The forgotten krill:

The biology and ecological function of *Thysanoessa macrura* in the Southern Ocean ecosystem

By

Jake Rodney Wallis

B.MarSc

M.MarAntSc

Submitted in fulfilment of the requirements for the degree of

Doctor of Philosophy in Quantitative Antarctic Science

Institute for Marine and Antarctic Sciences (IMAS)

University of Tasmania

May 2019

"You can swim all day in the Sea of Knowledge and still come out completely dry.

Most people do."

- Norman Juster

The Phantom Tollbooth, 1996

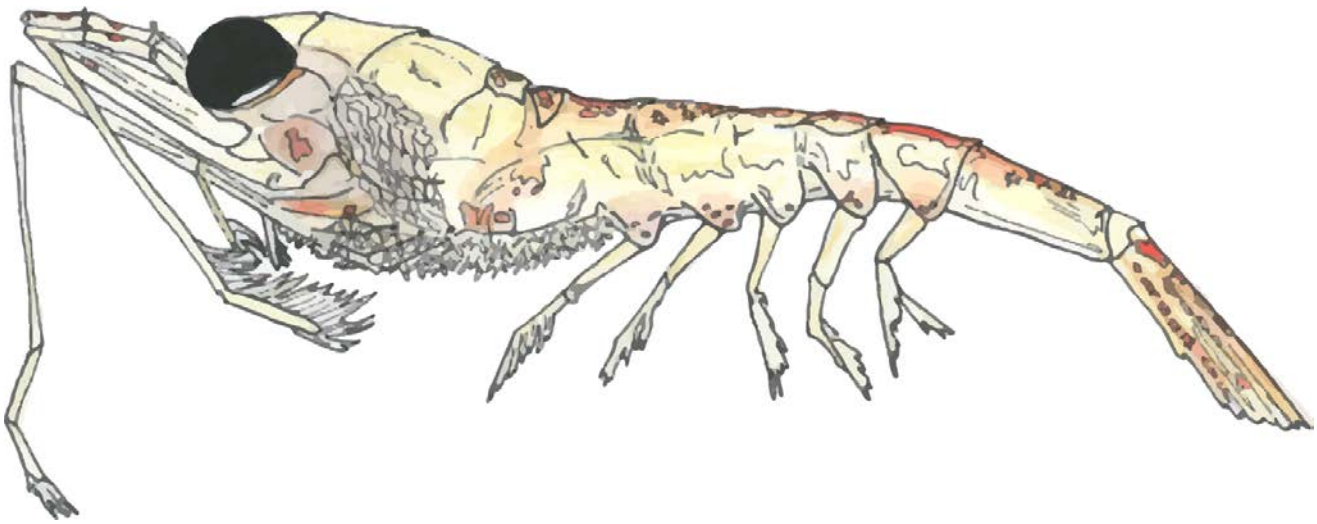

Statements and declarations

Declaration of Originality

This thesis contains no material which has been accepted for a degree or diploma by the University or any other institution, except by way of background information and duly acknowledged in the thesis, and to the best of my knowledge and belief no material previously published or written by another person except where due acknowledgement is made in the text of the thesis, nor does the thesis contain any material that infringes copyright.

Signed:

Date: 20th May, 2019

Authority of Access

This thesis may be made available for loan and limited copying and communication in accordance with the Copyright Act 1968.

Signed:

Date: 20th May, 2019

Statement regarding published work contained within this thesis

The publishers of the papers 1 – 6 hold the copyright for that content and access to the material should be sought from the respective journals. The remaining non-published content of the thesis may be made available for loan and limited copying and communication in accordance with the Copyright Act 1968.

Signed:

Date: 20th May, 2019

Statement of Co-authorship contributions

The following people, institutions, and organisations contributed to the publication of work undertaken as part of this thesis:

Jake Wallis, Institute for Marine and Antarctic Studies, University of Tasmania

Dr. Kerrie M. Swadling, Institute for Marine and Antarctic Studies, University of Tasmania

Dr. So Kawaguchi, Australian Antarctic Division, Kingston, Tasmania

Dale Maschette, Australian Antarctic Division, Kingston, Tasmania

Dr. Simon Wotherspoon, Institute for Marine and Antarctic Studies, University of Tasmania

Robert King, Australian Antarctic Division, Kingston, Tasmania

Jessica E. Melvin, Institute for Marine and Antarctic Studies, University of Tasmania

Abigail J.R. Smith, Institute for Marine and Antarctic Studies, University of Tasmania

Dr. Kohei Matsuno, Hakkaido University, Hakodate, Japan

Author details and their roles

Publication 1. Sexual differentiation, gonad maturation and reproduction of the Southern Ocean euphausiid *Thysanoessa macrura*.

This publication is reproduced in Chapter 2, and published in Journal of Crustacean Biology – Oxford Academic.

Wallis JR, Kawaguchi S, Swadling KM (2018) Sexual differentiation, gonad maturation and reproduction of the Southern Ocean euphausiid Thysanoessa macrura*. J Crustacean Biol 38:107-118*

- Jake R Wallis (75%)
- Dr. So Kawaguchi (10%)
- Dr. Kerrie M Swadling (15%)

Publication 2. A description of the post-naupliar development of Southern Ocean krill (*Thysanoessa macrura*).

This publication is reproduced in Chapter 3, published in Polar Biology – Springer.

*Wallis JR (2018) A Description of the post-naupliar stages of Southern Ocean krill (*Thysanoessa macrura*). Polar Biol 41:2399-2407*

- Jake R Wallis (100%)

Publication 3. *Thysanoessa macrura* in the southern Kerguelen region: population structure and biomass.

This publication is reproduced in Chapter 5 and is currently submitted to Deep-Sea Research II – Elsevier.

Wallis JR, Maschette D, Kawaguchi S, Wotherspoon S, Swadling KM (2019) Thysanoessa macrura *in the southern Kerguelen region: population structure and biomass. Submitted to Deep-Sea Research II.*

- Jake R Wallis (60%)
- Dale Maschette (15%)
- Dr. Simon Wotherspoon (10%)
- Dr. So Kawaguchi (5%)
- Dr. Kerrie Swadling (10%)

Publication 4. Discovery of gregarine parasitism in some Southern Ocean krill (Euphausiacea) and the salp *Salpa thompsoni*.

This publication is reproduced in Appendix E, published in Polar Biology – Springer.

Wallis JR, Smith AJR, Kawaguchi S. (2017). Discovery of gregarine parasitism in some Southern Ocean krill (Euphausiacea) and the salp Salpa thompsoni*. Polar Biol 40:1913-1917*

- Jake R Wallis (75%)
- Abigail JR Smith (15%)
- Dr. So Kawaguchi (10%)

Publication 5. In situ growth rate estimates of Southern Ocean krill, *Thysanoessa macrura*.

This publication is reproduced in Appendix F, in press in Antarctic Science – Cambridge University Press.

> *Wallis JR, Melvin JE, King R, Kawaguchi S. (2019). In situ growth rate estimates of Southern Ocean krill,* Thysanoessa macrura*. Antarct Sci DOI:10.1017/S0954102019000063*

- Jake R Wallis (65%)
- Jessica E Melvin (15%)
- Robert King (15%)
- Dr. So Kawaguchi (5%)

Publication 6. Big things come in small packages. Biomass contribution of the krill *Thysanoessa macrura* to the marine ecosystem in the Kerguelen Plateau region.

This publication is reproduced in Appendix G, in press in Proceedings of the 2nd Kerguelen Plateau Marine Ecosystem and Fisheries Symposium.

> *Wallis JR, Kawaguchi S, Matsuno K, Swadling KM (2019). Big things come in small packages. Biomass contribution of the krill* Thysanoessa macrura *to the marine ecosystem in the Kerguelen Plateau region. Proceedings of the 2nd Kerguelen Plateau Marine Ecosystem and Fisheries Symposium. In press*

- Jake R Wallis (70%)
- Dr. So Kawaguchi (10%)
- Dr. Kohei Matsuno (10%)
- Dr. Kerrie M Swadling (10%)

We the undersigned agree with the stated contributions for each of the above published or submitted peer-reviewed manuscripts contributing to this thesis.

Signed:

Dr. Kerrie Swadling

Primary Supervisor

Institute for Marine and Antarctic Studies

University of Tasmania

21st August, 2019

Signed:

Prof. Craig Johnson

Head, Ecology and Biodiversity Centre

Institute for Marine and Antarctic Studies

University of Tasmania

21st August, 2019

Acknowledgements

Firstly, I express my deepest gratitude to my supervisory team for their continued support and encouragement throughout my PhD. My sincerest thanks are extended to Dr. So Kawaguchi for his wealth of expert knowledge and enthusiasm for my research. Words cannot describe my appreciation for the support of Dr. Kerrie Swadling, not only throughout my PhD but for the entire 6 years we have worked together. I honestly don't think I would have got to where I am today without your thoughtfulness and most of all your patience. Together their guidance has helped me achieve more than I thought I could, allowing me to have confidence in my direction of research and providing me with the subtle nudges that I sometimes needed. A better and more supportive supervisory team does not exist.

I would like to thank Dr. Ruth Eriksen for her ever insightful eye and passion for Southern Ocean phytoplankton. Although I will never compare to her abilities, the time she took to impart some of her wisdom was immensely helpful. I am grateful to and thank Dr. Patti Virtue for not only teaching me but assisting in lipid extractions and analyses.

To the countless friends I have both here in Hobart and farther afield, without your support, advice, encouragement and understanding my PhD would not have been possible. Although there are too many to name personally there is one whom without their support I would not be submitting this thesis. I need to thank Christine Weldrick for her constant coffee-break companionship, a time in which much was discussed, plans were made, and everything felt possible, until the next coffee-break at least.

Last but by no means least, I would like to thank my family, my parents, sister and partner Tommy. Although they may not have understood half of the things I was on about most of the time, I appreciate their support and eagerness for me to the best I can be. Without their confidence in me over the past 3 years I would not have been able to finish my PhD.

General Abstract

The importance of euphausiids or 'krill' in the Southern Ocean has long been documented, establishing important links between lower trophic levels and apex predators. Although more than 20 species of euphausiids are found within these mid – high latitude waters of the Southern hemisphere our current understanding of the function and role of euphausiids as a collective is almost exclusively restricted to the Antarctic krill, *Euphausia superba*. Whilst the importance of *E. superba* is well documented, its role as a keystone species has overshadowed the study of other euphausiid species in the Southern Ocean and limited the research needed to understand fundamental biology and ecology of those species. Despite being considered the second most abundant euphausiid species in the Southern Ocean, *Thysanoessa macrura* is one of these largely understudied species. Although *T. macrura* is beginning to be recognised as a species that requires more attention due to its significant biomass and abundance, current studies are generally restricted to describing population demography and ecology; however, the lack of concise information on the fundamental biology of the species makes providing a context to the role of *T. macrura* impossible.

Despite being a smaller euphausiid, high and calorific-rich lipid reserves, coupled with an extensive and ubiquitous latitudinal distribution from the sub-Antarctic to the Antarctic continent, indicate an importance of *T. macrura* that is currently underexplored for the pelagic ecosystem of the Southern Ocean. Abundances of *T. macrura* often exceed those of *E. superba* in regions including Prydz Bay (east Antarctica), Bransfield Strait (west Antarctica Peninsula), lower latitudes of the Antarctic Pacific Ocean, and may form a more important trophic connection in the Indian Ocean region of the Southern Ocean. A winter reproductive period for *T. macrura* has been indicated by the appearance of larval stages during June to August, however no direct information is currently reported on the reproductive cycle and fecundity of this species. The quantitative information on the diet of *T. macrura* is scarce and lacks the detail required to conceptualise their role and function in the ecosystem. This shortage of foundation information often necessitates the use of assumptions based on *E. superba* to understand the ecology of *T. macrura* in an ecosystem context. The current understanding of *T. macrura*, despite being limited, indicates a difference in fundamental biological and ecological processes between the two species that make such assumptions tenuous at best.

This PhD thesis focuses on filling vital knowledge gaps in the biology and ecology of *T. macrura*. A bottom-up approach is taken by first providing a foundation of fundamental biological information, including reproduction and life history. Ecological processes of this species are then conceptualised and developed to understand feeding ecology and population dynamics. Specifically, this thesis provides (**1**) the first conceptual model of gonadal development, maturation and fecundity estimates, (**2**) descriptions of the larval development, and (**3**) the diet of *T. macrura* from early larval stages to adults, identifying ontogenetic shifts

and overlap in feeding ecology. Building upon these biological processes, (**4**) the population demography of *T. macrura* is explored in the important Kerguelen Plateau region. Key highlights of each chapter are summarised below.

(**1**) Gonadal development and maturation of *T. macrura* during late winter in high latitude waters confirms a winter reproductive period previously assumed from observational evidence of larvae. Analysis of ovaries and direct oocyte counts allowed for the first estimate of *T. macrura* fecundity, which scales strongly with female length, resulting in a surprisingly high egg production of > 2200 eggs female^{-1} during a reproductive period. (**2**) After hatching, the resulting larvae undertake a series of developmental steps, with the morphological characteristics of post-naupliar stages consisting of 3 calyptopis and 6 furcilia stages described in detail, allowing for the avoidance of misidentification with larvae of other euphausiid species with overlapping distributions. Despite expecting an influence of temperature on the size of larvae due to the latitudinal range of the species, *T. macrura* larvae appear to be able to capitalise on the increased primary productivity during their appearance in surface waters, indicating that food availability is a more important driver of larval growth and development than temperature.

(**3**) Although diatoms were common, protozoan and metazoan prey, particularly copepods identified by their mandibles, were found to be the most important contributor to the diet of adult *T. macrura*. Coupling microscopic examination of guts with analysis of lipid profiles and fatty acid biomarkers emphasised the importance of carnivory to *T. macrura*, particularly predation on the copepod *Calanoides acutus*. The first evidence of the diets of larval *T. macrura* confirm their ability to graze phytoplankton. Additionally, mouthpart morphology of larvae suggests a niche overlap with adults, consuming prey of similar size-range, although the ability of larvae to capture larger motile prey is reduced due to the lack of fully developed secondary feeding appendages.

(**4**) Despite a ubiquitous distribution at the oceanic scale, *T. macrura* populations are not homogenous, responding strongly to environmental drivers. Spatial heterogeneity of *T. macrura* over the Kerguelen Plateau was driven by water mass properties and the presence of the copepod *C. acutus*, a dominant prey source. Adult *T. macrura* reached abundances up to 162 ind. 1000 m^{-3} accompanied by high abundances of early furcilia stages in excess of 4000 ind. 1000 m^{-3}. The total lipids of *T. macrura* were found to be reaching their maximum recorded in the literature (> 40% of dry weight), stored as predominantly wax esters as a lipid mass within the free carapace space.

A conservative mean biomass of 1.66 mg m^{-3} was calculated for *T. macrura* across the southern Kerguelen Plateau region, with peaks up to 9.53 mg m^{-3}. This high biomass, coupled with high, energy-rich lipid content throughout most of the year indicates *T. macrura* forms a substantial energy source for vertebrate predators in the high productive Kerguelen Plateau region.

Explanatory note to thesis structure

A large proportion of this thesis has been published as peer-reviewed journal articles (or currently submitted and under peer-review) and therefore there is some textual overlap in introductory and discussion sections of Chapters. All Chapter references have been coalesced into a single reference list provided at the end of this thesis. For continuity, the main body of the thesis follows the referencing format of the journal *Polar Biology*.

Table of Contents

List of figures

List of tables

Chapter 1

Introduction and thesis overview

Thysanoessa macrura collected from Antarctic waters on board *RV Aurora Australis*

Photograph by Jake Wallis

1.1 Background

Euphausiids, commonly known as 'krill', are pelagic crustaceans and are amongst the most abundant groups in the Southern Ocean. Their broad-scale ecological role in the Southern Ocean is well documented, forming integral and direct links between lower trophic levels and apex predators (Atkinson et al. 2012). Twenty-three species of euphausiids currently occupy the Southern Ocean, accounting for 27% of species recognized globally (Mauchline 1980; Kirkwood 1982). Despite this high species diversity, fundamental biological and ecological information on many of these species is lacking and generally restricted to basic distributional information only. Temperature is an important environmental driver of euphausiid species distribution. The frontal systems associated with the Antarctic Circumpolar Current therefore play an important role in establishing clear latitudinal distributional limits of euphausiids of the Southern Ocean (Fig. 1.1).

Euphausia superba is the most well-studied euphausiid species in the Southern Ocean due to it being a 'keystone' species, forming an important resource exploited by many large vertebrate predators including marine birds, seals, baleen whales and humans. Due to its significance in the Southern Ocean pelagic ecosystem it is often referred to as 'krill' or 'Antarctic krill' to the exclusion of all other species, creating confusion in terminology when assessing the role of euphausiids as a collective. Whilst *E. superba* is the largest and most numerous species of euphausiid in the Southern Ocean, the smaller species *Thysanoessa macrura* is thought to be the second most abundant, with abundances exceeding those of *E. superba* in areas including Prydz Bay (East Antarctica), the Bransfield Strait (West Antarctic Peninsula) and it has even been reported to successfully replace *E. superba* within higher latitudes of the Antarctic Pacific Ocean (Makarov 1979; Hosie 1991; Nordhausen 1992). Moreover, while *E. superba* is confined by the Polar Front at its northern extent, *T. macrura* has a much larger latitudinal distribution that extends into the sub-Antarctic, north of the sub-Antarctic front, with a ubiquitous distribution throughout its range (Cuzin-Roudy et al. 2014; Haraldsson and Siegel 2014).

Although the current information on *T. macrura* is relatively restricted, information currently available on the biology and ecology of this abundant Southern Ocean euphausiid species suggests it is currently underappreciated in the Southern Ocean ecosystem. The lack of targeted investigations to fully describe the fundamental biological processes of *T. macrura* makes our understanding of the ecological roles of this species rudimentary at best.

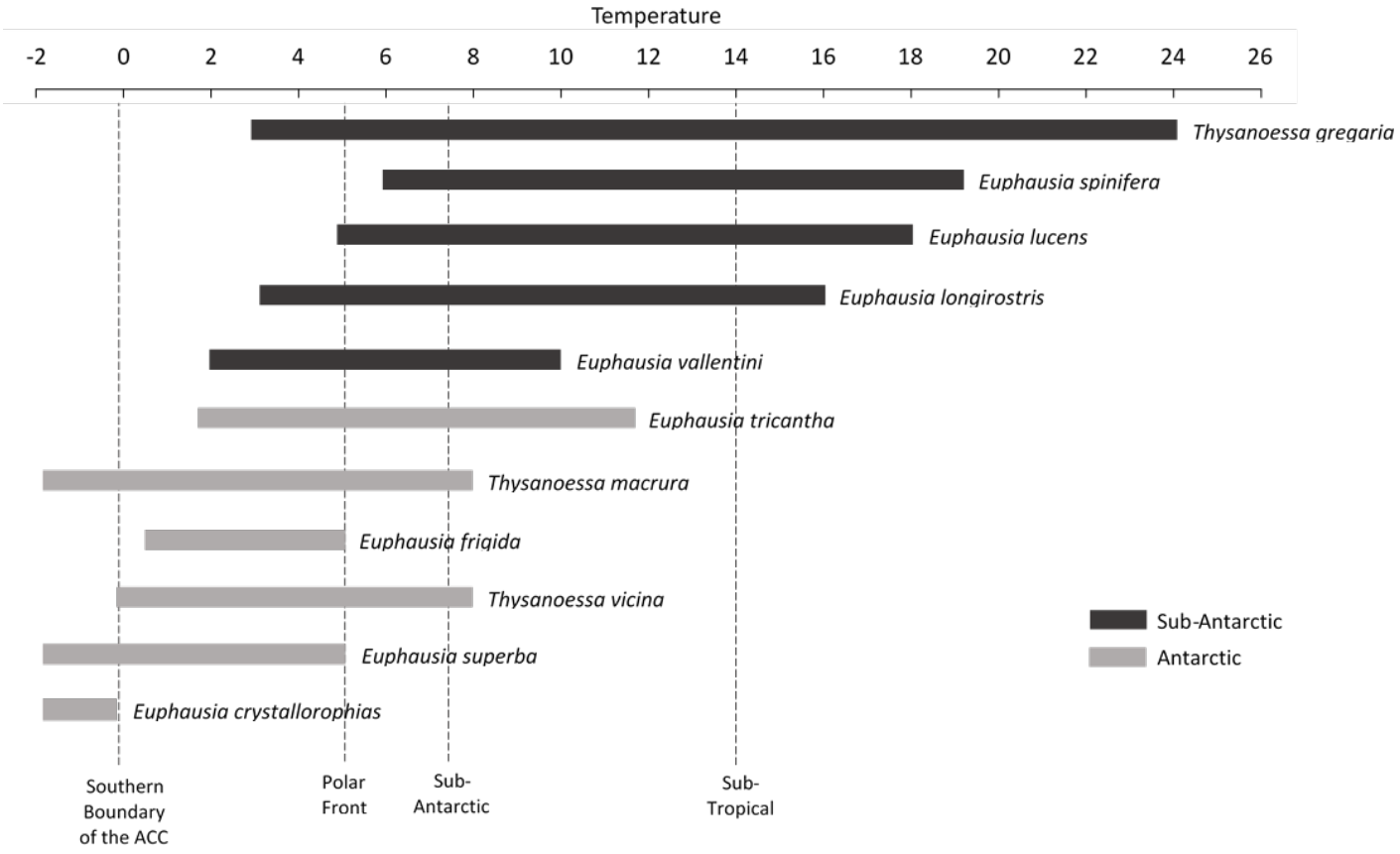

Figure 1.1. Distribution of the dominant euphausiid species commonly observed in the Southern Ocean (Sub-Antarctic and Antarctic) based upon their thermal tolerances (Kirkwood 1982; Cuzin-Roudy et al. 2014). Oceanic fronts associated with the Antarctic Circumpolar Current (ACC) are indicated by the dashed lines generalised from thermal properties of water masses reported by Orsi et al. 1995.

1.2 *Thysanoessa macrura* life history and reproduction

The timing of reproduction of euphausiids is species-specific in the Southern Ocean, with the common goal of the appearance of larval stages in surface waters during spring and summer, the period of increased primary productivity. The ability of adults to undertake gonadal maturation, and subsequent mating, restricts the onset of spawning, with most Southern Ocean and Antarctic euphausiids requiring periods of intense feeding during the onset of spring to fuel the energetic demands of gonad development and egg and sperm production (Falk-Petersen et al. 2000). *Thysanoessa macrura* is the earliest spawning euphausiid in the Southern Ocean, with spawning thought to begin during winter (Makarov 1979). Having a reproductive period that occurs before peaks in primary productivity in the Southern Ocean is highly advantageous as it ensures that larval stages are present in surface waters during the onset of spring blooms and ensures rapid

development of larvae without competition from other euphausiid species. This capital breeding strategy, using stored energy rather than relying upon feeding to fuel reproduction employed by *T. macrura* is possible due to the storage of large quantities of lipids during late spring and summer, a unique trait compared to other Southern Ocean euphausiids (Hagen and Kattner 1998).

Thysanoessa macrura stores a large proportion of their lipids as wax esters, which are used for long-term storage of metabolic energy. The use of wax esters by Southern Ocean euphausiids is not confined to *T. macrura* and is also common in the high-latitude species *Euphausia crystallorophias,* although at lower proportions of total lipid content (Falk-Petersen et al. 2000). Although *E. crystallorophias* uses wax esters to initiate spawning at the beginning of spring, periods of intense feeding during the onset of spring blooms are still required to fuel and increase the fecundity of females. Unlike *E. crystallorophias*, the wax esters stored by *T. macrura*, comprised of longer-chained alcohol components, have a high calorific content (Kattner et al. 1996). With with up to 65% of total lipids stored as these wax esters, the lipids deposited facilitates this decoupling of egg production from primary production for *T. macrura* (Hagen and Kattner 1998; Falk-Petersen et al. 2000).

Early reports on the spawning period were based upon the reproductive cycle of *E. superba* and the appearance of larval stages (Makarov 1979). More recent reports, however, suggest spawning begins between June and August, indicating a mid-winter spawning onset (Siegel 1987; Haraldson and Siegel 1987). Regional variation in reproductive periods are common for Antarctic euphausiids, in addition to prolonged spawning periods, and may account for the discrepancies in previously reported studies and suggests a relatively prolonged spawning period for *T. macrura*.

Despite the cursory information on the initiation of spawning, no data are available on the fecundity of *T. macrura* either based on egg production rates or clutch size. The lack of this critical component in understanding the life-history dynamics of *T. macrura* is hindered by their timing of spawning during winter and therefore their relative inaccessibility during this period, with sampling efforts for pelagic invertebrates generally confined to spring and summer. In other euphausiid species, fecundity is often heavily influenced by environmental factors including food quality and quantity both prior to and during spawning; however, due to the use of lipid reserves to fuel reproduction, it is unclear how food availability influences *T. macrura* (Ross and Quentin 2000). Furthermore, the relationship between body size and clutch size (the number of eggs produced), with larger females producing more eggs, remains unexplored for *T. macrura*.

Similarly, the information on the life history of *T. macrura* is fragmentary. The identification of *T. macrura* larvae from stratified depth sampling suggests an ontogenetic vertical migration from 1000 to 2000 m depth, similar to that documented for *E. superba*, confirming that *T. macrura* is a broadcast spawner, releasing their eggs freely into the water column with eggs that are negatively buoyant (Makarov 1979). Like other Southern Ocean euphausiids, *T. macrura* possess a complex developmental succession from eggs to juveniles consisting of two naupliar, one metanauplius, three calyptopis stages and six furcilia stages (Kirkwood 1982). Ontogenetic stratification has been identified for *T. macrura* larvae, with nauplius I and II and metanauplius stages generally found between 500 – 1000 m depth (Fig. 1.2) (Makarov 1979; Nordhausen 1994a; Nordhausen 1994b; Taki et al. 2009; Haraldsson and Siegel 2014). Calyptopis I is the first developmental stage to reach surface waters. This stage possesses mandibles that first developed in naupliar stages to facilitate swimming and these are accompanied by simple maxilla and maxillules to enable feeding (Mauchline 1967). All three calyptopis stages are generally found within the upper 200 m of the water column, with furcilia stages I – VI generally restricted to the upper 50 m (Makarov 1979; Nordhausen 1994a; Haraldsson and Siegel 2014). *Thysanoessa macrura* develop into juveniles at an approximate length of 8 mm, transitioning into adults that are reproductively active in as little as 13 months from hatching, although more conservative estimates suggest up to 2 years (Nordhausen 1994a; Haraldsson and Siegel 2014). Early estimates of the life-span of *T. macrura* suggested a maximum of three years (Siegel 1987). Recent evidence based upon cohort analysis of *T. macrura* in the Lazarev Sea, however, suggests a life span of 5+ years indicating a previously underestimated longevity (Haraldsson and Siegel 2014). Sexual dimorphism in growth, maturation and life-span is thought to be displayed by *T. macrura,* with females believed to take up to one year longer than males to reach sexual maturity. This difference in the timing of maturation is due to slower growth rates of females and would suggest that females can participate in up to 4 breeding seasons during their life span, with males growing fast and dying young (Haraldsson and Siegel 2014). This pattern in growth rates could explain why *T. macrura* populations are skewed toward female dominance.

The current information about *T. macrura* life history is fragmentary in nature, with information drawn from disparate studies in both space and time. The lack of definitive estimates of the timing of *T. macrura* reproduction and duration across their large distributional range hinders the description of the life-history of this abundant Southern Ocean euphausiid species

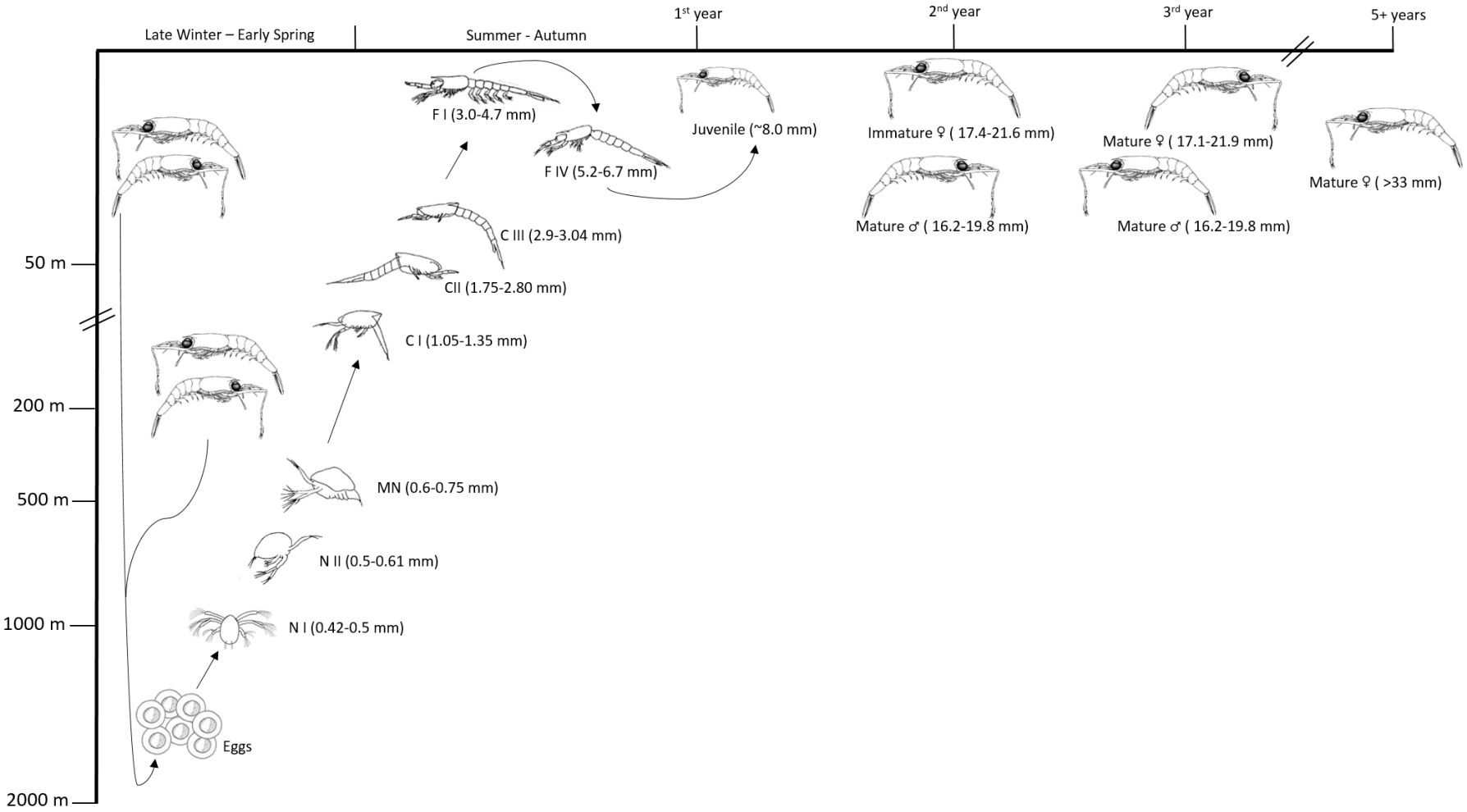

Figure 1.2. Lifecycle of *Thysanoessa macrura* showing the ontogenetic migration of larval stages and the depth where they are commonly found. Larval stages include N – nauplius, MN – metanauplius, C – calyptosis and F – furcillia. The average size of each stage is also provided, including the size of adults as they age.

1.3 Ecosystem niche

1.3.1 Feeding and diet

Thysanoessa macrura is believed to be omnivorous, consuming a large range of prey including diatoms, flagellates, protozoans and metazoans (Hopkins 1985; Hopkins and Torres 1989). The premise of a flexible diet of *T. macrura* is supported by morphological adaptations to the feeding mechanisms, direct analysis of the gut contents, lipid biomarkers and stable isotope analysis. These methods provide valuable information about the diet of *T. macrura* over a range of time scales, from hours in the case of gut content analysis to months for stable isotope analysis. Despite multiple lines of evidence that support an omnivorous feeding mode, there is a lack of targeted investigations, with direct analysis of the diet of *T. macrura* included in larger food-web based assessments, providing more generalised and coarse information on feeding patterns and dominant food items (Hopkins 1985; Hopkins and Torres 1989).

Euphausia superba possesses a highly developed feeding basket, created by the interlinkage of thoracopods to form a dense network of setae, to capture suspended prey items, primarily phytoplankton. *Thysanoessa macrura* does not have this structure and instead possesses modified and elongated second thoracopods that enable the capture of large, motile prey items such as copepods. Additional modifications to mouthpart morphology and the internal structures of the foregut facilitate the maceration and ingestion of both phytoplankton and crustacean prey (Mauchline 1967; Suh 1996). Feeding experiments to quantify the importance of protozoan ciliates, tintinnids, acanthans and foraminifera in the diet of adult and juvenile *T. macrura* highlight the efficiency in the capture of these prey items (Froneman et al. 1996). Furthermore, the elongation of thoracopods as individual *T. macrura* grow indicates that bigger individuals may be able to capture larger prey sources and thus allow for a shift from smaller prey to large motile prey, such as copepods (Fäber-Lorda and Mayzaud 2010). A transition to the importance of carnivory, with juveniles more reliant on herbivory than adults, highlights the complexity in feeding preferences of *T. macrura*.

Analysis of prey items identifiable in the guts of *T. macrura* from the two studies that have included them suggests a carnivory-based diet in Western Antarctica (Hopkins 1985; Hopkins and Torres 1989). Radiolarians and foraminifera were the dominant protozoan consumed, although the copepods *Calanoides acutus* and *Metridia gerlachei* were found to dominate the guts of *T. macrura* (Hopkins 1985; Hopkins and Torres 1989). Diatoms formed a constant, yet smaller, contribution to prey items identified. Lipid biomarkers support a similar understanding of diet. The abundant Antarctic copepod *C. acutus* has been identified as an important component of the diet of *T.*

macrura based upon the high presence of the alcohol 20:1(*n*-9), a biomarker for *C. acutus* (Hagen and Kattner 1998; Falk-Petersen et al. 2000). There is little evidence to suggest a large contribution from phytoplankton based upon fatty acids in the lipid profiles of *T. macrura*, with levels of trophic markers consistently low both spatially and temporally (Falk-Petersen et al. 2000). Stable isotope analysis, which is used to delineate trophic levels and connections, indicates that *T. macrura* functions as a secondary consumer, falling between the second and third trophic level within the Weddell Sea (Rau et al. 1991).

Unlike adult *T. macrura*, no investigation has been undertaken to understand the diet of progressive larval stages from calyptopis stage 1, the first larval phase with rudimentary mouthparts to enable feeding. Significant work has been undertaken to quantify the diet of *E. superba* larval stages (calyptopis 1 to furcilia 6) and for the purpose of this thesis it is assumed that *T. macrura* follows a similar pattern, utilising developing feeding appendages to capitalise on the high phytoplankton abundance present when larval stages reach productive surface waters. With the inclusion of four furcilia samples in their study Hagen and Kattner (1998) provide the only insights into prey preferences of late larval stages. The high proportion of the fatty acid indicator 18:4(*n*-3) suggests a heavy reliance upon phytoplankton by furcilia, predominately flagellate groups (Hagen and Kattner 1998). The preference for motile prey items may demonstrate an increasing ability to capture motile prey items that would later facilitate a transition to carnivory. The lack of dietary information for *T. macrura* larval stages, coupled with the spatially and temporally limited information on the diets of adults, limits our ability to understand the species dynamics of *T. macrura* and ultimately hinders our ability to describe their importance in the Southern Ocean ecosystem.

1.3.2 Role of *Thysanoessa macrura* in the Southern Ocean ecosystem

The high abundance of wax ester-rich lipids makes *T. macrura* a highly valuable resource for higher predators. A total lipid content up to 12% greater than *E. superba* and a sustained high lipid content throughout the winter months highlights their potential contribution to the marine ecosystem that remains relatively underappreciated (Falk-Petersen et al. 2000). Additionally, the ontogenetic ascent of larvae from up to 2000 m depth represents an additional contribution to the marine food-web. The role of *T. macrura* in the Southern Ocean is therefore not limited to surface waters where adults are predominantly located, but also reach the meso and bathypelagic systems, forming a substantial carbon source for marine predators over many trophic levels. The wide latitudinal distribution of *T. macrura* also provides an important prey source from predators from the sub-Antarctic to the Antarctic continent.

Thysanoessa macrura are common in the diets of many diving birds and fish from the sub-Antarctic to the Antarctic region (Raymond et al. 2011). The evaluation of *T. macrura* as an important contributor to the diets of mid-trophic levels and apex predators in the Southern Ocean is often hindered by the level of analysis performed. In many studies, due to the difficulties in differentiating the different euphausiid species during visual examinations of stomach contents, species-specific information is often not recorded. Recent comparisons of the circumpolar food webs of the major oceanic sectors of the Southern Ocean have highlighted the importance of *T. macrura* in food-web connectedness and energy flow. In particular, McCormack et al. (2019a) highlight the importance of krill other than *E. superba*, represented largely by *T. macrura* as the dominant mid-trophic resource in the diets of demersal fish, seabirds and penguins.

Understanding the role *T. macrura* play in the transfer of biogenic carbon through the pelagic food-web is restricted by lack of information about the diet of both adults and larvae. The lack of quantitative information on the diet of *T. macrura* outside of western Antarctica is required to appreciate spatial heterogeneity and how *T. macrura* responds to different prey types and assemblages, especially in the Indian Ocean sector of the Southern Ocean where they appear to play a more important role in ecosystem function than *E. superba*.

1.4 Study region

1.4.1 Southern Ocean

The Southern Ocean is the largest ocean in the southern hemisphere and is a highly complex system with no geographic barriers. It is bound by the sub-tropical front to the north and the Antarctic continent to the south (Orsi et al. 1995). In a broad setting, the Southern Ocean is often described based upon the three oceanic basins that comprise this oceanic system, linked by the eastward flowing Antarctic Circumpolar Current (ACC). Despite the lack of longitudinal borders, the Southern Ocean does not lack structure, with the ACC and its complex filamentous structure of frontal systems providing distinctive latitudinal bands. Sharp transitions in water column properties, primarily temperature and salinity, caused by the convergence and divergence of surface waters due to changes in wind stress create these latitudinal regions. The dominant fronts associated with the ACC, in increasing latitudinal location, include the sub-Antarctic front, Polar Front, southern ACC front and the southern boundary of the ACC, with each representing a transition in these important physical properties (Orsi et al. 1995). These fronts tend to show an increase in primary and secondary productivity due to the upwelling of nutrient-rich deep water (Schallenberg et al. 2018).

The sharp transitions in temperature associated with these frontal systems often act as physical barriers to the distribution of Antarctic invertebrates, based upon their thermal tolerance limits. This is especially true for krill in the Southern Ocean, with their distributional limits defined by these frontal systems (Fig. 1.1) (Kirkwood 1982; Cuzin-Roudy et al. 2014). The influence of these complex frontal systems is unique to three major sectors of the Southern Ocean, establishing unique bioregions, characterised by fundamental differences in underlying primary and secondary producers and consequently ecosystem level structure. Furthermore, the increased branching of the major fronts in the Indian Ocean sector of the Southern Ocean result in enhanced eddy action, increasing primary and secondary productivity in these eddy fields (Sokolov and Rintoul 2007).

1.4.2 Kerguelen Plateau

The Kerguelen Plateau has been identified as one of the most important regions for primary and secondary productivity in the Southern Ocean, supporting large fish biomass to the north and Antarctic krill to the south. The southern extent of the Kerguelen Plateau and the surrounding region (Australian-Antarctic Basin, Weddell-Enderby Basin and the Princess Elizabeth Trough) have been demonstrated to be a biologically important region, supporting many of the migratory whale species found in the Southern Ocean during the spring and summer months (Tynan 1998). The southern ACC front and southern boundary of the ACC are the dominant oceanic features in this region and play a key role in influencing biological productivity. The Antarctic Slope Front flows west along the Antarctic continental slope and shelf break. The Weddell-Enderby and Australian-Antarctic basins, flanking the southern extent of the Kerguelen Plateau, support relatively low levels of primary productivity due to being iron-limited (Schallenberg et al. 2018). Upwelling of water that is rich in iron close to the eastern boundary of the plateau and Princess Elizabeth Trough promotes and sustains long periods of phytoplankton blooms that persist well into summer (Schallenberg et al. 2018).

Due to the importance of this region to biological productivity in the Indian Sector of the Southern Ocean, the Southern Kerguelen Plateau was the focus of the Kerguelen Axis voyage during mid-January to mid-February 2016, a large-scale international study to assess the transition between krill-based and fish-based marine food webs and the underlying physical drivers (Fig. 1.3) (Bestley et al. 2018). Given the possibility of an ecological hotspot in this region and the recent revelations of the potential dominance of *T. macrura* in the food-web (McCormack et al. 2019a), the Kerguelen Plateau region represents a key area where the role of *T. macrura* needs to be assessed.

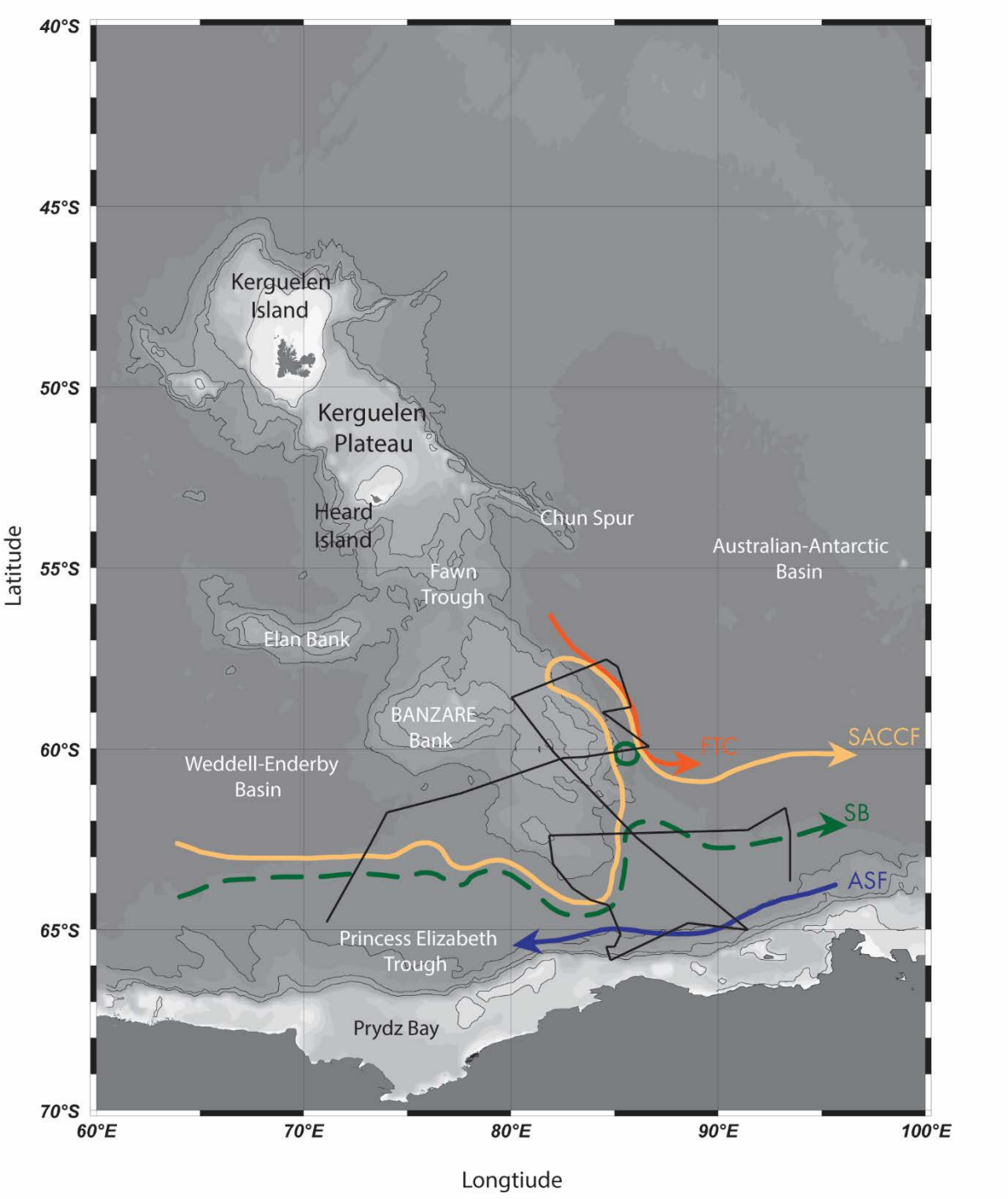

Figure 1.3. Kerguelen Plateau region with the Kerguelen Axis voyage track highlighted and the dominant oceanic fronts of the study region including the Fawn Trough Current (FTC), the Southern Antarctic Circumpolar Current Front (SACCF), Southern Boundary of the Antarctic Circumpolar Current (SB) and Antarctic Slope Front (ASF).

1.5 Context of the thesis

1.5.1 Aims of the thesis

Thysanoessa macrura is a dominant euphausiid in the Southern Ocean; however, despite high abundances, our current knowledge about the ecological functioning and role of this species is restricted. For example, a winter reproductive period has been demonstrated for *T. macrura*, yet no reproductive cycle or fecundity has been established. Although multiple lines of evidence confirm an omnivorous diet, there is a dearth of quantitative information on the diet of *T. macrura*. Furthermore, a lack understanding of feeding behaviour of larvae restricts the ability to conceptualise the integration of *T. macrura* within the pelagic ecosystem. These foundational biological end ecological processes are essential in providing context to the role of *T. macrura* in the Southern Ocean.

The objective of the thesis is to fill vital knowledge gaps in the biology and ecology of *T. macrura*. A bottom-up approach is taken by first describing fundamental biological processes including reproduction, life history and feeding. Building upon this information, knowledge of the ecological processes of this important Southern Ocean euphausiid is conceptualised and developed to understand feeding ecology and population dynamics (Fig. 1.4). Specifically, this thesis aims to:

1. Provide a conceptual model of gonadal development, maturation and fecundity estimates for *T. macrura*.

2. Explore the larval development of *T. macrura,* presenting comprehensive larval descriptions and photographic documentation.

3. Describe the diet of adult and larval *T. macrura,* identifying ontogenetic shifts and overlap in feeding ecology.

4. Understand and describe the population demography of *T. macrura* in the biologically important Kerguelen Plateau region of the Indian Ocean sector of the Southern Ocean.

1.5.2 Thesis structure

The body of work present in this thesis is provided in four main data chapters that are targeted to address the specific aims of the thesis Complementary information and stand-alone studies are also provided within the appendices that contribute to this thesis.

Chapter 2: Sexual differentiation, gonad maturation and reproduction of the Southern Ocean euphausiid *Thysanoessa macrura*.

This chapter focuses on conceptualising the reproductive cycle of *T. macrura* by establishing the stages of gonad development and maturation for both males and females. The egg production and batch size of females is explored by ovarian analysis and oocyte counts resulting in the first estimates of fecundity provided for *T. macrura*.

Chapter 3: A description of the post-naupliar development of Southern Ocean krill (*Thysanoessa macrura*).

A comprehensive description of the post-naupliar development of *T. macrura* is undertaken in this chapter. Accompanying photographs are presented, with this study documenting the developmental pathway of *T. macrura* and stage-specific characteristics to enable their identification. The effects of temperature on the size of larvae is also explored.

Chapter 4: Diet of *Thysanoessa macrura* in the Kerguelen region, with emphasis on carnivory and ontogenetic shifts.

This study focuses on the diet of *T. macrura* in the Kerguelen Plateau region of the Indian sector of the Southern Ocean using both microscopic examination of gut contents and lipid and fatty acid analyses. The diet of larval stages is explored in addition to describing mouthpart morphology to assess the ontogenetic shifts in feeding efficiencies and diet.

Chapter 5: *Thysanoessa macrura* in the southern Kerguelen region: population structure and biomass.

In this final study, the demography of *T. macrura* is described for the Kerguelen Plateau region. The distribution and population structure of *T. macrura* is assessed and environmental and biological drivers of population structure explored.

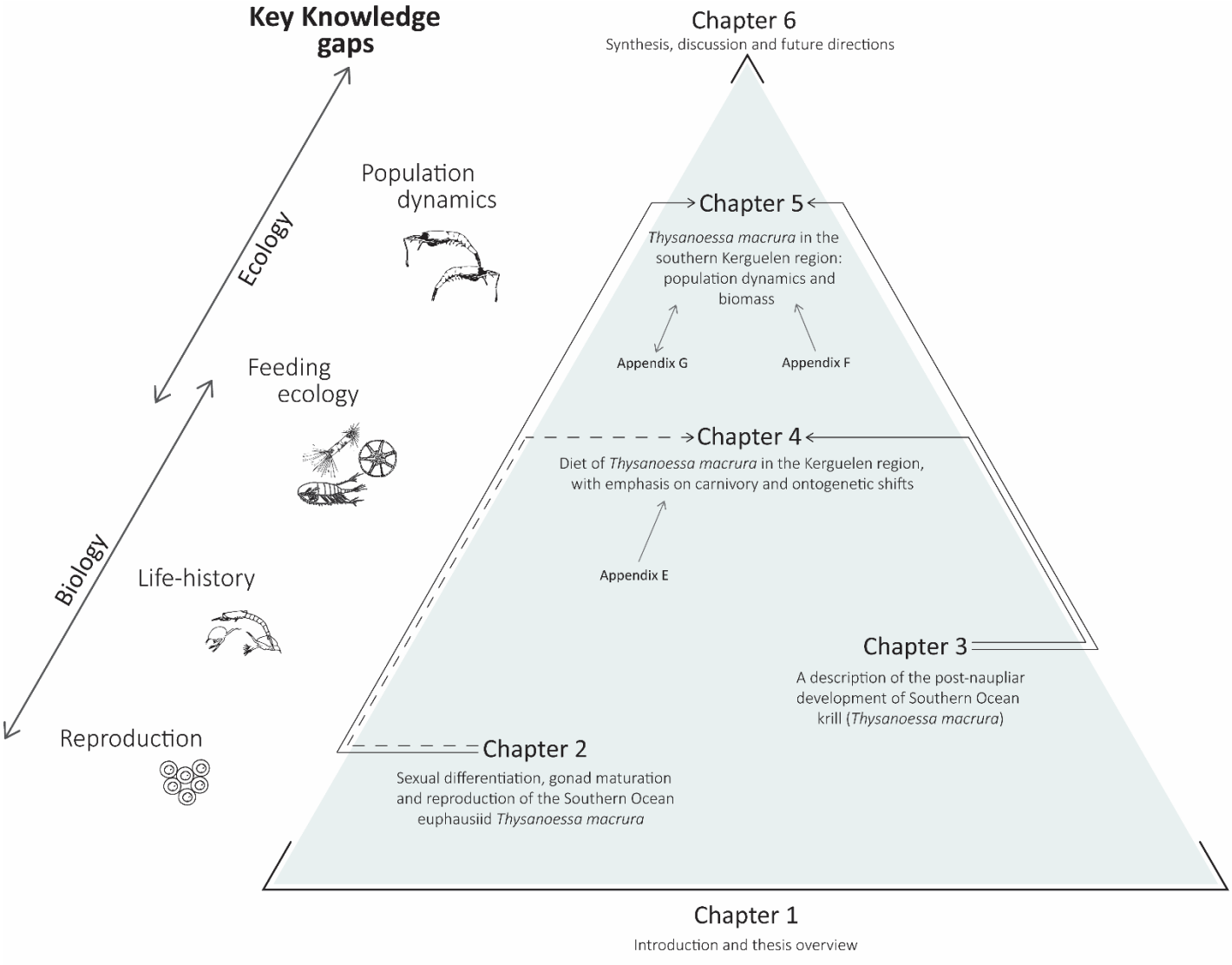

Figure 1.4. Thesis outline and structure indicating the development of understanding of the key knowledge gaps in *Thysanoessa macrura* biology and ecology.

Chapter 2

Sexual differentiation, gonad maturation and reproduction of the Southern Ocean euphausiid *Thysanoessa macrura*

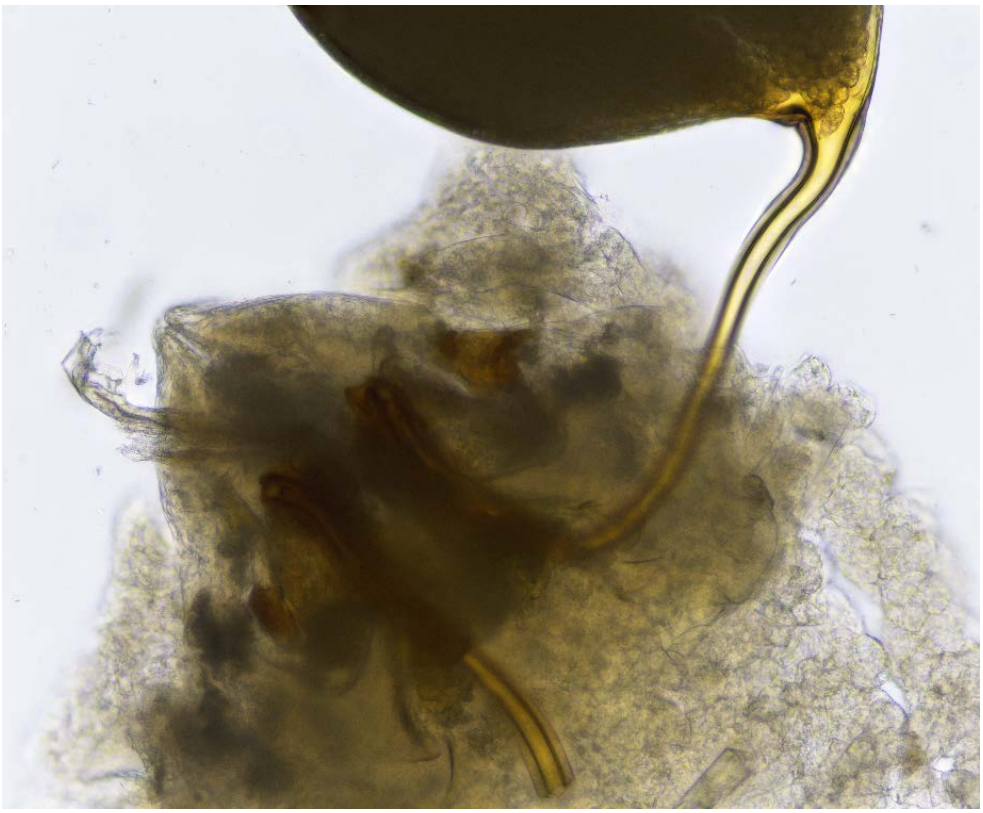

Attachment of spermatophore from a male *Thysanoessa macrura* to the external reproductive opening of a female.

Photo by Jake Wallis

All the research presented in this chapter is published in the Journal of Crustacean Biology

Wallis JR, Kawaguchi S, Swadling KM (2018) Sexual differentiation, gonad maturation and reproduction of the Southern Ocean euphausiid Thysanoessa macrura*. J Crustacean Biol 38:107-118*

2.1 Abstract

Thysanoessa macrura (Sars 1883) is a small, albeit highly abundant, Southern Ocean euphausiid. It has been reported that *T. macrura* undertakes reproduction during late winter, with the reproductive cycle decoupled from periods of high primary productivity in the highly seasonal Southern Ocean. Despite this uncommon reproductive strategy, there has been little work to describe this cycle and quantify the reproductive potential of this species. *Thysanoessa macrura* collected from Antarctic waters during early September to early October were used to establish sexual developmental stages, for both females and males, to provide a standard means for assessing the reproductive maturity of this species. Seven sexual developmental stages were established for females based upon the organisation of ovaries and their constituent oogonia and oocytes. Four sexual developmental stages were identified in males using secondary sexual characteristics. A large lipid deposit was identified in the carapace of both females and males, reducing in size with progressive gonadal development, likely fuelling egg and sperm production. Egg batch size was determined by direct ovarian counts and scaled allometrically with total wet weight. Predicted egg batch size ranged from 34 to 746 eggs batch^{-1} for the range of individual sizes present in this study (30.5–165.6 mg). Using the ratios of the different oocytes remaining after the first-spawning event of females, it was predicted that up to three egg batches can be produced by *T. macrura* in a single reproductive season. Consequently, the fecundity of *T. macrura* is estimated at 60 to >2200 eggs female^{-1} year^{-1}. A model of *T. macrura* reproductive cycle confirms a winter reproductive period and further highlights the reproductive potential of this small Southern Ocean euphausiid, providing the first estimates of fecundity reported for this species.

2.2 Introduction

Thysanoessa macrura (Sars 1883) is an abundant, though poorly understood, Southern Ocean euphausiid. The latitudinal distribution of *T. macrura* is the widest of Antarctic euphausiid species, extending from the Antarctic continent to north of the Sub-Antarctic front (Nordhausen 1992; Haraldsson and Siegel 2014). *Thysanoessa macrura* is the first spawning euphausiid species in the Southern Ocean, with reproduction thought to occur during late winter-early spring, before periods of high productivity in surface waters (Makarov 1979). This early spawning strategy is fuelled by the use of wax esters deposited during heavy feeding throughout the previous spring-summer, and it ensures that calyptopes, the first feeding larval stage, reach surface waters during the onset of periods of high productivity in spring (Makarov 1979). The lipid content of *T. macrura* remains high during winter, indicating that stored lipids are used for reproduction rather than winter survival (Hagen and Kattner 1998; Fäber-Lorda and Mayzaud 2010). Conclusions of a winter reproductive period are often extrapolated from the appearance of larval stages, predominantly naupliar and

calyptope stages, during early spring, however, due to the large latitudinal distribution of *T. macrura*, estimates of spawning onset varies seasonally, ranging from mid-winter to early spring (Makarov 1979; Siegel 1987; Haraldsson and Siegel 2014). Direct observations of females bearing spermatophores during mid-winter (June-July) and gravid females (August-October) infer a reproductive period that spans the winter-spring transitional period in high latitude waters, suggesting that reproduction is decoupled from periods of high primary productivity (Haraldsson and Siegel 2014). A lack of information regarding the sexual development of adults (via oogenesis and spermatogenesis) in preparation for spawning limits the ability to fully describe and quantify this uncommon reproductive cycle.

Sexual developmental staging of females, based upon the physiological phase of an individual, morphology of gonads and secondary sexual characteristics, has been developed for dominant euphausiid species in the global ocean, including Antarctic krill *Euphausia superba* (Dana, 1850) and northern krill *Meganyctiphanes norvegica* (Sars 1857; Cuzin-Roudy 1991; Cuzin-Roudy and Buchholz 1999). Euphausiid ovarian development follows patterns exhibited by most crustacean groups, with the maturation of germ cells from oogonia to mature oocytes via gametogenesis and subsequent oogenesis (Cuzin-Roudy 1991). The progressive development of these germ cells is punctuated by distinctive morphological differences that correspond to the physiological phase of the sexually developing female. The use of physiological phases in the establishment of these sexual developmental stages provides a more detailed approach to understanding the reproductive ecology of euphausiid species in contrast to early approaches that relied heavily upon the morphology and presence of external secondary sexual characteristics including the thelycum in females and ampullae and petasma of males. Applications of these sexual developmental stages allow for detailed information regarding the rate of sexual maturation, timing of spawning and the effects of environmental conditions on regional variation in spawning seasons.

The reproductive period of *T. macrura*, which encompasses the end of winter, generally inhibits the ability to undertake direct egg counts to quantify batch size and egg production rates due to their relative inaccessibility. Consequently, there are no current estimates of the reproductive potential of *T. macrura* within the Southern Ocean and high Antarctic waters. Studies of the population structure of *T. macrura* in the high Antarctic suggest that younger individuals (years 1-3) comprise the bulk of the population, despite an estimated life span of greater than 5 years (Haraldsson and Siegel 2014). Given the high abundance of *T. macrura* and a population dominated by younger individuals, population turnover rates and recruitment for this species must be high. Determining the reproductive biology of adults and their reproductive potential is critical to understanding the reproductive ecology of this highly abundant Southern Ocean euphausiid.

This study provides descriptions of sexual differentiation of *T. macrura* and the sexual development of males and females in preparation for reproduction. Here we establish sexual developmental stages of *T. macrura* using gonad morphology and maturation to provide a system for assessing the reproductive state of individuals and populations. Through detailed ovarian analysis, we also provide the first estimate of *T. macrura* fecundity from Antarctic waters.

2.3 Methods

Thysanoessa macrura were collected during the winter-spring transitional period (9th September – 11th October) during the Sea Ice Physics and Ecosystem eXperiment (SIPEX) voyage in 2007, in the area between 115°E - 125°E and 62°S - 66°S. Sampling was conducted using a Rectangular Midwater Trawl (RMT8), with standard double oblique tows from the surface to 200 m (Baker et al. 1973). Formaldehyde preserved (4% concentration) specimens were used to assess the sexual maturity of male and female individuals and establish sexual developmental stages (SDS) based upon gonad morphology and secondary sexual characteristics. Additionally, preserved females were used to estimate potential fecundity based upon direct counts of oocytes within fully developed ovaries.

2.3.1 Oocyte development

Ovarian germ cell maturation was assessed by dissecting whole ovaries from the carapace of females. Females with obvious differences in ovarian morphology, chiefly the relative volume of the carapace occupied, were chosen to assess the full spectrum of germ cell developmental stages. Germ cells within ovaries were examined using a modified 'squash technique' established by Cuzin-Roudy and Amsler (1991). Upon dissection, the left posterior lobe was removed, placed on a glass slide and gently compressed with a coverslip to disperse germ cells into a single layer. A weak concentration of methylene blue (0.5%) was added to slides prior to squashing to enhance the contrast between the nucleus and cytoplasm of oogonia and early oocyte stages and to visualise the germinal zone of ovaries. Germ cell stages were determined from characteristics provided by histological analysis of both northern krill, M. *norvegica* and Antarctic krill, *E. superba* (Cuzin-Roudy and Amsler 1991: Cuzin-Roudy and Buchholz 1999). Cell characteristics and appearance were recorded for the seven cell types identified in *T. macrura*. Due to the irregularity in the shapes of oocytes within the ovary, total length was recorded as the longest axis of the cell. Total cell area was also measured, with the nucleus-cytoplasm ratio for each cell type then calculated.

2.3.2 Sexual developmental stages

Female sexual developmental stages were determined by examining both secondary sexual characteristics and gonad morphology. Ovaries were dissected from the carapace of females and gross ovarian features recorded, including location within the carapace and abdomen. Ovaries were

examined and the relative contributions of developing oogonia and oocytes identified. Sexual maturation consists of seven stages (SDS 1-7) from sub-adults to adult females at the end of their reproductive period (Table 2.1). Sexual developmental stages were determined based on the physiological phase identified by the dominant germ cell types within the centre of ovaries, along with the development of the thelycum and attachment of spermatophores. Sexual developmental stages of males were established by examining the successive development of external sexual characteristics, including the petasma and ampullae and the appearance of spermatophores in ejaculatory ducts (Table 2.2).

Table 2.1. *Thysanoessa macrura* female sexual developmental stages (SDS) from ovarian analysis. Stages are based on the dominant ovarian cell type identifiable within the ovaries, corresponding to the major physiological phases of the reproductive cycle.

SDS	Physiological phase	Ovary morphology	Dominant ovarian cell type	Secondary sexual characteristics
1	Gametogenesis	Small, no lobe differentiation	Primary and secondary oogonia	No thelycum present
2	Oogenesis	Small with lobes differentiated	Primary oocytes	Small, underdeveloped thelycum
3	Pre-vitellogenesis	Large, lateral lobes small, posterior lobes reaching first abdominal segment	Type 1 oocytes	Fully developed thelycum, may have spermatophores attached
4	Vitellogenesis	Large, lateral lobes small, posterior lobes reaching mid of first abdominal segment	Type 2 and 3 oocytes	Fully developed thelycum, 1 - 2 spermatophores attached
5	Spawn-ready	Large, lateral lobes elongated, posterior lobes reaching base of first abdominal segment	Type 4 oocytes	Fully developed thelycum, 1 - 2 spermatophores attached
6	Post-first spawn	Anterior lobes retracted, reaching half way along the DG, posterior lobes thin	Residual type 4 oocytes	Fully developed thelycum
7	Spent (oosorbtion)	-	-	Fully developed thelycum

Table 2.2. *Thysanoessa macrura* male sexual developmental stages (SDSM) based upon observable features of secondary sexual characteristics and spermatophore production.

SDSM	Secondary sexual characteristics
1	Petasma developing
2	Petasma fully developed and ampullae clearly visible
3	Ampullae and ejaculatory ducts empty of spermatophores, testes visible through the carapace
4	Spermatophores stored in ampullae, or in the ejaculatory ducts

2.3.3 Egg batch size and fecundity

Seventy-four females that were scored as sexual developmental stage 4 and 5 were used to assess potential egg batch size based on ovarian oocyte counts. The total body length (BL), measured from the tip of the rostrum to the base of the sixth abdominal segment, and total wet weight (TWW) were recorded for each female. Ovary wet weight (OWW) was then measured after the complete dissection from the carapace and first abdominal segment. The left posterior lobe of the ovary was removed and weighed. Using the squash technique, the number of pre-vitellogenic oocytes (PVO: type 1 and 2 oocytes) and mature, vitellogenic oocytes (MO: type 3 and 4 oocytes) were counted. The total number of previtellogenic oocytes (NPVO) and mature oocytes (NMO) was then calculated respectively based upon the measured weights of the left posterior lobe and the entire ovary, with their sum representing the total number of developing oocytes (NOCT).

To determine the number of egg batches females can potentially produce in a single spawning season, 15 females that had already undertaken a single spawn (SDS 6) were selected. Morphometric measurements (BL, TWW and OWW) were recorded and the left posterior lobe of the ovary assessed for oocyte types. Each oocyte type was counted (primary oocytes, oocyte types 1, 2, 3 and 4) and the total number of each estimated for the entire ovary. The proportion of each oocyte type within the ovary was used as a proxy to determine the total number of potential egg batches that could be produced by each female during the reproductive period. The fecundity of females was then determined by the total number of eggs produced in each batch and the total number of potential batches, defined as the total number of eggs produced per year.

Allometric relationships for females using the morphological characteristics BL, TWW and OWW and the oocyte counts NMO and NOCT were established using the allometric power function

(2.1) $\mathrm{y} = \mathrm{a}x^{b}$

whereby the coefficient *a* represents the y-intercept and *b* determined from the slope using log-log transformed data. Model 1, ordinary least squares (OLS) and Model 2, reduced major axis (RMA) regression were performed to determine the most appropriate relationship due to the underlying differences in the approaches of both models (Cuzin-Roudy 2000). Person's coefficient of determination (R^2) and ANOVA *F* ratio from OLS regression were used to distinguish the allometric model with the highest predictive power of fecundity estimation.

2.4 Results

Mature *T. macrura* were collected from surface waters during the winter-spring transitional sampling period (9th September – 11th October). Females were identified by the presence of the thelycum on the sixth thoracic somite (Fig. 2.1A). The thelycum of reproductively active females is small, with each coxal plate measuring approximately 500 µm in length. The thelycum is generally obstructed by the gills and is best visualised by placing the individual with the ventral side up and parting the gills. Thelyca are not fully pigmented but are distinguishable by the presence of small orange-red chromatophores distributed throughout the coxal plates (Fig. 2.1A).

Males are identifiable by the presence of the petasma on the first pair of pleopods (Fig. 2.1B). Although the presence of ampullae on the seventh thoracic somite is also a distinguishing feature of mature males, the ampullae are often difficult to distinguish, especially in formalin-preserved individuals. The presence of the highly structured petasma provides a more accurate and rapid assessment of sex and, when fully developed, do not require the dissection of the first pair of pleopods. The absence of either male of female secondary sexual characteristics indicates that the individual is a juvenile.

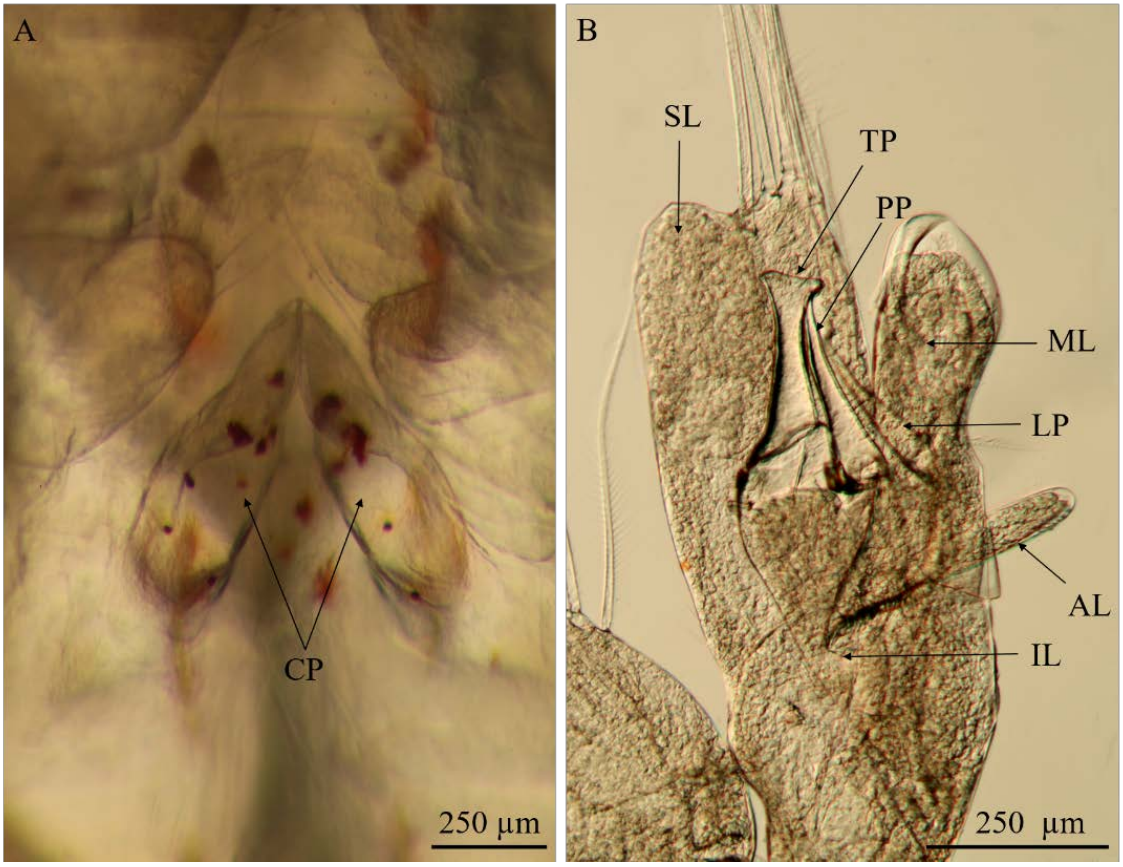

Figure 2.1. *Thysanoessa macrura* secondary sexual characteristics. **A**, Ventral view of a fully developed thelycum with pigment spots visible throughout the coxal plates (CP). **B**, Petasma of a reproductive male on the first pleopod. Auxillary lobe = AL, inner lobe = IL, lateral process = LP, middle lobe = ML, proximal process = PP, setiferous lobe = SL, terminal process = TP.

2.4.1 Ovarian development and Sexual developmental stages

The development of ovaries from sub-adults to actively reproducing females was identified. The successive developmental phases of ovarian morphology in preparation for spawning (gametogenesis, oogenesis, pre-vitellogenesis and vitellogenesis) and corresponding ovarian cells were identified (Fig. 2.2). A full description of the morphology of each ovarian cell type in developing ovaries is provided in the Appendix Table A1. Seven sexual developmental stages (SDS) were established for female *T. macrura* based upon the physiological phase of females, identified by the ovarian cells present, overall ovarian morphology and secondary sexual characteristics (Table 2.1).

Females of SDS 1 possess small, undifferentiated ovaries located ventrally to the heart. Gametogenesis is evident in these females, with ovaries comprised predominately of primary and secondary oogonia. Primary and secondary oogonia are small (35 µm and 52 µm, respectively), nondescript cells with the nucleus occupying most of the internal cellular space (Fig. 2.2 A and B). Staining increased the contrast of nuclear material and allowed the differentiation of the two oogonia cell types present. Primary oogonia were commonly found in various stages of mitotic division (Fig. 2.2A), forming secondary oogonia. Secondary oogonia are slightly larger than primary oogonia and have a nucleus that appears reticulated (Fig. 2.2B). SDS 1 females do not have an evident thelycum and are difficult to differentiate from sub-adult males without dissection.

The differentiation of secondary oogonia into primary oocytes by oogenesis defines SDS 2 females (Fig. 2.2C). The nucleus of primary oocytes are large, however, the overall cell size is much greater than that of secondary oogonia, increasing from 52 µm to 117 µm (Appendix A, Table A1). Ovaries of SDS 2 females are larger than those of SDS 1 due to the increase in size and abundance of primary oocytes. Ovaries have clearly defined anterior and posterior lobes, with primary oocytes primarily occupying the centre of each lobe. In relation to the carapace cavity, ovaries are still relatively small, however, they may be visible as a mass through the carapace of preserved individuals, located below the heart. The thelycum is beginning to develop and is translucent, lacking distinctive differentiation of the coxal and sternal plates seen in fully mature females.

Pre-vitellogenesis marks the transition of primary oocytes into type 1 oocytes seen in SDS 3 females (Fig. 2.2D). These oocytes are large (up to 212 µm), with a reduced nucleus, clear cytoplasm and a nuclear to cytoplasm ratio of approximately 50% (Appendix A, Table A1). Ovaries of SDS 3 females are considerably larger than those of earlier stages due to the increase in size of type 1 oocytes. Three distinct ovarian lobes are evident, with the anterior lobe extending forward to the mid-dorsal carapace region, the posterior lobes reaching the first abdominal segment and the lateral lobes distinct, albeit small (Fig. 2.3B). At this stage, ovaries are evident through the carapace of females and appear as a golden mass in formaldehyde preserved specimens. The thelycum is fully developed and may bear spermatophores in preparation for spawning (Fig. 2.4 A-C).

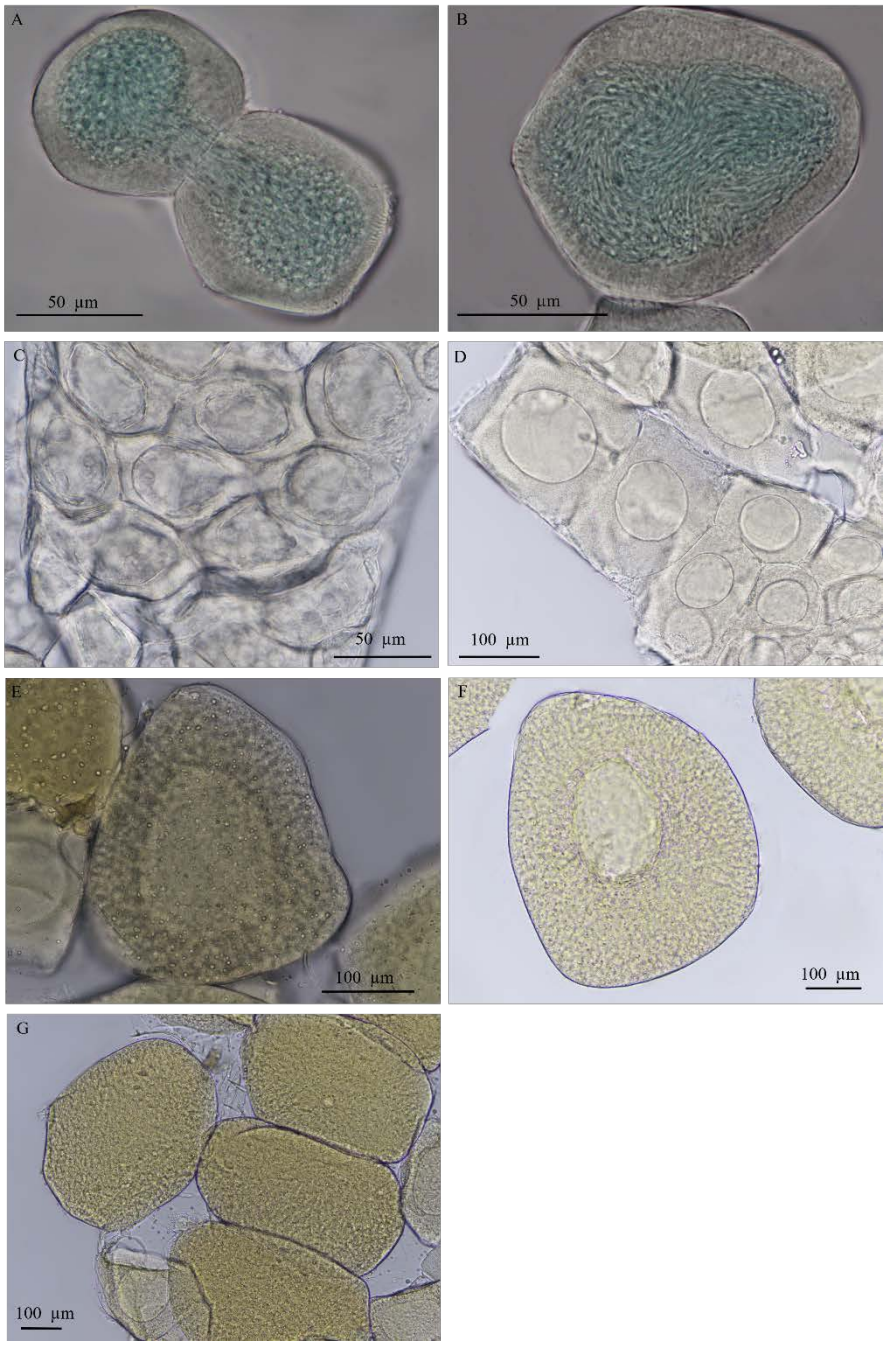

Figure 2.2. *Thysanoessa macrura*, female germ cell maturation phases. **A**, Primary oogonia during late telophase, with nuclear material stained using 0.5% methylene blue. **B**, Secondary oogonia with large, reticulated nucleus stained with methylene blue (0.5% solution). **C**, Primary oocytes. **D**, Pre-vitellogenic type 1 oocytes with large nuclei and transparent cytoplasm. **E**, Type 2 oocytes with granulated and cloudy cytoplasm during early vitellogenesis. **F**, Vitellogenic type 3 oocyte. A relatively small nucleus is apparent in the centre of cells, with the cytoplasm filled with lipid droplets. **G**, Mature type 4 oocytes. No clear nucleus is visible, with the cells appearing golden-brown and filled with lipid granules.

Figure 2.3. *Thysanoessa macrura* ovary. **A**, Lateral view of a spawn-ready female (SDS 5), with the dotted white line indicating the maximum extent of the ovaries within the carapace and first abdominal segment. **B**, Ventral view of an ovary dissected from a pre-vitellogenic female (SDS 3) indicating the three dominant regions of the ovary, Anterior Lobe (AL), Lateral Lobe (LL) and Posterior Lobe (PL). **C**, Lateral view of a post first-spawn female with full spermatophores (sp) attached to the thelycum. The white dotted line indicates the extent of the ovary, showing the ventral contraction after first spawn.

SDS 4 females are vitellogenic, with type 2 and 3 oocytes found within the mid regions of the ovarian lobes. The accumulation of lipids becomes evident in type 2 oocytes, which are large (approximately 300 µm), with the cytoplasm appearing cloudy and slightly granulated (Fig. 2.2E). Lipid accumulation is very evident in type 3 oocytes in which the entire cytoplasm is comprised of lipid droplets (Fig. 2.2F). Type 3 oocytes are large (>400 µm) and have a clear nucleus present within the centre of cells. Females are generally mated at this stage, with up to two spermatophores attached to the thelycum.

The development of type 4 oocytes typifies the transition to SDS 5, in which females are ready to spawn. Type 4 oocytes are large, greater than 500 µm, and have no visible nucleus (Fig. 2G). Ovaries reach their maximum extent, with the lateral lobes rounded and extending to the base of the first abdominal segment. Due to the presence of large oocytes, oocytes within the ovary are visible through the carapace (Fig. 2.3A). Attached spermatophores appear empty, with spermatozoa transferred from the spermatophore to the gonopores of females (Fig. 2.4D). After the first spawning event, the ovary retracts posteriorly, although it remains relatively large and robust (SDS 6) (Fig. 2.3C). Ovaries contain residual type 4 oocytes within the centre of ovarian lobes with primary oocytes, type 1 and type 2 oocytes found in the peripheries of ovarian lobes. Due to the timing of the voyage, females had not yet undertaken oosorption (SDS 7) and therefore this stage was not identified in this study.

Figure 2.4. *Thysanoessa macrura* spermatophore attachment. **A**, Full spermatophore. **B**, spermatophore (sp) attached to the gonopores of the thelycum of a female below the Coxal Plates (CP). **C**, Dissected thelycum of a female bearing spermatophores (sp), indicating the attachment of the spermatophoral stalk within the gonopores of females at the base of the thelycum. **D**, Non-flagellated spermatozoan (spz) travelling from the ampullae (sac like structure) to the gonopore of a female during fertilisation.

2.4.2 Male development

The development of males was identified by the observable changes in external morphology (Fig. 2.5). Four sexual developmental stages of males (SDSM) were identified and correspond to the physical development of males from sub-adults, which are difficult to differentiate from females of a comparable developmental stage, to males actively producing spermatophores (Table 2.2). The development of the petasma on the endopod of the first pair of pleopods, identified as a small, undifferentiated lobe characterises SDSM 1. The full development of the petasma and clearly visible ampullae characterise SDSM 2, with the sexual copulatory and spermatophore storage structures ready for mating. The full development of the testes, which are clearly visible as a large golden mass within the carapace of preserved individuals, marks the ability of males to begin sperm production, however no spermatophores have yet been produced (SDSM 3). The production of spermatophores signifies the capacity to undertake mating and is characteristic of SDSM 4 (Fig. 2.5A). As the production of spermatozoa (sperm) (Fig. 2.4D) and consequently spermatophores is a continual process during reproductive periods; during this stage spermatophores are always identifiable within either the ampullae, ready for transfer to females or within the ejaculatory ducts as they transition to the ampullae (Fig. 2.5B).

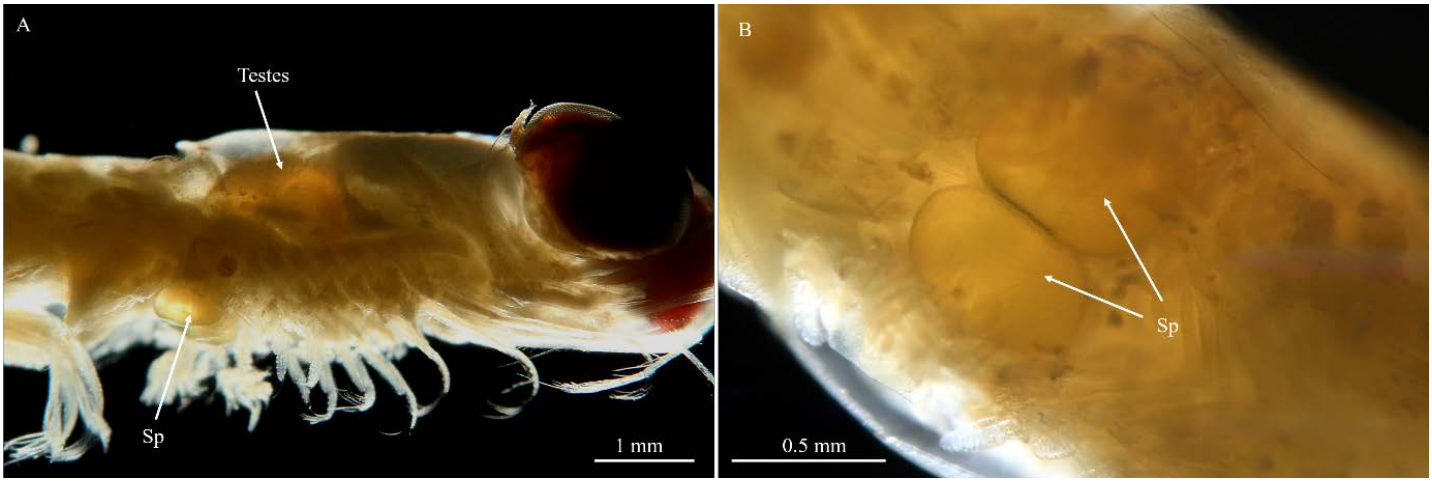

Figure 2.5. *Thysanoessa macrura* male. **A**, Lateral view of the male with testes visible through the carapace and spermatophores stored in the ampullae. **B**, Ventral view of a pair of spermatophores (sp) stored in the ampullae.

2.4.3 Lipid deposit

A large lipid deposit was identified within the carapace of all sub-adult and adult *T. macrura* individuals. In non-reproductive individuals, the lipid deposit fills the entire carapace cavity, extending from the rostrum to the base of the first abdominal segment (Fig. 2.6A). In both males and females that were reproductively active, the size of this lipid deposit varied depending upon their relative sexual developmental stage. In females, this lipid deposit was diminished and replaced with the enlarging ovary. By SDS 3 the lipid deposit was restricted to the free space within the anterior region of the carapace (Fig. 2.6B). In later stage females, the lipid deposit is generally completely diminished or, if present, it straddles the tip of the anterior ovarian lobes as a thin film.

In males, the size of the lipid deposit varied and did not diminish with sexual development. The lipid deposit occupied most of the free carapace space in all sexual developmental stages (Fig. 2.6C). In SDSM 4, the testes are encompassed by the lipid deposit. Only at this stage did the lipid deposit vary in size, likely relating to the time spent at this developmental stage and therefore sperm production.

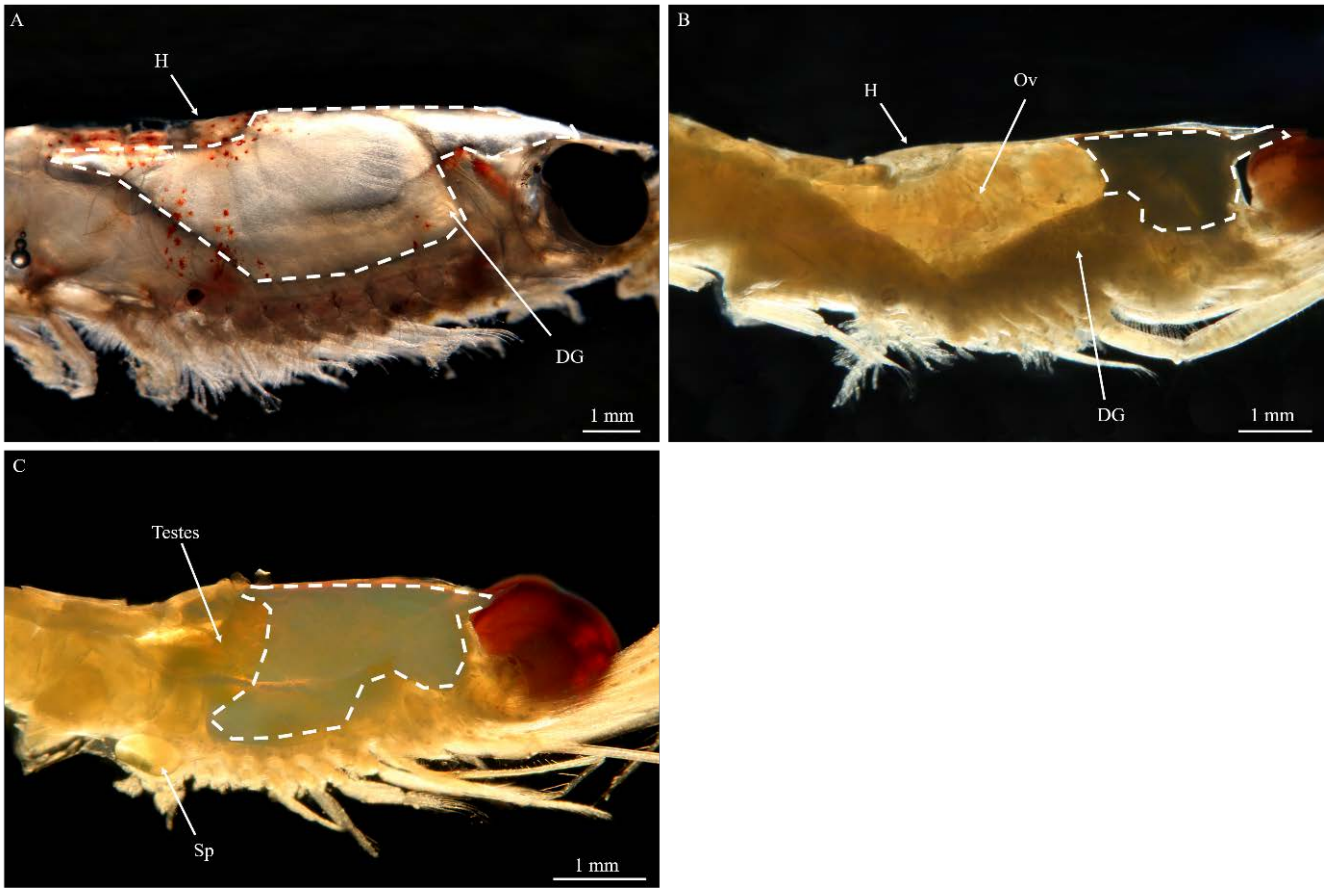

Figure 2.6. *Thysanoessa macrura* lipid deposit. **A**, Maximum extent of the lipid deposit (tip of the rostrum to the first abdominal segment) in a non-reproductively active female, saddling the digestive gland (DG) and sitting below the heart (H), with its extent indicated by the white dashed line. **B**, Cross-section of a pre-vitellogenic (SDS 3) female with the lipid deposit retracted to the anterior region of the carapace cavity as indicated by the white dashed line, directly adjacent to the anterior lobes of the developing ovary (ov). **C**, Cross-section of a reproductively active male showing the testes embedded within the lipid deposit (indicated by the white dashed line) with spermatophores (sp) stored within the ampullae.

2.4.4 Egg batch size, fecundity and the reproductive cycle

Egg batch size was estimated by examining the total number of vitellogenic and mature oocytes in the ovaries of 74 females. There was a relatively small size range for females with mature ovaries (SDS 4 and 5): 13.2 mm – 25.7 mm (Table 2.3). OWW scaled positively with BL, with OWW averaging 9% of TWW. Allometric relationships were established for *T. macrura* using both OLS and RMA regression analysis using log-log transformed data (Table 2.4). Significant correlations were found for all allometric relationships of female morphology, with a relatively high degree of variance explained using OLS regressions; TWW/BL (82%), OWW/BL (34%) and OWW/TWW (44%), with all relationships allometric. Significant correlations between egg batch size (NMO) and OWW, BL and TWW of females were described using OLS, with TWW best describing the variance of NMO at 20% (Table 2.4). NPVO increased positively with OWW, indicating that larger females not only have larger egg batches but also larger stocks of previtellogenic oocytes suggesting the capacity to produce multiple egg batches in a single reproductive period.

Table 2.3. Morphological characteristics of female *Thysanoessa macrura* and estimates of egg batch size (NMO) by ovarian cell counts of SDS 4 and 5 females. For SDS 5 and 6 females, NPVO includes type 1 and 2 oocytes, NMO is the sum of type 3 and 4 oocytes. All oocyte stages were counted individually for SDS 6 females to determine the number of potential egg batches produced during the reproductive cycle. (N = number of females included in the analysis, SE = standard error. NOTE: 0 values were omitted from calculations of mean if oocyte category was not present.)

	N	Range	Mean	SE
Vitellogenic and spawn-ready females (SDS 4 and 5)				
Total length (TL), mm	74	13.2 - 25.7	17.6	0.24
Total wet weight (TWW), mg	74	30.5 - 165.6	64.4	2.78
Ovary wet weight (OWW), mg	74	1.2 - 12	5.8	0.27
Number of previtellogenic oocytes (NPVO)	74	0 - 1175	263	22.5
Number of mature oocytes (NMO)	74	20 - 747	150	11.7
Post first-spawn females (SDS 6)				
Total length (TL), mm	15	14.4 - 19.3	16.7	0.46
Total wet weight (TWW), mg	15	37.4 - 83.3	57	3.87
Ovary wet weight (OWW), mg	15	1 -12.4	3.7	0.45
Number of primary oocytes	15	18 - 370	152	28.39
Number of type 1 oocytes	15	32 - 419	149	24.63
Number of type 2 oocytes	15	17 - 247	79	17.98
Number of type 3 oocytes	15	0 - 36	5	3.59
Number of type 4 oocytes	15	0 - 12	2	1.00

Table 2.4. Allometric relationships ($y = ax^b$) using total length (TL), total wet weight (TWW), ovary wet weight (OWW) and mature oocytes (NMO) and the total number of developing oocytes within the ovary (NOCT) in vitellogenic and spawn-ready females (SDS 5 and SDS 6). The R^2 and ANOVA *F* ratio (F) are provided for the log-log OLS linear regression (model 1). The coefficient *a* represents the y-intercept and *b* the coefficient of regression, determined from the slop using log-log transformed data and is provided for both OLS and RMA (model 2) regression. Based upon the allometric relationships, the range of the predicted egg batch size and its mean is calculated for both OLS and RMA estimated coefficients of regression (N = the number of individuals included in each analysis).

		Model 1 (OLS)								Model 2 (RMA)			
Allometric relationship (y/x)	N	*a*	*b*	*b* SE	R^2	F	p	Predicted egg batch size (range)	mean	*a*	*b*	Predicted Batch size (range)	mean
TWW/BL	73	0.022	2.77	0.14	0.816	305.5	<0.005			0.00871	3.09		
OWW/BL	73	0.005234	2.43	0.37	0.34	36.70	<0.005			0.000118	3.754		
OWW/TWW	73	0.135	0.898	0.113	0.44	56.15	<0.005			0.0359	1.22		
NPVO/OWW	70	7.78	1.81	0.3	0.33	35.47	<0.005	10-699	170	0.789	3.179	1.4 - 2127	178
NMO/OWW	73	43.85	0.608	0.151	0.19	16.32	<0.005	49 - 199	124	6.934	1.712	9 - 488	77
NMO/BL	73	0.115	2.439	0.5812	0.17	14.97	<0.005	62 - 316	125	0.000005	5.92	23 – 1,111	118
NMO/TWW	73	4.217	0.822	0.193	0.2	23.57	<0.005	70 - 382	129	0.0833	1.781	34 - 746	139
NOCT/OWW	70	70.469	0.9093	0.158	0.318	33.17	<0.005	83 - 675	332	24.774	1.534	33 - 1121	339
NOCT/BL	70	0.0265	3.294	0.6915	0.242	22.69	<0.005	130 - 1168	336	0.00006	5.449	72 - 2890	367
NOCT/TWW	70	1.977	1.245	0.212	0.327	34.50	<0.005	139 - 1145	353	0.204	1.802	96 - 2034	371

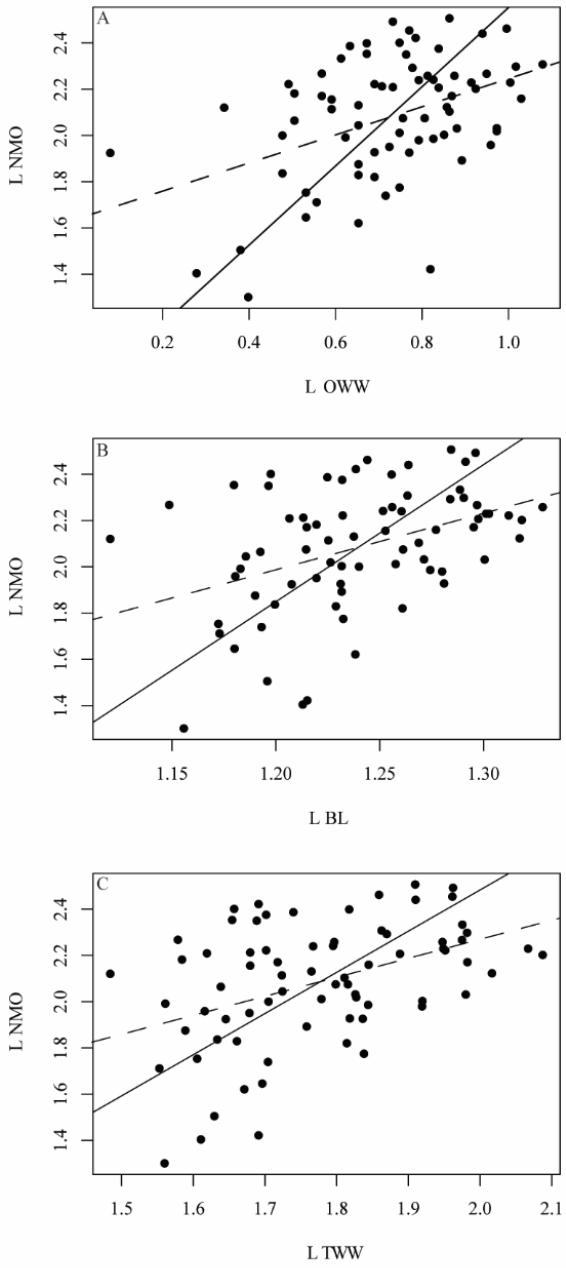

Figure 2.7. Relationships between the number of mature oocytes (NMO) used to estimate egg batch size within the ovaries of vitellogenic and spawn-ready female *T. macrura* and morphometric predictors on a log-log scale. Model 1, ordinary least squares (OLS) regression is indicated by the dashed line and model 2, reduced major axis (RMA) relationships are represented by the solid line (*N*=73). **A**, NMO (L NMO) and ovarian wet weight (L OWW) relationship, $R^2 = 0.19$. **B**, NMO and total body length (L BL), $R^2 = 0.107$. **C**, NMO and total wet weight (L TWW), $R^2 = 0.2$.

RMA regression provided better estimates of egg batch size than OLS when the allometric relationships were applied. Egg batch size estimates, based on the RMA and TWW, ranged from 34 – 746 eggs batch^{-1}, closely matching the observed range of 20-747 eggs batch^{-1}. A comparison of the mean predicted egg batch size of 139 eggs batch^{-1} and the observed mean of 150 eggs batch^{-1} highlights the skew in the data obtained, with few larger females in the present study (Fig. 2.7).

Post first-spawn females (SDS 6) were used to assess the potential for the production of multiple egg batches in a reproductive season. Very few SDS 6 females were present throughout the sampling region, with only 15 individuals identified. Despite the retracted ovary, females generally had a large number of previtellogenic oocytes (Table 2.3). Residual type 3 and 4 oocytes were often present in relatively low numbers and were likely representative of partial spawns not yet released. Primary oocytes and type 1 oocytes were present in approximately equal proportions, with the number of type 2 oocytes slightly lower and indicating up to 2 additional egg batches developing. Type 2 oocytes and type 1 oocytes would likely form the next batch of eggs to be released, with the large number of primary oocytes indicating a potential third batch. The smallest females identified as reproductively active, that is those < 15 mm, generally had extremely low numbers of previtellogenic oocytes (Table 3), indicating that the ability to incubate multiple batches is size dependent. Based on the estimates of a mean sized female weighing 64.4 mg (equivalent to 17.6 mm) and the ability to produce up to 3 egg batches, the potential mean fecundity of *T. macrura* is estimated at 420 eggs female^{-1} year^{-1}, however it is >2200 eggs female^{-1} year^{-1} for the largest individuals identified in this study.

The sexual development of males and females and the production of egg batches is conceptualised in Fig. 2.8. The seasonal cycle of sexual development of both females and males during egg production, and the utilisation of the large lipid deposit found in the carapace of individuals of both sexes begins in late September-early October. Maturing sub-adult females first develop via gametogenesis and oogenesis (SDS 1 and 2) prior to the spawning period, whilst 2+ year adult females begin the egg production cycle at SDS 3, with females producing up to 3 egg batches in a single reproductive period. Male development progresses linearly, with males fully developed (SDSM 4) and having stored spermatophores and ready for mating prior to females reaching SDS 3. As 2+ year males retain fully developed secondary sexual characteristics at the end of the spawning period, and therefore regress to SDSM 2, sub-adult males first develop through SDSM 1 and 2 prior to the reproductive period. The lipid deposit is heavily depleted in both females and males during reproduction, fuelling egg and sperm production whilst also allowing for the growth of the developing ovary in adult females.

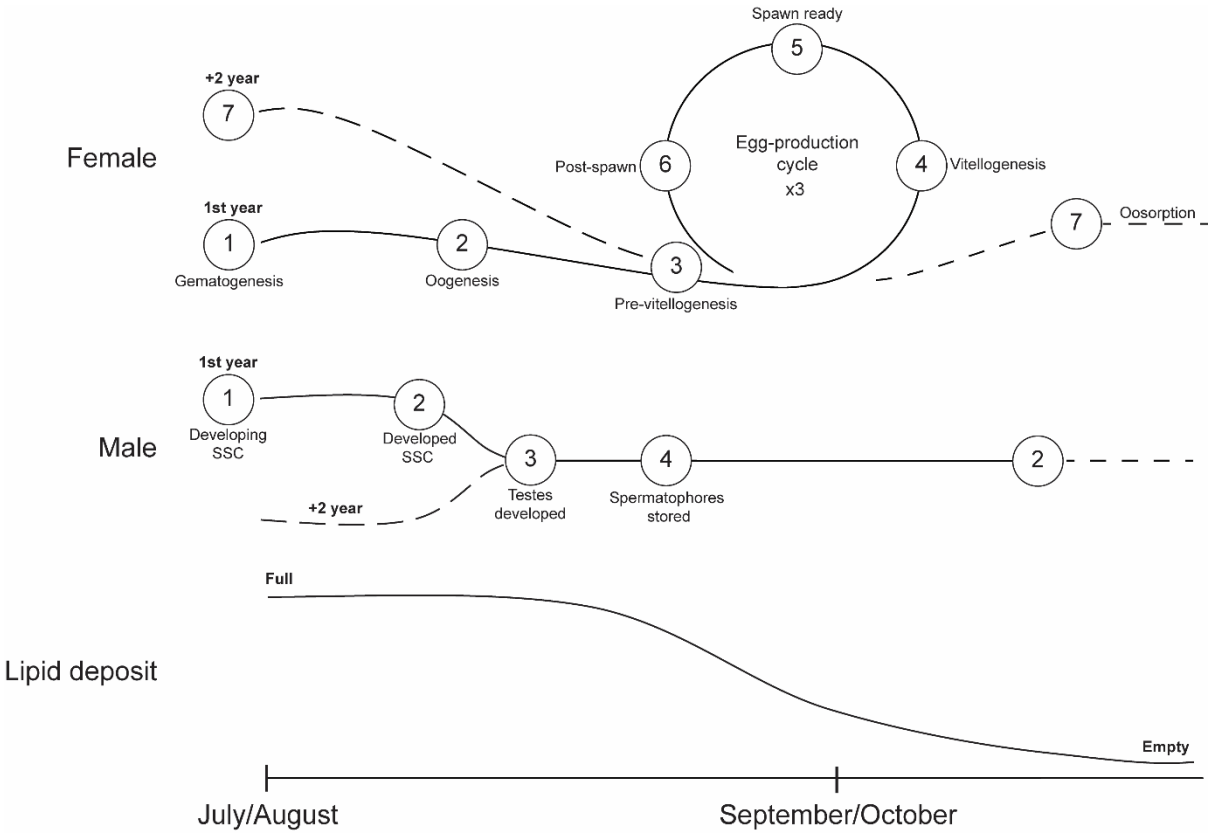

Figure 2.8. Seasonal cycle of sexual development and lipid content of male and female *T. macrura* in Antarctic waters. **Female** sexual development is conceptualised by successional sexual developmental stages (SDS), with the reproductive season begging with pre-vitellogenic females (SDS 3). Sub-adult females complete SDS 1 and 2 prior to commencing egg development, while females 2+ years beginning the cyclical process of egg batch development at SDS 3 (indicated by the dashed line). The cyclical process of egg batch development (SDS 4-6) occurs in late September with up to 3 egg batches produced in a reproductive period. Sexual development stages of **males** (SDSM) progress linearly, with SDSM 2 indicating they are ready to partake in copulation and reproduction, with fully developed secondary sexual characteristics (2°SC). 2+ year males therefore begin the reproductive period at SDSM 3, with both sub-adult males and 2+ year males reproductively ready (SDSM 4) prior to the production of egg batches by females, with spermatophores (sp) stored for copulation. Due to the seasonal regression of testes, males remain at SDSM 2 during the non-reproductive period (indicated by the dashed line). During the cycle of mating and egg production (late Sep-early Oct), the **lipid deposit** stored in the carapace of *T. macrura* rapidly decreases from occupying the total available space, fuelling egg and sperm production whilst also allowing the development of ovaries and testes within the carapace of females and males respectively.

2.5 Discussion

The patterns in ovarian development and organisation of developing oogonia and oocytes provide valuable insights into the reproductive strategies of *T. macrura* and confirm the presence of a winter-spring spawning period. The establishment of sexual developmental stages based upon underlying variations in gonad morphology during periods of reproductive activity provide a means of consistent and detailed analysis of a population's reproductive state. The cellular organisation and development of female ovaries examined in *T. macrura* are consistent with those reported for *E. superba* and *M. norvegica* (Cuzin-Roudy 1991; Cuzin-Roudy and Buchholz 1999). The development of oocytes in the ovaries of *Thysanoessa longicaudata* (Kroyer 1846), *T. inermis* (Kroyer,1846) and *T. raschi* (Sars 1864) has previously been used to map the development of ovaries, as females prepare for spawning based upon the relative size of developing oocytes (Mauchline 1968; Dalpadado and Skjoldal 1991). Whilst the five stages of development established previously closely resemble those described in our study, they are based upon the increase in size of maturing oocytes and the relative volume of the nucleus and not the physiological phase of development. Despite the overlap between the stages established by Mauchline (1968) for *Thysanoessa* spp., the presence of oogonia filled ovaries in sub-adult females (gametogenesis SDS 1) is unaccounted for. Furthermore, the use of these arbitrary stages of ovarian development do not include the potential for multiple spawning events within a single reproductive period (Kulka and Corey 1978; Dalpadado and Skjoldal 1991). Observations of ovarian re-organisation after a single spawning event in both *E. superba* and *M. norvegica* demonstrate the ability of euphausiids to incubate multiple egg batches in a single reproductive period (Cuzin-Roudy 2000). Developing sexual developmental stages based upon the cellular structure of ovaries and corresponding physiological phases of reproduction has demonstrated a similar pattern in reproductive strategies of *T. macrura* in the present study.

Developing oocytes within *T. macrura* ovaries are considerably larger than comparable oocyte stages of northern hemisphere *Thysanoessa* species (Mauchline 1968; Kulka and Corey 1978). Analysis of ovaries from our study show that the most mature oocytes (type 4) are up to 0.6 mm in diameter, almost double the 0.27-0.36 mm size range reported from studies for the congeners *T. inermis* and *T. raschi* (Mauchline 1968). Furthermore, the size of developing oocytes of *T. macrura* are equivalent in size to the larger Antarctic species, *E. superba*, despite *T. macrura* being only approximately half the total body length of E. superba (Cuzin-Roudy and Amsler 991). This disparity in the size of oocytes with northern hemisphere congeners suggests a relatively large maternal contribution to developing eggs from *T. macrura*, with the nauplii of both *T. macrura* and *E. superba* of comparable size (Kirkwood 1982). The potential fecundity of *T. macrura* reflects this, with a small batch size compared to the larger Antarctic species *E. superba* with the large oocytes of *T. macrura*

comparative to its body size occupying a greater proportion of ovarian space. Although ovarian counts likely overestimate the potential egg batch size, an average of 150 eggs per batch^{-1} is comparable to estimates of egg production rates based on bottle incubations for *T. inermis* (Mauchline 1968; Pinchuk and Hopcroft 2006). The presence of residual mature oocytes in post first spawn females (SDS 6) indicates that developing egg batches are released in small periodic spawning events, a feature that is commonly reported for euphausiids (Siegel 2000). When establishing allometric relationships to predict egg batch size based upon the morphometrics of ovarian wet weight, total body length and total wet weight of *T. macrura* in this study, these variables were only able to account for 17-20% of egg batch size. This is likely a result of the condition of females prior to the onset of the spawning season, with the condition of their lipid deposit influencing ovarian development and oocyte maturation in preparation for spawning. Despite this, egg batch size was best described by an allometric relationship with total wet weight for *T. macrura*, with strong agreement between predicted and recorded egg batch sizes. The average length of *T. macrura* in this study was 17.6 mm, considerably smaller than the maximum size of 40 mm reported by previous studies (Haraldsson and Siegel 2014). The size range of females present probably reflects a young population comprised of first and second year individuals (Haraldsson and Siegel 2014). Despite this, the smallest individual of 13 mm, which had fully developed ovaries, indicates that females can be reproductively active at one year of age; however, egg batch estimates of these females were low at only 20 eggs batch^{-1} compared to 747 eggs batch^{-1} for the largest female (25.7 mm).

Ovarian organisation after the first spawning event of *T. macrura* indicates the potential for up to two additional egg batches developing as primary oocytes and type 1 and 2 oocytes. The large lipid reserve of *T. macrura* is responsible for the winter-spring breeding period prior to an increase in oceanic productivity seen in spring. The presence of the large lipid deposit and its steady decline during ovarian development reflect the use of these reserves to fuel reproduction and support the development of successive egg batches during the spawning period. Analysis of the seasonal total lipid content of *T. macrura* shows them falling to their lowest during winter-spring (Hagen and Kattner 1998). The use of these large lipid reserves has previously been reported in *T. inermis* as a reservoir to initiate gonad maturation and an overwintering reserve (Buchholz et al. 2010). Whilst *T. inermis* requires periods of intense feeding to continue gonad development and spawning, it appears that the role of this lipid deposit in *T. macrura* is functionally different, and is used predominantly for reproduction by both males and females. The ability to produce up to three egg batches in a reproductive period provides an estimate of 420 eggs female^{-1} year^{-1} for a mean sized female in this study; however, larger females can produce over 2200 eggs year^{-1}, considerably more than estimates for *T. inermis* which release only one egg batch per year (Pinchuk and Hopcroft

2006). The small size range of females captured in the present study restricts our estimates of maximum fecundity of *T. macrura*. Using the largest *T. macrura* recorded by Haraldsson and Siegel (2014) at 40 mm body length, equating to 600 mg (total wet weight) by applying the allometric relationships established in this study, a maximum fecundity of over 22,000 eggs year^{-1} is predicted. This estimate therefore suggests a comparable fecundity to the largest age classes of *E. superba* (Cuzin-Roudy 2000).

This study demonstrates the use of gonad analysis in assessing and describing the reproductive pattern of the poorly understood Southern Ocean krill *T. macrura*. The cycle of ovarian development is consistent with the well-documented Antarctic species *E. superba*, with the timing of physiological changes in both males and females in preparation for reproduction supporting a winter-spring spawning period for *T. macrura*. The establishment of sexual developmental stages of both males and females provides a means for evaluating the reproductive status of populations consistently. We show that egg batch size scales allometrically with total wet weight, with the potential for up to 3 successive egg batches developed during a single spawning season providing fecundity estimates much greater than the northern hemisphere congener *T. inermis*. These primary estimates of *T. macrura* fecundity are restricted to the small size range of adults present in the population studied and require further investigations to fully assess the reproductive potential of this small Southern Ocean euphausiid.

Chapter 3

A description of the post-naupliar development of Southern Ocean krill (*Thysanoessa macrura*)

Close-up photograph of the head of a *Thysanoessa macrura* larvae (furcilia stage V)

Photograph by Jake Wallis

All the research presented in this chapter is published in Polar Biology

*Wallis JR (2018) A Description of the post-naupliar stages of Southern Ocean krill (*Thysanoessa macrura*). Polar Biol 41:2399-2407*

3.1 Abstract

Southern Ocean krill (*Thysanoessa macrura*) is one of the most abundant euphausiid species in the Southern Ocean. Despite a wide distribution and high abundance this species remains poorly understood. Unique ecological traits of this species, including a late-winter reproductive period, highly omnivorous diet and large lipid deposits within the carapace, suggest *T. macrura* is attuned to the seasonal patterns of the Southern Ocean. The absence of the descriptions of *T. macrura* larval stages limits the development of a comprehensive understanding of the early life-history of this species. Here I provide the first detailed descriptions of the post-naupliar larval developmental stages of *T. macrura* with accompanying photographic documentation. Three calyptopis and 6 furcilia stages were identified and described for *T. macrura*, providing an accessible guide for their identification in both historical samples and for future investigations.

3.2 Introduction

Southern Ocean krill, *Thysanoessa macrura* possess one of the largest latitudinal distributions of the mid-high latitude euphausiids in the Southern Hemisphere, with a range that extends from the Sub-Antarctic Front to the Antarctic continent (Cuzin-Roudy et al. 2014). Moreover, *T. macrura* is considered to be the second most abundant euphausiid in the Southern Ocean, with a more ubiquitous distribution than the dominant species, *Euphausia superba* (Nordhausen 1992; Haraldsson and Siegel 2014). Despite observations of physiological and ecological traits, including high, energy-dense lipid content and a broad omnivorous diet, the role of *T. macrura* in the Southern Ocean ecosystem is currently underappreciated due to a lack of targeted investigations of the species (Makarov 1979; Kattner et al. 1996). Late winter reproduction in *T. macrura*, confirmed in Chapter 2 of this thesis, makes this species the earliest known spawning euphausiid in the Southern Ocean.

A winter reproductive period limits the ability to observe the larval development of *T. macrura* due to the difficulties associated with sampling in southern, ice-covered regions during their reproductive period (Chapter 2). Consequently, there are few observations on the life-history of *T. macrura* and descriptions of their larvae are currently sparse and incomplete, leading to ambiguity in the identification of larval stages. *T. macrura* has been described as following a typical euphausiid development, with four distinct phases of development punctuated by 12 specific stages (Kirkwood 1982). Ontological development includes two nauplius, one metanauplius, 3 calyptopis (CI – CIII) and 6 furcilia stages (FI – FVI) (Makarov 1979). Similar to other Southern Ocean euphausiids, it is theorised that spawned eggs, due to their negative buoyancy, sink through the water column and hatch at depth. An ontogenetic ascent then occurs with calyptopis I, the first developmental stage with functional feeding appendages, appearing in surface waters (Makarov 1979). The wide

geographic range of *T. macrura* and the associated changes in their physical environment, chiefly temperature, likely causes regional variation in the timing and duration of larvae as seen in other polar euphausiid species (Ross et al. 1988).

This study provides descriptions of the post-naupliar stages of *T. macrura* to aid in identification of these larval stages, furthering the ability to fully understand the life-cycle of this dominant Southern Ocean euphausiid. Descriptions and accompanying photographic documentation of the key diagnostic features from calyptopis I to furcilia VI are provided.

3.3 Methods

Larval *T. macrura* were collected during summer (late January – mid February) in the Indian sector of the Southern Ocean. Sampling was conducted as part of the Kerguelen-Axis marine science voyage of the *RV Aurora Australis*. *T. macrura* larvae were collected by standard double oblique tows from the surface to 200 m using a Rectangular Midwater Trawl net (RMT) 8+1 configuration (Baker et al. 1973). The sampling region (61°S - 66°S, 115°E - 130°E) extended from the BANZARE Bank, located on the southern extent of the Kerguelen Plateau, to the Antarctic continent. It was flanked by the Davis Sea on the eastern side and the Cooperation Sea as the western extent, encompassing the Princess Elizabeth Trough. Larval *T. macrura* were isolated from the RMT 1 net (1 m^2 mouth area, 315 µm mesh size) and immediately stored in 10% buffered formalin solution.

T. macrura larvae were sorted according to gross morphological development. The general descriptions of larval development provided by Kirkwood (1982) were used to aid in the identification of the different stages of *T. macrura* larvae. Accordingly, morphological characteristics including size, appearance and number of limbs, eye morphology and rostrum shape were used to differentiate larval *T. macrura* from other euphausiid species (Kirkwood 1982). No naupliar stages were identified from net samples and therefore only post-naupliar stages were examined in this study. Nine post-naupliar stages were identified and examined using a Leica M205C microscope. The key morphological characteristics of each developmental stage, including eye morphology, body segmentation, the appearance and morphology of appendages and the appearance and number of spines on the posterior end of the telson, were recorded for each stage. Due to the lack of knowledge of the development of the closely related species, *Thysanoessa vicina* it should be noted that they may have been included in this study due to the inability to distinguish them from *T. macrura*. Fifty individuals of each stage were measured for their total length. Measuring was performed from the anterior end of the carapace, rounded in calyptopis stages and the tip of the rostrum in furcilia stages, to the base of the telson, not including their spines due to their fragility. Measuring was performed using a calibrated eye-piece micrometre and photographs of the key

diagnostic features of each larval stage taken using a Canon 6D camera integrated into the microscope. The possible effects of temperature on the size of larval stages was assessed by comparing 25 of each late furcilia stage (FIV – FVI) from north and south of the Southern Antarctic Circumpolar Current Front (SACCF).

3.4 Results

3.4.1 Calyptopis phase

The calyptopis phase of larval development includes 3 specific stages (Table 3.1). Calyptopis are distinguishable from nauplius and metanauplius stages (not documented) by a differentiated cephalothorax and abdomen. In calyptopis I, the cephalothorax is rounded in the dorsal view with a rounded rostrum and the abdomen is unsegmented (Fig. 3.1A). Developing eyes are visible beneath the carapace and are unpigmented. Rudimentary thoracic limbs are developing and protrude from beneath the carapace (Fig. 3.1A). The transition to calyptopis II is identified by the segmentation of the abdomen. Calyptopis II possess five abdominal segments, with the fifth segment not differentiated from the telson (Fig. 3.1B). Eyes remain enclosed within the carapace and have increased in size (Fig. 3.1C). The differentiation of the sixth abdominal segment is diagnostic of calyptopis III (Fig. 3.1D). Additionally, the abdomen elongated compared with the cephalothorax. Eyes of calyptopis III are more developed, with a crease indicating the constriction that forms the bilobed eyes characteristic of adult individuals (Fig. 3.1E)

.

Table 3.1. Key diagnostic features of each larval stage in the post-naupliar development of *Thysanoessa macrura*.

Developmental phase	Stage	Rostrum	Eyes	Abdominal segmentation	Pleopods	Telson Terminal spines	Telson Postero-lateral spines
Calyptopis	C I	Rounded	Rounded, visible through and enclosed by carapace. Pigment absent	No segmentation	Absent	7	3
	C II	Rounded	Rounded, visible through and enclosed by carapace. Pigment absent	5	Absent	7	3
	C III	Rounded	Rounded, visible through and enclosed by carapace. Pigment absent	6	Absent	7	3
Early furcilia	F I	Pointed, extending midway to eyes	Eyes rounded with pigment present in the centre. Eyes on stalks, protruding from beneath the carapace	6	Absent	7	3
	F II	Pointed, extending midway to eyes	Eyes visibly bilobed. Pigment present in the centre. Eyes on stalks, protruding from beneath the carapace	6	5 pairs, all without setae	7	3
	F III	Pointed, extending midway to eyes	Eyes visibly bilobed. Pigment prominent throughout. Eyes on stalks, protruding from beneath the carapace	6	5 pairs, all bearing setae	7	3
Late furcilia	F IV	Pointed, extending midway to eyes	Eyes visibly bilobed. Pigment prominent throughout. Eyes on stalks, protruding from beneath the carapace	6	5 pairs, all bearing setae and well developed	5	3
	F V	Pointed, extending midway to eyes	Eyes visibly bilobed. Pigment prominent throughout. Eyes on stalks, protruding from beneath the carapace	6	5 pairs, all bearing setae and well developed	3	3
	F VI	Pointed, extending midway to eyes	Eyes visibly bilobed. Pigment prominent throughout. Eyes on stalks, protruding from beneath the carapace	6	5 pairs, all bearing setae and well developed	1	2

Figure 3.1. Calyptopis stages of *Thysanoessa macrura*. **A.** lateral view of Calyptopis I with distinct non-segmented abdomen and cephalothorax with developing thoracic limbs. **B**. Calyptopis II with 5 abdominal segments. **C.** Calyptopis II dorsal view with rudimentary eyes visible through the carapace. **D**. Calyptopis III with 6th abdominal segment differentiated from the telson. **E**. Developing eyes of calyptopis III indicating the crease which will latter develop into the eye constriction forming bilobed eyes.

3.4.2 Furcilia Phase

The furcilia phase of larval development consists of 6 specific stages and is differentiated from the calyptopis phase by the emergence of eyes on mobile stalks from beneath the carapace, further development of thoracic appendages and mouthparts and the development of a pointed rostrum (Table 3.1). The development from furcilia I to furcilia VI can be further separated into early (furcilia I – III) and late (furcilia IV –VI) stages based upon the appearance of pleopods on the abdomen and their setation and the number of spines on the telson.

3.4.3 Early Furcilia

The most notable morphological changes occur during the early furcilia stages (Table 3.1). Furcilia I possess no pleopods on their abdomen and have a prominent pointed rostrum (Fig. 3.2A). The eyes of furcilia I are the first stage to develop mobile eye stalks, protruding the eyes from beneath the carapace (Fig. 3.2B). Further, the eyes have begun to develop the complexity as seen in adults, with pigmentation evident within the centre of the eyes. The telson of furcilia I possess 7 terminal spines, all with small spinules on both margins and three pairs of postero-lateral spines (Fig. 3.2C). The postero-lateral spines increase in size from 1-3 (anterior to posterior), with the second and third pair having spinules on their inner margins.

By furcilia II, the eyes have become characteristically bilobed in shape, however the transverse constriction between lobes is inconspicuous (Fig. 3.3A). The eyes are fully pigmented and the compound structure of the eyes is evident (Fig. 3.3B). The abdomen bears five pairs of pleopods, none of which are setose (Fig. 3.3C). The structure of the telson remains unchanged with 7 terminal spines all bearing spinules and three pairs of postero-lateral spines, with the second and third postero-lateral spines with spinules on their inner margins (Fig. 3.3D).

Furcilia III closely resemble the furcilia II stage (Fig. 3.4A). However, pleopods are evident and have developed setae, with all five pairs setose at their tips (Fig. 3.4B). The arrangement of spines on the distal border of the telson remains consistent with the earlier furcilia stages (Fig. 3.4C). Prior to moulting into Furcilia IV, the 5 developing terminal spines of the telson are visible on the new cuticle (Fig. 3.4C).

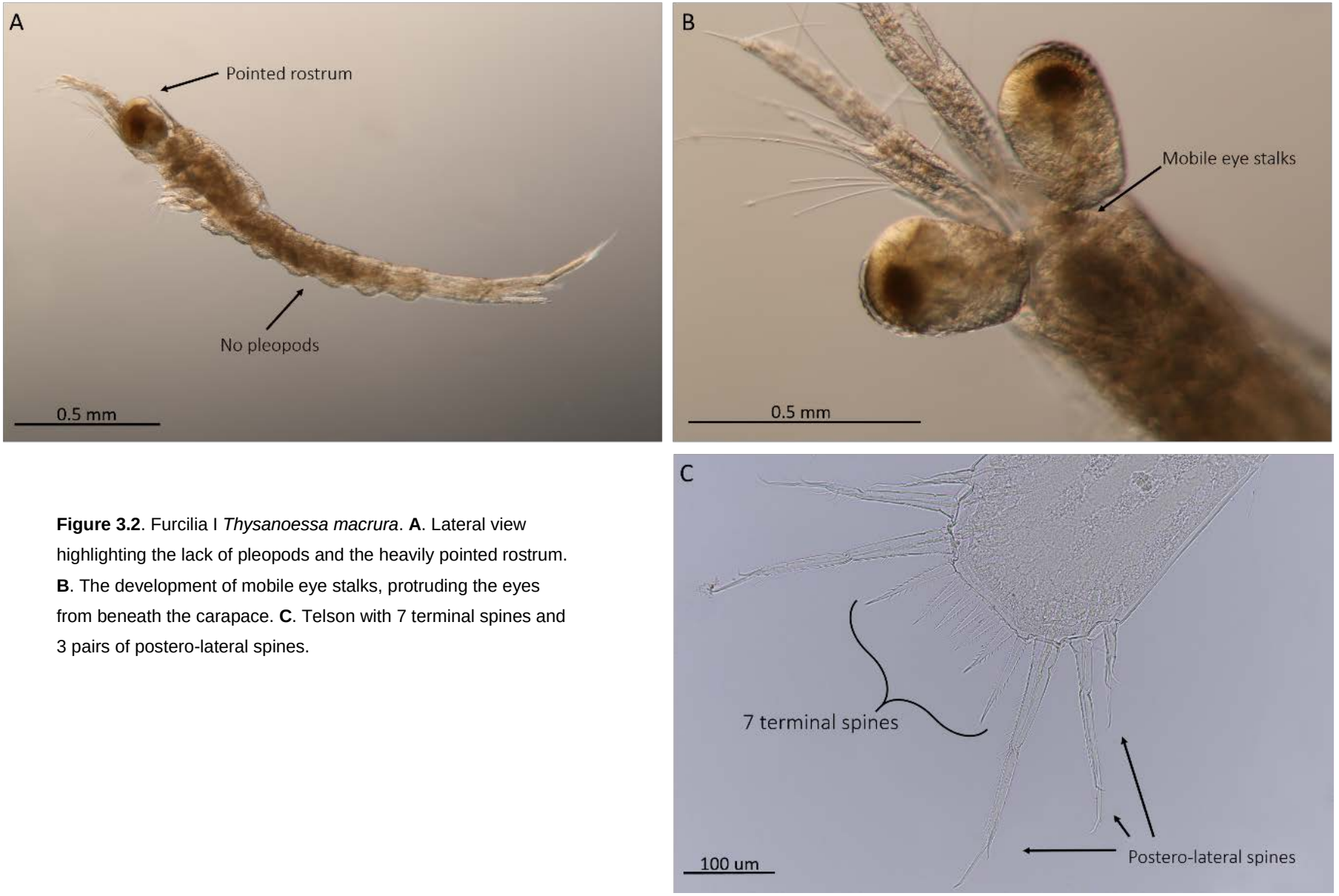

Figure 3.2. Furcilia I *Thysanoessa macrura*. **A**. Lateral view highlighting the lack of pleopods and the heavily pointed rostrum. **B**. The development of mobile eye stalks, protruding the eyes from beneath the carapace. **C**. Telson with 7 terminal spines and 3 pairs of postero-lateral spines.

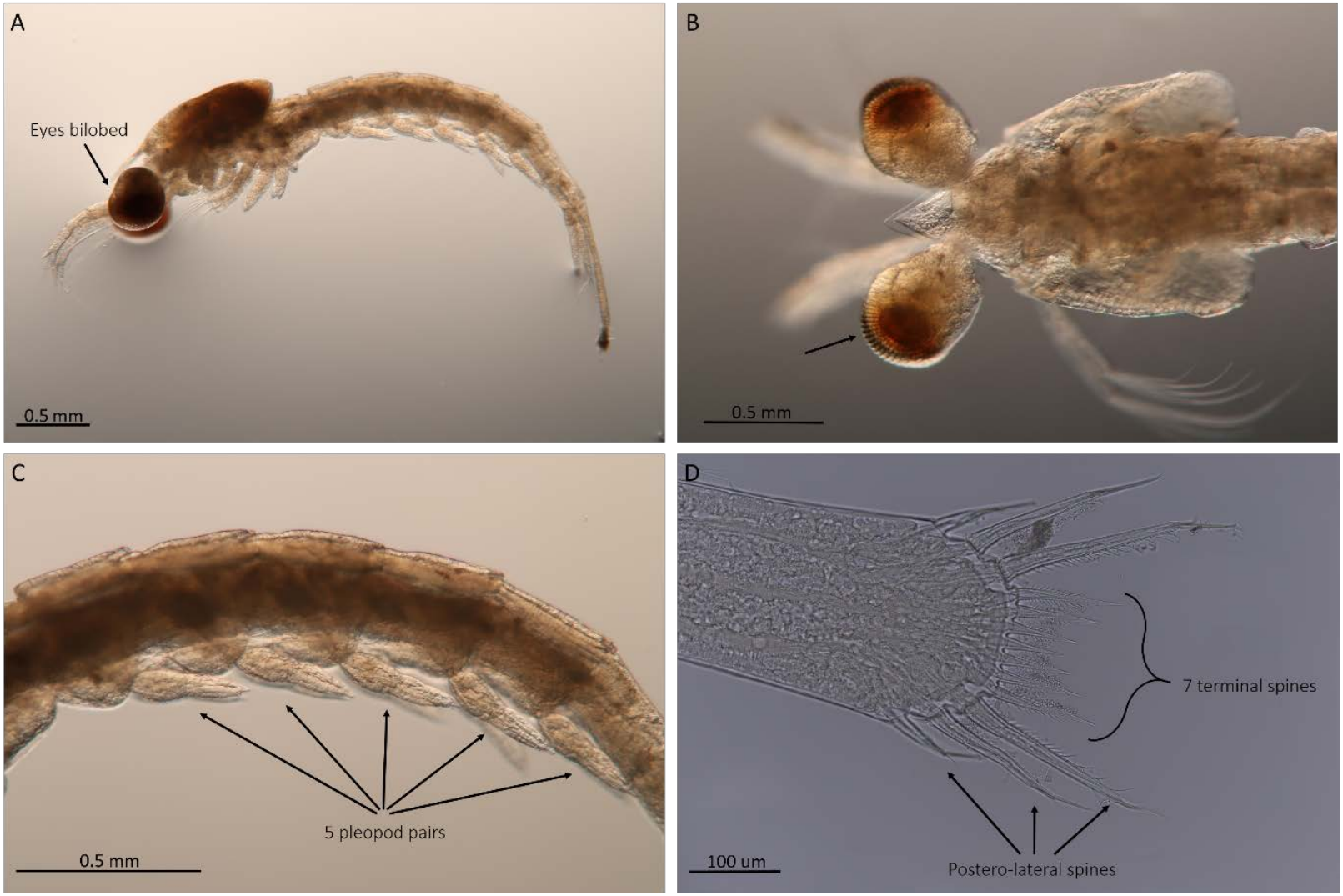

Figure 3.3. Furcilia II *Thysanoessa macrura*. **A**. Lateral view with clearly bilobed eyes. **B**. Dorsal view indicating the development of cones of the eyes. **C**. Abdomen bearing 5 pairs of non-setose pleopods. **D**. Telson bearing 7 terminal spines and 3 pairs of postero-lateral spines.

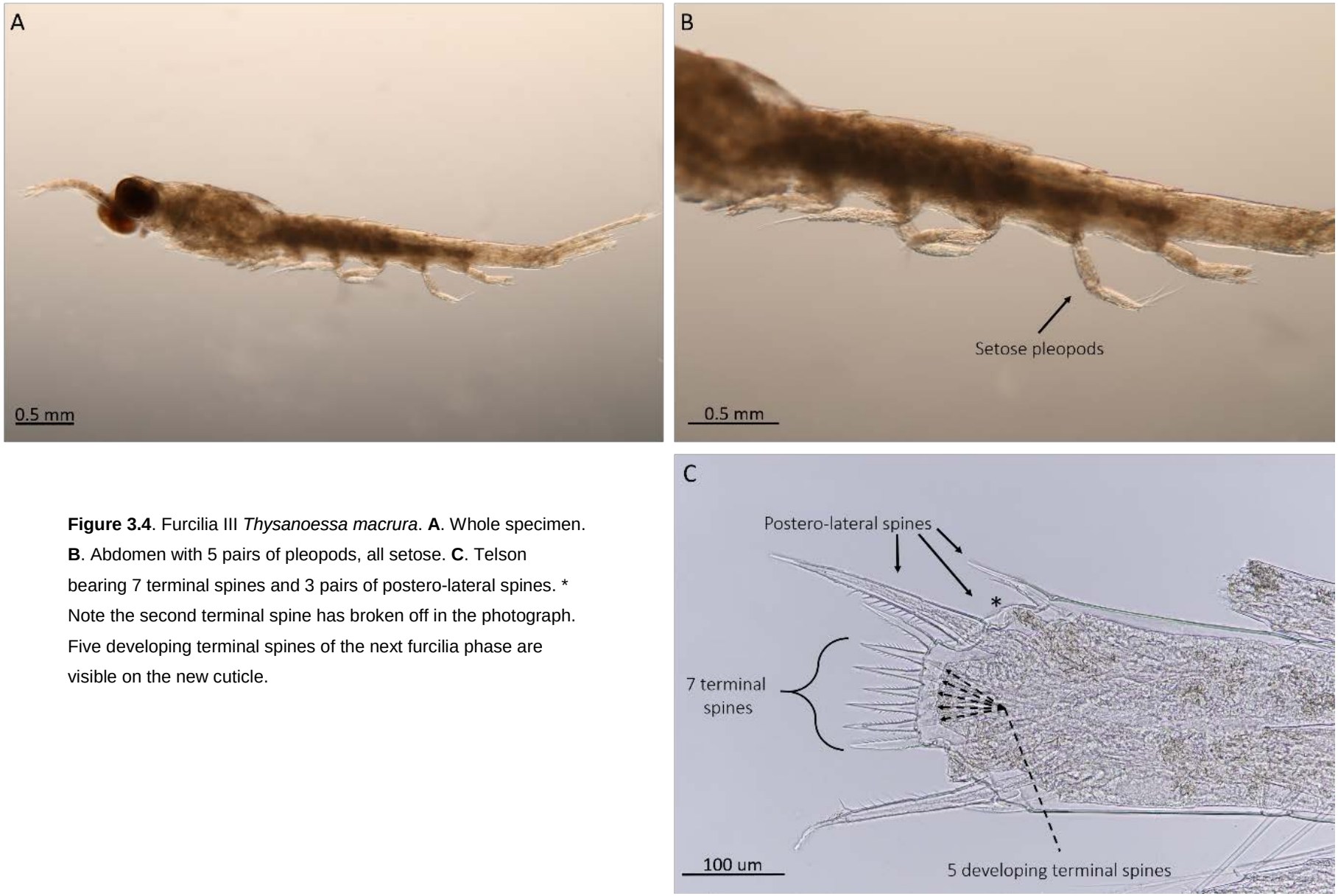

Figure 3.4. Furcilia III *Thysanoessa macrura*. **A**. Whole specimen. **B**. Abdomen with 5 pairs of pleopods, all setose. **C**. Telson bearing 7 terminal spines and 3 pairs of postero-lateral spines. * Note the second terminal spine has broken off in the photograph. Five developing terminal spines of the next furcilia phase are visible on the new cuticle.

3.4.4 Late Furcilia

Later furcilia stages begin to resemble juveniles in their appearance and are differentiated from each other chiefly by changes in the number of terminal and postero-lateral spines on the posterior end of the telson (Table 3.1). Furcilia IV, shown in Fig. 3.5A possesses five terminal spines on the telson, all of which have spinules on both their inner and outer margins (Fig. 3.5B). Developing terminal spines on the telson of Furcilia V are visible on the new cuticle (Fig. 3.5B).

Furcilia V have fully developed mouthparts and thoracic appendages used for filter feeding (Fig. 3.5C). The number of terminal spines on the telson is reduced to three, with the centre spine having lost all spinules (Fig. 3.5D). Furcilia V retain three pairs of postero-lateral spines, however the third pair have enlarged to approximately three times the length of the second pair, with spinules only present on the distal region of the inner margins (Fig. 3.5D). By furcilia VI individuals resemble juveniles (Fig. 3.5E). There is only one smooth terminal spine on the telson, and two pairs of poster-lateral spines (Fig. 3.5F).

3.4.5 Latitudinal variation in larval development

The larval size of *T. macrura* varied at each stage of development and showed considerable overlap between each stage (Table 3.2). Despite overlapping size, the mean size increased between each stage of development from 1.4 mm for calyptopis I to 6.3 mm at furcilia VI. There was no substantial increase in larval size between the calyptopis and furcilia phases of development, with the largest difference in mean size recorded between calyptopis I and II (Table 3.2).

Temperature data collected by CTD deployments from sites from which larvae were assessed indicate a temperature difference of 3.4°C based upon minimum temperatures recorded in the upper 50m in each region (data not shown). Larvae north of the SACCF were collected from waters with a mean temperature of 1.8°C and south of the SACCF, -1.6°C. Despite a considerable difference in temperature between these two sub-regions of the sampling area no significant difference in size of late furcilia stages were evident from individuals found north and south of the SACCF. Each of the three late furcilia stages however displayed a large spread in size regardless of location (Fig. 3.6).

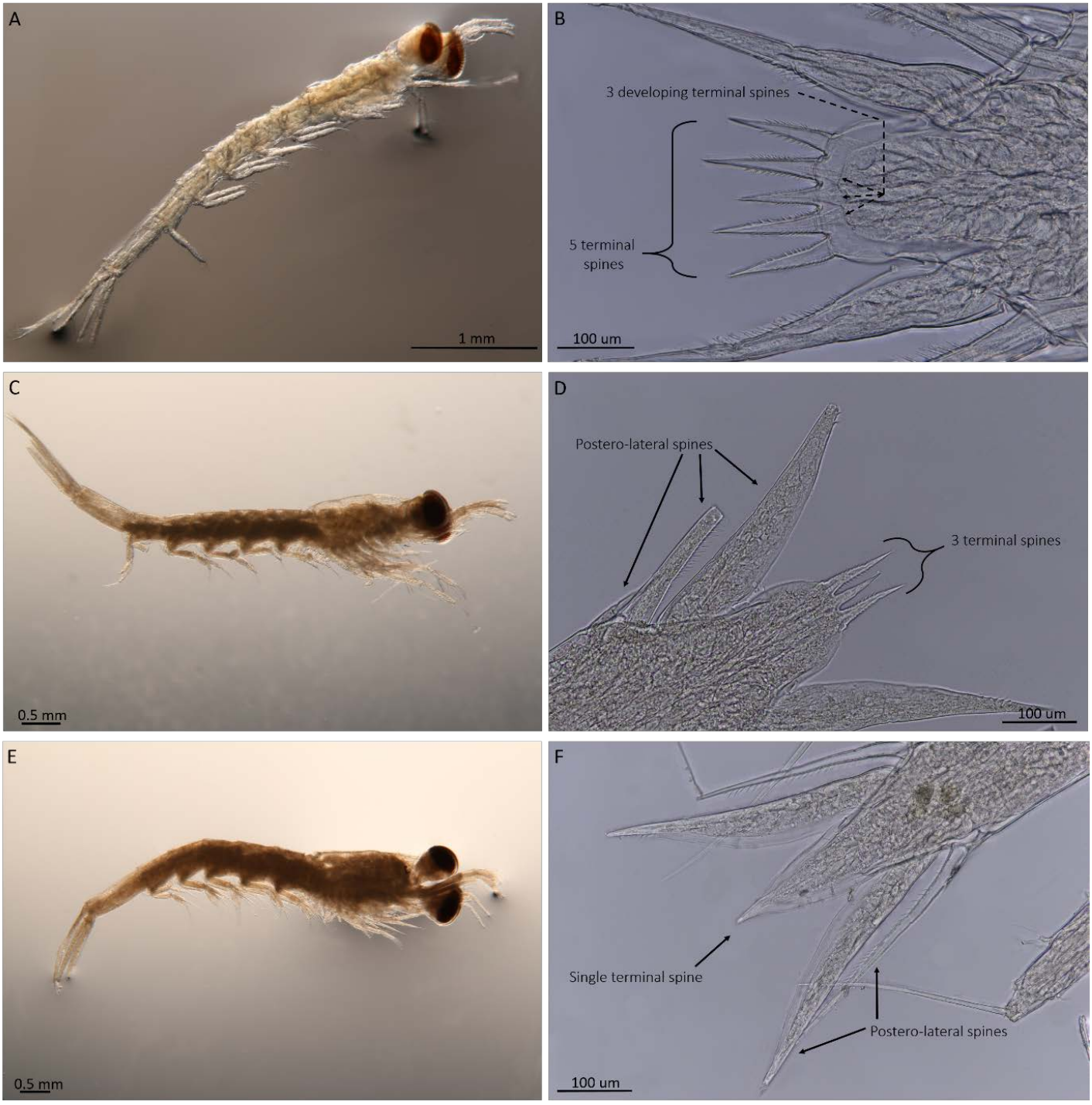

Figure 3.5. Late Furcilia (F IV- VI) *Thysanoessa macrura*. **A**. Furcilia IV whole specimen. **B**. Furcilia IV Telson with 5 terminal spines. Three developing terminal spines of the next furcilia phase are visible on the new cuticle. **C**. Furcilia V whole specimen. **D**. Furcilia V Telson with 3 terminal spines and 3 pairs of postero-lateral spines. **E**. Furcilia VI whole specimen. **F**. Furcilia VI Telson with 1 terminal spine and 2 pairs of postero-lateral spines.

Table 3.2. Size (mean and range) of the different larval stages in the post-naupliar development of *Thysanoessa macrura* including a graphic of the size distribution overlap of the 9 specific stages. N= 50 individuals for all developmental stages.

Development stage	Size mean (mm)	Size range (mm)	Size distribution
Calyptopis I	1.4	1 - 2.2	
Calyptopis II	2.4	1.5 - 3.5	
Calyptopis III	3.0	2 - 4.1	
Furcilia I	3.3	2.4 - 3.9	
Furcilia II	3.9	3.1 - 5.1	
Furcilia III	4.5	3.4 - 5.6	
Furcilia IV	5.2	1 - 5.8	
Furcilia VI	5.4	4.4 - 6.2	
Furcilia VI	6.3	5.4 - 7.8	

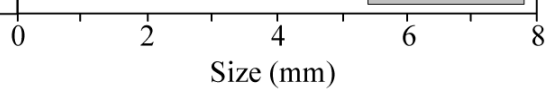

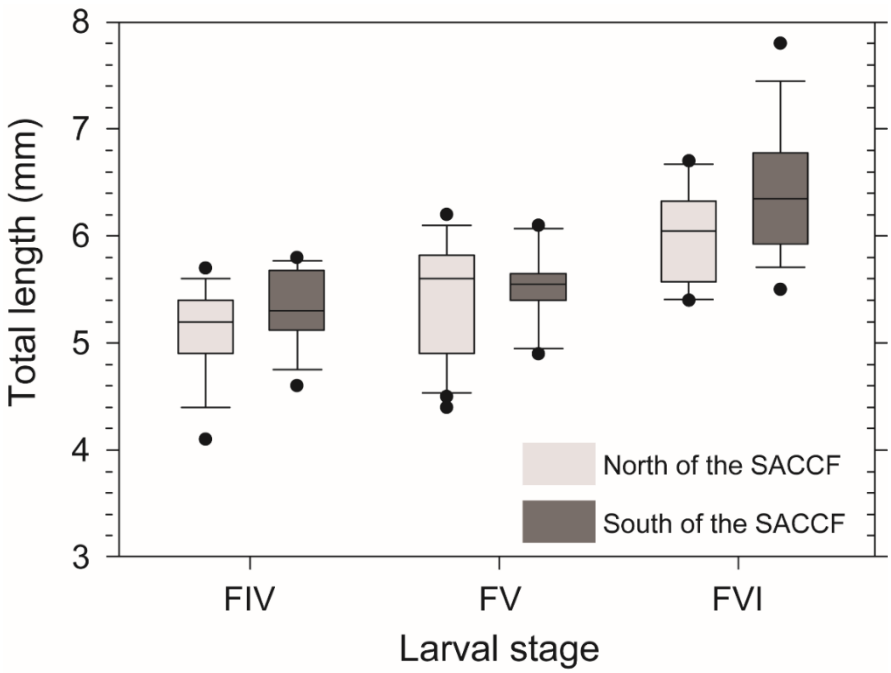

Figure 3.6. Size distribution of late furcilia stages of *Thysanoessa macrura* from north and south of the Southern Antarctic Circumpolar Current Front (SACCF) representing a 3.4°C difference in temperature. N = 25 for each group.

3.5 Discussion

The post-naupliar larval development of *T. macrura* is consistent with other euphausiid species in the Southern Ocean. The nine specific stages described (3 calyptopis and 6 furcilia) show a progressive development in morphology that easily allows for the differentiation of each stage. The ability to identify the larval stages of *T. macrura* and distinguish them from other euphausiid species with overlapping distributions is vital for improving the descriptions of the early-life cycle of this species. Despite being the earliest spawning euphausiid in the Southern Ocean, the extended reproductive period of *T. macrura* via multiple spawning events, as described in Chapter 2, inevitably leads to the overlap in occurrence of larvae with other Southern Ocean euphausiids, including *Euphausia superba*, *Euphausia crystallorophias*, *Euphausia frigida*, *Euphausia triacantha*, *Euphausia vallentini* and *T. vicina* due to their overlapping distributions (Cuzin-Roudy et al. 2014). Due to the hatching of *T. macrura* eggs at depths below 500 m, deeper than routinely sampled in the Southern Ocean, naupliar stages were not collected during sampling of this study and therefore could not be described (Makarov 1979). The ability to readily identify the post-naupliar larval stages of *T. macrura* is important in establishing a comprehensive understanding of the early-life cycle for this species.

The key diagnostic features of *T. macrura* developmental stages described here are commonly used in the identification of larval stages of the dominant euphausiids (Jia et al. 2014). *T. macrura* larvae are relatively robust and remain intact when sampled with large nets. The key features used to separate the different stages of each developmental phase are easily identifiable with microscopic examination. The spines used on the posterior end of the telson (terminal and postero-lateral) are the most likely feature to break or become damaged during sampling and/or preservation. These features however are vital for the identification of late furcilia stages, with the reduction in the number of terminal spines with successive development of furcilia stages a key identifier used for all euphausiid species. I found that the points of attachment of both the terminal and postero-lateral spines remain identifiable on the telson, appearing as a pocket in the cuticle. In conjunction with the other described diagnostic features of later stage furcilia, larval specimens are still readily identifiable. Furthermore, the developing terminal spines of the successive larval developmental stages are visible developing with the new cuticle, aiding with the identification of furcilia stages.

A comparison with congener species in the northern hemisphere, particularly *Thysanoessa raschii* and *Thysanoessa longipes*, reveals strikingly different larval development pathways. Whilst all three species have three stages within the calyptopis phase of larval development, *T. raschii* and *T. longipes* have been documented to have 11 and 9 furcilia stages, respectively (Mauchline 1965; Endo and Komaki 1979). These differences among the number of developmental stages identified for *T. macrura* and its congeners are attributable to the common occurrence of indirect development

observed in the northern *Thysanoessa* species (Mauchline 1965; Endo and Komaki 1979). Variations in instar morphology, the interval between successive moults within a larval stage have been recorded separately for these northern species. Such indirect larval development, influenced by temperature and food quality and availability is common among oceanic euphausiids (Feinberg et al. 2006). No indirect larval development was identified for *T. macrura* in this study, however I cannot preclude its existence due to the limited geographic range of sampling. Additionally, the identification of developing telson terminal spines within the new cuticle of furcilia that correspond to the spine arrangement of the next developmental stage suggests intermediate instars are not common for *T. macrura*.

The influence of different water mass temperatures for larvae measured north and south of the SACCF showed no difference in the overall size of *T. macrura* larvae. Despite expecting lower growth rates in cooler waters south of the SACCF, corresponding to larger larvae, no size differences were identified (Ross et al. 1988). It is relatively common under poor conditions, i.e. food limitation, for larvae to remain at a single stage for an extended time, moulting without further ontogenetic development (Feinberg et al. 2006). This lack of progression in development was not identified for any individuals of all stages, with the terminal spine arrangement of the next developmental stage identifiable within the new cuticle. This suggests that *T. macrura* larvae capitalise on the increase of primary productivity during spring, when they reach surface waters where food availability is likely to be a more important driver of larval growth and development than temperature.

T. macrura remains an enigmatic species within the Southern Ocean. The ability to successfully identify the different stages of larval development and differentiate them from other species with overlapping distributions will facilitate further studies to describe the early life-cycle of *T. macrura* and provide a context for the life-history of this abundant Southern Ocean euphausiid.

Chapter 4

Diet of *Thysanoessa macrura* in the Kerguelen region, with emphasis on carnivory and ontogenetic shifts

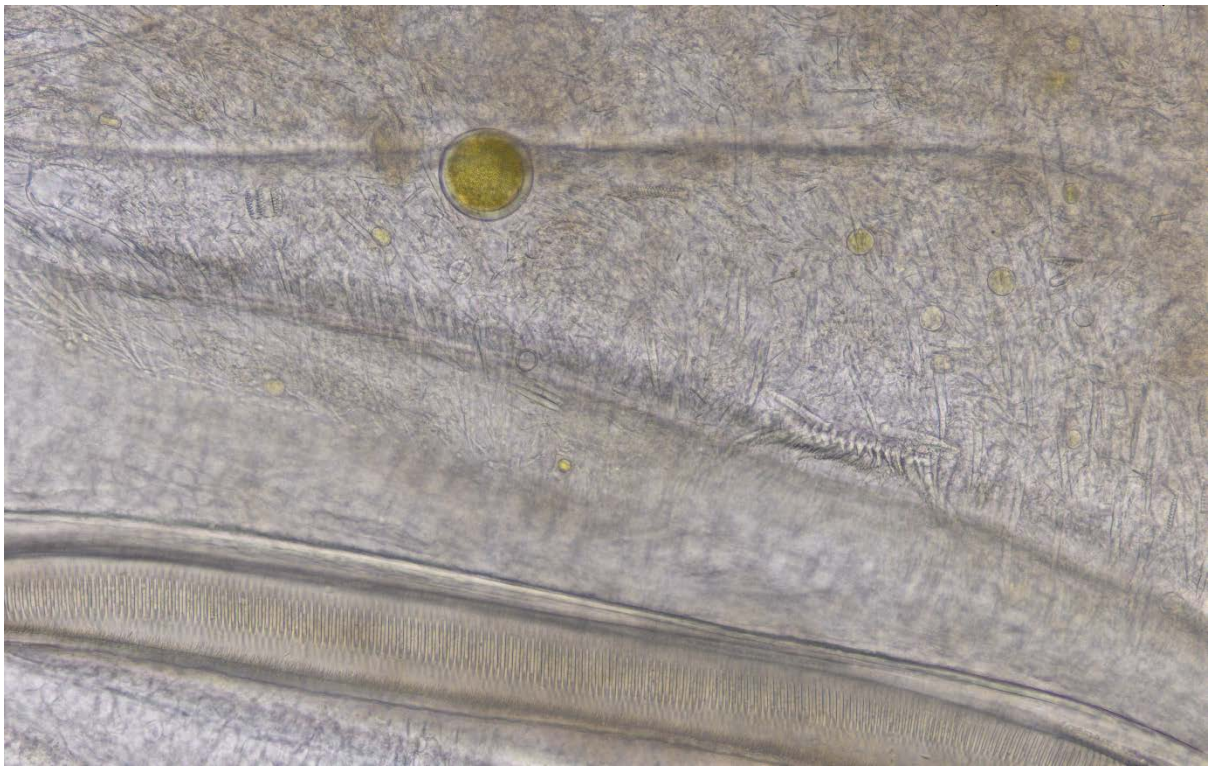

Microscopic image of the foregut of *Thysanoessa macrura* showing the intricate components of the gastric mill used to grind food particles within the stomach

Photograph by Jake Wallis

4.1 Abstract

Thysanoessa macrura are an omnivorous species, readily consuming a large range of food items including phytoplankton, protozoans and metazoans. The assumption of this broad, flexible diet is based on morphological characteristics of feeding appendages, primarily an elongated second thoracopod, and a few studies that analysed gut contents and lipid biomarkers. Although the methods used to assess the diet of *T. macrura* have confirmed an omnivorous diet, with predation on copepods the most significant component of metazaon feeding, there is a lack of quantitative information about the diets of *T. macrura*. Furthermore, a lack of little information on the feeding of *T. macrura* larval stages (calyptopis – furcilia) represents a critical gap in understanding of the life-history and feeding ecology of *T. macrura*. The work in this Chapter incorporated mouthpart and feeding appendage morphometrics, microscopic analysis of gut contents and lipid biomarkers, and represents the most detailed analysis of the diet of adult *T. macrura* at the population scale, over the southern Kerguelen Plateau region. Due to the fragile nature of larvae, dietary information is based upon mouthpart morphometrics and the identification of silicified organisms only, with acid digestions used to removed body tissues. For adults, the level of carnivory was variable and generally accounted for 30% of the diet of individuals based upon carbon contribution. Cluster analysis revealed spatial variability in the diet of adults, with those in the north of the study region more reliant upon carnivorous feeding, and those in the south consuming more phytoplankton, corresponding to increased primary production in the south. Phytoplankton was readily grazed by adults across the study region, with mainly diatoms identified, reflecting the available phytoplankton standing stock. This unselective phytoplankton grazing was countered with positive selection for the copepod *Calanoides acutus*, identified by mandibles in the guts of *T. macrura*. Analysis of lipid biomarkers confirmed the importance of carnivory in the diet of *T. macrura*, especially *C. acutus,* highlighting the close relationship between these two crustaceans. The presence of diatoms and the characteristics of the mandibles, maxillae and maxillules of larval stages confirmed herbivorous feeding on phytoplankton, with the capacity to effectively clear particles as small as 2 µm.

4.2 Introduction

In the Southern Ocean, euphausiids play an important and dominant role in linking lower trophic levels with large vertebrate predators, primarily fish, seals, birds and whales. Despite their influence on higher trophic levels, understanding the connections between euphausiids and primary producers and consumers is largely restricted to the dominant Antarctic krill *Euphausia superba*. Although *E. superba* is valued as a keystone species, a shift to understanding the role of other dominant Southern Ocean euphausiids is underway. *Thysanoessa macrura* is at the forefront of this effort due to its high abundance and wide latitudinal distribution from the sub-Antarctic to the

Antarctic continent. Although abundances of *T. macrura* are known to exceed those of *E. superba* in regions including Prydz Bay, the Bransfield Strait and lower latitude waters of the Antarctic (Makarov 1979; Hosie 1991; Nordhausen 1992), descriptions of their role in connecting lower trophic levels with vertebrate predators are largely cursory. Compared to the diet of *E. superba*, which has been thoroughly investigated using DNA analysis, microscopic gut examination, lipid profiles and stable isotope analysis, indicating a largely herbivorous diet with opportunistic carnivorous feeding (Schmidt and Atkinson 2016), the dietary preference of *T. macrura* is relatively poorly described. Despite descriptions of an omnivorous diet, the lack of detailed analysis makes understanding the role of diet in facilitating the life history of *T. macrura*, including a winter reproductive period, rapid lipid accumulation during summer and growth and development of larval stages, difficult. Furthermore, the lack of quantitative information on dietary preferences, and their variation over space and time, makes incorporating the role of *T. macrura* in a broader ecosystem framework difficult.

A largely omnivorous diet of *T. macrura* has been indicated by microscopic analysis of gut contents and the presence of lipid biomarkers assessed during lipid analysis. Despite these multiple lines of evidence that support an omnivorous feeding mode, there is a general lack of quantitative information on the dietary components of *T. macrura*. Microscopic analysis of the guts of *T. macrura* in western Antarctica indicates a high level of carnivory, with copepods the most important dietary components (Hopkins 1985; Hopkins and Torres 1989). Although diatoms were consistently identified, they were found to contribute a small proportion to the diet of *T. macrura* during these ecosystem-based studies, with copepods, particularly *C. acutus* and *Metridia gerlachei*, comprising up to 80% of their diet in the western Weddell Sea and Crocker Passage in the Antarctic Peninsular region (Hopkins and Torres 1989). The results of these studies, however, lack precision in the identification of phytoplankton prey sources and provide only a semiquantitative analysis that inhibits the ability to identify spatial variation in diet. Furthermore, sexual differences in diet are not explored.

Thysanoessa macrura demonstrate a seasonal pattern in lipid accumulation. Lipid reserves that are acquired during summer and autumn, reaching up to 56% of dry weight and stored mainly as wax esters, are used to fuel a winter reproductive period before falling to their lowest values during spring (Hagen and Kattner 1998; Chapter 2). A rapid accumulation of lipids during summer would indicate a period of intense feeding on energy-rich food sources during this short season. Faster accumulation of lipids by females compared to males would also seem to suggest sexual differentiation in feeding behaviour (Mayzaud et al. 2003), although this has not yet been proven. Analysis of the lipid stored by *T. macrura* can also provide evidence of the feeding strategy through

the identification of biomarkers. Although lipid analysis is not able to provide detailed information on the species-specific dietary components of *T. macrura*, it can provide broad information about the relative importance of phytoplankton and metazoan-derived prey based upon ratios of the dominant fatty acids. Accordingly, carnivory has been identified as more important than herbivory based upon high levels of fatty acids derived from metazoans (Hagen and Kattner 1998; Falk-Petersen et al. 2000). *Calanoides acutus* has been identified as an important prey item for *T. macrura* due to the high proportion of the alcohol 20:1(*n*-9) present, which is a unique and important contributor to the wax esters created by *T. macrura* (Hagen and Kattner 1998).

Thysanoessa macrura has modified and elongated second thoracopods that are thought to assist in the capture of large metazoans such as copepods (Fäber-Lorda and Mayzaud 2010). Modifications and adaptations to feeding appendages, including the mandibles, maxillules and maxilla, in addition to internal structures of the digestive tract, facilitate an omnivorous diet (Mauchline 1967: Suh 1996). Along with carnivory, feeding experiments have highlighted the efficient capture of protozoans by *T. macrura* (Froneman et al. 1996).

Although general dietary trends have been identified for adults, the diet of larval *T. macrura* remains largely unknown. Calyptopis I is the first stage with sufficiently developed mouthparts to facilitate feeding, appearing in surface waters after an ontogenetic ascent during the onset of spring (Makarov 1979; Nordhausen 1992). Unlike adults, euphausiid larvae have little lipid reserves and are only able to survive short periods of feeding inactivity, requiring continuous feeding for survival, growth and further development (Meyer et al. 2002). Given that the development of mouthparts is relatively rudimentary and only supports filter feeding, it is assumed that larval *T. macrura* ingest a similar diatom-based diet to that recorded for *E. superba* larvae (Marschall 1985).

This Chapter aims to provide a comprehensive and detailed analysis of the diet of *T. macrura*, incorporating information gained form mouthpart morphology, microscopic analysis of gut contents and lipid analysis in the highly productive southern Kerguelen Plateau region. The diet of larval stages is explored for the first time, enabling the assessment of ontogenetic shifts in feeding abilities and diet.

4.3 Methods

Thysanoessa macrura were collected during the Kerguelen Axis voyage between late January and mid-February over the Southern Kerguelen Plateau region (Figure 4.1a). The study region was predominantly situated over the BANZARE Bank, extending into the Princess Elizabeth Trough to the south and the Weddell-Enderby Basin to the west. Three major oceanographic features punctuated

the region: the Antarctic Slope current front, the Southern Boundary of the Antarctic Circumpolar Current Front and the Southern Antarctic Circumpolar Current Front (Figure 4.1b).

A Rectangular Midwater Trawl (RMT) 8+1 configuration (Baker *et al.* 1973), equipped with a flow meter, was used to sample post-naupliar larval stages and adult *T. macrura*. Sampling was performed by standard double oblique trawls from the surface to 200 m, with adult *T. macrura* collected from RMT 8 samples (8 m^2 mouth area, 4.5 mm mesh size) and larvae from the RMT 1 (1 m^2 mouth area, 315 µm mesh size). Additional target trawls (T1 and T10) were also performed for regions of interest, identified by the ship's echosounder. The RMT was deployed to the depth of interest with trawling lasting 5-7 minutes. After collection, RMT 8 samples were sieved immediately and, if the sample volume exceeded 1 L of 'wet sample', the total sample was split volumetrically, and a subsample taken. When subsampling was performed *T. macrura* was removed from the remaining sample and immediately frozen at -80 °C. RMT 1 samples were subsequently fractionated onboard after collection using a Motoda Box plankton splitter (Motoda 1959). Both the RMT 8 samples (or subsamples) and RMT 1 samples were preserved in 10% buffered formalin.

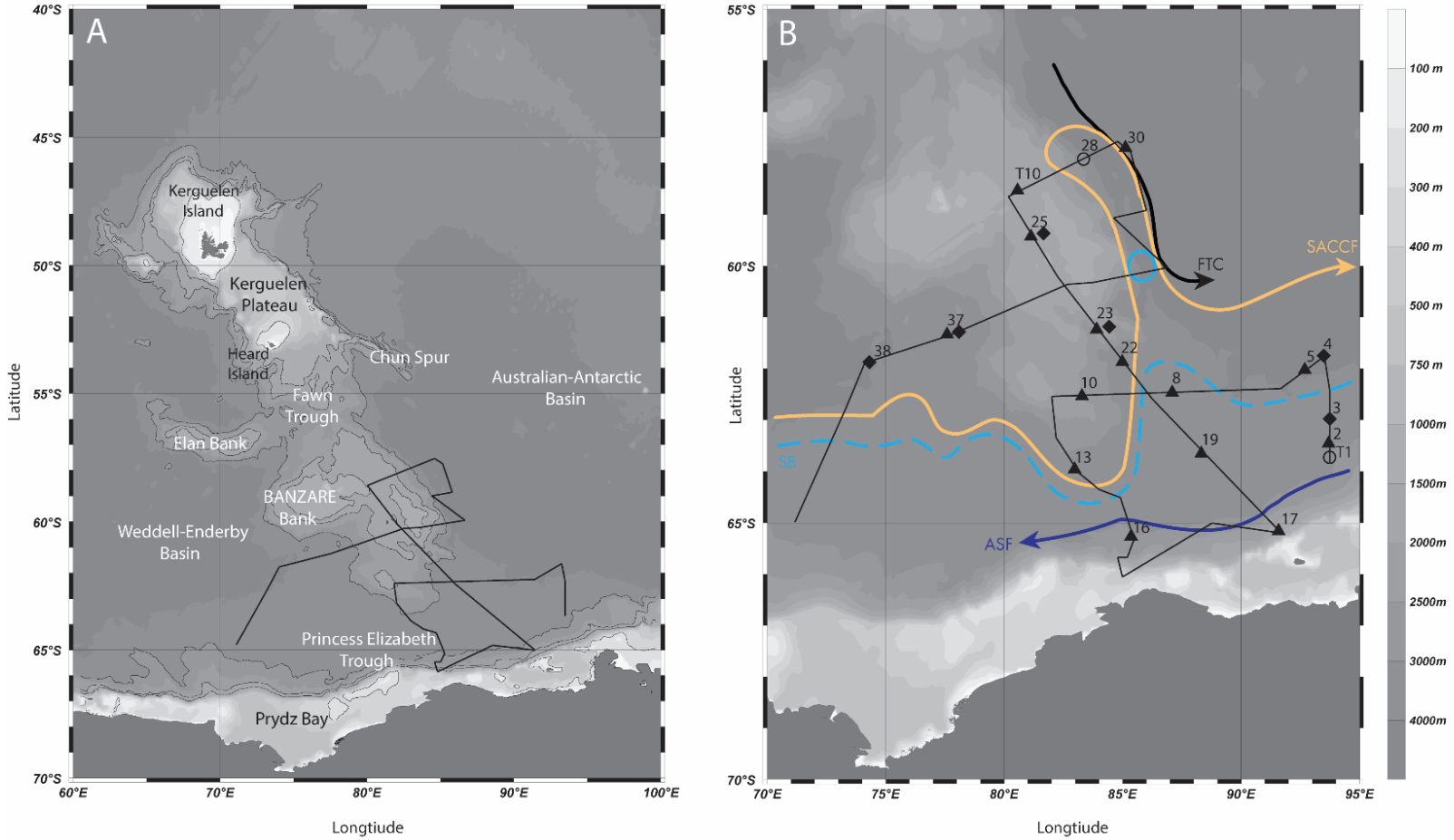

Figure 4.1. Sampling region on the Southern extent of the Kerguelen Plateau. **A**. Large scale map highlighting the voyage track undertaken during sampling. The major regions are identified. The bathymetric contours indicate 300 m, 1500 m and 2000 m **B**. Sampling sites used to assess the diet of *T. macrura*. The major oceanographic features of the region are highlighted, including the Fawn Trough Current (FTC), the Southern Antarctic Circumpolar Current Front (SACCF), Southern Boundary of the Antarctic Circumpolar Current (SB) and the Antarctic Slope Front (ASF). Filled triangles indicate sites where gut contents analysis on adults was performed, filled diamonds indicate larval analysis and open circles show lipid analysis.

4.3.1 Microscopic analysis of krill guts

4.3.1.1 Adults

A total of 161 adults, including 112 females and 49 males across 13 sites, was used to examine gut contents via microscopy of *T. macrura* in the study region (Figure 4.1b). Prior to dissection, sex and total length, in mm, from the tip of the rostrum to the base of the sixth abdominal segment (standard measurement 2; Mauchline 1981) were recorded. Adult krill were then dissected, and the entire length of the gut removed. Gut sections were mounted on slides and analysed using a Nikon Eclipse Ci-L compound microscope equipped with a camera. Each region of the gut (fore-, mid- and hindgut) was photographed under low magnification (10x) and a 500 μm^2 grid overlayed on the photos, using the analytical photography software package NIS Elements (Nikon Instruments, NY, USA), to assess total surface area. Guts were then analysed under high magnification (40x) and large prey items, including mandibles, zooplankton appendages and foraminifera documented using the microscope described above. UV-B fluorescence (Excitation filter: EX365/10, Dichroic mirror: DM400, Barrier filter: BA400) was used to assist in the identification of copepod mandibles as it caused them to fluoresce blue. During this initial examination of ingested items, the relative 'gut fullness' was recorded on a qualitative scale from 1-4, where by 1 = 25% or less, 2 = 25%-50%, 3= 50% - 75% and 4 = 75% - 100%. Photographs were then taken under high magnification (40 x) along the length of each gut section and a 100 μm^2 grid overlayed. The photographs were examined, and food items identified within the gridded area. Examined grids included both the empty regions of the gut (if present) and full regions to ensure a representative analysis. Additionally, the relative proportion of unidentifiable contents, often visible as a mush or matrix was determined using this gridded technique. The number of grids counted under high magnification was then used to extrapolate the total number of individual food items present in the entire gut.

4.3.1.2 Larvae

Direct dissection and enumeration of the gut contents of larval *T. macrura* was not possible due to both their small size and preservation in formaldehyde – seawater solution. When preserved with formaldehyde larval *T. macrura* become brittle, and, due to their small and fragile bodies, efforts to dissect the them resulted in tearing or breaking. To determine if larval *T. macrura* were ingesting particles from the water column, acid digestions were performed, allowing for the identification of most siliceous prey items (e.g. diatoms) if present.

Larvae were divided into three broad post-naupliar developmental phases of calyptopis (CI – CIII), early furcilia (FI – FIII) and late furcilia (FIV- VI) (see Chapter 3). Individuals of each developmental phase were pooled from adjacent sites to provide sufficient numbers for analysis. Due to their

scarcity, a total of 17 calyptopes was analysed from samples pooled across the entire sampling area. 63 early furcilia and 62 late furcilia were analysed from the eastern and western boundaries of the study region and north of the SACCF (Table 4.3). Prior to acid digestion, individuals were rinsed thoroughly using Milli-Q water to dislodge any phytoplankton trapped within feeding appendages during collection and sample preservation. Pooled individuals were then placed into 10 mL of concentrated nitric acid and left at room temperature for 18 hours, which removed all soft biological material including the body tissues of larvae. Samples were diluted using Milli-Q water and filtered onto 0.45 µm mixed cellulose ester filters under low vacuum (<50 mg Hg) to avoid damage to fragile diatoms and diatom chains (adapted from Elder and Elbrächter 2010). Samples were then rinsed from the filter using Milli-Q water and examined by compound microscopy using a Sedgewick Rafter counting chamber. A total of 100 grids was counted per sample due to low phytoplankton presence within samples, and the number and type of species determined. The total number of items was then tallied for the entire sample and the mean number of items calculated per individual in the pooled sample.

4.3.1.3 Particle identification and diet composition

Ingested items were identified to the lowest taxonomic resolution possible, and, for chain forming species, the length of the chain was recorded. To provide a consistent methodology for enumerating the contents of *T. macrura* guts, a set of rules was established for all phytoplankton, protozoan and metazoan items identified. For the major phytoplankton groups, at least 25% of the individual cell needed to be identifiable for the cell to be counted. For the fragile pennate diatoms, *Rhizosolenia* sp. and *Trichotoxon* sp., at least one apex (end of the cell) needed to be identifiable, however, if two apices were present only one individual was counted. Due to the variation in the size of *Thalssiosira* species observed in the guts, and the inability to confidently differentiate between species because of both the magnification and obstruction of cells by other items in the guts, three size categories of *Thalassiosira* were established to capture this size diversity: <20 µm, between 10-20 µm and >20 µm. The identification and enumeration of protozoans was based upon the presence of their tests. Tests were generally isolated within small regions of the gut and counted as one individual. If fragments of test were identified strewn through the length of the gut (which was rare), only one individual was counted due to the inability to distinguish between the number of possible individuals ingested. For the enumeration of copepods, the presence of two mandibles was taken to indicate the ingestion of a single individual. If mandibles and other copepod body parts were identified, including antennae and legs, the mandible rule was used to distinguish the number of copepods consumed. However, if copepod body parts were identified and no mandibles were

identified then 1 copepod was counted as having been ingested due to the inability to distinguish how many individuals had been consumed.

To enable a direct comparison of identifiable gut contents, phytoplankton were first converted to their respective biovolumes (μm^3). For diatoms, appropriate cell dimensions were measured and the biovolume was calculated based upon standards provided by Leblanc et al. (2002), applying the best-approximate three-dimensional geometric shape. The biovolumes of dinoflagellates and protozoans were estimated assuming a spherical shape. Conversion to carbon content was then performed using the relationships provided by Leblanc et al. (2002) for diatoms and Menden-Deuer and Lessard (2002) for dinoflagellates and protozoans. For copepods, the generalised relationship provided by Karlson and Bamstedt (1994) to estimate copepod dry weight from mandible width was used, and then a dry weight : carbon conversion of 45% was applied (Conover and Huntley 1991). Dry weight of dissected *T. macrura* was calculated using the allometric relationship provided in Appendix C of this thesis. An assumed carbon content for *T. macrura* of 50% of dry weight (Froneman et al. 1996) was then used to estimate the carbon content of each individual. Consequently, the proportion of body carbon ingested could then be calculated to identify the relative importance of herbivorous and carnivorous food sources to individual *T. macrura*.

4.3.1.4 Lipid analysis

Lipids were extracted from frozen *T. macrura* over 24 hours using a modified Bligh and Dyer (1959) method consisting of a methanol:dichloromethane:water solvent mixture of 20:10:7 (v:v:v). The addition of 10 mL dichloromethane and 10 mL of saline Milli-Q water achieved phase separation, resulting in a final methanol:dichloromethane:water solvent ratio of 1:1:0.85. Rotary evaporation was used to concentrate the extract, with the sample then dried under a continuous flow of nitrogen gas, and the total lipid extract quantified gravimetrically. Prior to analysis, fatty acids were converted to their fatty acid methyl ester derivatives (FAME). A subsample of the total lipid extract was removed and treated with 3 mL of methylating solution of methanol:dichloromethane:hydrochloric acid at 10:1:1 (v:v:v), then heated for 75 min at 90 –100 °C. After cooling, 1 mL of Milli-Q water and 1.8 mL of hexane:dichloromethane at 4:1 (v:v) was added. Samples, with the addition of an internal injection standard (23:0 FAME), were analysed by gas chromatography using an Agilent Technologies 7890A GC-FID system (Palo Alto, CA, USA), equipped with a non-polar Equity® fused-silica capillary column (15 m length, 0.1 mm internal diameter, 0.1 µm film thickness). Samples were injected at an oven temperature of 120 °C using the helium as a carrier gas. The oven temperature was increased to 270 °C at a ramping rate of 10 °C min^{-1} then further increased to 310 °C at a rate of 5 °C min^{-1}. Peaks were identified and quantified using Agilent

Technologies ChemStation software (Palo Alto, CA, USA) based upon the retention times of fully characterised standards.

4.3.1.5 Statistical analysis

Hierarchical cluster analysis based upon sex and the proportion of carbon within the identifiable gut contents was performed on the 159 individuals analysed to examine any underlying spatial changes in the level of carnivory. Cluster analysis was performed based upon complete linkage and Euclidean distance (using the package dyplr in R).

4.3.2 Morphological adaptations to feeding and prey capture

4.3.2.1 Mouthpart morphology and development

The ontogenetic development of the major mouthparts of *T. macrura* was assessed for all post-naupliar developmental stages. Formaldehyde-preserved specimens were used and the mandible, maxillule and maxilla dissected and characterised for each developmental stage. The major morphological characteristics of each mouthpart were recorded to assess their development in relation to dietary preferences and prey handling ability as the krill grow (Figure 4.2). All measurements were performed using the open-source photographic analysis software ImageJ™ (Rasband 1997-2018).

Mandible: total length was measured as the longest axis from the tip of the pars incisiva to the base of the coxa. To provide a measure of the cutting and grinding ability of the mandibles, the pars incisiva and pars molaris were also measured (Figure 4.2 a and b). The length of the pars incisiva was measured from the most apical tooth to its base at the intersection with the pars molaris. The surface area of the par molaris was estimated by measuring the total diameter of the region and the assumption of a circular shape.

Maxillule: total length was measured from the tip of the endopod to the base of the coxa. The primary spine interval on the outer margin of the endite and secondary spine interval was measured (Figure 4.2 c and d). The total area of this spine region was calculated by measuring the length of the outer margin of the endite and the total length of the spines.

Maxilla: total length was measured from the tip of the endopod to the base of the coxa and the filtering area provided by the primary and secondary setae calculated by multiplying the length of the filtering region and the length of the primary setae. The primary and secondary setae intervals were measured, providing an approximation of the prey items and particles that can be effectively processed by *T. macrura* (Figure 4.2 e and f).

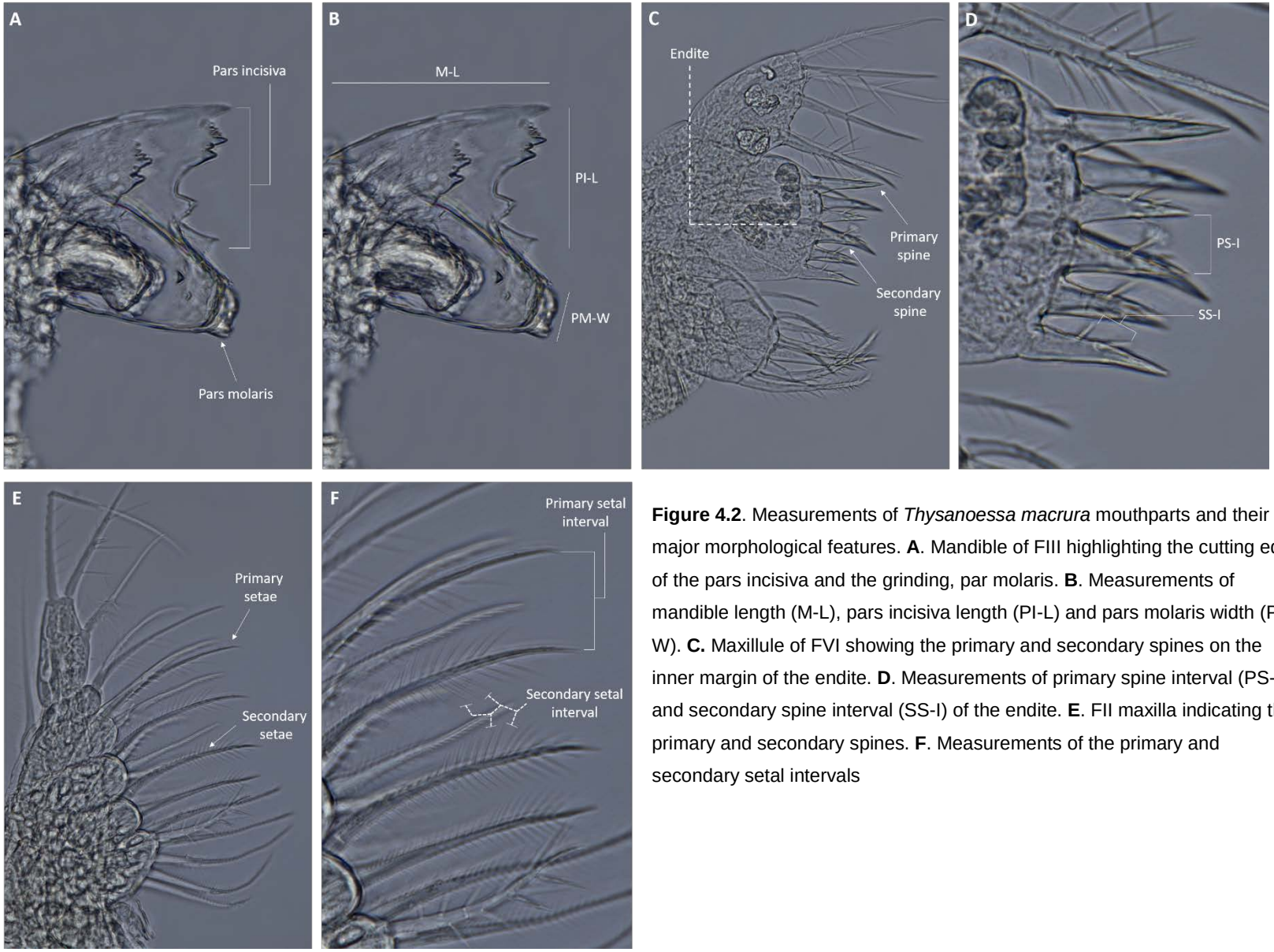

Figure 4.2. Measurements of *Thysanoessa macrura* mouthparts and their major morphological features. **A**. Mandible of FIII highlighting the cutting edge of the pars incisiva and the grinding, par molaris. **B**. Measurements of mandible length (M-L), pars incisiva length (PI-L) and pars molaris width (PM-W). **C.** Maxillule of FVI showing the primary and secondary spines on the inner margin of the endite. **D**. Measurements of primary spine interval (PS-I) and secondary spine interval (SS-I) of the endite. **E**. FII maxilla indicating the primary and secondary spines. **F**. Measurements of the primary and secondary setal intervals

4.3.2.2 Thoracopods

The development of the second thoracopod, which becomes elongated and is thought to be responsible for active prey capture required for carnivory, was described for the late furcilia stages. The segmentation and length of each segment were recorded for each developmental stage and adults. The primary and secondary setal intervals of the ischium and merus of the third and fourth thoracopods of adult were additionally measured, providing an estimate of the filtering capacity of the filtering basket.

4.4 Results

4.4.1 Diet of Thysanoessa macrura

4.4.1.1 Adults

161 *T. macrura* from 13 sites were subjected to microscopic analysis of gut contents (Table 4.1). The proportion of males and females analysed per site was relatively consistent, with females dominating samples at all sites. The relative gut fullness of *T. macrura* was variable across the study region, although tended to be generally low (<25%). Sites 19 and T10 had the fullest guts, scoring an index between 50% and 75% (Figure 4.3). Under high magnification, it became evident that portions of many dissected guts were filled with unidentifiable contents, appearing as an organic matrix often interspersed with identifiable particles. Due to the inability to quantify this organic matrix or 'mush', an estimate of its contribution to gut fullness was made. Subsequent data analysis is based only upon the clearly identifiable prey items quantified under microscopic examination. The proportion of unidentifiable prey items tended to be variable both between individuals and between sampling sites, however on average tended to be lower than 35% of total gut contents, excepting site 19 which had an average of 70% of this organic matrix.

Table 4.1. Adult *Thysanoessa macrura* sampled for gut contents analysis. The number of individuals, sex ratio and gut carbon content (mean ± SD) is provided.

Site summary							Proportion of body carbon ingested (%)	
Site	Number of Individuals	Proportion males (%)	Proportion females (%)	Mean Total Length (mm)	Mean DW (µg)	Gut carbon (ug)	Herbivory	Carnivory
2	7	29	71	20.4 ± 4.3	25.8 ± 13.7	$2.6x10^{-4} \pm 7.0x10^{-4}$	$1.5x10^{-6} \pm 3.9x10^{-6}$	0
5	12	42	58	17.6 ± 3.3	16.1 ± 11.9	17.28 ± 46.7	$3.1x10^{-3} \pm 2.4x10^{-3}$	$1.9x10^{-1} \pm 5.1x10^{-1}$
8	12	42	58	18.7 ± 3.1	19.0 ± 9.9	29.42 ± 42.3	$1.1x10^{-2} \pm 9.7x10^{-3}$	$2.6x10^{-1} \pm 3.8x10^{-1}$
10	12	25	75	18.4 ± 2.9	18.0 ± 7.7	94.77 ± 102.4	$8.1x10^{-3} \pm 1.7x10^{-2}$	1.3 ± 1.4
13	12	17	83	20.0 ± 2.1	22.3 ± 7.7	14.56 ± 27.8	$3.0x10^{-3} \pm 4.5x10^{-3}$	$1.6x10^{-1} \pm 3.2x10^{-1}$
16	12	17	83	20.3 ± 2.8	24.0 ± 11.9	14.97 ± 27.5	$8.9x10^{-4} \pm 3.1x10^{-3}$	$1.41x10^{-1} \pm 2.7x10^{-1}$
17	10	50	50	15.2 ± 3	10.3 ± 6.3	$5.7x10^{-3} \pm 0.02$	$1.5x10^{-4} \pm 4.8x10^{-4}$	$6.2x10^{-5} \pm 2.0x10^{-4}$
19	20	35	65	17.0 ± 2.3	13.9 ± 7.2	5.0 ± 13.35	$2.3x10^{-4} \pm 2.1x10^{-4}$	$7.1x10^{-2} \pm 1.9x10^{-1}$
22	8	38	63	16.4 ± 0.9	11.6 ± 1.9	16.1 ± 22.2	$4.1x10^{-4} \pm 1.0x10^{-3}$	$3.2x10^{-1} \pm 4.5x10^{-1}$
25	10	30	70	16.5 ± 2.5	12.8 ± 6.8	6.6 ± 15.2	$1.2x10^{-2} \pm 1.1x10^{-2}$	$5.5x10^{-2} \pm 1.0x10^{-1}$
30	20	15	85	16.6 ± 2.1	12.6 ± 5.0	77.2 ± 71.6	$3.1x10^{-3} \pm 5.5x10^{-3}$	1.4 ± 1.7
37	10	10	90	22.8 ± 2.5	33.8 ± 11.7	59.9 ± 55.2	$4.6x10^{-4} \pm 6.5x10^{-4}$	$4.0x10^{-1} \pm 4.0x10^{-1}$
T20	14	43	57	17.0 ± 3.5	14.7 ± 9.8	6.6 ± 16.7	$1.9x10^{-4} \pm 5.2x10^{-4}$	$8.3x10^{-2} \pm 2.3x10^{-1}$

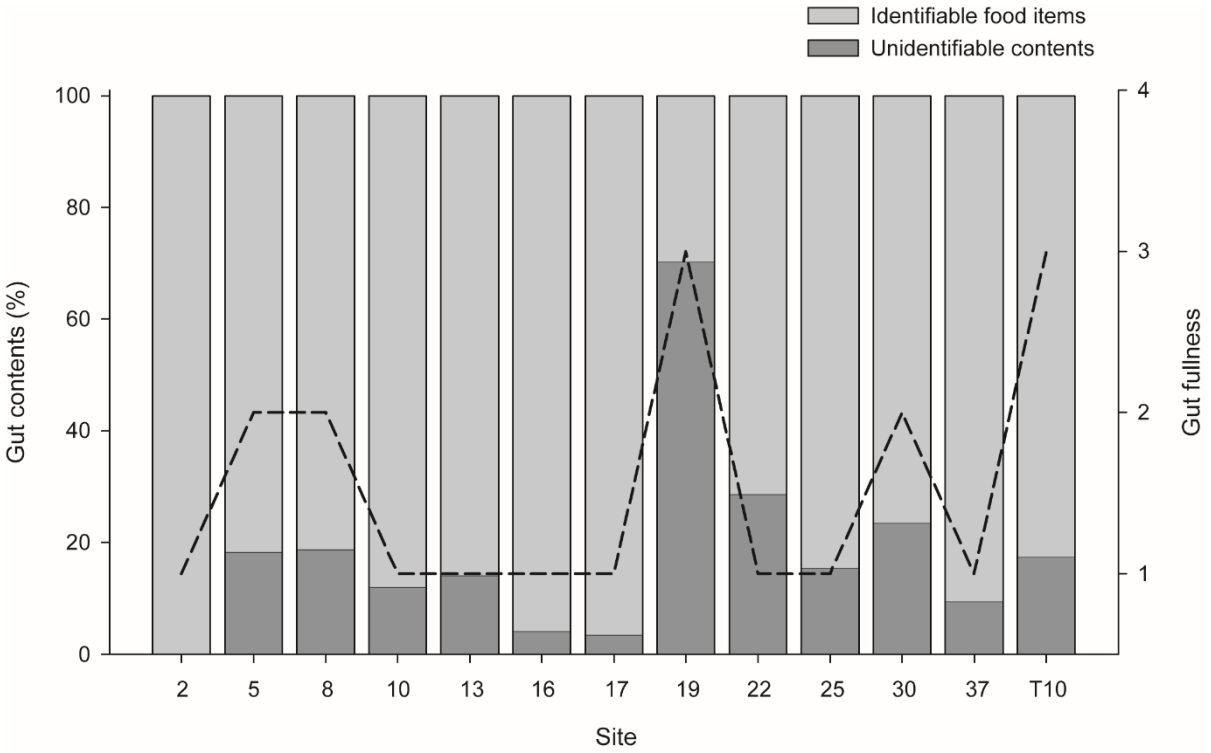

Figure 4.3. The mean proportion of identifiable and unidentifiable prey items and mean gut fullness (dashed line) of adult *Thysanoessa macrura* from each sample site.

The conversion of particles identified in the guts of *T. macrura* to carbon content was applied to provide an equal weighting to phytoplankton, protozoan and metazoan prey sources. Due to the soft bodied nature of copepod tissues, identifying them in the guts of *T. macrura* relied upon the presence of hard body parts, primarily the mandibles. The proportion of carnivory in the diet, identified through the presence of mandibles and appendages of copepods and the tests of foraminiferans and radiolarians, was variable throughout the study region, and generally accounted for greater than 30%. Maximum gut carbon derived from carnivory reached up to 99% for some individuals at site 37 (Figure 4.4). Evidence of carnivory tended to be more common in females than in males, with protozoan and metazoan prey significantly contributing to female diet at all sites except site 2 at which no carnivory was identified in either males or females. A detailed list of prey sources and respective biovolumes, and size used for the calculation of carbon content per individual prey item is provided in Table 4.2.

Table 4.2. The species/groups identified within the guts of adult *Thysanoessa macrura*, their mean biovolume and carbon content. The mean smallest and largest axis of each food item identified (± standard deviation) is also provided. Note that other common items identified within the guts are also provided, although they were not included in the analysis of gut contents.

	Mean biovolume (μm^3)	Mean Carbon content (ug C)	Smallest axis (µm)	Largest axis (µm)
Herbivorous				
Fragilariopsis curta	$2.8x10^2$	$1.4x10^{-5}$	4.1 ± 2.7	15.0 ± 2.4
Fragilariopsis ritscheri	$2.4x10^3$	$1.6x10^{-4}$	5.3 ± 0.8	53.8 ± 5.6
Fragilariopsis kerguelensis	$1.9x10^3$	$1.4x10^{-4}$	8.1 ± 1.1	29.0 ± 9.2
Fragilariopsis rhombica	$3.4x10^2$	$4.9x10^{-5}$	11.0 ± 2.9	12.9 ± 3
Thalassiosira spp. < 10 µm	$2.2x10^2$	$2.7x10^{-5}$	4.1 ± 0.6	8.2 ± 1.2
Thalassiosira spp. 10 - 20 µm	$1.7x10^3$	$9.4x10^{-5}$	7.0 ± 1.2	14.0 ± 2.4
Thalassiosira sp. > 20 µm	$3.5x10^4$	$1.2x10^{-3}$	21.0 ± 5.4	42.0 ± 10.8
Rhizosolenia sp.	$3.2x10^5$	$5.6x10^{-4}$	22.3 ± 5.8	765.2 ± 156.1
Chaetoceros spp.	$6.3x10^2$	$5.9x10^{-5}$	5.0 ± 1.1	15.2 ± 3.2
Trichotoxon sp.	$4.3x10^4$	$1.5x10^{-3}$	28.9 ± 2.4	50.9 ± 28.7
Asteromphalus spp	$2.4x10^5$	$5.4x10^{-3}$	30.0 ± 5.6	100.1 ± 7.9
Eucampia sp.	$1.3x10^3$	$1.0x10^{-4}$	7.1 ± 2.4	18.2 ± 3.1
Dinoflagellate	$5.8x10^3$	$9.1x10^{-4}$	-	73.9 ± 6.9
Carnivorous				
Protozoans				
Silicoflagellate	$3.1x10^3$	$5.5x10^{-4}$		87 ± 20.46
Radiolarian	$6.4x10^3$	$9.8x10^{-4}$		75.8 ± 22.5
Ciliates	$4.6x10^3$	$4.6x10^{-4}$		66.1 ± 12.4
Foraminifera	$1.6x10^4$	2.0		122.8 ± 25.2
Copepods				
Metridia mandibles	-	$3.3x10^1$		126.6 ± 21.6
Calanus propinquus & *Calanoides acutus* mandibles	-	$4.3x10^1$		137.5 ± 37.3
Rhincalanus gigas mandibles	-	$4.1x10^1$		140.8 ± 18.9
Not included in analysis of gut carbon				
Gregarine parasite				
Euphausiid eye trichomes				
Copepod appendages				

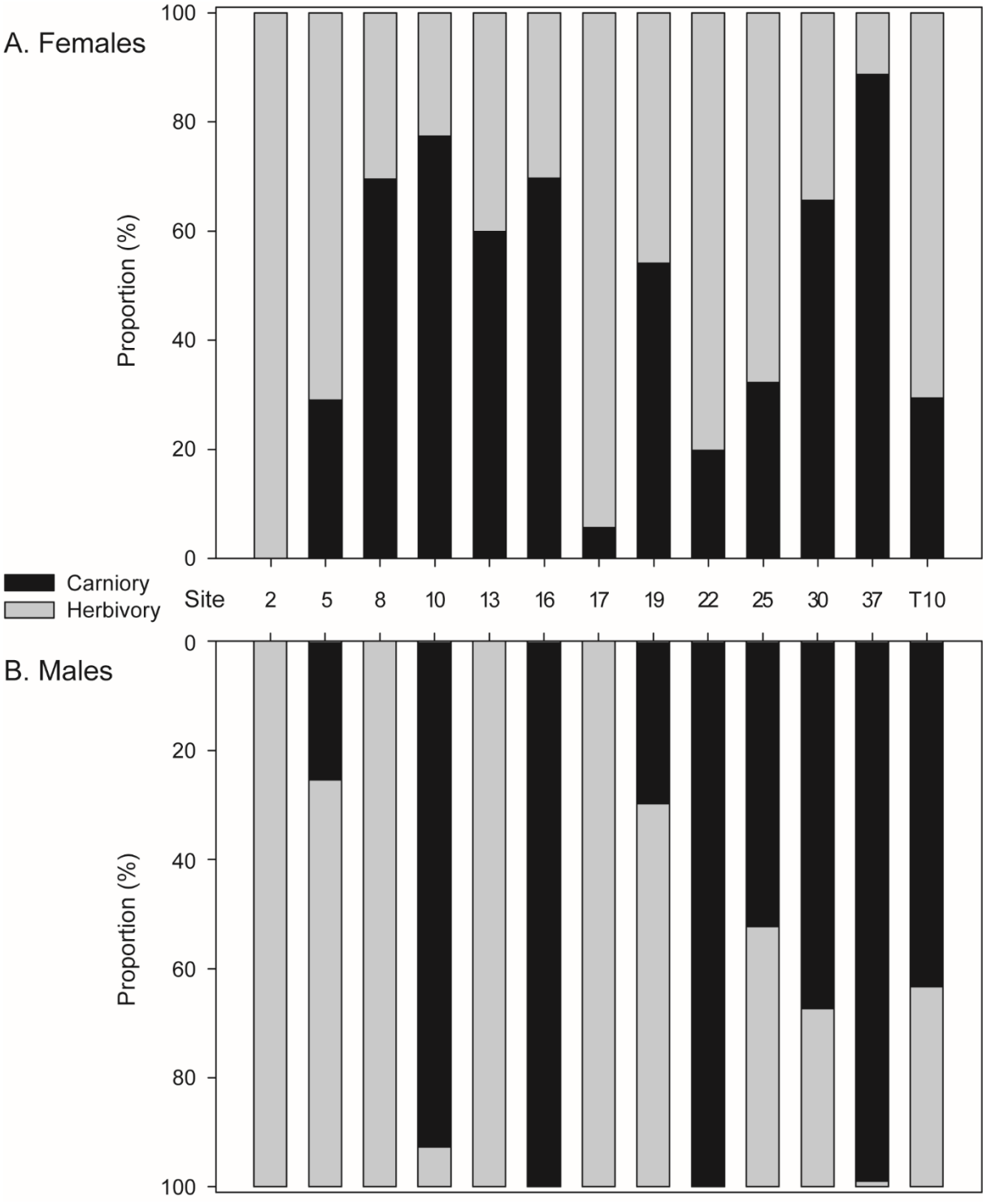

Figure 4.4. The relative proportions of carbon in the diet of *Thysanoessa macrura* from herbivorous and carnivorous feeding. **A.** Adult females. **B**. Adult males.

Phytoplankton identified within the guts of *T. macrura* were dominated by diatoms. The diatom *Fragilariopsis kerguelensis* was the numerically abundant phytoplankton identified and was present both as single cells and chains up to 13 cells long. Consequently, *F. kerguelensis* was a major contributor to gut carbon (Figure 4.5). *Asteromphalus* spp. and *Trichotoxon* sp., although occurring in low proportions, were also major contributors to phytoplankton carbon ingested due to their large call sizes of 100 µm and 50.9 µm, respectively. *Thalassiosira* spp. size fractions of <10 µm and >20 µm and *Rhizosolenia* sp. were also identified across the study region although at lower proportions, however, at site 17, *Thalassiosira* spp. >20 µm was the dominant phytoplankton present in guts (Figure 4.5a). Dinoflagellates and the intermediate size fraction of *Thalassiosira* 10-20 µm contributed little to gut carbon. All other taxa, including *Fragilariopsis rhombica, Fragilariopsis curta, Fragilariopsis ritscheri*, *Chetocerous* sp. and *Eucampia* sp., had a cumulative contribution to gut carbon of less than 2.5% at all sites. Copepod mandibles were the most common evidence for carnivorous feeding at all sites (Figure 4.5b). Mandibles and large copepod body parts, including legs and carapace sections, were readily identifiable in both the foregut and hindguts of *T. macrura*, aided with the use of UV-B fluorescence (Figure 4.6).

Mandibles belonging to the copepods *Calanus propinquus and/*or *Calanoides acutus* were identified in the guts of *T. macrura* at all sites except 2 and 17 (Figure 4.5b). The identification of these mandibles could not be resolved between the two species due to their high similarity in morphology. A mean mandible width of 137.5 µm, corresponding to a calculated carbon content of 42.8 µg carbon per individual ingested, made these calanoid copepods the highest single contributor to gut carbon of all identified prey sources. Mandibles of *Rhincalanus gigas* and *Metridia* sp. were also identified within the guts of *T. macrura*: *Metridia* sp. was identified at sites 16 and 37, and *R. gigas* was identified only at site 16 (Figure 4.5b). The dominant protozoan taxa that contributed to carnivory included radiolarians, ciliates and foraminifera. Due to their relatively small size compared to copepods, these protozoans contributed less carbon to the diets of *T. macrura* across the study region (Figure 4.5b). To assess the importance of carnivory to the diet of adult *T. macrura* the carbon ingested from herbivorous and carnivorous feeding as a proportion of total body carbon was determined. Carnivorous feeding contributed an average of 0.3% of body carbon ingested, with a minimum of 0% (no carnivory identified at site 2) and a maximum of 1.4% (Table 4.1). Herbivorous feeding ranged from <0.001% to 0.01% of total body carbon, with an average of 0.003% for the entire study region (Table 4.1).

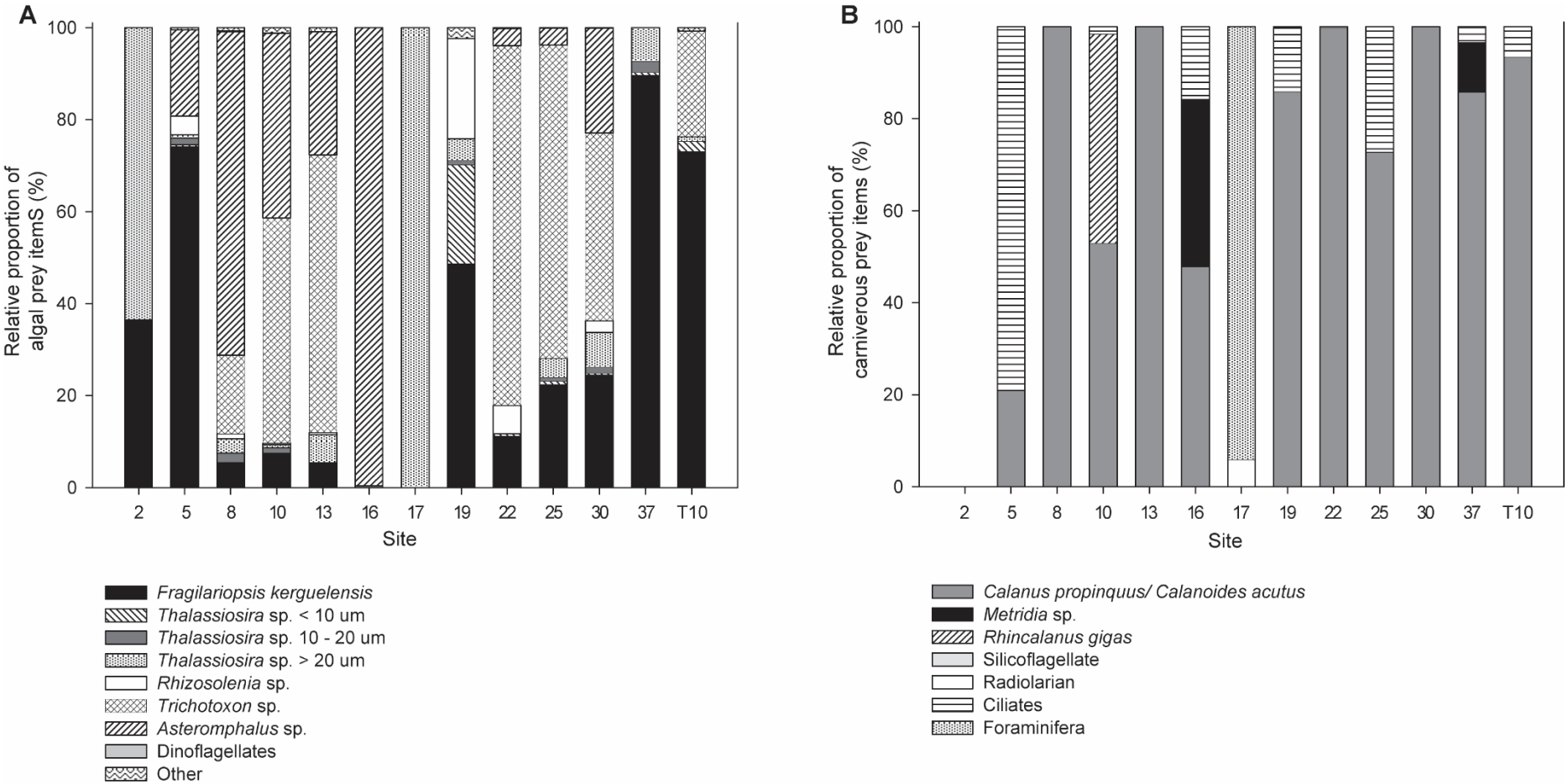

Figure 4.5. The relative contribution of the major food items from herbivorous and carnivorous feeding of total gut carbon content. **A.** The dominant algal taxa/groups that contributed to the diet of *Thysanoessa macrura* based upon their carbon contribution. **B**. The protozoan and metazoan prey sources and their relative contribution based upon carbon content. Note there was no recorded carnivory at site 2.

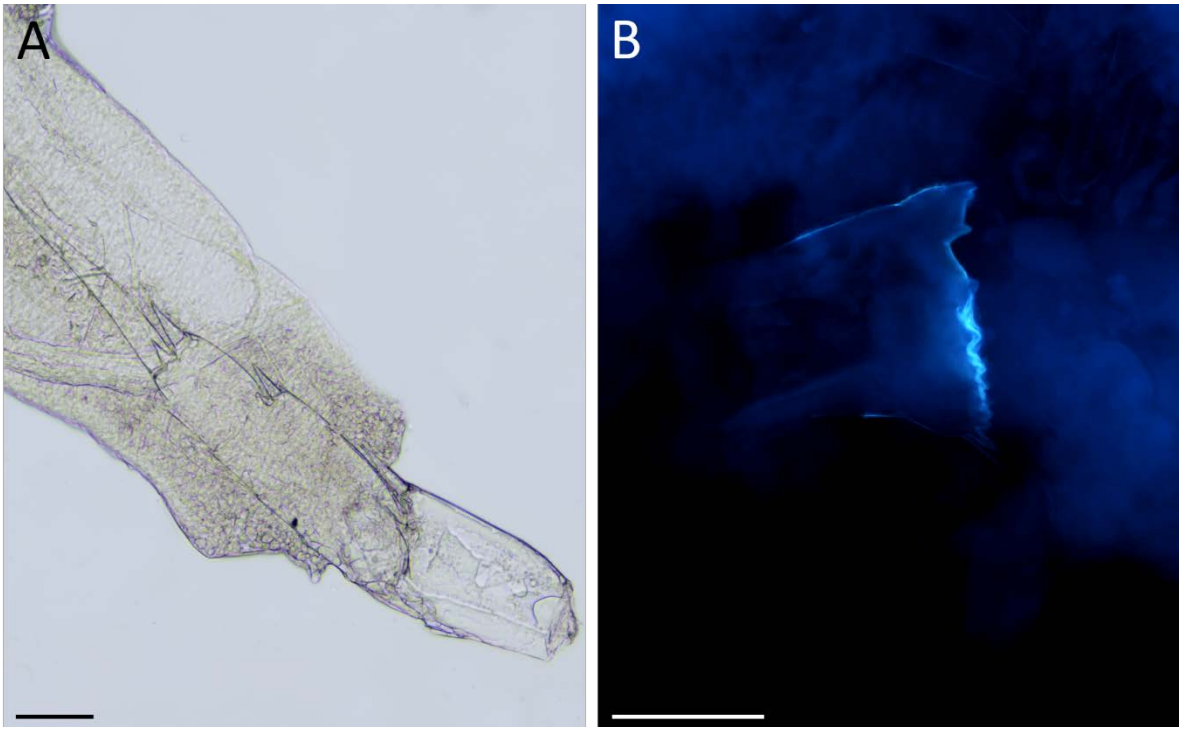

Figure 4.6. Evidence of carnivory in the guts of *Thysanoessa macrura*. **A**. Segments from copepod leg **B**. Copepod mandible. Scale bar = 100 µm.

Despite the dominance of carnivory in the diet of *T. macrura,* and continuous background presence of algal prey items in the gut, cluster analysis based upon the proportion of herbivorous and carnivorous contributions to total gut carbon for both males and females suggested spatial variation in the north and south of the study region (Figure 4.7). Qualitatively, the Southern Antarctic Circumpolar Current Front (SACCF) appears to be the delineating oceanographic feature between the two clear clusters identified. Carnivory appeared to be more important in individuals north of the SACCF compared to those south of the SACCF. In the north, carnivory represented an average of 52% and 70% of the gut contents of females and males, respectively. In the south carnivory contributed only an average of 37% to the gut carbon of females and 9% of males.

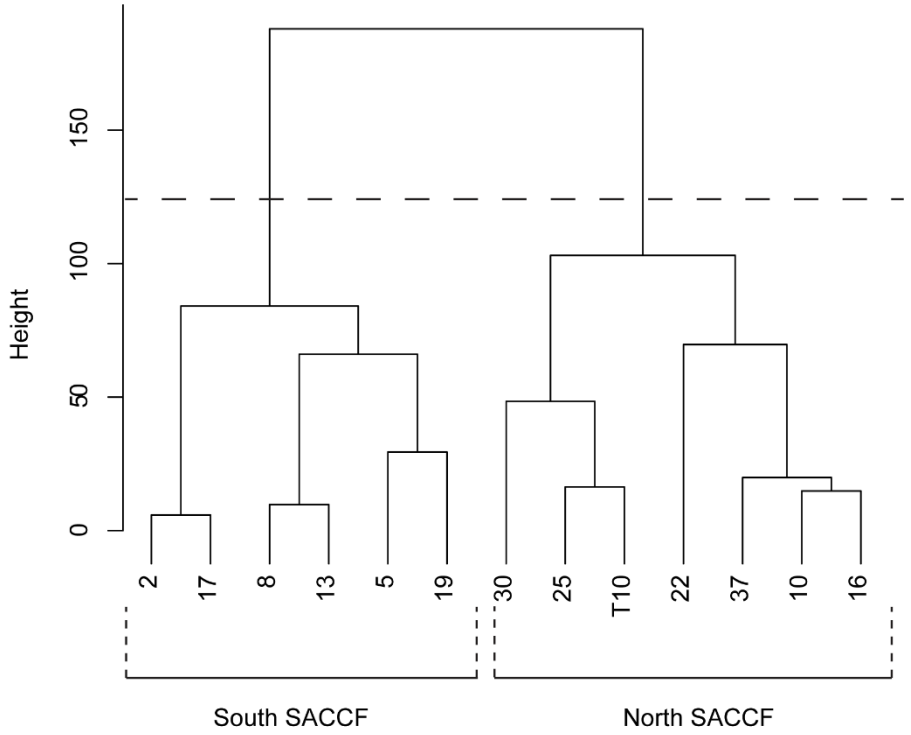

Figure 4.7. Cluster analysis representing the importance of carnivory, represented as the proportion of protozoan and metazoan-derived carbon in the identifiable prey items of the gut contents based upon sex. Height indicates the average Euclidean distance between clusters.

4.4.1.2 Larvae

Due to the destructive nature of the acid digestion used to assess the diets of *T. macrura* larvae, diatoms were the only food items identified. Five diatom taxa were identified from larval stages across the study region (Table 4.3). Both *F. kerguelensis* and *Thalassiosira* spp. 10-20 µm were the most commonly identified diatoms and dominated the food items identified from early furcilia phases. *Rhizosolenia* sp. and *Chaetocerous* sp. were identified in early furcilia phases in individuals assessed from the western edge of the study region. Late furcilia had higher proportions of *F. kerguelensis* than any other diatom taxa, however *Thalassiosira* spp. 10-20 µm were found to the exclusion of all other taxa in the eastern area. Like early furcilia, *Rhizosolenia* sp. and *Chaetocerous* sp. were found in individuals within the western area of the study region, however *Chaetocerous* sp. were also identified within individuals north of the SACCF. Despite pooling calyptopis stages from the entire study region, no diatoms were identified.

Table 4.3. Analysis of siliceous items ingested by *Thysanoessa macrura* larval stages. Data are represented as the total number of items ingested by individual larval from the pooled samples.

Sampling Summary					Prey items per individual larvae				
Developmental Phase	Pooled Stages	Sampling Area	Number of Individuals	Sites	*Fragillariopsis kerguelensis*	*Rhizosolenia* sp.	*Chaetoceros* sp.	*Thalassiosira* sp. (10-20 um)	**Total**
Calyptopis	C II - C III	Pooled Sampling Region	17	3,4,23,25,37,38	0	0	0	0	**0**
Early Furcilia	F I - F III	Eastern	18	3,4	6	0	0	11	**17**
		North SACCF	15	23,25	13	0	0	20	**33**
		Western	30	37,38	7	3	5	0	**15**
Late Furcilia	F IV - FVI	Eastern	14	3,4	0	0	0	11	**11**
		North SACCF	24	23,25	10	0	8	4	**23**
		Western	24	37,38	21	6	6	0	**33**

4.4.1.3 Lipids as an indication of prey source

The main fatty acid and alcohol components of total lipids extracted from males and females are provided in Table 4.4. Total lipids were dominated by saturated fatty acids (SFA), primarily 14:0 and 16:0, which were present in equal proportions in both males and females and accounted for approximately 50% of total fatty acids. Polyunsaturated fatty acids (PUFA) were dominated by 20:5(*n*-3), which accounted for 16% in females and 18% in males. 22:6(*n*-3) and 18:1(*n*-9) were also important, contributing 7.5% and 9.7% to females and 8.9% and 9% to males, respectively (Table 4.4). Fatty alcohols were mainly composed of 18:1(*n*-9) and 18:1(*n*-7), both contributing equal proportions to male and female *T. macrura*. 20:1(*n*-9) was also a significant contributor, accounting for 21% in females and 18% in males.

Biomarkers were assessed for *T. macrura* based upon relative ratios of dominant fatty acids. The ratio of PUFA to SFA has been used in *E. superba* to demonstrate carnivory, with higher ratios indicating an increased level of carnivory; however, this has yet to be applied to other euphausiid species (Cripps and Atkinson 2000). For females this ratio yielded 0.7 and 0.8 in males indicating low levels of carnivory. The biomarker ratio 18:1(*n*-9)/18:1(*n*-7) indicates a high degree of carnivory, with ratios of 2.8 and 2.7 recorded for *T. macrura* males and females, respectively. To discriminate between the major phytoplankton dietary sources, diatoms and flagellates, several biomarkers can be used (Table 4.4). The ratio between 16:1(*n*-7) and 18:4(*n*-3) indicates the importance of flagellates in the diet due to their high levels of 18:4(*n*-3) compared to diatoms (Graeve et al. 1994). Consequently, the low levels of 18:4(*n*-3) measured in this study indicates that diatoms were more important than flagellates to the diets of both males and females. This is confirmed by the ratio of 20:5(*n*-3)/22:6(*n*-3), which indicates a high level of diatom input.

Table 4.4. Major fatty acid and alcohols as lipid mass percentage of adult *Thysanoessa macrura*. Only fatty acids and alcohols that were greater than 1% for each group are presented. The dominant ratios of fatty acids used to elucidate feeding history are also presented. SFA = saturated fatty acid, MUFA = monounsaturated fatty acid, PUFA = polyunsaturated fatty acid. Values are provided as mean ± SD.

Fatty Acid	Females (n=17)	Males (n=9)	Biomarker
14:0	20.7 ± 6.2	19.2 ± 5.2	
16:0	22.6 ± 1.9	20.2 ± 4.2	Flagellates[3]
16:1(*n*-7)	4.0 ± 0.8	4.9 ± 0.9	Diatoms[3]
16:1(*n*-5)	1.3 ± 0.4	1.2 ± 0.3	
18:0	0.9 ± 0.1	0.96 ± 0.3	
18:1(*n*-9)	9.7 ± 1.1	9.0 ± 1.3	Metazoans[5]
18:1(*n*-7)	3.7 ± 1.1	3.5 ± 1.0	
18:2(*n*-6)	2.1 ± 0.4	2.1 ± 0.3	
18:4(*n*-3)	1.2 ± 0.5	1.0 ± 0.2	Flagellates[3]
20:1(*n*-9)	1.0 ± 0.6	0.7 ± 0.4	
20:5(*n*-3)	16.0 ± 4.5	18.0 ± 2.7	
22:6(*n*-3)	7.5 ± 1.3	8.9 ± 0.6	
24:1(*n*-9)	0.8 ± 0.6	1.2 ± 0.5	
% SFA	50.0 ± 6.0	42.3 ± 5.0	
% MUFA	24.3 ± 4.0	24.4 ± 3.1	
% PUFA	29.7 ± 4.4	33.3 ± 3.0	
PUFA/SFA	0.7 ± 0.2	0.8 ± 0.1	Carnivory v Herbivory[1]
16:1(*n*-7)/18:4(*n*-3)	3.9 ± 1.9	5.1 ± 1.2	Flagellates v Diatoms[2]
20:5(*n*-3)/22:6(*n*-3)	2.2 ± 0.8	2.0 ± 0.3	Diatoms v Flagellates[4]
16:1(*n*-7)/16:0	0.2 ± 0.04	0.3 ± 0.1	Diatoms v Flagellates[3]
18:1(*n*-9)/18:1(*n*-7)	2.8 ± 0.7	2.7 ± 0.7	Carnivory v Herbivory[5]
Alcohols			
15:0	1.9 ± 0.6	1.7 ± 0.4	
17:0	7.9 ± 21.6	2.9 ± 0.6	
18:1(*n*-9)	30.4 ± 11	33.8 ± 8.8	
18:1(*n*-7)	30.2 ± 8.3	34.7 ± 5.1	
22:0	1.0 ± 0.3	1.2 ± 0.2	
20:1(*n*-9)	21.3 ± 7.2	18.2 ± 5.5	*Calanoides acutus*[6]
22:1(*n*-11)	3.2 ± 3.9	3.3 ± 3.7	
Cholesterol	86.2 ± 21.7	89.8 ± 4.1	

[1]Cripps and Atkinson 2000

[2] Graeve et al. 1994

[3]Stübing and Hagen 2003

[4]Nelson et al. 2001

[5]Cripps et al. 1999

[6]Hagen and Kattner 1998

4.4.2 Prey capture and mouthpart morphology

4.4.2.1 Mandibles

The development of the mandible, maxillule and maxilla was documented and described for stages of *T. macrura* from calyptopis II to adults (Table 4.5). The morphometric characteristics of the major components of the three mouthparts are also provided in Table 4.6. The mandibular palp of *T. macrura* is present as a single lobe until late furcilia stage VI, when the mandibular palp then resembles that of adults, having two articulated lobes. The pars incisiva, the cutting regions of the mandibles, are prominent in all larval stages, although their development is marked by transitions in the cutting edges. In early larval stages, incisor teeth are small and pointed, with prominent regions of serrations. By furcilia VI, serrations are heavily reduced and are lost entirely in adults. The pars molaris is the region of the mandibles responsible for the grinding of food items. In calyptopis stages, the pars molaris is relatively small in total surface area, with undefined specialist features (Tables 5 and 6). The region becomes more defined and enlarged in early furcilia stages, with the obvious development of serrated marginal teeth that protrude from the distal side of the molar. Finely divided marginal teeth on the proximal region of the molar in late furcilia stages become evident. When the par molaris is developed fully in adults clear definition of the major regions of the molar is apparent, including the serrated and fine marginal teeth and marginal pores (Table 4.5). A full photographic record of mandibular development between stages is provided in Appendix B.

4.4.2.2 Maxillules

Maxillules are present on all post-naupliar stages of *T. macrura* as a three-segmented appendage (Table 4.5). The development of the spines on the outer margin of the endites, used in manipulating and holding prey items for maceration by the mandibles, is the only marked difference in the morphological development between larval stages. In calyptopis stages, only three outer spines are evident, however spines are robust with small secondary spines present on all three. The number of spines in this region increases between each developmental stages, reaching six by FVI, with adults having up to 15, with no secondary spines evident (Table 4.5). The spine interval in all stages remains consistent, between 6.6 µm and 13 µm, but increases to 35.7 µm in adults (Table 4.6). Similarly, the secondary spine interval is consistent between developmental stages, between 3.3 and 6.2 µm. Photographic documentation of maxillule morphology is listed in Appendix B.

4.4.2.3 Maxilla

The number of primary setae present on the maxilla increases from 16 in CI individuals to 24 in FVI and greater than 40 in adults (Table 4.5). Maxilla are responsible for the filtering packaging of prey items for maceration by the mandibles prior to digestion. The primary setae distance remained consistent across all larval stages and into adults. Similarly, the secondary setae distance remained consistent between 2.6 and 5.6 µm (Table 4.6). The area of the filtering region, defined as the region of primary setae, increased between each larval stage due to the increase in the number of primary setae and the overall size of the maxilla, increasing from 5,278 μm^2 in CII to 13,045 μm^2 in adults. See Appendix B for supporting photographic documentation.

4.4.2.4 Thoracopod development

Furcilia IV are the first larval stage to possess a fully developed second thoracopod (Table 4.5). An increase in length of the ischium, merus, carpus and propodus of the second thoracopod of FIV – FVI stages was recorded; however, the length of the dactylus as the tip of the thoracopod remained small, < 50 µm, in all three stages and lacked the fully developed spines seen in adults (Table 4.7). The primary and secondary setae intervals of the third and fourth thoracopods of adults were also assessed to determine their filtering and prey capturing abilities along the inner margins of both the ischium and merus (Table 4.7). The primary setal distances of both the ischium and merus were similar on both the third and fourth thoracopods, between 40 – 50 µm. Similarly, the secondary setal distances were consistent, ranging from 14 to 22 µm on both thoracopods. Photographic documentation of thoracopod development is provided is Appendix B.

Table 4.5. Characteristics of the development of the mouthparts; mandible, maxillule and maxilla and the second thoracopod of *Thysanoessa macrura*. The major morphological components of each mouthpart are described, enabling an assessment of food handling ability. Note that due to a lack of individuals information about calyptopis stage I is incomplete for maxillules and maxilla.

	Mandible			**Maxillule**			**Maxilla**		**2nd Thoracopod**
Stage	Pars incisiva	Pars molaris	Mandibular palp	Segment	Spines on outer margin of the endite	Secondary spines	Segment	Number of primary setae	Number of segments?
C I	Incisor teeth small and pointed with obvious serrations between points	Small region with undefined specialist ridges and plates	1						
C II	Incisor teeth a pointed with serrations present between teeth points	Small region with undefined specialist ridges and plates	1	3	3	Small secondary spines present at the upper ends of all primary spines.	3	16	-
C III	Incisor teeth a pointed with serrations present between teeth points	Small region with undefined specialist ridges and plates	1	3	4	Small secondary spines present at the upper ends of all primary spines.	3	16	-
F I	Incisor teeth a pointed with serrations present between teeth points	Defined serrated marginal teeth present	1	3	4	Small secondary spines present at the upper ends of all primary spines.	3	18	4
F II	Incisor teeth short and pointed. Serrations between points more defined	Defined serrated marginal teeth present	1	3	5	Small secondary spines present at the upper ends of the primary spines.	3	20	4
F III	Incisor teeth short and pointed. Serrations between points more defined	Defined serrated marginal teeth present	1	3	5	Small secondary spines present at the upper ends of all primary spines.	3	20	4

Table 4.5 continued.

	Mandible			Maxillule			Maxilla		2nd Thoracopod
Stage	Pars incisiva	Pars molaris	Mandibular palp	Segment	Spines on outer margin of the endite	Secondary spines	Segment	Number of primary setae	Number of segments?
F IV	Incisor teeth short and pointed. Serrations between points more defined	Defined serrated marginal teeth present	1	3	5	Small secondary spines present at the upper ends of all primary spines.	3	20	5
FV	Incisor teeth short and pointed. Serrations between points more defined	Defined serrated marginal teeth and finely divided marginal present	1	3	5	Small secondary spines present at the upper ends of all primary spines.	3	24	5
FVI	Incisor teeth elongated. Serrations between teeth heavily reduced.	Defined serrated marginal teeth and finely divided marginal teeth present	2	3	6	Small secondary spines present at the upper ends of the primary spines.	3	24	5
Adult	Incisor teeth robust and prominent. No serration present between teeth.	Fully defined. Serrated marginal teeth and finely divided marginal teeth present. Marginal pores evident	2	3	10 - 15	No secondary spines evident		>40	5

Table 4.6. Mouthpart morphometrics of the developmental stages of *Thysanoessa macrura*. All measurements are provided as mean ± standard deviation.

		C II	C III	F I	F II	F III	FIV	FV	FVI	Adult
Mandible	Total Length (μm)	105.2 ± 9.4	111.2 ± 13.4	111.8 ± 11.6	176.2 ± 9.5	183.7 ± 7.2	185.4 ± 3.7	327.9 ± 7.1	345.1 ± 170.2	628.1 ± 60.9
	Pars incisiva length (μm)	54.4 ± 3.5	71.0 ± 6	76.8 ± 4.8	123.8 ± 6.2	104.6 ± 5.4	111.5 ± 7.3	115.3 ± 4.5	157.3 ± 11.4	485.0 ± 14.6
	Pars molaris surface area (μm^2)	287.5 ± 72.4	413.4 ± 241.6	513.2 ± 165	738.1 ± 269.9	970.4 ± 191.8	857.3 ± 128.8	838.6 ± 74.8	2586.6 ± 639.7	7457.2 ± 769.5
Maxillule	Total length (μm)	160.4 ± 17.8	226.2 ± 17.8	177.2 ± 14.3	243.3 ± 9.1	264.4 ± 12.7	204.1 ± 5.1	352.6 ± 19.0	318.3 ± 11.0	981.1 ± 24.3
	Area of spine region (μm^2)	1462.0 ± 284	1523.8 ± 154.4	1559.4 ± 351.5	2282.0 ± 155.3	2671.8 ± 307.7	2240.5 ± 174.5	3324.6 ± 269.8	3732.5 ± 678.3	27732.0 ± 1966.1
	Spine interval (μm)	8.44 ± 0.8	7.5 ± 0.8	7.1 ± 0.6	9.6 ± 0.5	7.7 ± 0.5	6.6 ± 0.8	7.5 ± 0.5	13.3 ± 2.0	35.7 ± 3.8
	Secondary spine interval (μm)	3.3 ± 0.5	6.2 ± 0.5	3.2 ± 0.4	3.5 ± 0.4	5.5 ± 0.5	4.0 ± 0.6	3.5 ± 0.5	6.6 ± 1.0	9.9 ± 0.9
Maxilla	Total length (μm)	204.0 ± 26.3	166.2 ± 8.9	276.9 ± 6.7	326.0 ± 4.3	316.4 ± 5.5	255.1 ± 14.6	405.5 ± 5.9	358.1 ± 18.5	928.7 ± 52.6
	Area of filtering region (μm^2)	5278.4 ± 878.7	7221.2 ± 476.9	14363.5 ± 2019	18476.5 ± 1745.9	20344.0 ± 2983.8	13720.1 ± 1729.1	24241.2 ± 2746.3	20403.2 ± 2815.1	130849.9 ± 9506.1
	Primary setal interval (μm)	11.8 ± 3.2	18.9 ± 1.8	10.6 ± 1.3	9.5 ± 0.9	10.4 ± 0.6	13.1 ± 0.4	14.4 ± 0.5	13.2 ± 1.2	15.2 ± 1.3
	Secondary setal interval (μm)	2.8 ± 0.3	2.8 ± 0.2	4.1 ± 0.4	2.6 ± 0.4	3.2 ± 0.4	3.0 ± 0.2	4.1 ± 0.1	3.5 ± 0.5	5.6 ± 0.5

Table 4.7. Development of the 2nd thoracopod of *Thysanoessa macrura,* showing the length of the segments of the exopod. The setal intervals of the ischium and merus of the 3rd and 4th thoracopod of adults are also provided.

2nd Thoracopod						**3rd Thoracopod**				**4th Thoracopod**			
	Length (µm)					Ischium		Merus		Ischium		Merus	
Stage	Ischium	Merus	Carpus	Propodus	Dactylus	Primary setal interval (µm)	Secondary setal interval (µm)	Primary setal interval (µm)	Secondary setal interval (µm)	Primary setal interval (µm)	Secondary setal interval (µm)	Primary setal interval (µm)	Secondary setal interval (µm)
FIV	200 ± 10	318 ± 31	107 ± 9.1	64 ± 24	41 ± 5								
FV	163 ± 14	285 ± 22	98 ± 5	67 ± 7	40 ± 3								
FVI	222 ± 12	545 ± 23	236 ± 18	160 ± 8	51 ± 2								
Adult	1260 ± 163	6131 ± 144	4143 ± 92	1490 ± 162	1548 ± 203	52 ± 30	14 ± 2	55 ± 9	22 ± 6	41 ± 2	17 ± 2	61 ± 8	19 ± 2

4.5 Discussion

4.5.1 Prey diversity

Analysis of gut contents of adult *T. macrura* revealed a diverse range of prey items available across the study region. Consistently low feeding activity was observed, with gut fullness generally 25% or less, excepting individuals at sites 19 and T10 which had guts up to 75% full. The identification of particles identified in guts was confined to hard items that were robust enough to remain intact during mechanical digestion of the mandibles and gastric mill. Accordingly, diatoms dominated the phytoplankton identified, while large, armoured dinoflagellates were also observed intact in hind guts at several sites. Both protozoans and copepods were common, with silicoflagellates, radiolarians and foraminifera identified by their tests and copepods observed by the presence of mandibles and appendages in both fore and hind guts. Although these robust prey items were readily identifiable, a relatively constant level of unidentifiable 'mush' was also present. This mush only occurred in individuals that were feeding (with additional identifiable prey items), never occurring in adults with fully evacuated guts. The presence of mush-like gut contents was common in similar studies of other euphausiid species and was attributed to heavily macerated phytoplankton (Hopkins 1985; Schmidt et al. 2006). The lack of identifiable fragments of diatoms, protozoan tests or crustacean exoskeletons within this mush suggests its presence may result from the ingestion of soft bodied prey items. Despite the common appearance of gregarine parasites in analysed individuals, identified and described by Wallis et al. 2017 (Appendix E), they were not considered for this study as they do not relate directly to the diet of *T. macrura*. Furthermore, the appearance of crystalline cones (eye structure of euphausiids) in the foregut of *T. macrura* occurring predominantly at sites with high *T. macrura* abundance was attributed to net feeding and also precluded from the study.

The use of UV-B fluorescence was valuable for identifying crustacean remains, with mandibles and appendages fluorescing vibrant blue. Without the application of UV-B fluorescence, mandibles were often difficult to identify, appearing translucent against the contents of guts. Unlike protists, where the remains of entire tests stayed relatively intact, the assessment of predation on known copepod species relied upon the identification of mandibles, a standard method in microscopic analysis of gut contents (Karlson and Bamstedt 1994; Schmidt 2006). Mandibles belonging to *Calanus propinquus* or *Calanoides acutus* were the most common and numerous mandibles were identified. Due to the similarities in gnathobase structure, these two species could not be differentiated using light microscopy (Michels and Schnack-Schiel 2005). *Metridia* sp, and *Rhincalanus gigas* were more easily distinguished based upon mandibular morphology, although they were identified less frequently. As the presence of two mandibles (of the same species and size) is used to indicate the ingestion of a single copepod, it requires the assumption of the complete

ingestion of each copepod. Odd numbers of mandibles identified within the guts of *T. macrura* indicates that this isn't always the case and therefore predation of copepods is likely underestimated using this method. Furthermore, a lack of species-specific mandible width-weight relationships for the species identified in the gut contents of *T. macrura* also contributes to an underestimation of predation, with calculated carbon content of ingested copepods lower than reported values (Froneman et al. 1996). Despite the consistent occurrence of both protozoans and metazoans, their relative contribution to the diet was heavily outnumbered by phytoplankton. Numerically, the diatom *Fragillariopsis kerguelensis* was the most dominant phytoplankton ingested by *T. macrura* at all sites except those beyond its geographic distribution (sites 16 and 17). Only at these sites did large centric diatoms become an important component of herbivorous grazing.

4.5.2 Diet and importance of carnivory

Despite the numerical dominance of phytoplankton in the diet of adult *T. macrura*, their contribution based on carbon is less than that for carnivory. Although biovolumes are often used to weight prey counts, carbon was chosen due to both its biological significance and the large differences in carbon content of the prey consumed by *T. macrura*, especially between phytoplankton and copepods (Schmidt et al. 2006). Despite this weighting, the proportion of phytoplankton was still higher than expected compared to previous diet studies (Hopkins 1985; Hopkins and Torres 1989).

The diet of *T. macrura* from the western Weddell Sea during a similar period to that assessed in this study showed a consistent but low contribution from diatoms (Hopkins and Torres 1989). An even lower contribution from diatoms was observed in the Croker Passage during Autumn (Hopkins 1985). In both these early studies, diatoms were the only phytoplankton identified, with those diatoms identified in the guts of *T. macrura* reflective of the dominant components of the phytoplankton community present. Although several large dinoflagellates were identified in the current study, a similar pattern in phytoplankton grazing was observed. The fatty acid ratios of both 16:1(*n*-7):16:0 and 16:1(*n*-7):18:4(*n*-3) show that diatoms were more important food items than flagellates (Cripps and Atkinson 2000; Stübing and Hagen 2003). The high levels of sustained primary production over the southern Kerguelen Plateau observed during this study, primarily due to the dynamics of the frontal systems (Schallenberg et al. 2018) is significantly higher than those reported in the studies by Hopkins (1985) and Hopkins and Torres (1989). Phytoplankton therefore represent a more accessible resource in the Southern Kerguelen region and this is reflected in the larger contribution to the diet of *T. macrura* in this region.

Protozoans and metazoans comprised a maximum of 99% of the numerical diet composition of *T. macrura* and contributed at least 35% to gut carbon content, although with a high level of spatial variability. Accounting for the proportion of body carbon ingested which takes into account the size of individual *T. macrura* being assessed, provides a more accurate description of the relative role of carnivorous and herbivorous feeding. The proportion of body carbon ingested via carnivorous feeding was significantly higher than that consumed via phytoplankton grazing, often by several orders of magnitude. Although this information is based upon a snapshot of diet at the time of sampling and does not enable the assessment of temporal variability, the use of lipid biomarkers supports a more significant role for carnivory than concluded by gut content contribution alone.

Lipid biomarkers, due to the time taken for assimilation, modification and accumulation, provide a valuable source of information of more generalised feeding trends at longer time scales. The ratio of the 18:1 isomers, 18:1(*n*-9):18:1(*n*-7), commonly used to assess the importance of carnivory (Cripps et al. 1999; Stübing and Hagen 2003), was high for both males and females over the Kerguelen Plateau. The ratio between PUFA and SFA has similarly been used as a measure of carnivory for *E. superba* (Cripps and Atkinson 2000), suggesting it might be applicable to other euphausiid species. However, the use of PUFA:SFA in the present study indicates this isn't the case for *T. macrura*, with low ratios calculated that would seem to indicate little to no carnivory and is likely due to the fundamental differences in lipid storage between these two euphausiids (Falk-Petersen et al. 2000). Unlike *E. superba,* which deposit predominantly triacylglycerols, *T. macrura* synthesises wax esters, accounting for up to 70% of their total lipids (Hagen and Kattner 1998). High levels of the alcohol 20:1(*n*-9), an important component of the wax esters of *T. macrura* have been used to indicate predation on the copepod *C. acutus*, the only known other species with substantial levels of this alcohol (Hagen and Kattner 1998; Falk-Petersen et al. 1999). Accordingly, the dominant copepod ingested by *T. macrura* in the present study is likely to be *C. acutus* rather than *C. propinquus*, due to this strong biomarker signal.

4.5.3 Sexual differentiation and spatial changes in diet

Sexual differentiation in the importance of carnivory was observed across the study region, with females having consistently higher proportions of carnivory than males, which may relate to their efficiency at capturing copepods by raptorial feeding. Fäber-Lorda and Mayzaud (2010) demonstrated that larger individuals have a greater capacity to perform raptorial feeding due to increase in the length of both the second thoracopods and the heavily spinous dactylus, used for grasping prey. Although the ability to capture large motile prey items, such as copepods, is not sex-dependant females tend to be larger than males due to slower growth rates and lower mortality (Haraldsson and Siegel 2014), a trend that is consistent for the population examined in this study.

Accordingly, females may be more efficient at copepod capture than males. A peak in the proportion of dietary-derived carbon from carnivory was found in females at site 37, where the largest individuals were measured (mean length of 22.8 mm), supports this theory. Furthermore, this may also explain the faster accumulation rate of lipids by females compared to males described by Mayzaud et al. (2003). Alternatively, the sexual differences in the relative contribution of carnivory to diet and the apparent lipid accumulation rates previously described may indicate a stronger selective feeding on copepods by females, requiring larger lipid reserves to fuel reproduction in the following winter (Falk-Petersen et al. 2000; Chapter 2). Due to the low numbers of males in this study, a larger sample size is required to evaluate fully whether feeding efficiencies, selective feeding or both come into play.

Spatial differences in the diet of adult *T. macrura* were observed for both males and females, with adults in the north having a higher proportion of carnivory than those in the south. A high phytoplankton biomass in the southern extent of the study region, remnant of the Princess Elizabeth Trough phytoplankton bloom that occurred during early spring (Schallenberg et al. 2018), coincided with individuals with higher proportions of phytoplankton-based diet. Northern sites over the plateau, especially those in the Weddell-Enderby basin where primary production was at its lowest during the sampling period, had *T. macrura* with the highest levels of carnivory. This pattern in feeding highlights a plastic diet for *T. macrura*, readily consuming phytoplankton when present in high proportions due to the low energetic costs associated with filter feeding. Despite reaching similar conclusions on the importance of carnivory and especially predation on the copepod *C. acutus* as previous studies (Hopkins 1985; Hopkins and Torres 1989), the role of herbivory and carnivory in the diet of *T. macrura* is still highly variable and driven by prey availability and accessibility.

The observed sexual differentiation in dietary preferences, trends in total lipid accumulation between males and females and the apparent influences of phytoplankton standing stocks on the diet of *T. macrura* highlight the need to assess seasonal dietary shifts. Based upon the current understanding of feeding ecology, the dietary preferences of *T. macrura* during the end of winter and spring are likely very different than those described for summer over the southern Kerguelen Plateau. Depletion of lipid reserves due to the fuelling of gonadal development of both males and females and subsequent reproduction, and low phytoplankton availability prior to spring, indicate that carnivory represents the sole feeding mode of *T. macrura* during winter. A period of intense feeding during spring would then be required to facilitate both somatic growth and the rapid accumulation of lipids of more than 20% of dry weight (Hagen and Kattner 1998). Although lipids continue to increase into autumn, this initial increase is more than double recorded for any other

time-span, indicating a relatively short period of intense feeding (Hagen and Kattner 1998). This pattern in lipid accumulation coincides with the appearance of many of the dominant copepod species in surface waters during late spring, particularly *C. acutus*, which undertakes winter diapause at depth (Marin 1988; Atkinson 1998). Upon their ascent from deep waters, *C. acutus* retains high levels of stored wax esters, which are used to fuel their reproduction (Atkinson 1998). High levels of the fatty alcohol 20:1(*n*-9) in *T. macrura* sampled during this period would therefore indicate intense feeding on *C. acutus*.

4.5.4 Larval feeding

The first evidence of feeding by post-naupliar stages of *T. macrura* provided in this study confirms that larval stages are able to graze effectively. Because of long-term formalin preservation, the guts of the larvae were fragile, making classical dissection very difficult. Consequently, the use of acid digestions to remove the gut tissue was the only option available to examine feeding; therefore, only those diatoms were observed. Lipid reserves of larvae are sufficient for the development from nauplii to calyptopis, the stage in which the first rudimentary mouthparts are developed to allow feeding (Meyer et al 2002). Lipid reserves of further developmental stages, however, are low and do not support continued development, so larvae are required to feed (Meyer et al. 2002; Meyer et al. 2003). The diet of larval *T. macrura* has yet to be explored, restricting the ability to understand their ontogenetic development. Diatoms have been shown to play an almost exclusive role in the diet of larval *E. superba,* with the development of a functional feeding basket in F II aiding their capture and ingestion (Marschall 1985). Given that filter feeding represents the only mode of feeding available for larvae, especially early stages, diatoms were unsurprisingly identified in both early (FI-FIII) and late (FIV-VI) stages. Similar quantities of diatoms ingested by both early and late furcilia however was unexpected, due to the increase in size from early to late furcilia and the advancement in feeding appendage morphology (Chapter 3, Appendix B). A lack of identifiable particles in calyptopis stages may indicate a period of feeding inactivity, with larvae able to survive short periods of non-feeding (Meyer et al. 2002). Alternatively, the extremely small setal distances of secondary setae of the maxilla of 2.8 µm would allow them to feed on small flagellates, which would not be evident with the methods used in this study to assess larval diets.

A high filter feeding efficiency of post-naupliar *T. macrura* larvae is identified by the arrangement of primary and secondary setae of the maxilla. The densely packed primary setae of the maxilla, less than 15 µm spacing and small secondary setal distances, generally lower than 4 µm, indicate efficient grazing on a large size spectrum of phytoplankton, similar to that recorded for larval *E. superba* (Marschall 1985). Like *E. superba*, thoracopods of larval stages have begun to develop by F II, however the second thoracopod has yet to become elongated and is likely not involved in the

capture and handling of motile prey items in early stages. Unlike adults, lipid profiles of late furcilia stages indicates a dependence on flagellates over diatoms, the same developmental phase in which thoracopods are fully developed (Hagen and Kattner 1985; Chapter 3).

4.5.5 Feeding Mode of *T. macrura*

The mechanics of *T. macrura* feeding remain unclear. Unlike other genera of euphausiids, the feeding basket of *T. macrura* is relatively rudimentary without any complex interlocking systems present in other Southern Ocean euphausiid species (Hamner 1988). Although intersetal distances of primary setae of the thoracopods are comparable to those of *E. superba*, at 40-50 µm, the distances between secondary setae are considerably larger in *T. macrura* (McClatchie and Boyd 1983). Furthermore, thoracopod secondary setae of adult *T. macrura* are substantially shorter than those of *E. superba*, inhibiting the formation of a fine feeding basket created by the interlocking of these primary and secondary setae (McClatchie and Boyd 1983; Hamner 1988). The dense, interlocked structure of *E. superba* feeding baskets have been suggested to acts more like paddles than sieves as determined by Reynolds numbers that express the ratio of internal to viscous forces in fluid flow. McClatchie and Boyd (1983) found that at high velocities of water flow experienced during filter feeding, Reynolds numbers of <1.0 indicate that flow is dominated by viscous forces, impeding flow through interlocked primary, secondary and tertiary setae. Using the same assumptions of seawater density and molecular viscosity at high flow velocity, the Reynolds number of secondary setae of *T. macrura* thoracopods are up to 4 times greater than those estimated for *E. superba*. The structure of the feeding basket of *T. macrura* would therefore suggest its primary use is for predation, with more streamlined thoracopods, not impeded by viscous forces on primary and secondary setae, allowing for the rapid spreading and contracting of thoracic limbs to capture copepods (Mauchline and Fisher 1969). Although there is no substantial evidence as to the role of the second thoracopods, it is likely they play an important role in grasping and manipulating prey.

The underlying structure of the feeding basket of *T. macrura* appears to be well adapted to capturing large motile prey items. The second thoracopod, bending between the merus and carpus, is likely used to grasp and manipulate prey towards the mandible for slashing and cutting. This is aided by both the mandibular palp and large, robust spines on the outer margins of the maxillules. The ability to efficiently graze phytoplankton, however, does not appear to be supported by the feeding basket. The distances between primary and secondary setae of the thoracopods are substantially larger than the dominant phytoplankton species identified in guts of *T. macrura*. The biomechanics of feeding by compression filtration used by *E. superba* has been well described, allowing efficient grazing of particles as small as 2 µm (Hamner 1988). The relatively large spacing of primary and secondary setae indicates that this method of particle filtration would be inefficient,

and not account for the size range and quantity of phytoplankton ingested by *T. macrura*. It is possible that, like larval stages, adult *T. macrura* rely upon maxillules and mandibles to filter feed, with the mesh provided by primary and secondary setae small enough to allow the capture of the diatoms. Although this method is inefficient compared to the volume swept clear by the feeding basket of *E. superba*, it supports the trends observed in this study where phytoplankton are ingested when present in high abundances; this warrants further investigation.

4.6 Conclusions

The morphological traits of *T. macrura* indicate adaptations suitable to an omnivorous diet. Previous studies that employed the use of coarse dietary analysis and lipid biomarkers have confirmed this trait, however the level of detail in these earlier studies has been insufficient to fully evaluate the diversity and extent of variation in diet. The results of this study corroborate that *T. macrura* are omnivorous, however the relative importance of herbivory and carnivory varied both between sexes and spatially. The Antarctic copepod *C. acutus* was the most important dietary component of *T. macrura* and was identified by unique lipid biomarkers and mandibles that resemble those of *C. acutus*. Herbivory also played a more important role in the diet of *T. macrura* than expected and was likely a response to the sustained high primary productivity of the region, highlighting the plastic nature of *T. macrura*. Variations in primary production of the Southern Ocean prompt the need for further investigation into the temporal changes in dietary preferences, especially during the onset of spring when intense feeding is required due to the energetic demands associated with reproduction.

Feeding in larval stages was confirmed with diatoms observed in the guts of furcilia. The species of diatoms identified corresponded with those consumed by adults, highlighting an overlap in feeding. Unlike adults, larvae do not yet have the morphological modifications to feeding appendages needed to facilitate carnivory, and their small size precludes them from feeding on metazoans such as copepods. However, there is evidence to suggest that late furcilia stages (FIV-FVI) do ingest flagellates and therefore are beginning to develop the capacity to capture motile prey. These observations illustrate a succession in the relative importance of herbivory to the diet of larval *T. macrura*, with calyptopes and early furcilia relying upon diatoms and late furcilia, with the use of developing thoracopods feeding upon energy rich motile flagellates.

Chapter 5

Thysanoessa macrura in the southern Kerguelen region: population structure and biomass

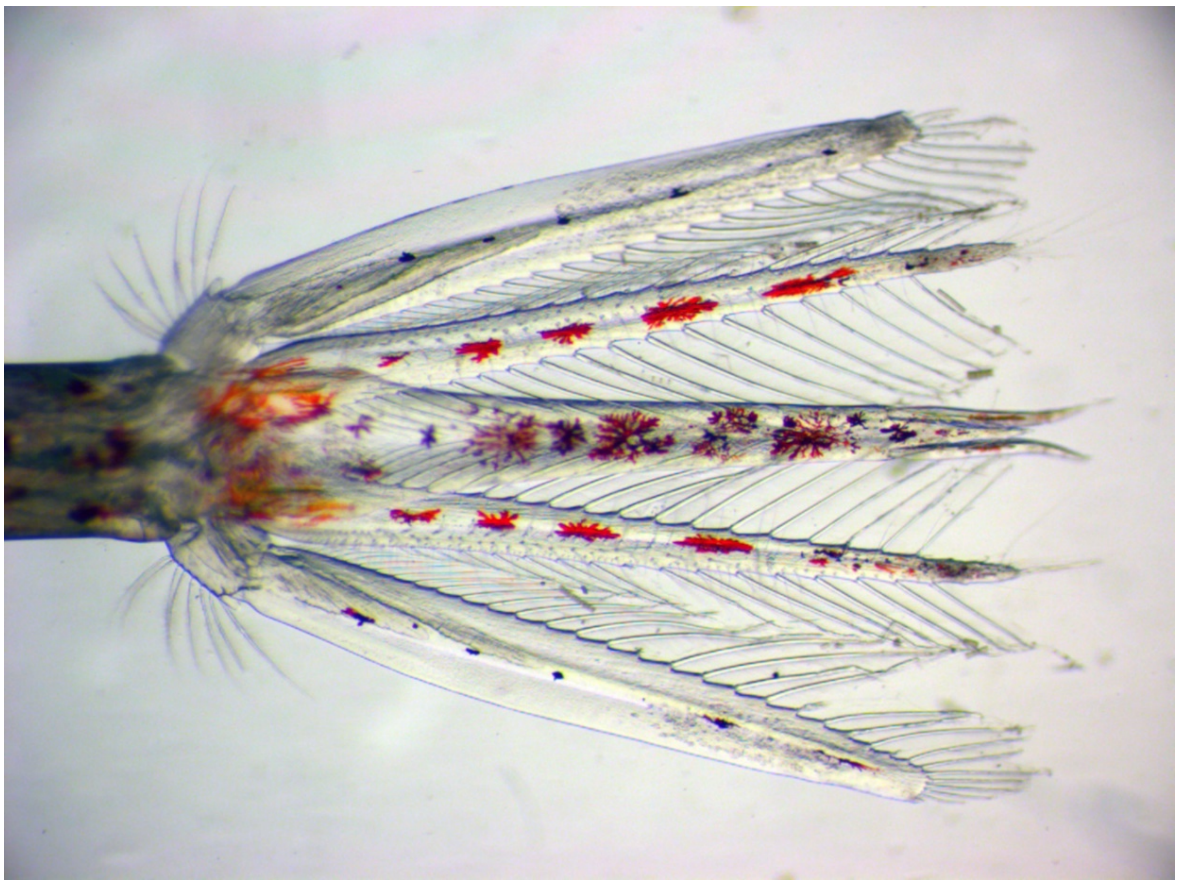

Microscopic image of the telson of *Thysanoessa macrura*

Photograph by Jessica Melvin

All the research presented in this chapter is currently submitted to Deep-Sea Research II

Wallis JR, Maschette D, Kawaguchi S, Swadling KM (2019) Thysanoessa macrura *in the southern Kerguelen region: population structure and biomass. Submitted to Deep-Sea Research II.*

5.1 Abstract

Thysanoessa macrura is well adapted to the strong seasonality of the Southern Ocean. A flexible diet, large lipid reserves and a winter reproductive period provide *T. macrura* with the ability to capitalise on the pulses of primary and secondary reproduction in spring and summer. The population dynamics of *T. macrura* were examined over the southern Kerguelen Plateau region as part of a large-scale ecosystem assessment. Larval stages were present in high abundances, exceeding 4000 Ind. 1000 m^{-3}, with a peak in early furcilia (FI – FIV) and lower abundances of calyptopis stages (CI – CIII) indicating the end of a prolonged spawning period. High abundances of *T. macrura* were recorded throughout the entire study region, although they tended to be highest over the southern extent of the BANZARE bank and Princess Elizabeth Trough. This maximum appeared to be driven by the presence of the copepod *Calanoides acutus*, a dominant prey source. The first biomass estimates of *T. macrura* were determined for the region using length-frequency and abundance distributions. A mean biomass of 1.66 mg m^{-3} was calculated, however localised biomass over the southern tip of the BANZARE Bank exceeded 9 mg m^{-3} in the upper 200 m of the water column. The high biomass of *T. macrura* highlights their significance as an energy-rich resource for larger predators, inferring they play a currently underappreciated role in pelagic food-webs of the Southern Ocean.

5.2 Introduction

Euphausiids are one of the most abundant taxonomic groups of Southern Ocean zooplankton, and their importance as a key link in the Southern Ocean food-web has been well documented (Atkinson et al., 2012). New insights into the heterogeneity in food-web structure of the Southern Ocean have highlighted differences in the role of 'krill' in the major oceanic sectors, with the importance of *E. superba* reduced compared to other euphausiid species in both the Indian Ocean and West Pacific sectors (McCormack et al. 2019a). East Antarctica supports lower densities of *E. superba* compared to the South Atlantic (Constable et al. 2000; Kawaguchi et al. 2010), suggesting that other lower trophic level species could fill important roles in the food web. *Thysanoessa macrura* is a species of euphausiid that is highly abundant and has a wide distribution, from the sub-Antarctic to the Antarctic continent (Cuzin-Roudy et al. 2014; Haraldsson and Siegel 2014). The Kerguelen Plateau has been identified as one of the most important regions for productivity in the Indian sector of the Southern Ocean, supporting a high biomass of primary consumers and vertebrate predators including mesopelagic fish, birds and migrating whales (Tynan 1998; Trebilco et al. 2019). The unique oceanography of the southern extent of the Plateau causes upwelling of nutrient-rich deep water across the shallowing Plateau. This upwelling supports high levels of

primary productivity, extending into mid-late summer and well beyond typical 'spring blooms' that occur in other regions (Schallenberg et al. 2018).

Life-history traits of *T. macrura* demonstrate that this small euphausiid species is well adapted to the seasonality of the Southern Ocean, where there are light-driven pulses of high productivity during spring and summer contrast with little to no productivity during the dark autumn and winter months. The diet and lipid storage of *T. macrura* facilitate a decoupling of gonad maturation and spawning from these peaks in primary productivity, allowing for an advantageous winter reproductive period (Chapter 2). Lipids stored within the carapace fuel gonad maturation and spawning occurs during mid – late winter, with larval stages reaching surface waters after an ontogenetic ascent during the onset of spring. The development from larvae to juveniles occurs within the first year, fuelled by the ability of larvae to feed at the beginning of peaks in primary productivity. Furthermore, sexual maturation occurs within 13 months from hatching, with adults potentially reproducing in the year after hatching (Nordhausen 1994a; Chapter 2).

A broad latitudinal distribution that encompass both sub-Antarctic and Antarctic waters demonstrates the ability of *T. macrura* to thrive in a wide temperature range from -2 °C to 8 °C. This temperature tolerance indicates the capacity of *T. macrura* to cope with predicted increases in temperature in high latitude waters, with evidence to suggest they may be positively affected by these changes, such as increased growth rates (Driscoll et al. 2015). Recent descriptions of their life-history and population dynamics in the Southern Ocean have provided new insights into the ecology of *T. macrura* (Chapters 2-4; Wallis et al. 2019a – Appendix F). *Thysanoessa macrura* have been found to live for 5+ years, with a highly skewed ratio of females to males and females growing larger and living longer than males, a similar pattern observed for *E. superba* populations (Haraldsson and Siegel 2014).

Dietary plasticity, with opportunistic feeding on both phytoplankton and copepods, is intrinsically linked to the flexibility and success of this species. Predation on the copepod *Calanoides acutus* has been identified through the wax esters stored by *T. macrura* (Hagen and Kattner 1998; Chapter 4). Despite being decoupled from seasonal trends in primary productivity it appears that *T. macrura* has a close association with *C. acutus*, with an increase in total lipids in *T. macrura* during summer co-occurring with the ascent of lipid-rich *C. acutus* after their winter diapause (Atkinson 1998). High total lipids that are depleted when fuelling gonadal development and reproduction during winter (Chapter 2), which are regained during summer, can account for greater than 50% of dry weight, significantly higher than most other euphausiids (Falk-Petersen 2000). Their high abundance and calorie-rich lipid content suggest that *T. macrura* could provide a valuable resource for foraging

predators; however, large-scale estimates of the biomass contribution of *T. macrura* to the pelagic ecosystem have yet to be made.

Here we report on the population ecology of *T. macrura* in the Kerguelen Plateau region, exploring abundance, distribution and the key drivers thereof. We also calculated the biomass of *T. macrura* over the southern Kerguelen Plateau, the first estimate for the region and the east Antarctic.

5.3 Methods

5.3.1 Study region and sampling regime

Specimens of *Thysanoessa macrura* were collected between late January and mid-February during the Kerguelen Axis research voyage by the *RV Aurora Australis* in the southern Kerguelen Plateau region. The study area encompassed the southern Kerguelen Plateau, situated over the BANZARE Bank in the north and bounded by the Princess Elizabeth Trough in the south (Figure 5.1a). The eastern extent was situated in the Australian-Antarctic Basin and the western extent in the Weddell-Enderby Basin. The area was transected by both the Southern Antarctic Circumpolar Current Front (SACCF) and the Southern Boundary of the Antarctic Circumpolar Current (SB), and bound by the westward flowing Antarctic Slope Front (ASF) at its southern extent.

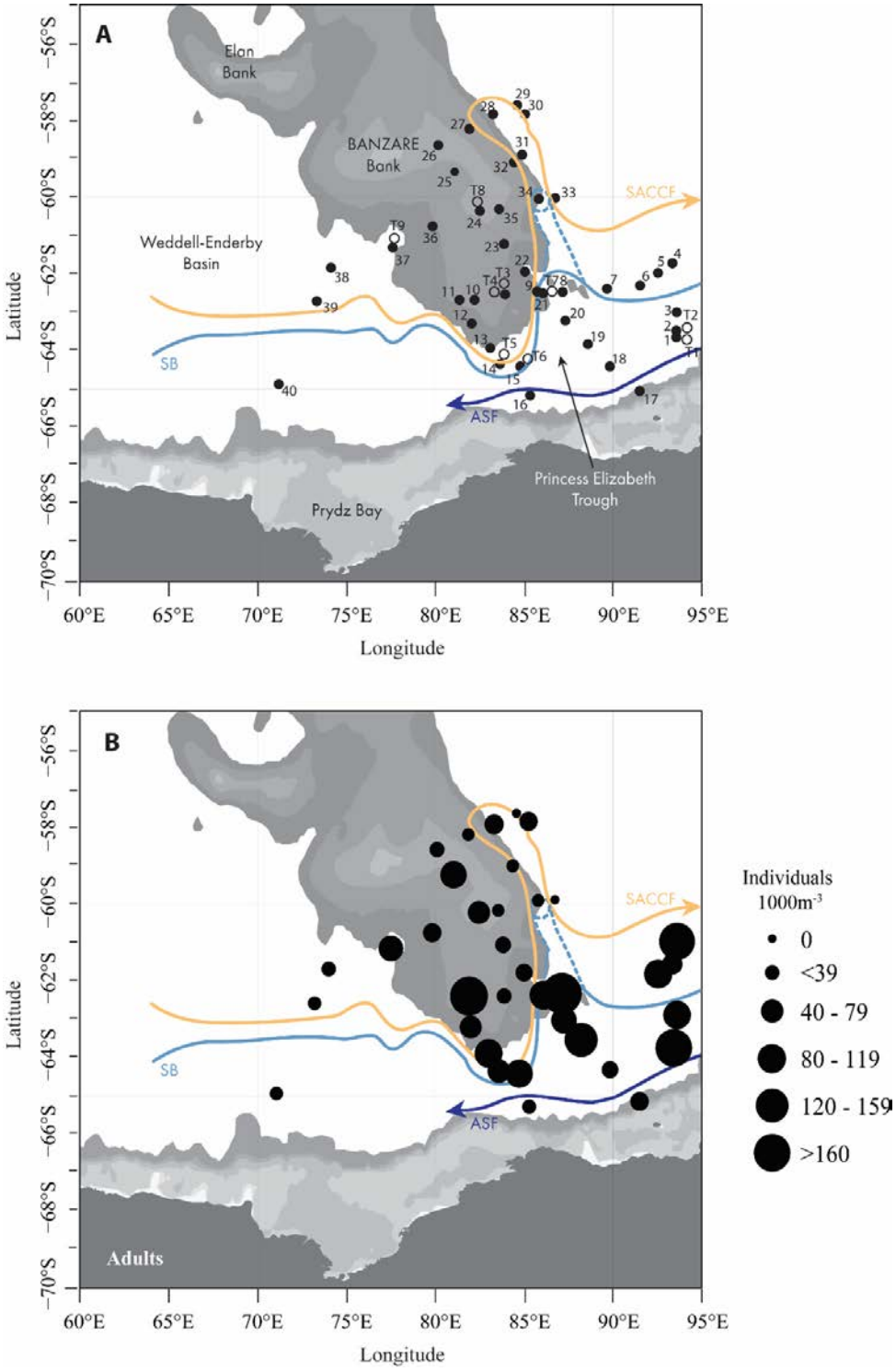

Figure 5.1. Sampling region of the southern Kerguelen plateau. Major oceanographic features of the area are indicated: the Southern Antarctic Circumpolar Current Front (SACCF), the Southern Boundary of the Antarctic Circumpolar Current Front (SB) including an inferred northern incursion (dashed line) and the Antarctic Slope Front (ASF). **A**. Sampling sites for *Thysanoessa macrura* using RMT8+1 nets. Filled circles indicate routine trawls and open circles indicate target trawls. **B.** Abundance of adult *Thysanoessa macrura* collected from routine RMT8 net trawls (Ind. 1000 m^{-3}).

A Rectangular Midwater Trawl (RMT) 8+1 net, equipped with a flow metre, was deployed from the surface to 200 m depth in standard double oblique tows to sample *T. macrura* at 40 sites (Baker et al. 1973). Seven additional target trawls were performed for regions of interest, identified by the ship-equipped scientific echo-sounder. The RMT was then deployed to the depth of interest and towed for 5-7 minutes. At each site, adult *T. macrura* were collected from the RMT8 net (8 m^2 mouth area, 4.5 mm mesh size) and larval stages from the RMT1 net (1 m^2 mouth area, 315 µm mesh size). Upon collection, RMT8 samples were sieved and the total volume of the sample recorded. If the total sample exceeded 1 L in volume, the sample was split volumetrically, and a subsample removed and immediately stored in 10% buffered formalin. When samples required subsampling, *T. macrura* (when present) were removed from the remaining sample and frozen at -80°C. RMT1 samples were fractionated using a Motoda Box plankton splitter (Motoda 1959) prior to preservation in 10% buffered formalin.

5.3.2 Lipid content and allometry

Frozen adult *T. macrura* were used to quantify the total lipid content and lipid class profiles. Prior to dissection, individuals were measured for their total length and wet weight and then the carapace portion of the krill was carefully dissected while frozen to minimise the loss of lipids from the lipid deposit. Body length measurements of adults were measured using length standard 2, from the tip of the rostrum to the anterior edge of the sixth abdominal segment (Mauchline 1981).

A modified Bligh and Dyer (1959) method, using a methanol:dichloromethane:water solvent mixture of 20:10:7 was used to quantitatively extract lipids over 24 hours. Phase separation was then achieved by the addition of 10 mL dichloromethane and 10 mL of saline Milli-Q water. The extracted lipid was concentrated via rotary evaporation and the total lipid measured gravimetrically. Extracted lipids were then used to assess the dominant lipid classes present using IATROSCAN MK-5 TLC/FID (Iatron Laboratories, Tokyo, Japan) thin layer chromatography-flame ionisation detection. Aliquots of 1 µL were spotted onto chromarods and developed for 25 min in a hexane:diethyl-ether:acetic acid solution (v:v:v 90:10:0.1) and dried at 100 °C for 10 minutes. Lipid class peaks were then identified and quantified by comparison to a standard solution of known quantities of wax esters, triacylglycerols, free fatty acids, sterols and phospholipids (Virtue et al. 2016).

Adult individuals frozen immediately after collection were also used to establish allometric relationships between wet weight and dry weight, and both with body length. Specimens were measured from the tip of their rostrum to the base of their 6^{th} abdominal segment, blotted dry and weighed. Larval stages, both calyptopis and furcilia, were formalin-preserved prior to measuring and weighing and were measured from the tip of the rostrum to the base of the telson. Both calyptopis

stages (CI – CIII) and furcilia stages (FI – FVI) were pooled, providing allometric relationships for calyptopis and furcilia respectively. All individuals were dried at 60 °C for 24 h or until constant mass was reached. The allometric power function was used to describe the relationships between body length and wet weight, dry weight and lipid content;

(5.1) $y = ax^b$

where y is the biomass parameter: wet weight (mg), dry weight (mg) or lipid content (mg Ind^{-1}) and x is body length (mm).

5.3.3 Population analysis

Generalised additive models (GAMs) were used to assess the influence of environmental and biotic variables on the abundance of adult *T. macrura* over the southern Kerguelen Plateau (the mgcv package in R; Wood 2004). Predictor variables included total depth of site, photosynthetically active radiation (PAR), chlorophyll *a* concentration, surface temperature and temperature at 200 m depth, abundance of *C. acutus* and abundance of foraminifera, both of which are dominant food items for *T. macrura* in the region (Chapter 4). Models were fitted using a negative binomial distribution and model selection was carried out with a stepwise approach using the Akaike Information Criterion (AIC). Models within 2 AIC units were considered possible.

The biomass of *T. macrura* was determined using kernel k-nearest neighbour interpolation. The length frequency distributions were used at each site to determine the total wet weight of *T. macrura* based on the allometric relationship between length and wet weight established for the region. Total wet weight of *T. macrura* was then scaled to the abundance determined for each site. Bootstrapped k-nearest neighbour interpolation was used to determine the biomass of *T. macrura* in the upper 200 m of the water column across the entire sampling region. Bootstrapped resampling was performed with 100 replicates and the nearest 8 neighbours (sites) used. Points were then masked using a convex hull with a 1-degree buffer to ensure that biomass was only calculated within the region of sampling.

5.4 Results

5.4.1 Abundance and distribution

Thysanoessa macrura were collected at 40 sites sampled by RMT trawls, with total abundance ranging from 0 - 5231 Ind. 1000 m^{-3} (Table 5.1). Due to the high abundances of *T. macrura* at site 1, exceeding 5000 Ind 1000 m^{-3}, this site was excluded from all subsequent analysis. Abundances tended to be higher in the southern extent of the region, reaching up to 160 Ind. 1000 m^{-3} over the tip of the BANZARE Bank and Princess Elizabeth Trough (Figure 5.1b). Abundances in the north were approximately half of those measured in the south, reaching a maximum of 80 Ind. 1000 m^{-3}. No evidence of reproduction was found for adults, with females identified as sexual development stage (SDS) 7 and males as sexual developmental stage (SDSM) 2 (Chapter 2).

A similar distributional pattern for larvae was observed, with the highest abundances centred over the southern tip of the BANZARE Bank (Figure 5.2). Larval stages were grouped by developmental stage according to Chapter 2 to identify potential larval cohorts present in the region. Calyptopis stages (CI – CIII) had the lowest abundance of all larval groups, with abundances ranging from 0 – 502 Ind. 1000 m^{-3} (Table 5.1). Early furcilia (FI – FIII) had the highest abundance (0 – 4270 Ind. 1000 m^{-3}), followed by late furcilia (FIV -FVI) with a range of 0 – 2512 Ind. 1000 m^{-3} (Table 5.1). Despite large differences in total abundances of the three larval groups, with a clear peak in early furcilia stages, all groups were spread throughout the study region, with calyptopis stages present at 31 sites and early and late furcilia stages found at 35 sites.

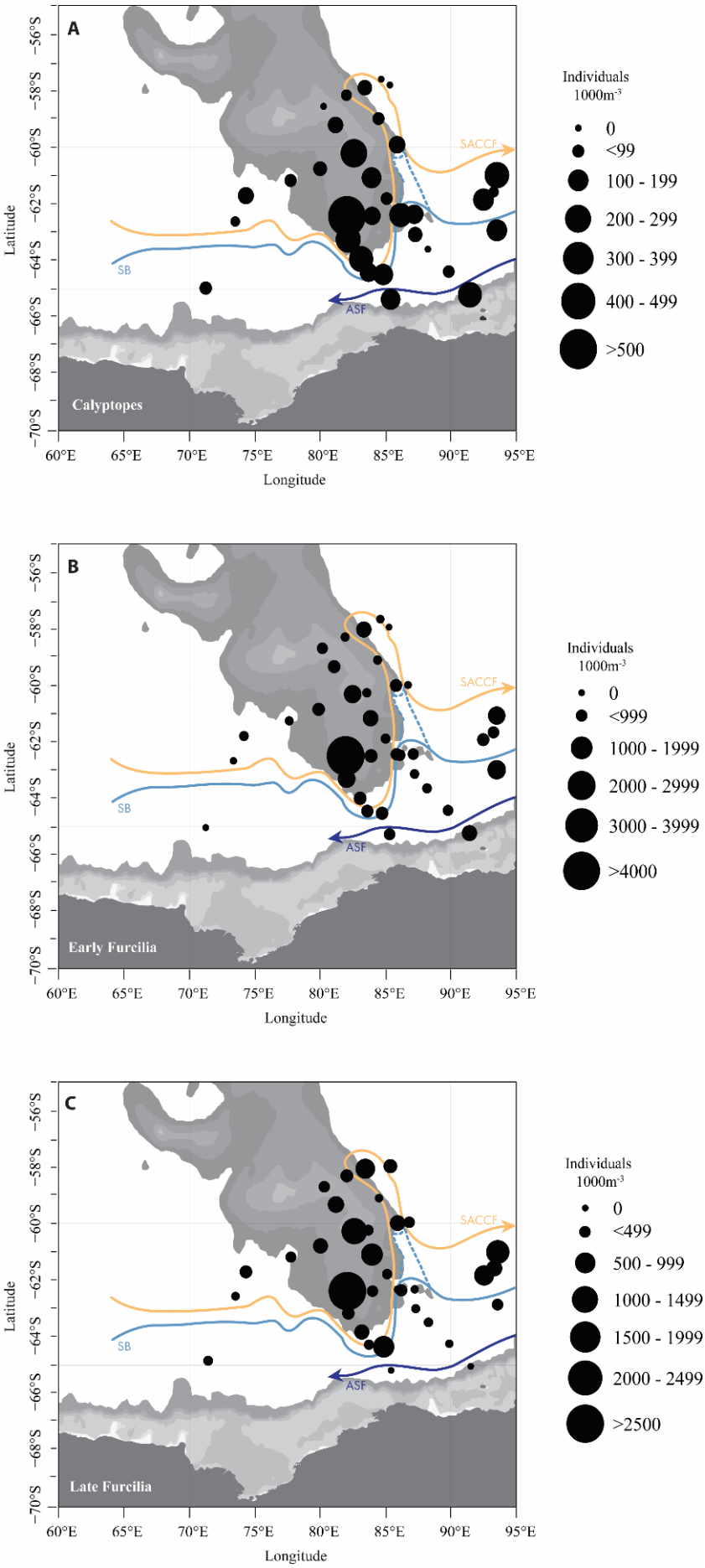

Figure 5.2. Abundance of the larval stages of *Thysanoessa macrura* collected from routine RMT1 trawls. **A.** Calyptopis stages (CI-CIII) **B**. Early furcilia (FI-FIII) and **C**. Late furcilia (FIV-FVI).

Table 5.1. Population characteristics including the female : male ratio, sex-specific abundance of adults and abundance of pooled developmental stages; calyptopis (CI - CIII), early furcilia (FI – FIII) and late furcilia (FIV -FVI) of *Thysanoessa macrura* for the three areas identified with the southern Kerguelen Plateau region. Values are provided as mean ± standard deviation (and range). N indicates the number of sampling sites within each area. Note that site 1 is only included in the whole region overview of adult abundance.

Area	Number of sites	Sex ratio (F:M)	Adult abundance (Ind. 1000 m^{-3})			Larval abundance (Ind. 1000 m^{-3})		
			Adult	Female	Male	Late furcilia	Early Furcilia	Calyptopis
Whole region	40	5:1	281 ± 225	216 ± 171	66 ± 54	226 ± 74	290 ± 117	85 ± 21
		(1:1 - 12:1)	(6 – 5231)	(5 - 3978)	(1 - 1254)	(0 - 2512)	(0 - 4270)	(0 - 581)
1	13	4:1	44 ± 12	32 ± 11	12 ± 6	340 ± 189	475 ± 319	101 ± 37
		(1:1 - 12:1)	(6 - 143)	(5 - 92)	(1 - 51)	(9 - 2512)	(2 - 4270)	(5 - 502)
2	16	4:1	50 ± 12	39 ± 14	11 ± 3	250 ± 78	221 ± 84	87 ± 42
		(1:1 - 4:1)	(18 - 124)	(13 - 100)	(5 - 24)	(0 - 947)	(0 - 1114)	(0 - 581)
3	10	4:1	57 ± 18	47 ± 15	11 ± 4	44 ± 22	147 ± 59	62 ± 18
		(2:1 - 10:1)	(4 - 162)	(3 - 131)	(1 - 32)	(0 - 227)	(0 - 617)	(0 - 159)

A qualitative assessment of the lipid deposit indicated that all adults had full deposits, causing a swelling of the carapace, extending from the tip of the rostrum to the posterior region of the carapace. The quantitative lipid extraction from adult *T. macrura* confirmed large lipid contents, with females possessing a mean lipid content of 43% of dry weight and males, 35% of dry weight (Table 5.2). A comparison of total lipid content of adults with the lipid stored within the carapace indicates that a large proportion of the lipids stored by *T. macrura* is located within the lipid deposit, which comprised 90% and 92% of total lipid content by wet weight for females and males, respectively (Table 5.2). The proportions of the major lipid classes were consistent between females and males. Wax esters and polar lipids were the dominant classes, contributing greater than 50% and 40%, respectively (Table 5.2). The proportions of the major lipid classes were consistent between whole *T. macrura* and the lipid deposit. Length-weight relationships for *T. macrura* followed traditional allometric relationships, with a summary of derived equations provided in Table 5.3.

5.4.2 Population structure

Cluster analysis separated three distinct clusters based upon length-frequency data of adult males and females (Figure 5.3a). The clusters were used to explore spatial differences in *T. macrura* population structure, with clusters geographically linked. Based on this, the study region was categorised into three distinct areas (Figure 5.3b). Area 1 was located over the southern tip of the BANZARE Bank, restricted to the south and east by the SB. Area 2 was located adjacent to area 1, and encompassed the northern reaches of the study region with the SB forming the boundary with area 3 to the south; area 3 encompassed the entire study region south of the SB.

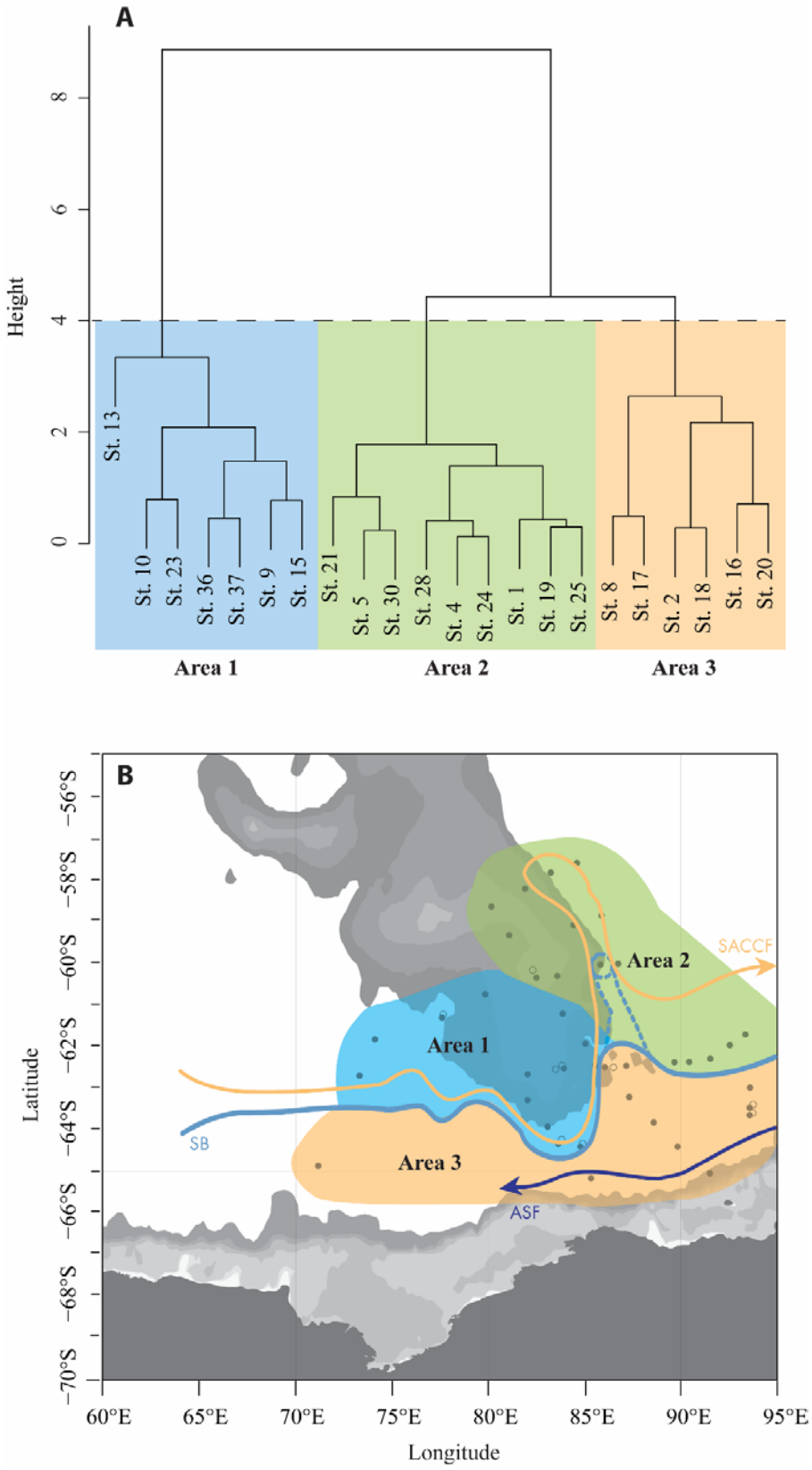

Figure 5.3. The three areas defined by cluster analysis based upon length-frequency distributions of male and female *Thysanoessa macrura*. **A**. Dendrogram defining clusters **B**. Spatial coverage of clusters.

Table 5.2. Quantitative lipid content of adult *Thysanoessa macrura*. Total lipids are reported as both % of wet weight and % of dry weight for whole individual males and females, for comparison with lipid deposits within the carapace. The carapace : body ratio is reported for those individuals that were dissected for their lipid deposits. Lipid class data include free fatty acids (FFA), polar lipids (PL), sterols (ST), triacylglycerols (TAG) and wax esters (WE). Values are provided as mean ± SD.

							Percentage lipid class (of total lipids)				
	n	Wet weight (mg)	Dry Weight (mg)	Carapace:Body (%)	Total lipids (% of wet weight)	Total lipids (% of dry weight)	*n*	FFA	PL	ST	TAG	WE
Whole												
Female	11	78.58 ± 14	21.43 ± 5.79	-	10.89 ± 2.18	42.46 ± 15.6	12	1.39 ± 0.58	43.15 ± 3.62	0.7 ± 0.28	0.7 ± 0.92	54.06 ± 4.71
Male	6	52 ± 10.6	15.43 ± 4.16	-	9.76 ± 1.64	34.93 ± 13.7	6	1.82 ± 0.35	40.47 ± 7.97	1.07 ± 0.49	2.36 ± 0.49	54.68 ± 8.20
Carapace												
Female	5	60.64 ± 42.75	-	66.04 ± 7.06	9.73 ± 2.68	-	5	1.82 ± 1.21	40.02 ± 4.34	0.8 ± 0.51	2.25 ± 1.39	55.11 ± 4.21
Male	3	32	-	63.3	9.02	-	4	2.08 ± 1.47	43.6 ± 4.35	0.92 ± 0.44	2.63 ± 1.68	50.77 ± 2.01

Table 5.3. Allometric relationships ($y = ax^b$) established for *Thysanoessa macrura*. Relationships are provided for adults and pooled developmental stages (calyptopis and furcilia). N indicates the sample size for each analysis.

Allometric relationship (y/x)	Developmental stage	N	Total length (mm)	*a*	*b*	*b* SE	R^2	F	P
Wet weight/Total length	Calyptopis	5	1.0 - 1.72	0.234	0.090	0.200	0.059	0.188	0.694
	Furcilia	21	5.8 - 9.6	0.006	3.340	0.351	0.777	66.187	<0.001
	Adults	327	11.63 - 23.23	0.005	3.230	0.121	0.698	749.235	<0.001
	Total	353	1.0 - 23.23	0.005	3.223	0.116	0.769	1166.900	<0.001
Dry weight/Total length	Calyptopis	5	1.0 - 1.72	0.006	1.221	0.399	0.737	8.396	0.0626
	Furcilia	21	5.8 - 9.6	0.0003	3.855	0.288	0.863	119.728	<0.001
	Adults	327	11.63 - 23.23	0.002	3.111	0.136	0.629	550.861	<0.001
	Total	353	1.0 - 23.23	0.002	3.117	0.130	0.769	896.300	<0.001
Lipid content/Total length	Adults	18	12.94 - 22.45	0.196	1.217	0.711	0.203	4.062	0.061

Analysis of the fixation experiment indicated that *T. macrura* shrinks when preserved in a 10% formalin solution. After 1.5 years, *T. macrura* shrunk by an average of 1.4% (±3.7 SD) in total body length, with shrinkage linear across their size range whereby;

(5.2) Unpreserved length = 0.896 x preserved body length + 2.04 (R^2= 0.88) (Figure C2; Appendix C).

The size of adult *T. macrura* was variable across the study region. A large disparity in body length was observed between females and males, with females between 11.6 mm – 28 mm in total length and males from 10.8 mm – 21.7 mm. Despite each of the three defined areas possessing distinctive size-structured adult populations (Figure 5.4), there was no difference in the mean sex ratio of *T. macrura*, with a female : male ratio of 4:1 (Table 5.1). Area 1 had the largest females in the region, with a mean total length of 21.4 mm (± 2.46 SD) while males were on average 17 mm (± 1.8 SD). Area 2 had the smallest females and males, with females measuring 16.8 mm (±2.2 SD) and males 15.8 mm (±1.5 SD). Area 3 was defined by females with a mean length of 19.2 mm (±2.8 SD) and males of 16.1 mm (± 2.1 SD).

Little variation in the abundance of females and males was observed between the three areas, with patterns in abundance consistent with the whole region mean abundance of 39 Ind. 1000 $^{-3}$ and 11 Ind. 1000 m^{-3} for females and males, respectively (Table 5.1). Variations in the abundances of the three larval groups, however, was observed. Area 1 possessed the highest abundances of all three larval stages and area 3 the lowest; within all three areas, early furcilia were the most abundant larval group (Table 5.1)

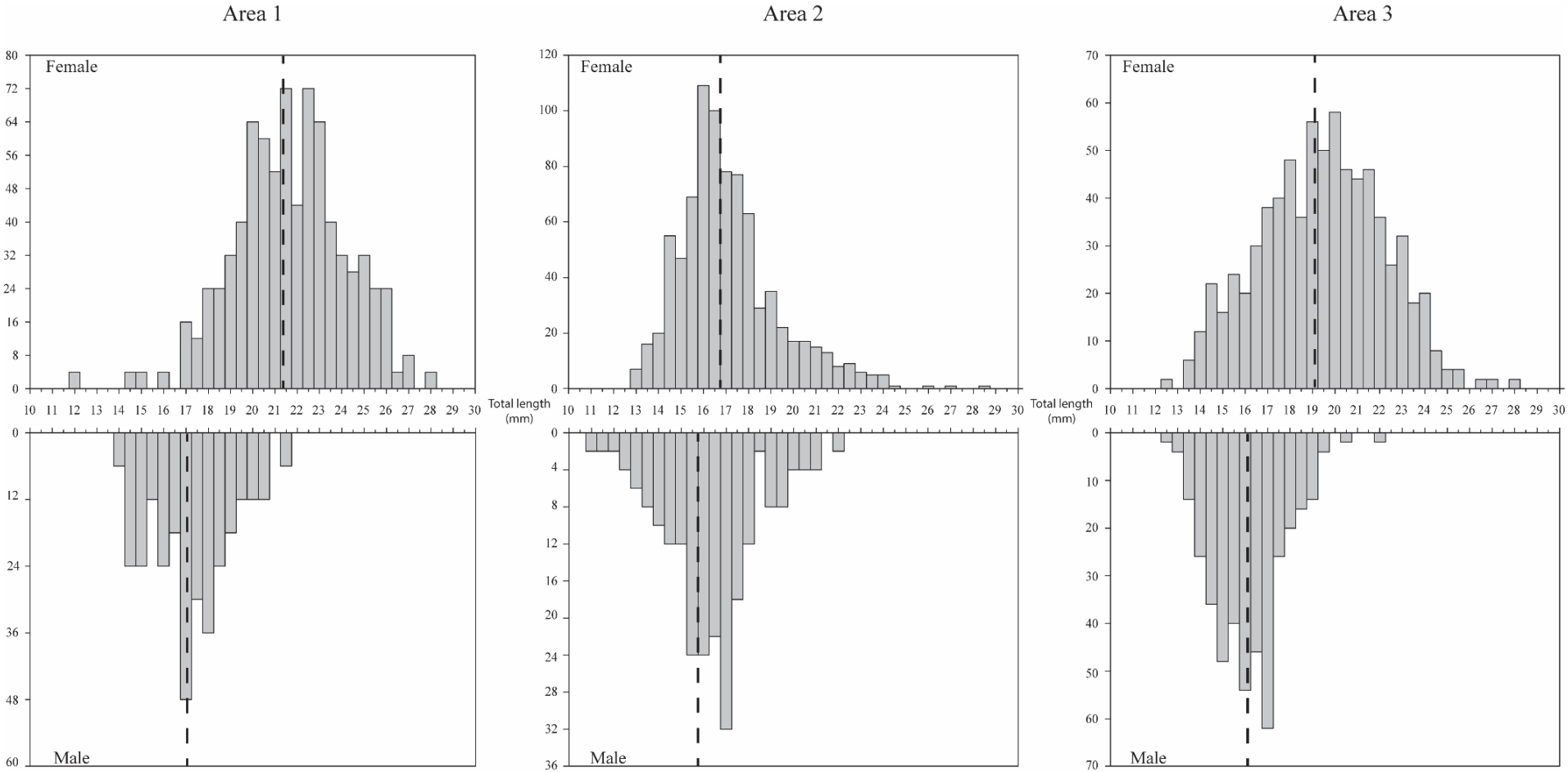

Figure 5.4. Length-frequency distribution of male and female *Thysanoessa macrura* from routine RMT8 trawls for the three areas identified based upon length-frequency cluster analysis. Dashed lines indicate the mean length of each sex from the defined areas.

5.4.3 Population drivers and biomass

The best model to describe the abundance of adult *T. macrura* is given by:

(5.3) Abundance ~ β_0 + salinity$_s$ + Log (*C. acutus*)$_s$ + temperature$_{200s}$

where β_0 is the intercept and subscript *s* denotes spline smoothing (adjusted R^2 = 0.126, deviance explained = 56.7%, n = 36). The abundance of adult *T. macrura* increased in abundance at the highest salinities recorded (34.2 – 34.4), increased with the abundance of *C. acutus* and slightly decreased with increasing temperature. A full description of the model is provided in Appendix D (Table D1 and Figure D1)

Based on wet weight, allometric relationships of total length-wet weight and abundance, a total of 339,124 t (320,918 t - 357,331 95% confidence interval) of adult *T. macrura* was estimated to be present within the upper 200 m of the southern Kerguelen Plateau, within the sampling region (masked to 1 degree) of 1,011,493 km^2. The biomass of *T. macrura* varied from a low of 0.04 mg m^{-3} to 9.53 mg m^{-3} with a mean biomass of 1.68 mg m^{-3} (± 0.045 mg m^{-3}) (Figure 5.5, Table D2; Appendix D).

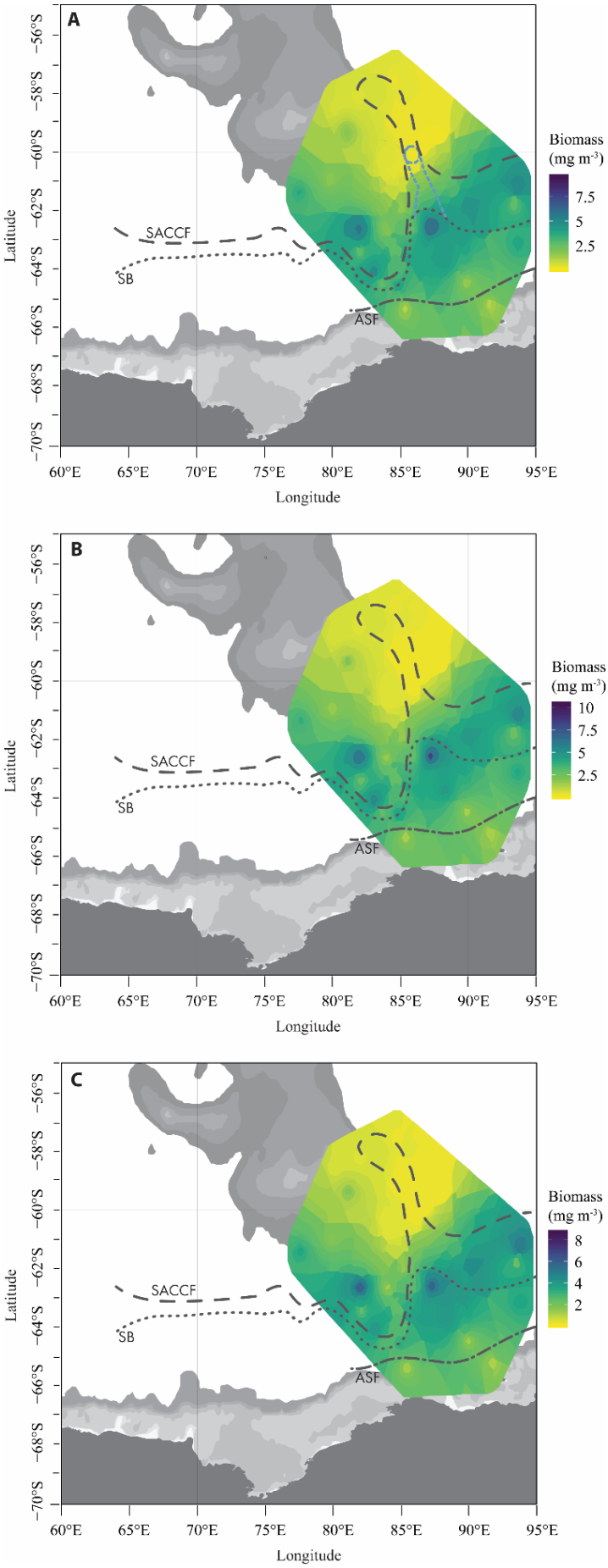

Figure 5.5. Calculated biomass of *Thysanoessa macrura* in the upper 200 m of the southern Kerguelen Plateau. **A**. Mean biomass **B**. Upper estimate of biomass based upon upper 95% confidence interval **C**. Lower estimate of biomass based upon lower 95% confidence interval

5.5 Discussion

5.5.1 Population structure

Thysanoessa macrura is consistently identified as a dominant species, dominating zooplankton assemblages in all major regions of the Southern Ocean (Cuzin-Roudy et al. 2014). Abundances regularly exceed those of other euphausiids with overlapping distributions, including *Euphausia crystallorophias*, *Euphausia triacantha* and *E. superba* in both western and eastern Antarctica (Hosie et al. 2000; Steinberg et al. 2015). Abundances of *T. macrura* over the southern Kerguelen Plateau were comparable to regions of the west Antarctic (Steinberg et al. 2015), and typical of the southern Indian Ocean (Hosie et al. 2000; Swadling et al. 2010). Abundances were variable over the southern Kerguelen Plateau. The very high abundance of >5000 Ind. 1000 m^{-3} observed at site 1 exceeds any other abundances of *T. macrura* recorded from the southern Indian Ocean. *Thysanoessa macrura* at this site had formed a dense mat, observable on the echosounder, providing a rare sight of aggregative behaviour by this species. Abundances of *T. macrura* were highest over the tip of the BANZARE Bank and Princess Elizabeth Trough, a similar trend identified for the dominant copepod species (Matsuno et al. 2019), driven by high primary productivity that flanked the plateau (Schallenberg et al. 2018). The copepod *C. acutus*, an important prey item of *T. macrura* (Hagen and Kattner, 1998; Chapter 4), was identified as a key driver of the abundance of adults within the study region, highlighting the strong association between these two planktonic crustaceans.

Abundances of larvae, especially early furcilia (FI – FIII) exceeded those previously documented for Prydz Bay, an area adjacent to the study region, with mean abundance of *T. macrura* larvae 50% higher and maximum abundances four times greater (Hosie et al. 2000). The pattern in abundance of larvae was similar to that described for adults, however whilst adults were responding to *C. acutus*, larvae were likely driven by the underlying primary productivity. The higher abundances of early (FI – FIII) and late (F IV – FVI) furcilia compared to calyptopis (CI – CIII) stages suggest these larvae are a result of the last spawn of the season. The presence of *T. macrura* larvae 6 months after the spawning season begun (beginning in September/October the previous year; Chapter 2) suggests either a relaxed or prolonged spawning period or a late spawn from recently matured adults. Nordhausen (1994a) has indicated that sexual maturity of *T. macrura* may be reached in as little as 13 months from hatching, confirmed by the analysis of gonadal development Chapter 2, with females as small as 13 mm being reproductively active. This would indicate a duel spawning period of *T. macrura*, with the dominant winter spawning followed by a spring spawn from recently matured adults that hatched the previous year.

5.5.2 Population structure of *Thysanoessa macrura*

The size range of adult *T. macrura* is generally considered to be between 15 – 36 mm (Nordhausen 1994a; Siegel 2000), although the largest individual recorded exceeded 42 mm in length (Haraldsson and Siegel 2014). The size distribution of *T. macrura* during the present study, however, was considerably smaller than those identified in previous population-based analyses (Haraldsson and Siegel 2014). The three geographical areas of the southern Kerguelen Plateau, identified through length frequency distribution of males and females, were mainly determined by changes in female length, with males relatively consistent in their length frequency distribution across the entire study region. Small males and dominance of females are common attributes of many euphausiid populations (Kawaguchi et al. 2007; Haraldsson and Siegel 2014), and was the case for *T. macrura* on the Kerguelen Plateau. In other populations of *T. macrura*, the size difference and skewed sex ratio of males and females have been attributed to the possible inability of males to survive periods of low food availability during winter due to lower lipid reserves than females, with males reported to have lipid reserves of approximately 1.5% of dry weight (Mayzaud et al. 2003; Haraldsson and Siegel 2014). Total lipids of both males and females during the present study were high at 36% and 42.5% of dry weight, respectively. Through examination of seasonal lipid content, Hagen and Kattner (1998) have shown that the lipid reserves of both females and males do not differ considerably, consistent with the total lipid content of *T. macrura* reported in the present study.

Seasonal patterns in lipid storage would therefore not account for the differences in survival rates of males and females over winter. Alternatively, this difference in survival rates of males and females could be attributed to seasonal vertical migration patterns. Haraldsson and Siegel (2014) have indicated that *T. macrura* migrate to depth (up to 2000 m). This migration however appears to be exhibited predominantly by females, leaving overwintering surface populations dominated by males. The migration of mainly females coincides with the vertical migration and diapause of *C. acutus* (Atkinson 1998). Individuals remaining in surface waters during winter could therefore be exposed to a higher predation mortality by fish and diving predators and would account for a decrease in both the abundance of males and the presence of few large males in *T. macrura* populations. Additional winter sampling and assessment of the size structure of the sub-population remaining in surface waters and those that migrate to depth is required to fully explore this important seasonal trend.

Regardless of the mechanisms that influence the size structure over the southern Kerguelen Plateau, the high larval abundances and the large proportion of relatively small individuals of *T. macrura* suggest a high population turnover rate and recruitment.

5.5.3 Biomass and ecosystem contribution

Despite being considered one of the most abundance euphausiids in the Southern Ocean, biomass estimates of *T. macrura* at large scales have yet to be produced. The need to understand the role and importance of *T. macrura* in the marine ecosystem is gaining attention due to the uncertainty of ecosystem responses to a potential decrease in the biomass of *E. superba* in future climates (Hill et al. 2013; Kawaguchi et al. 2013). The southern Kerguelen Plateau region, with its ecological importance in the Indian sector of the Southern Ocean as a key foraging ground for fish, birds and large mammals, provides a good opportunity to assess the role of *T. macrura* in pelagic marine ecosystems. The biomass density of *T. macrura* over the southern Kerguelen Plateau (1.66 mg m^{-3} corresponds to 0.33 g m^{-2}) highlights that *T. macrura* is an important component of the pelagic ecosystem. As we could not determine the frequency of the aggregative behaviour of *T. macrura* observed at site 1, abundances at this site were not included in biomass calculations and therefore the estimates provided are conservative. This biomass estimate is large for a single species, especially given the size range of *T. macrura*, and is similar to net-derived estimates of *E. superba* biomass from the southern Indian Ocean of 0.15 g m^{-2} – 0.64 g m^{-2} (Nicol et al. 2000). However, the biomass of *T. macrura* is considerably lower than biomass estimates of *E. superba* based on large-scale acoustic surveys of the southern Indian Ocean, (5.54 g m^{-2}; Pauly et al. 2000). Areas of high numbers however correspond to peaks in biomass of up to 9.53 mg m^{-3} (1.9 g m^{-2}), comparable to biomass estimates of *E. superba*. In the west Antarctic Peninsula, the biomass of *T. macrura* has been reported to exceed 300 g m^{-2}, equal to that of *E. superba* in the region (Herr et al. 2016).

The high abundance and biomass of *T. macrura* highlight their importance in the Southern Ocean ecosystem. Over the southern Kerguelen Plateau, *T. macrura* represents a significant component of the mid-trophic level biomass, providing an energy dense resource for larger, higher-trophic predators, including birds, fish and baleen whales during spring and summer months (Tynan 1998; Bocher et al. 2000; Trebilco et al. 2019). Mesopelagic fish sampled during the voyage were identified as important consumers of *T. macrura*, with dominant species all found to be feeding on *T. macrura* based upon DNA signatures within fish stomachs (Clarke et al. 2019). Microscopic examination of these stomach contents confirmed high predation on *T. macrura*, especially by younger and smaller species of fish, and this was attributed to mouth-gape size (Riaz et al. 2019). Similarly, *T. macrura* plays an important role in the diets of many diving bird species that nest on Kerguelen Island north of the study region, including common diving petrels (*Pelecanoides urinatrix*) and blue petrels (*Halobaena caerulea*) (Bocher et al. 2000; Cherel et al. 2002). Predation by fish and birds may account for the smaller size range of *T. macrura* (particularly females) across the Southern Kerguelen

Plateau region during summer and spring, with larger individuals easier to capture and providing greater nutritional content than smaller individuals.

In the Indian sector of the Southern Ocean, krill other than *E. superba* form the dominant trophic connection that influences structure and energy flow (McCormack et al. 2019a). Given the abundance and biomass in the region, *T. macrura* forms the dominant component of this 'other krill' group. *Thysanoessa macrura* have been found to form important dietary components of many large predators throughout the Southern Ocean, including macaroni penguins (Niemandt et al. 2016) and petrel species (Bocher et al. 2000). Additionally, crocodile icefish (*Cryodraco antarcticus*) have been found to exclusively feed on *T. macrura* furcilia, highlighting the significance of high abundances of not only adults but also larval stages (Hubold and Ekau 1990). More significantly, in the western Antarctic peninsula, fin whales have been shown to feed heavily on *T. macrura*, despite *T. macrura* being more dispersed throughout the water column than *E. superba* (Herr et al. 2016). Interpreting the current role of *T. macrura* in the Southern Ocean food web is limited by the ability to identify predation on this small euphausiid species, with analysis of gut contents often unable to distinguish between krill species. Furthermore, current methods used to assess the relative importance of prey to predators such as fish and birds often relies upon the relative contribution of species or groups to the total weight of ingested prey (Bocher et al. 2000; Riaz et al. 2019). These methods down-play the importance of *T. macrura* as a food-source, not accounting for the high nutritional content provided by the high calorific-rich lipid content during summer, autumn and winter.

5.6 Conclusions

This study of the southern Kerguelen Plateau provides a unique opportunity to not only assess the population dynamics of *T. macrura* across a large and highly dynamic oceanographic region, but also to consider the role of *T. macrura* in the ecosystem. The Kerguelen Plateau region supports a hotspot of *T. macrura* abundance in the southern Indian Ocean. There is increasing evidence to support that *T. macrura* is an integral component of the pelagic food-web of the Southern Ocean. *Thysanoessa macrura* are often more abundant than *E. superba*, with regional biomasses that support predation by many vertebrate predators. The mounting evidence to support the importance of *T. macrura* to the Southern Ocean ecosystem calls for the need for a broader understanding of population dynamics on a basin scale, with current information restricted to relatively small regional studies. Furthermore, winter sampling is required to understand the overwintering strategy of this species and further elucidate the current understanding that *T. macrura* migrates to depth during winter with surface populations dominated by males.

Chapter 6

Synthesis, discussion and future directions

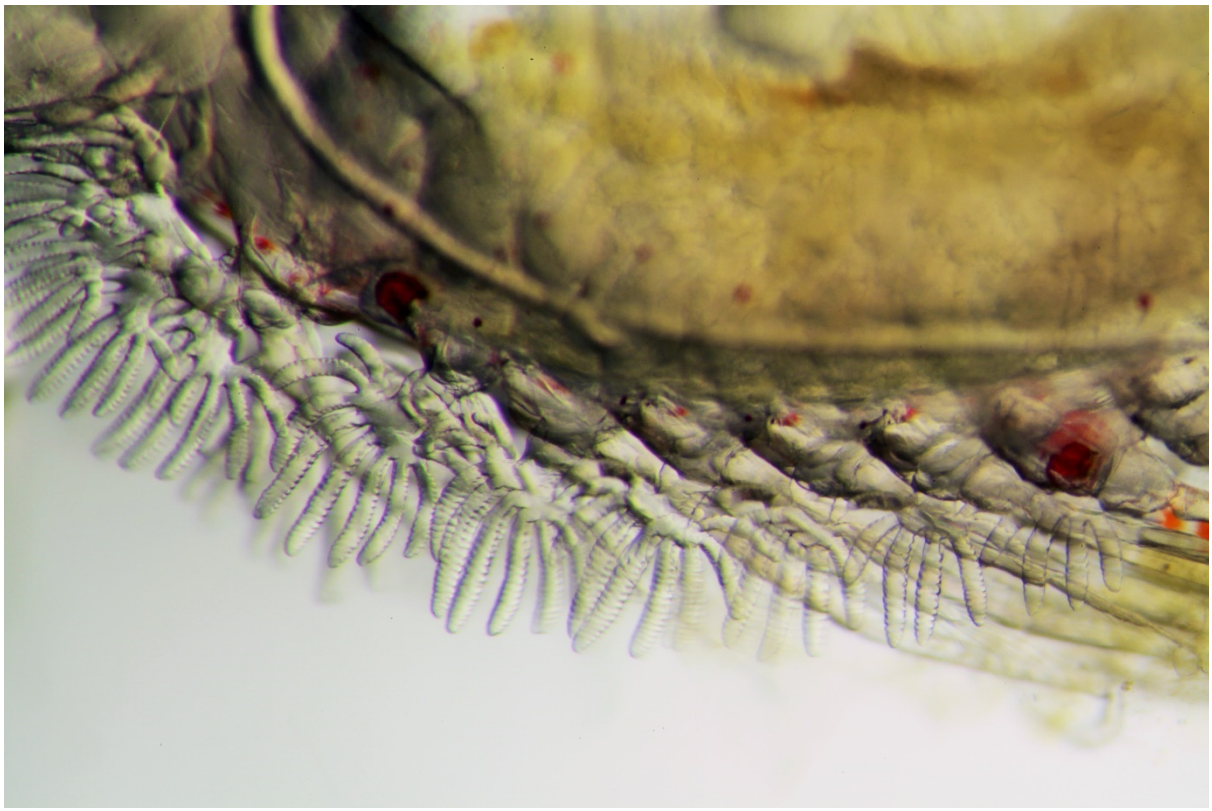

Gills of *T. macrura*

Photograph by Jake Wallis

6.1 Key research findings

Thysanoessa macrura is recognised as an important species of euphausiid in the Southern Ocean, based on its high abundance, a circum-Antarctic distribution and large latitudinal range. Understanding of the function and role of *T. macrura* in the Southern Ocean ecosystem has been hindered by the lack of consolidated information regarding fundamental biological and ecological processes of the species. Historically, the lack of attention towards *T. macrura* results from the strong interest in Antarctic krill (*Euphausia superba*), a keystone species within high latitude food-webs of the Southern Ocean and subject of a large single-species fishery (Constable et al. 2000). This is reflected in the number of targeted studies of both species, with *E. superba* currently the focus of over 1,800* peer-reviewed publications, and only 90* for *T. macrura*. The legacy of being considered a background or "other krill" species in the Southern Ocean is changing, with a shift away from an Antarctic krill-centric view of euphausiids in the Southern Ocean due to the uncertainties associated with a changing climate. As the second most abundant species of euphausiid, with abundances exceeding those of *E. superba* in regions of both east and west Antarctica (Makarov 1979; Hosie 1991; Nordhausen 1992), studies of *T. macrura* are leading this transition.

The body of research this thesis presents adds significantly to the current understanding of the Southern Ocean euphausiid species *T. macrura*. The approach taken, by first filling key knowledge gaps in fundamental biology, then building an understanding of the ecology, provides a comprehensive first insight into the function and role of *T. macrura*. This thesis focuses on the southern Kerguelen Plateau region in the Indian Ocean sector of the Southern Ocean; its findings are applicable beyond the study region and provide a broad framework for building further research.

* Peer-reviewed publications accessible through Scopus that include "Antarctic krill" or "*Euphausia superba*" for *E. superba* studies and "*Thysanoessa macrura*" for *T. macrura*.

Specifically, in this thesis I found that:

- Female *T. macrura* undergo seven distinctive sexual developmental stages based upon ovarian organisation and oogonia and oocyte development. Males undertake four, which are defined by the development of secondary sexual characteristics and presence of spermatophores in ejaculatory ducts.
- A large lipid deposit stored in the carapace of both males and females accounts for the high recorded lipid content of *T. macrura*, fuelling gonad maturation during winter and facilitating the decoupling of spawning from primary productivity peaks in spring.
- Egg batch size scales allometrically with female size (wet weight), with females producing up to three egg batches per season and resulting in an estimated fecundity of >2200 eggs female^{-1} year^{-1}.
- The ontogeny of *T. macrura* is consistent with the developmental pathways of other euphausiids in the Southern Ocean.
- The appearance of larvae in surface waters during the onset of spring promotes rapid larval growth.
- The development of mandibles, maxillules and maxilla of calyptopis and furcilia stages facilitate phytoplankton grazing, with inter-setal distances of maxillae indicating effective grazing on particles as small as 2 – 3 µm.
- Copepods are the dominant food-source in the diets of adult *T. macrura*, particularly the abundant calanoid *Calanoides acutus*.
- The extent of herbivorous grazing by adult *T. macrura* is driven by food availabilities and is spatially variable.
- *Thysanoessa macrura* are commonly infected with gregarine gut parasites; the first evidence and descriptions of *Cephaloidophora thysanoessae* that host within the hindgut are provided (Appendix E).
- The southern Kerguelen Plateau supports high abundances of *T. macrura*, reaching up to 162 Ind. 1000 m^{-3}.
- *Thysanoessa macrura* can form dense aggregations close to the surface, with abundances exceeding 5000 Ind. 1000 m^{-3}.
- High larval abundances during mid-summer, up to 4000 Ind. 1000 m^{-3}, and the regression of sexual traits of adults indicate reproduction has ceased by mid-summer and suggests a spawning season that lasts up to 6 months.

- Slow and short target trawls successfully capture live *T. macrura* for live experimentation, with individuals maintained under natural conditions in ship-board laboratories (Appendix F).
- Both males and females have similar low growth rates during summer of 0.011 mm day^{-1} and 0.012 mm day^{-1}, respectively (Appendix F).
- Juveniles maintain a high growth rate throughout summer, at 0.055 mm day^{-1} (Appendix F).
- Abundances of *T. macrura* in the southern Kerguelen Plateau increase as *Calanoides acutus* increases, highlighting a strong association between the two species.
- The high abundances of *T. macrura* over the southern Kerguelen Plateau correspond to a high biomass, with a mean of 1.66 mg m^{-3} (0.33 g m^{-2}) and localised peaks greater than 9 mg m^{-3} (1.9 g m^{-2}) in the upper 200 m of the water column.

6.2 Synthesis of research findings and discussion

Figure 6.1 provides a conceptual diagram that summarises how this thesis has grown our understanding of biology and ecology of *T. macrura*. *Thysanoessa macrura* have an atypical euphausiid life history, not conforming to several of the key principles of euphausiid biology and ecology demonstrated for well-studied species including *E. superba* in the southern hemisphere and *Meganyctiphanes norvegica* in northern hemisphere waters. Notably, *T. macrura* undertake a winter reproductive period facilitated by a high lipid content stored, predominantly as high calorific wax esters, as an aggregated mass within the carapace. The presence of high numbers of larvae, mainly early furcilia (FI – FIII), indicates a prolonged spawning season, with a second spawning period during spring resulting from recently matured adults.

Due to their high energetic demands; reproduction, lipid accumulation and somatic growth, generally do not occur concurrently due to internal energy partitioning. The accumulation of high lipid reserves, which are maintained during winter, is associated strongly with predation on the copepod *Calanoides acutus*, a large Southern Ocean copepod with high wax ester content. The appearance of *C. acutus* in surface waters during summer coincides with the beginning of a rapid increase in lipid deposition by *T. macrura*. Due to accumulation of lipids during summer and autumn, somatic growth of adult *T. macrura* is restricted to spring, after the end of spawning, with somatic growth minimal during summer. Juveniles however, maintain high growth rates throughout spring and summer and only accumulate lipid reserves in autumn. This disparity between adults and juveniles ensures juveniles have an accelerated growth rate, allowing them to mature rapidly and undertake reproduction the following year.

The diet of *T. macrura* progresses from an herbivorous, phytoplankton-based diet in larval stages to an omnivorous diet in juveniles and adults. Diatoms form the base of the diet of furcilia and likely also for calyptopis stages. With development and increasing complexity of feeding appendages, late furcilia (FIV – VI) transition to flagellates due to their higher energy content and the developing feeding behaviours that enable carnivory in adults. Feeding of adults is plastic, relying on the underlying biomass of available resources, although they show a marked preference for feeding upon copepods during summer. This plasticity enables a broad diet, taking full advantage of all available food items including phytoplankton, protozoa and copepods.

The high abundance of all stages of *T. macrura* from larvae to adults throughout the Southern Ocean provide a valuable resource for carnivorous predators. *Thysanoessa macrura* form a substantial single species biomass in the Southern Ocean. In the southern Kerguelen Plateau region, *C. acutus*, reflecting the close relationship between these two species, is a key driver of *T. macrura* abundances and subsequent biomass. Given that predation is often size-dependant, larval *T. macrura* form a substantial resource for carnivorous zooplankton and small fishes. Adults, with their high lipid contents throughout most of the year, are regularly consumed by diving birds, mesopelagic fish and large vertebrate predators including seals and baleen whales.

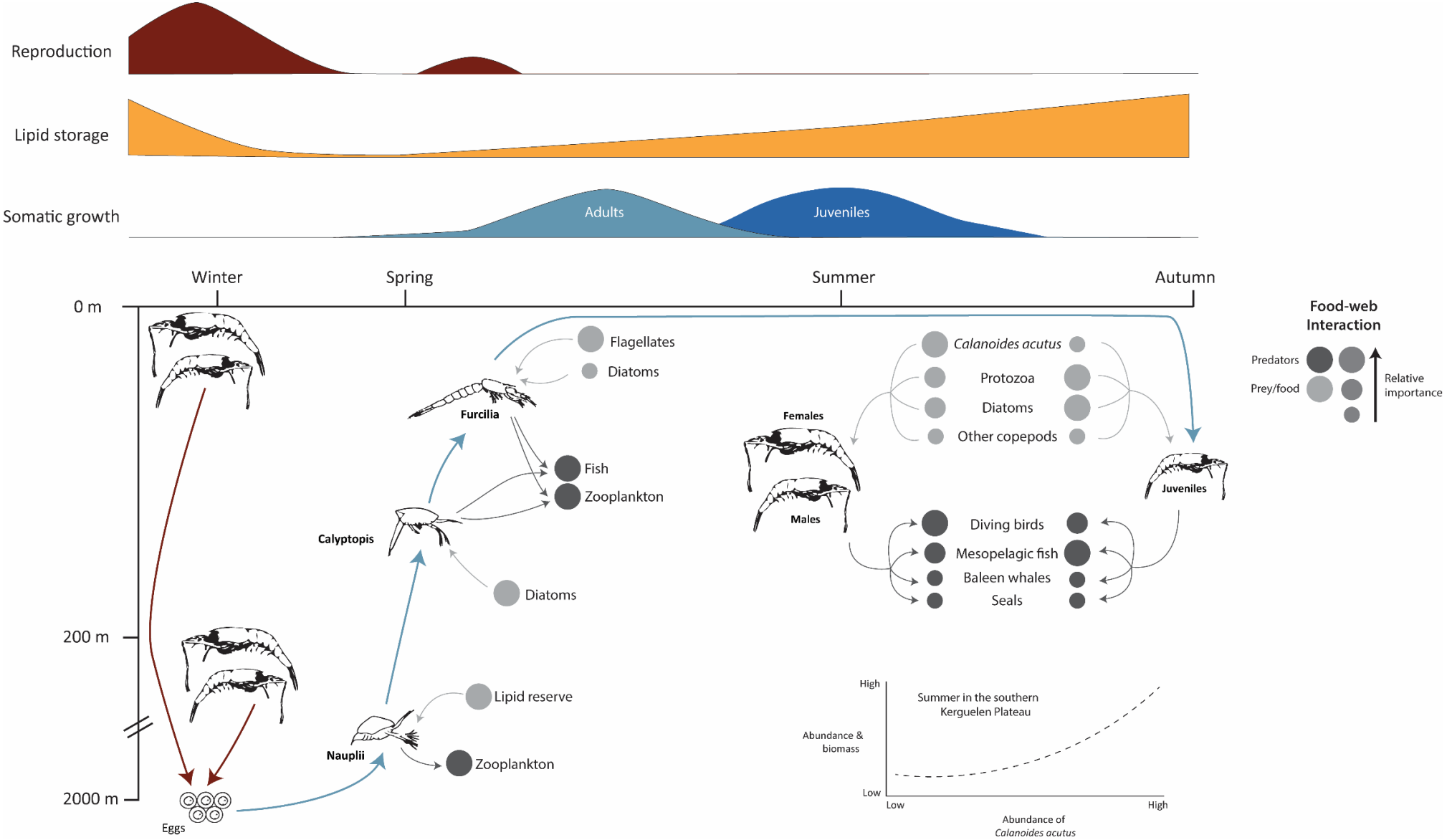

Figure 6.1. Synthesis of research finding of *Thysanoessa macrura*, incorporating information on reproduction, life history, diet and the seasonal partitioning of energy across the internal pathways of reproduction, lipid storage and somatic growth.

6.2.1 Reproduction and early life history

In the Southern Ocean, the life cycle and life-history of all species is intrinsically linked to the strong seasonality associated by the shifts in light regime between summer and winter. For the low- to mid-trophic levels, this seasonality is driven by the increase in primary productivity in surface waters during spring, induced by the increase in light availability and upwelling of nutrient-rich deep-water during winter. For euphausiids, the timing of reproduction is tightly coupled to these peaks in productivity during spring, with their life-history developed to ensure their larvae reach surface waters during these periods of high productivity. *T. macrura*, the earliest spawning euphausiid of the Southern Ocean relies upon stored lipids to fuel this development, with indirect observations of spawning, primarily the observation of larvae indicating a winter reproductive period (Makarov 1979; Siegel 1987).

Despite high abundances, the mechanisms and reproductive potential of *T. macrura* that facilitate these sustained high abundances had yet to be explored. Chapter 2 provides the first quantitative assessment of the reproductive cycle of *T. macrura*, assessing both gonadal development and fecundity. Analysis of ovaries and oogonia and oocyte development was used to assess both the sexual maturation of female *T. macrura* and the potential fecundity by direct counts of mature oocytes. The development of germs cells within the ovaries from oogonia and oocytes was also assessed, with seven stages identified. The development of *T. macrura* oogonia and oocytes were consistent with generalised euphausiid development (Cuzin-Roudy and Amsler 1991; Cuzin-Roudy and Bucholz 1999).

Although the analysis confirms a winter reproductive period, the single study was unable to resolve the effects of environmental conditions on regional variation in spawning onset. Furthermore, the cues that initiate spawning remain unresolved. In high latitude euphausiids, the onset of spawning is tightly linked to changes in light regimes and increases in phytoplankton biomass in surface waters during spring, resulting in highly synchronous reproduction at regional scales (Quetin and Ross 2001; Tarling and Cuzin-Roudy 2003). The initiation of spawning by *T. macrura* during winter, a time when light is consistently low, suggests that these environmental cues do not apply to *T. macrura*. Reports on the beginning of spawning of *T. macrura* based upon observations of larvae range from mid-winter (June-August) in the Antarctic Peninsula, south-eastern Weddell Sea and Lazarev Sea (Siegel 1987; Haraldsson and Siegel 2014) to early spring (October-November) in the Scotia Sea (Makarov 1979), indicating regional variation in spawning onset. Given the wide latitudinal distribution of *T. macrura*, it is likely this regional variation is greater on a north-south gradient. The establishment of sexual developmental stages of both male and females provides a framework for assessing the reproductive 'status' of populations from other

regions across the large distribution of *T. macrura* and the influence of environmental conditions on regional variations in spawning onset.

The length of the spawning season is still unclear. The high numbers of larvae present across the southern extent of the southern Kerguelen Plateau suggests that the spawning season of *T. macrura* extends well beyond the winter-spring period. The lack of active reproduction identified during the population analysis of the Kerguelen Axis study indicates that larvae present during summer are the result of the final spawn of the reproductive season. The lack of information on the developmental rates of *T. macrura* makes it impossible to accurately determine when these eggs were laid. The presence of calyptopis stages six months after the reproductive period begun suggests a prolonged spawning season of *T. macrura*. However, it remains unclear if reproduction occurs consistently throughout this six-month period or if the presence of larvae so late after reproduction begun is a result of recently matured individuals from the previous year undertaking their first spawn. If this is the case, *T. macrura* would have a duel spawning period, with the dominant winter spawn followed by a spring spawning period from recently matured adults.

Despite their small size, *T. macrura* have high reproductive potential. Like *E. superba*, *T. macrura* develop multiple eggs batches within their ovaries concurrently, increasing their ability to continuously and rapidly produce eggs. The ovaries of *T. macrura* act as a conveyor belt, with the free space created once an egg batch is laid immediately replaced by the next batch of developing eggs. The size of ovaries of *T. macrura*, when assessed relative to their body size are considerably larger than *E. superba*, with the number of eggs produced in a single egg batch by *T. macrura* approximately double that of *E. superba* for individuals of the same total length. For example, for the smallest cohort of *E. superba* assessed by Cuzin-Roudy (2000) of 39-40 mm were found to produce approximately 200 eggs in a single batch. For *T. macrura*, an egg batch size of 200 eggs would be produced by an individual female of only 16 mm, highlighting the high fecundity of *T. macrura*. A winter spawning period, large egg size and high fecundity indicate that *T. macrura* places an extremely large maternal investment in reproduction, higher than other species in the Southern Ocean, sustaining their high abundances.

6.2.2 The trade-off between lipid accumulation and somatic growth

Energy is partitioned between three major internal pathways, reproduction, somatic growth and lipid accumulation. For *T. macrura*, lipid accumulation and reproduction are not mutually exclusive, with lipid storage used to fuel a winter reproductive period. Patterns in lipid accumulation of *T. macrura* show a sharp decline in stored lipids during winter, coinciding with gonad maturation and subsequent reproduction (Hagen and Kattner 1998). Lipids are then re-accumulated during spring

and summer when food availability is high due to the seasonal patterns in productivity of the Southern Ocean. Unlike other euphausiid species that accumulate lipids to facilitate overwintering, *T. macrura* appear to maintain a relatively constant lipid content prior to reproduction. High lipid contents of *T. macrura,* which can reach more than 50% of dry weight (Hagen and Kattner 1998; Falk-Petersen et al. 2000), is facilitated by the accumulation of these lipids within the free space of the carapace, forming a concentrated lipid mass. The direct analysis of the lipid masses in the carapace of adult *T. macrura* suggests that, unlike *E. superba* that store lipids throughout their body tissues and organs (Mayzaud et al. 1998), *T. macrura* store more than 90% of their lipids in the lipid deposit (Chapter 2). The dedication of a specialised region for the accumulation of lipid reserves, similar to the large sacs used by many Antarctic copepod species (Atkinson 1988), facilitates the largest lipid reserves (by proportion of body weight) of all dominant Southern Ocean euphausiids (Falk-Petersen et al. 2000). The high lipid content of both females and males assessed during the Kerguelen Axis voyage in summer follow the seasonal trend in lipid accumulation of *T. macrura* reported by Hagen and Kattner (1998). The cessation of reproduction and the accumulation of lipids indicates that by mid-summer, *T. macrura* are actively investing in energy storage for winter and subsequent reproduction.

Due to the high energetic demands of the accumulation of high calorific wax esters, somatic growth during summer is low. This was identified via live experiments, measuring growth from moulting individuals by the Instantaneous Growth Rate (IGR) method (Appendix F). Although *T. macrura* are often considered too fragile to be used in live experiments (R. King, personal communication), short trawling was found to be successful in catching individuals that were able to be maintained at sea. The experiments conducted using live *T. macrura* represent forward momentum, proving the ability to successfully capture and maintain healthy individuals for extended periods of time. Growth rates of adults measured by the IGR method during this study identified a period of low growth during summer, with both females and males estimated to have highly similar growth rates (Appendix F). Estimates of juvenile growth, up to 5 times higher than adults during summer, highlights their rapid growth, capitalising on high food availability and only storing large quantities of lipids during autumn (Hagen and Kattner 1998). This extended period of growth of juveniles allows the rapid maturation rates of *T. macrura* reported, with reproductive maturity reached in as little as 13 months after hatching (Nordhausen 1994a; Chapter 2). The pattern in energy partitioning between the three major internal pathways suggests that for adults, lipid accumulation, with the primary role of fuelling reproduction preferential over somatic growth. This raises the question of when adults undertake growth?

Traditional growth rate methods that rely upon length frequency distribution models to assess cohort growth is difficult for *T. macrura* due to the significantly smaller size distribution compared to the *E. superba,* for which such techniques are used extensively (Kawaguchi et al. 2010). The approach taken by Driscoll et al. (2015), where change in the length of quartiles was used to assess growth, rather than traditional cohorts provides a more reliable approach to assessing growth rates at these large population scales. The growth of *T. macrura* estimated by Driscoll et al. (2015) was positively related to temperature and indicated a period of high somatic growth during the beginning-mid summer, noting that larger individuals unexpectedly were growing faster than smaller individuals. Despite seeming counter-intuitive, a slower growth rate of smaller individuals may be explained by their later reproductive period, only becoming sexually mature in early spring and likely undertaking a second reproductive period, as underpinned by the high abundances of larvae during mid-summer. The seasonal lipid accumulation of *T. macrura* (Hagen and Kattner 1998), in addition to the high growth rates reported by Driscoll et al. (2015) and the low growth rates of adults during summer (Appendix F), *T. macrura* appears to undertake a relatively short period of somatic growth during spring and early summer before transitioning to accumulating lipids.

6.2.3 Diet plasticity

Thysanoessa macrura has long been believed to have an omnivorous diet, although there has been little quantitative evidence to assess food selectivity and determine the relative importance of herbivorous and carnivorous feeding. Gut contents analysis of *T. macrura* performed in the Croker Passage and western Weddell Sea indicates a high feeding pressure on copepod species, forming up to 80% of identifiable food items (Hopkins 1985; Hopkins and Torres 1989). Further evidence produced from fatty acid analysis and lipid biomarkers has highlighted the importance of carnivory compared to herbivory (Hagen and Kattner 1998; Falk-Petersen et al. 2000). Although these studies provide valuable insights into the diet of adult *T. macrura*, the multi evidence-based approach used in this thesis to assess the diet of *T. macrura*, i.e. combining microscopic analysis of gut contents and lipid biomarkers, provides the first comprehensive analysis of *T. macrura* at the population scale.

Spatial variability in their gut contents over the southern Kerguelen Plateau highlights the plasticity in the diet of *T. macrura*. Changes in diet were associated with the hydrography of the region, with adults north of the Southern Antarctic Circumpolar Current Front (SACCF) found to have higher carnivory than those to the south. Differences in the underlying productivity of the region accounted for this spatial pattern, with copepods more numerous to the north (Matsuno et al. 2019) and primary production higher to the south (Schallenberg et al. 2018). In both regions, copepods, in particular *Calanoides acutus*, were the dominant food item consumed by *T. macrura*.

6.2.4 *Thysanoessa macrura* in an ecosystem context

Thysanoessa macrura plays an important role as a low- mid trophic consumer in Southern Ocean food-webs. It forms considerable biomass and represents an energy dense resource for large predators, with energy-rich lipids present throughout most of the year. Over the southern Kerguelen Plateau *T. macrura* were estimated to have a mean biomass of 1.66 mg m^{-3} (0.33 g m^{-2}), with peaks up to 9.53 mg m^{-3} (1.9 g m^{-2}). These estimates are considerably lower than those initially produced by Wallis et al. (2019b; Appendix G), which calculated a mean of 3.1 g m^{-2} for the same region. This discrepancy is due to the omission of sites in the more recent calculations where large surface aggregations of *T. macrura* were identified, due to the inability to predict the frequency of their occurrence. Despite this, the conservative estimates produced in Chapter 5 are comparable to estimates of *E. superba* biomass based on the same net sampling techniques (Nicol et al. 2000), and signify the potential importance of *T. macrura* to the pelagic food-web of the region. To date there are few estimates of *T. macrura* biomass, with the values presented in Chapter 5 the first quantitative estimate for the southern Indian Ocean. Estimates from the Antarctic Peninsula represent the only other values, with *T. macrura* recorded to contribute up to 50% of total euphausiid biomass, exceeding 300 g m^{-2} (Herr et al. 2016).

A recent analysis of food-web structure by McCormack et al. (2019a) using literature-based dietary database has highlighted the Indian sector of the Southern Ocean as a region that is structured by euphausiids other than *E. superba*. Understanding the predators of *T. macrura* is complicated by the methods used to identify feeding by large vertebrate predators. These methods often rely upon the analysis of scat and stomach contents, with macerated euphausiid species often difficult to differentiate. When species identification is possible, the relative contribution and therefore importance of prey is generally represented by their relative mass. Despite their small size, the high lipid contents of *T. macrura*, especially during summer and autumn when the lipids of other euphausiid species are still relatively low (Falk-Petersen et al. 2000), means this assessment down-plays the relative contribution of *T. macrura* to these apex predators (Bocher et al. 2000; Riaz et al. 2019). Mesopelagic fish (Riaz et al. 2019), diving birds (Bocher et al. 2000), sub-Antarctic penguins (Niemandt et al. 2016) and fin whales (Herr et al. 2016) have been identified as major consumers of *T. macrura* and likely play an important role in shaping the size structure of *T. macrura* populations. Given their high abundances, larval stages also represent a significant resource for many smaller carnivorous groups, a facet of the contribution of euphausiids to food-webs that is often overlooked. For example, crocodile icefish were found to feed exclusively on *T. macrura* furcilia (Hubold and Ekau 1990). Although assessing predation on larval stages by carnivorous zooplankton groups including

copepods, chaetognaths and amphipods is difficult, theoretical predator : prey ratios indicate that larvae would fall within optimum prey sizes of many of these groups (Hansen et al. 1994).

Understanding the role of *T. macrura* in structuring pelagic food-webs has been hindered by their board amalgamation as "other krill" (euphausiid species other than *E. superba*). The recent evidence of the substantial biomass *T. macrura* represents within the ecosystem suggests their role is understated by this broad aggregation. Furthermore, their life-history, diet and ecology differentiate them from these other krill species with which they are combined indicating the need to be their own functional group in models that aim to describe ecosystem energy pathways and food-web structure. In a recent ecopath model established for Prydz Bay and BANZARE Bank, based upon information of biomass and functional group interactions of the southern Indian ocean, McCormack et al. (2019b) balance their model with an 'other krill' biomass of 1.8 g m^{-2}. Within this other krill functional group, ice krill, *Euphausia crystallorophias*, are considered the biomass dominant. There is likely a transition in the relative importance of *T. macrura* in the northern extent of the region, to *E. crystallorophias* on the Antarctic shelf due to the distributions of these species (Thomas and Green 1998). Given the biomass of *T. macrura* provided in Chapter 5, which is within this Prydz Bay model domain, *T. macrura* are highly underrepresented.

In a future Southern Ocean, with increasing temperatures and uncertain impacts of ocean acidification on the range and biomass of *E. superba*, *T. macrura*, with its flexible biological and ecological traits may not be adversely affected. Modelling the biomass change of *T. macrura* under future climate scenarios, Richerson et al. (2018) has demonstrated that due to the positive relationship of growth with temperature, *T. macrura* may undergo an increase in both abundance and geographic range. This suggests that in the short-term *T. macrura* may buffer the flow-on trophic impacts of a declining *E. superba* biomass and distribution. Given that the southern Indian Ocean already supports low densities of *E. superba* (Constable et al. 2000; Kawaguchi et al. 2010), and with *T. macrura* already an important component of apex predators' diets (McCormack et al. 2019a), the southern Indian Ocean provides important insights into the current role of *T. macrura* in the pelagic ecosystem and may represent a model of potential ecosystem shifts in other regions of the Southern Ocean.

6.3 The future of *Thysanoessa macrura* research

Thysanoessa macrura is an interesting species that doesn't fit the mould of 'typical' euphausiid biology and ecology demonstrated for *Euphausia superba*. An approach to future *T. macrura* research requires a duel approach, employing complementary sampling and experimentally- based

studies to fill the current gaps in understanding of biological and ecological processes at both the small and large scale (Figure 6.2).

The methods and approach used in this thesis provide a framework for assessing populations of *T. macrura* from both current and historical samples from the Southern Ocean. Archived samples of *T. macrura* have provided an easy and cost-effective means of increasing both the temporal and spatial coverage of *T. macrura* information, including assessing reproductive status, diet and population ecology. Although archived samples provide an easily accessible resource, further targeted sampling is required to fill the vital gap in winter distributions, a significant period in the life-history of *T. macrura*. Although the diet of *T. macrura* is reasonably well resolved, considerable information is still required for understanding the feeding patterns and capabilities of larval stages, with effort placed upon both analysis of consumed prey items and stored lipids.

Live experimentation represents an important development in *T. macrura* research. Field-based experimental approaches are required to not only validate the current understating of *T. macrura*'s biology and ecology but to further the understanding of early life-history, feeding ecology and responses to the environment. Feeding and selectivity experiments using incubation methods will help resolve the extent of plasticity in the diet of *T. macrura* whilst also producing quantified feeding rates, which are currently lacking. Consequently, describing the method of feeding and food capture is needed. Morphological characteristics of the feeding appendages of *T. macrura* reflect an adaptation for capturing large mobile prey, however, it is not clear how they capture and ingest smaller food items including phytoplankton. Experiments using high-speed cameras to record feeding behaviour would be a valuable addition to future feeding experiments. The successful use of the IGR method to assess the growth of *T. macrura* signifies that efforts to increase the spatial and temporal spread of IGR experiments would improve understanding of the seasonal patterns in the growth of both adults and juveniles. Furthermore, the effectiveness of this method in assessing relationships between growth and environmental influences including temperature and food availability is only possible with large numbers of studies in both space and time. Given that estimates of the impacts of increasing temperature in the future Southern Ocean may positively affect *T. macrura* populations, effort now needs to be placed on assessing both the impacts of temperature and acidification on the larvae and eggs of *T. macrura*. As demonstrated by experiments conducted with *E. superba*, early life stages of euphausiids are those that are most susceptible to these environmental changes due to the reduced capacity for internal buffering against non-optimal conditions (Kawaguchi et al. 2013; Ericson et al. 2018).

The key information gained from both sampling and experimentally- based research will aid in a more comprehensive understanding of *T. macrura* and facilitate the understanding of production using the framework established from *E. superba* research by Constable and Kawaguchi (2017). A stronger integration of *T. macrura* in ecosystem models directed at understanding the ecosystem structure and energy flow is also required to better describe the current role of *T. macrura* in the food-webs of the Southern Ocean. Although *T. macrura* may be a small species, an understanding of its importance in the Southern Ocean ecosystem is growing, leading the movement away from an Antarctic krill-centric view of euphausiids in this dynamic and fast-changing ecosystem, with future research strengthening the current understanding of the important role of *T. macrura*.

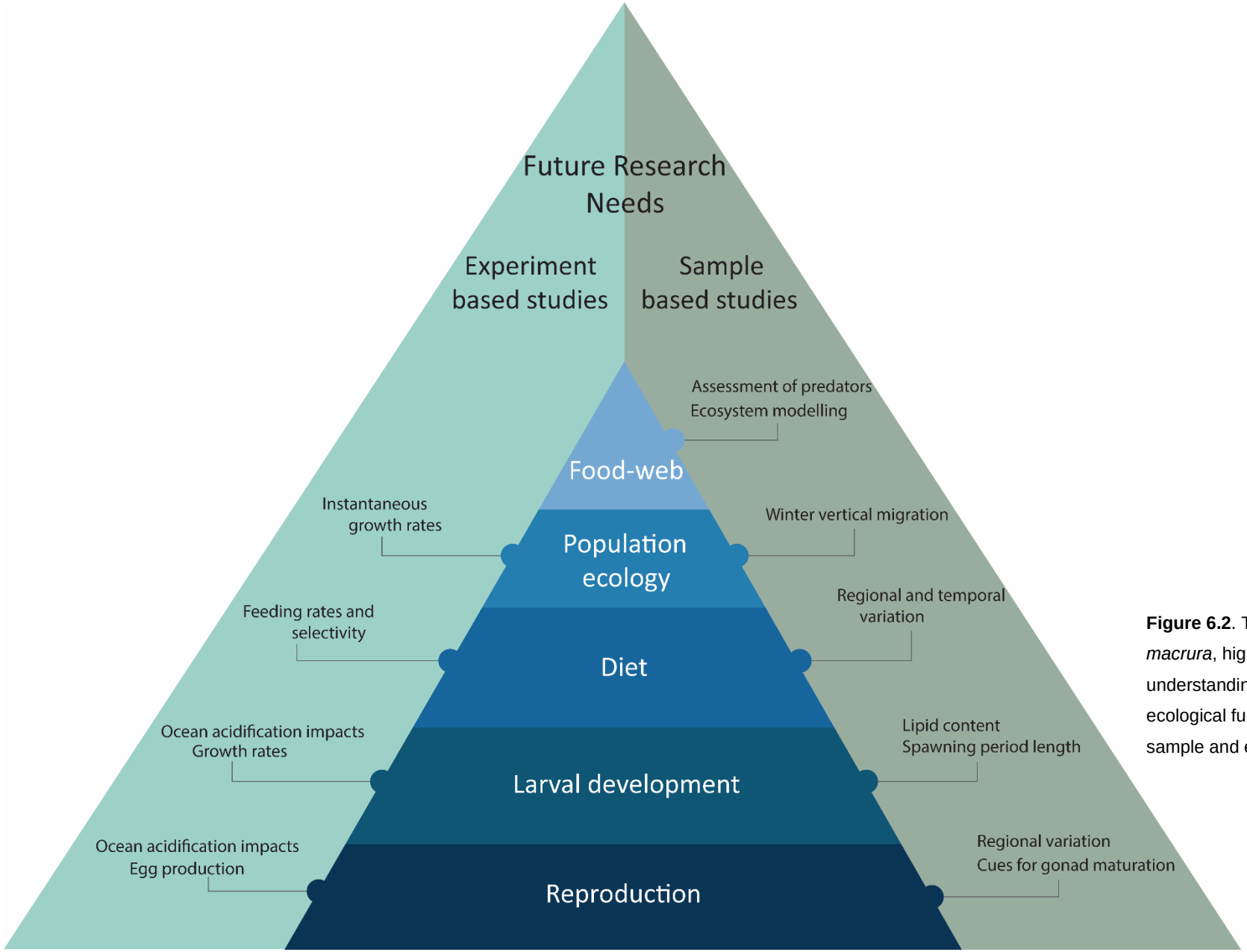

Figure 6.2. The future research needs for *T. macrura*, highlighting the need for increased understanding of the major biological and ecological functions of the species, using both sample and experiment-based studies.

References

Atkinson A (1998) Life cycle strategies of epipelagic copepods in the Southern Ocean. Journal of Marine Systems 15, 289-311.

Atkinson A, Shreeve RS, Hirst AD, Rothery P, Tarling GA, Pond DW, Korb RE, Murphy EJ, Watkins JL (2006) Natural growth rates in Antarctic krill (*Euphausia superba*): II Predictive models on food, temperature, body length, sex and maturity stage. Limnol Oceanogr 51:973-987

Atkinson A, Ward P, Hunt BVP, Pakhomov EA, Hosie GW (2012) An overview of Southern Ocean zooplankton data: Abundance, biomass, feeding and functional relationships. CCAMLR Sci 19:171-281

Baker AC, Clarke MR, Harris MJ (1973) The N.I.O. combination net (RMT 1+8) and further developments of rectangular midwater trawls. J Mar Biol Assoc U.K 53:176–184

Bestley S, van Wijk E, Rosenberg M, Eriksen R, Corney S, Tattersall K, Rintoul S (2018) Ocean circulation and frontal structure near the southern Kerguelen Plateau: The physical context for the Kerguelen Axis ecosystem study. Deep Sea Res II DOI: 10.1016/j.dsr2.2018.07.013

Blight, E.G., Dyer, W.J. 1959. A rapid method of total lipid extraction and purification. Can. J. Biochem. Phys. 37:911-917

Bocher P, Labidoire B, Cherel Y (2000) Maximum dive depths of common diving petrels (*Pelecanoides urinatrix*) during the annual cycle at Mayes Island, Kerguelen. J Zool Lond 251:517-524

Buchholz F, Buchholz C, Weslawski JM (2010) Ten years after: krill as indicator of changes in the macro-zooplankton communities of two Arctic fjords. Polar Biol 33:101–113

Cherel Y, Bocher P, Trouvé C, Weimerskirch H (2002) Diet and feeding ecology of blue petrels *Halobaena caerulea* at Iles Kerguelen, Southern Indian Ocean. Mar Ecol Prog Ser 228:283-299

Clarke LJ, Trebilco R, Walters A, Polanowski AM (2019) DNA-based diet analysis of mesopelagic fish from southern Kerguelen Axis. Deep Sea Res II DOI:10.1016/j.dsr2.2018.09.001

Conover RJ, Huntley M (1991) Copepods in ice-covered seas – distribution, adaptations to seasonally limited food, metabolism, growth pattern and life cycle strategies in polar seas. J Mar Syst 2:1-41

Constable AJ, de la Mare WK, Agnew DJ, Everson I, Miller D (2000) Managing fisheries to conserve the Antarctic marine ecosystem: practical implementation of the Convention on the Conservation of Antarctic Marine Living Resources (CCAMLR). ICES J Mar Sci 57:778-791

Constable AJ, Kawaguchi S (2017) Modelling growth and reproduction of Antarctic krill, *Euphausia superba*, based on temperature, food and resource allocation amongst life history functions. ICES J Mar Sci 75:738-750

Cripps GC, Watkins JL, Hill HJ, Atkinson A (1999) Fatty acid content of Antarctic krill, *Euphausia superba*, at South Georgia related to regional populations and variations in diet. Mar Ecol Prog Ser 181:177–188

Cripps GC, Atkinson A (2000) Fatty acid composition as an indicator of carnivory in Antarctic krill, *Euphausia superba*. Can J Aquat Sci 57:31-37

Cuzin-Roudy J (2000) Seasonal reproduction, multiple spawning, and fecundity in northern krill, *Meganyctiphanes norvegica*, and Antarctic krill, *Euphausia superba*. Can J Fish Aquat Sci 57:6–15

Cuzin-Roudy J, Amsler MO (1991) Ovarian development and sexual maturity staging in Antarctic krill, *Euphausia superba* Dana (Euphausiacea). J Crust Biol 11:236–249

Cuzin-Roudy J, Buchholz F (1999) Ovarian development and spawning in relation to the moult cycle in Northern krill, *Meganyctiphanes norvegica* (Crustacea: Euphausiancea), along a climatic gradient. Mar Biol 133:267–281

Cuzin-Roudy J, Irisson J-O, Penot F, Kawaguchi S, Vallet C (2014) Southern Ocean Euphausiids in De Broyer C., Koubbi P., Griffiths HJ, Raymond B., Udekem d'Acoz, Cd', et al. (Eds.), The Biogeographic Atlas of the Southern Ocean. Scientific Committee on Antarctic Research, Cambridge, pp. 2-9

Dalpadado P, Skjoldal HR (1991) Distribution and life history of krill from the Barents Sea. Polar Res 10:443–460

Driscoll RM, Reiss CS, Hentschel BT, (2015) Temperature-dependant growth of *Thysanoessa macrura*: inter-annual and spatial variability around Elephant Island, Antarctica. Mar Ecol Prog Ser 529:49-61

Edler L, Elbrächter M (2010) The Utermöhl method for quantitative phytoplankton analysis. In: Karlson B, Cusack C, Bresnan E (eds) Microscopic and molecular methods for quantitative phytoplankton analysis. International Oceanographic Commission of UNESCO, IOC Manuals and Guides, Paris, p 13-20

Endo Y, Komaki Y (1979) Larval stages of Euphausiid with descriptions of those of *Thysanoessa longipes* BRANDT. Bulletin of Japan Sea Regional Fisheries Research Laboratory 30:97-1

Ericson JA, Hellessey N, Kawaguchi S, Nicol S, Nichols PD, Howm N, Virtue P (2018) Adult Antarctic krill proves resilient in a simulated high CO_2 ocean. Commun Biol DOI: 10.1038/s42003-018-0195-3

Fäber-Lorda J, Mayzaud P (2010) Morphology and total lipids in *Thysanoessa macrura* from the southern part of the Indian Ocean during summer. Spatial and sex differences. Deep Sea Res II 57:565–571

Falk-Petersen S, Hagen W, Kattner G, Clarke A, Sargent J (2000) Lipids, trophic relationships, and biodiversity in Arctic and Antarctic krill. Can J Fish Aquat Sci 57:178–191

Feinberg LR, Shaw TC, Peterson WT (2006) Larval development of *Euphausia pacifica* in the laboratory: variability in development pathways. Mar Ecol Prog Ser 316:127-137

Froneman PW, Pakhomov EA, Perissinotto R, McQuaid CD (1996) Role of microplankton in the diet and daily ration of Antarctic zooplankton species during austral summer. Mar Ecol Prog Ser 143:15-23

Graeve M, Kattner G, Hagen W (1994) Diet-induced changes in the fatty acid composition of Arctic herbivorous copepods: experimental evidence of trophic markers. J Exp Mar Biol Ecol 182:97–110

Hagen W, Kattner G (1998) Lipid metabolism of the Antarctic euphausiid *Thysanoessa macrura* and its ecological implications. Limnol Oceanogr 43:1894–1901

Hamner WM (1988) Biomechanics of filter feeding in the Antarctic krill *Euphausia superba*: Review of past work and new observations. J Crust Biol 8:149-163

Hansen B, Bjørnsen PH, Hansen PJ (1994) The size ratio between planktonic predators and their prey. Limnol Oceanogr 39:395-403

Haraldsson M, Siegel V (2014) Seasonal distribution and life history of *Thysanoessa macrura* (Euphausiacea, Crustacea) in high latitude waters of the Lazarev Sea, Antarctica. Mar Ecol Prog Ser 495:105-118

Herr H, Viquerat S, Siegel V, Kock K-H, Dorschel B, Huneke WGC, Bracher A, Schröder M, Gutt J (2016) Horizontal niche partitioning of humpback and fin whales around the West Antarctic Peninsula: evidence from concurrent whale and krill survey. Polar Biol 39:799-818

Hill SL, Phillips T, Atkinson A (2013) Potential climate change effects on the habitat of Antarctic Krill in the Weddell quadrant of the Southern Ocean. PLOS One DOI:10.1371/journal.pone.0072246

Hopkins TL (1985) Food web of an Antarctic midwater ecosystem. Mar Biol 89:197-212

Hopkins TL, Torres JJ (1989) Midwater food web in the vicinity of a marginal ice zone in the western Weddell Sea. Deep Sea Res 36:543-560

Hosie GW (1991) Distribution and abundance of euphausiid larvae in the Prydz Bay region, Antarctica. Antarct Sci 3:167-180

Hosie GW, Schultz MB, Kitchener JA, Cochran TG, Richards K (2000) Macrozooplankton community structure off East Antarctica (80-150°E) during the Austral summer of 1995/1996. Deep Sea Res II 47:2437-2463

Hubold G, Ekau W (1990) Feeding patterns of post-larval and juvenile Notothenoids in the Southern Weddell Sea (Antarctica) Polar Biol 10:255-260

Jia Z, Virtue P, Swadling KM, Kawaguchi S (2014) A photographic documentation of the early development of Antarctic krill (*Euphausia superba*) from egg to early juvenile. Polar Biol 37:165-179

Karlson, K. Bamstedt, U. 1994. Planktivorous predation on copepods. Evaluation of mandible remains in predator guts as a quantitative estimate of predation. Mar Ecol Prog Ser 108:79-89

Kattner G, Hagen W, Falk-Petersen S, Sargent JR, Henderson RJ (1996) Antarctic krill *Thysanoessa macrura* fills a major gap in marine lipogenic pathways. Mar Ecol Prog Ser 134:295-298

Kawaguchi S, Nicol S, Virtue P, Davenport SR, Casper R, Swadling KM, Hosie GW (2010) Krill demography and large-scale distribution in the Western Indian Ocean sector of the Southern Ocean (CCAMLR Division 58.4.2) in Austral summer of 2006. Deep Sea Res II 57:934-947

Kawaguchi S, Finley LA, Jarman S, Candy SG, Ross RM, Quetin LB, Siegel V, Trivelpiece W, Naganobu M, Nicol S (2007) Male krill grow fast and die young. Mar Ecol Prog Ser 345:199-210

Kawaguchi S, Ishida A, King R, Raymond B, Waller N, Constable A, Nicol S, Wakita M, Ishimatsu A (2013) Risk maps for Antarctic krill under projected Southern Ocean acidification. Nat Clim Change 3:843-847

Kirkwood JM (1982) A guide to the Euphausiacea of the Southern Ocean. ANARE Research Notes 1, 1-45

Kulka DW, Corey S (1978). The life history of *Thysanoessa inermis* (Kroyer) in the Bay of Fundy. Can J Zool 56:492–506

Leblanc et al (2012) A global diatom database – abundance, biovolume and biomass in the world ocean. Earth Syst Sci Data 4:149-165

Makarov RR (1979) Larval distribution and reproductive ecology of *Thysanoessa macrura* (Crustacea: Euphausiacea) in the Scotia Sea. Mar Biol 52:377-386

Marin V (1988) Quantitative models of the life cycles of *Calanoides acutus*, *Calanus propinquus*, and *Rhincalanus gigas*. Polar Biol 8:439-446

Marschall HP (1985) Structural and functional analyses of the feeding appendages of krill larvae. In Siegfried WR, Condy PR, Laws RM (eds.) Antarctic nutrient cycles and food webs. Springer, Berlin pp 346-354

Matsuno K, Wallis JR, Kawaguchi S, Bestley S, Swadling KM, (2019). Zooplankton community structure and dominant copepod structure on the southern Kerguelen Plateau in the Southern Ocean during austral summer 2016. Deep Sea Res II *Submitted*

Mauchline J (1965) The larval development of the euphausiid, *Thysanoessa raschii* (M. Sars). Crustaceana 9:31-40

Mauchline J (1967) Feeding appendages of the Euphausiacea (Crustaceans). J Zool 153:1-43

Mauchline J (1968) The development of eggs in the ovaries of Euphausiids and estimation of fecundity. Crustaceana 14:155–163

Mauchline J (1980) The biology of mysids and euphausiids. Adv Mar Biol 18:1-681

Mauchline J (1981) Measurement of body length of *Euphausia superba* Dana. BIOMASS Handbook 4. 9 pp.

Mauchline J, Fisher LR (1969). The biology of euphausiids. In: Russel, F. S., Yonge, M. (eds.) Advances in Marine Biology. Academic Press, London

Mayzaud P, Albessard E, Cuzin-Roudy J (1998) Changes in lipid composition of the Antarctic krill *Euphausia superba* in the Indian Ocean sector of the Antarctic Ocean: influence of geographical location, sexual maturity stage and distribution among organs. Mar Ecol Prog Ser 173:149-162

Mayzaud P, Boutoute M, Alonzo F (2003) Lipid composition of euphausiids *Euphausia valentini* and *Thysanoessa macrura* during summer in the Southern Indian Ocean. Antarct Sci 15:463-475

McClatchie S, Boyd CM (1983) Morphological study of sieve efficiency and mandibular surfaces in the Antarctic krill, *Euphausia superba*. Can J Fish Aquat Sci 40:955-967

McCormack SA, Melbourne-Thomas J, Trebilco R, Blanchard JL, Raymond B, Constable A. (2019a) It's not all about Antarctic krill – Food web structures are fundamentally different across the Southern Ocean. Ecography *In Press*

McCormack SA, Melbourne-Thomas J, Trebilco R, Blanchard JL, Constable A (2019b) Alternative energy pathways in Southern Ocean food webs: Insights from a balanced model of Prydz Bay, Antarctica. Deep-Sea Res II. *In Press*

Menden-Deuer S, Lessard EJ (2000) Carbon to volume relationships for dinoflagellates, diatoms and other protist plankton. Limnol Oceanogr 45:569-579

Meyer B, Atkinson A, Stübing D, Ottel B, Hagen W, Bathmann UV (2002) Feeding and energy budgets of Antarctic krill *Euphausia superba* at the onset of winter-I. Furcilia III larvae. Limnol Oceanogr 47:943-952

Meyer B, Atkinson A, Blume B, Bathmann UV (2003) Feeding and energy budgets of larval Antarctic krill *Euphausia superba* in summer. Mar Ecol Prog Ser 257:167-177

Michels J, Schnack-Schiel S (2005) Feeding in dominant Antarctic copepods – does the morphology of the mandibular gnathobases retlate to diet? Mar Biol 146:483-495

Motoda S (1959) Devises of simple plankton apparatus. Mem Fac Fish Hokkaido Univ 7:73-94

Nelson MM, Mooney BD, Nicholas PD, Phleger CF (2001) Lipids of Antarctic Ocean amphipods: food chain interactions and the occurrence of novel biomarkers. Mar Chem 73: 53-64

Nicol S, Kitchener J, King R, Hosie G, de la Mare WK (2000) Population structure of Antarctic krill (*Euphausia superba*) off East Antarctica (80–150°E) during the Austral summer of 1995/1996. Deep Sea Res II 47:2489–2517

Niemandt C, Kovacs KM, Lydersen C, Dyer BM, Isaksen K, Hofmeyer GJG, Mehlum F, De Bruyn PJN (2016) Chinstrap and macaroni penguin diet and demography at Nyrøysa, Bouvetøya. Antarct Sci 28:91-100

Nordhausen W (1992) Distribution and growth of larval and adult *Thysanoessa macrura* (Euphausiacea) in the Bransfield Strait region, Antarctica. Mar Ecol Prog Ser 83:185-196

Nordhausen W (1994a) Distribution and diel vertical migration of the euphausiid *Thysanoessa macrura* in Gerlache Strait, Antarctica. Polar Biol 14:219-229

Nordhausen W (1994b) Winter abundance and distribution of *Euphausia superba*, *E. crystallorophias*, and *Thysanoessa macrura* in Gerlache Strait and Crystal Sound, Antarctica. Mar Ecol Prog Ser 109:131-142

Orsi AH, Whitworth III T, Nowlin Jr WD, (1995) On the meridional extent and fronts of the Antarctic Circumpolar Current. Deep Sea Res I 42:641-673

Pauly T, Nicol S, Higginbottom I, Hosie G, Kitchener J (2000) Distribution and abundance of Antarctic krill (*Euphausia superba*) off East Antarctica (80-150°E) during the Austral summer of 1995/1996 Deep Sea Res II 47:2465-2488

Pinchuk AI, Hopcroft RR (2006) Egg production and early development of *Thysanoessa inermis* and *Euphausia pacifica* (Crustacea: Euphausiacea) in the northern Gulf of Alaska. J Exp Mar Biol Ecol 332:206–215

Quetin LB, Ross RM (2001) Environmental variability and its impact on the reproductive cycle of Antarctic krill. Amer Zool 41:74-89

Rasband, W.S., ImageJ, U. S. National Institutes of Health, Bethesda, Maryland, USA, https://imagej.nih.gov/ij/, 1997-2018

Rau GH, Hopkins TL, Torres JJ (1991). $^{15}N/^{14}N$ and $^{13}C/^{12}C$ in the Weddell Sea invertebrates: implications for feeding diversity. Mar Ecol Prog Ser 77:1-6

Raymond B, Marshall M, Nevitt G, Gillies C, van den Hoff J, Stark JS, Losekoot M, Woehler EJ, Constable AJ (2011) A Southern Ocean dietary database. Ecology 92:1188

Riaz J, Walters A, Trebilco R, Bestley S, Lea M-A (2019) Stomach content analysis of mesopelagic fish from the southern Kerguelen Axis. Deep Sea Res II *In press*

Richerson K, Driscoll R, Mangel M (2018) Increasing temperature may shift availability of euphausiid prey in the Southern Ocean. Mar Ecol Prog Ser 588:59-70

Ross RM, Quentin LB, Kirsch E (1988) Effect of temperature on developmental times and survival of early larval stages of *Euphausia superba* Dana. J Exp Mar Biol Ecol 121:55-71

Schallenberg C, Bestley S, Klocker A, Trull TW, Davies DM, Gault-Ringold M, Eriksen R, Roden NP, Sander SG, Sumner M, Townsend AT, van der Merwe P, Westwood K, Wutting K, Bowie A (2018) Sustained upwelling of subsurface iron supplies seasonally persistent phytoplankton blooms around the southern Kerguelen Plateau, Southern Ocean. J Geophys Res Oceans 123:5986-6003

Schmidt K, Atkinson A (2016) Feeding and food processing in Antarctic krill (*Euphausia superba* Dana). In: Siegel J (ed.) Biology and ecology of Antarctic krill. Springer, Switzerland, pp 175-224

Schmidt K, Atkinson A, Petzke K-J, Voss M, Pond DW (2006) Protozoans as a food source for Antarctic krill, *Euphausia superba*: Complementary insights from stomach content, fatty acids, and stable isotopes. Limnol Oceanogr 51:2409-2427

Siegel V (1987) Age and growth of Antarctic Euphausiacea (Crustacea) under natural conditions. Mar Biol 96:483–495

Siegel V (2000). Krill (Euphausiacea) life history and aspects of population dynamics. Can J Fish Aquat Sci 57:130–150

Sokolov S, Rintoul SR (2007) Multiple jets of the Antarctic Circumpolar Current south of Australia. J Phys Oceanogr 37:1394-1412

Steinberg D, Ruck K, Gleiber MR, Garzio LM, Cope JS, Bernard KS, Stammerjohn SE, Schofield OME, Quetin LB, Ross RM (2015) Long-term (1993-2013) changes in macrozooplankton off the Western Antarctic Peninsula. Deep Sea Res II 101:54-70

Stepnik R (1982) All-year populational studies of Euphausiacea (Crustacea) in the Admiralty Bay (King George Island. South Shetland Islands Antarctic). Pol Polar Res 3:49–68

Stübing D, Hagen W (2003) Fatty acid biomarker ratios – suitable trophic indicators in Antarctic euphausiids? Polar Biol 26:774-782

Suh H-L (1996) The gastric mill of euphausiid crustaceans: a comparison of eleven species. Hydrobiol 321:235-244

Swadling KM, Kawaguchi S, Hosie GW (2010) Antarctic mesozooplankton community structure during BROKE-WEST (30°E-80°E), January-February 2006. Deep Sea Res II 57:887-904

Tarling GA, Cuzin-Roudy J (2003) Synchronization in the molting and spawning activity of northern krill (*Meganyctiphanes norvegica*) and its effects on recruitment. Limnol Oceanogr 48:2020-2033

Taylor F, McMinn A, Franklin D (1997) Distribution of diatoms in surface sediments of Prydz Bay, Antarctica. Mar Micropaleontol 32:209-229

Thomas PG, Green K (1998) Distribution of *Euphausia crystallorophias* within Prydz Bay and its importance to the inshore marine ecosystem. Polar Biol 8:327-331

Trebilco R, Walters A, Melbourne-Thomas J, Bestley S, Cox M, Gasteur S, Sumner M, Constable A (2019) Mesopelagic community structure on the southern Kerguelen Axis. Proceedings of the 2nd Kerguelen Plateau Marine Ecosystem and Fisheries Symposium. In press

Tynan CT (1998) Ecological importance of the Southern Boundary of the Antarctic Circumpolar Current. Nature 392:708-710

Virtue P, Meyer B, Freier U, Nichols PD, Jia Z, King R, Virtue J, Swadling KM, Meiners KM, Kawaguchi S (2016) Condition of larval (furcilia VI) and one year old juvenile *Euphausia superba* during the winter-spring transition in East Antarctica. Deep Sea Res II 131:182-188

Wallis JR, Melvin JE, King R, Kawaguchi S (2019a) *In situ* growth rate estimates of Southern Ocean krill, *Thysanoessa macrura*. Antarct Sci DOI: 10.1017/S0954102019000063

Wallis JR, Kawaguchi S, Matsuno K, Swadling KM (2019b). Big things come in small packages. Biomass contribution of the krill *Thysanoessa macrura* to the marine ecosystem in the Kerguelen Plateau region. Proceedings of the 2nd Kerguelen Plateau Marine Ecosystem and Fisheries Symposium. In press

Wallis JR, Smith AJR, Kawaguchi S (2017) Discovery of gregarine parasitism in some Southern Ocean krill (Euphausiacea) and the salp *Salpa thompsoni*. Polar Biol 40:1913-1917

Wood SN (2004) Stable and efficient multiple smoothing parameter estimation for generalized additive models. J Am Stat Assoc 99:673-686

Appendix A

The following accompanies the information provided in Chapter 2 “Sexual differentiation, gonad maturation and reproduction of the Southern Ocean euphausiid *Thysanoessa macrura*”

Table A1. Reproductive cells identified in the developing ovaries of *Thysanoessa macrura*. Morphological characteristics are provided for each cell type. N = the number of cells used for cellular measurements, showing mean ± SE (range). N:C = nucleus to cytoplasm ratio based upon surface area.

Cell type	Size (µm)	Cell area (µm^2)	Nucleus area (µm^2)	Cytoplasm area (µm^2)	N:C (%)	Appearance
Primary oogonia (n=37)	35 ± 1 (24 - 33)	826 ± 31 (478 - 1369)	439 ± 23 (255 - 938)	387 ± 15 (201 - 619)	117 ± 6 (67 - 217)	Small, relatively rounded cells. Nucleus occupies most of the cell and often seen in the stages of mitosis
Secondary oogonia (n=50)	52 ± 1 (37 - 79)	1563 ± 76 (791 - 3155)	802 ± 39 (435 - 1640)	761 ± 40 (356 - 1515)	107 ± 4 (71 - 234)	Small, nucleus occupying most of the cell with the nucleus appearing reticulated
Primary oocyte (n=40)	117 ± 5 (55 - 167)	7590 ± 810 (1680 - 19830)	3048 ± 308 (767 - 8130)	4542 ± 512 (913 - 11992)	74 ± 3 (41 - 123)	Cytoplasm clear, nucleus occupying majority of the cell
Type 1 oocyte (n=45)	212 ± 5 (138 - 270)	25464 ± 1358 (10839 - 48932)	8013 ± 476 (3660 - 17315)	17451 ± 954 (6648 - 31617)	47 ± 2 (23 - 83)	Cytoplasm transparent, nucleus occupies a large proportion of the cell, cells irregular in shape and not rounded
Type 2 oocyte (n=43)	300 ± 5 (235 - 390)	53389 ± 1523 (34036 - 78145)	15764 ± 553 (10672 - 26490)	37624 ± 1208 (23364 - 57652)	43 ± 2 (25 - 67)	Cytoplasm appears cloudy and granulated, cells irregular in shape and not circular
Type 3 oocyte (n=50)	436 ± 7 (367 - 543)	140656 ± 2812 (75216 - 173101)	19780 ± 671 (11344 - 28298)	99101 ± 2538 (58327 - 149929)	17 ± 1 (9 - 23)	Nucleus visible in centre of cell, cytoplasm filled with lipid droplets
Type 4 oocyte (n=51)	506 ± 8 (395 - 624)	170263 ± 29649 (13101 - 1641429)	- -	- -	- -	Nucleus not visible, filled with lipid droplets, cell relatively rounded

Table A2. Allometric relationships ($y = ax^b$) using total length (TL), total wet weight (TWW), ovary wet weight (OWW) and mature oocytes (NMO) and the total number of developing oocytes within the ovary (NOCT) in vitellogenic and spawn-ready females (SDS 5 and SDS 6). The R^2 and ANOVA *F* ratio (F) are provided for the log-log OLS linear regression (model 1). The coefficient *a* represents the y-intercept and *b* the coefficient of regression, determined from the slop using log-log transformed data and is provided for both OLS and RMA (model 2) regression. Based upon the allometric relationships, the range of the predicted egg batch size and its mean is calculated for both OLS and RMA estimated coefficients of regression. N = the number of individuals included in each analysis.

		Model 1 (OLS)								Model 2 (RMA)			
Allometric relationship (y/x)	N	*a*	*b*	*b* SE	R^2	F	p	Predicted egg batch size (range)	mean	*a*	*b*	Predicted Batch size (range)	mean
WWT/TL	73	0.022	2.77	0.14	0.816	305.5	<0.005			0.00871	3.09		
OWW/TL	73	0.005234	2.43	0.37	0.34	36.70	<0.005			0.000118	3.754		
OWW/TWW	73	0.135	0.898	0.113	0.44	56.15	<0.005			0.0359	1.22		
NPVO/OWW	70	7.78	1.81	0.3	0.33	35.47	<0.005	10-699	170	0.789	3.179	1.4 - 2127	178
NMO/OWW	73	43.85	0.608	0.151	0.19	16.32	<0.005	49 - 199	124	6.934	1.712	9-488	77
NMO/TL	73	0.115	2.439	0.5812	0.24	14.97	<0.005	62 - 200	124	0.000005	5.92	23 - 402	125
NMO/TWW	73	4.217	0.822	0.193	0.19	23.57	<0.005	70 - 219	127	0.0833	1.781	34-435	133
NOCT/OWW	70	70.469	0.9093	0.158	0.318	33.17	<0.005	83 - 675	332	24.774	1.534	33 - 1121	339
NOCT/TL	70	0.0265	3.294	0.6915	0.242	22.69	<0.005	130 - 630	329	5.64E-05	5.449	72 - 979	335
NOCT/TWW	70	1.977	1.245	0.212	0.327	34.50	<0.005	139 - 785	342	0.204	1.802	96 - 1178	354

Appendix B

The following provides a photographic documentation of the feeding appendages of *Thysanoessa macrura* from calyptopis I to furcilia FVI and adults whilst also documenting the morphological characteristics of the gut. This accompanies the information provided in Chapter 4 “Diet of *Thysanoessa macrura* with respect to carnivory and ontogenetic shifts”

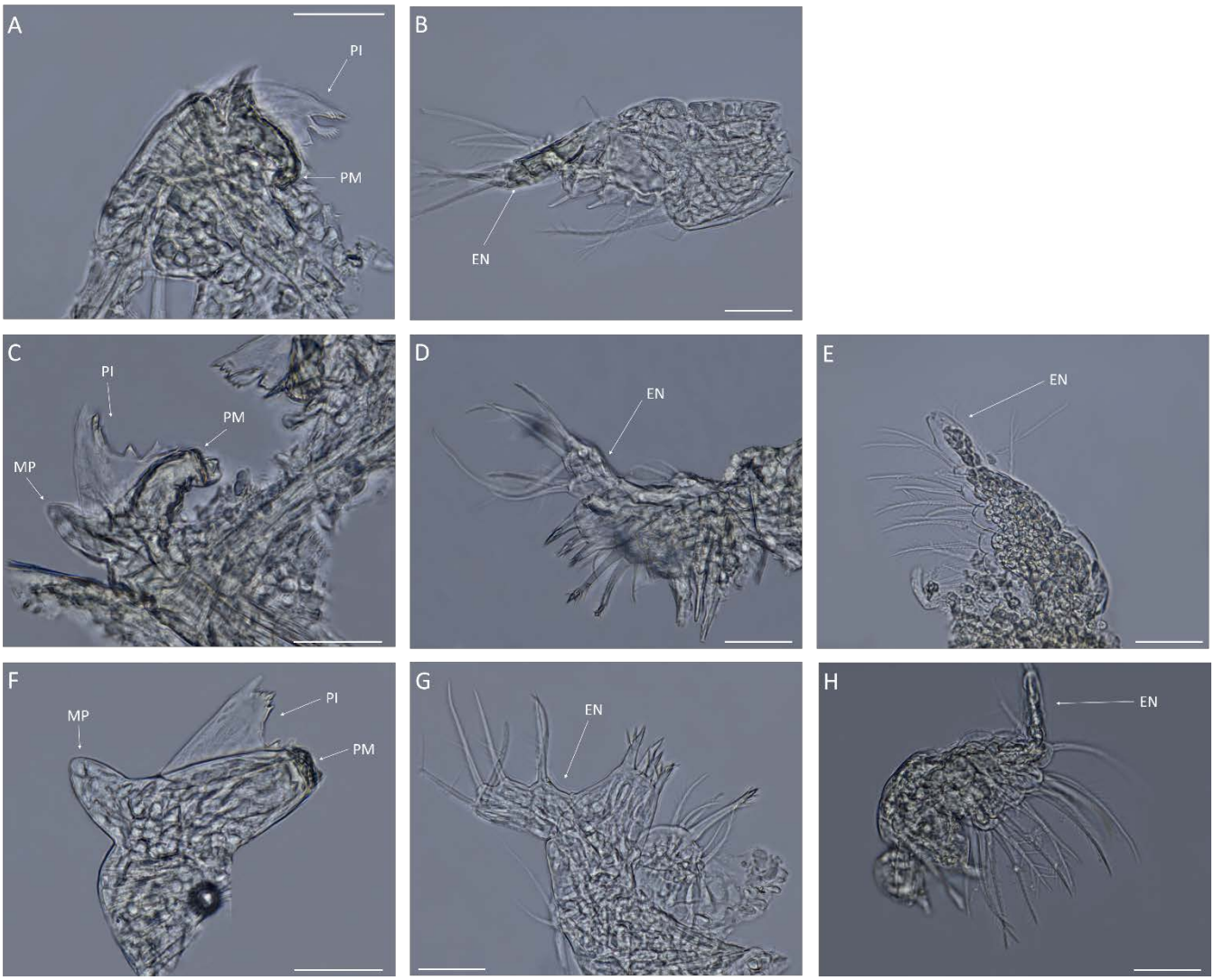

Figure B1. Feeding appendage morphology of *Thysanoessa macrura* calyptopis stages. A. C I mandible B. C I maxillule C. C II mandible D. C II maxillule E. C II maxilla F. C III mandible G. C III maxillule H. C III maxilla. Scale bar = 50 µm. PI = pars incisiva, PM = pars molaris, MP = mandibular palp, EN = endopod.

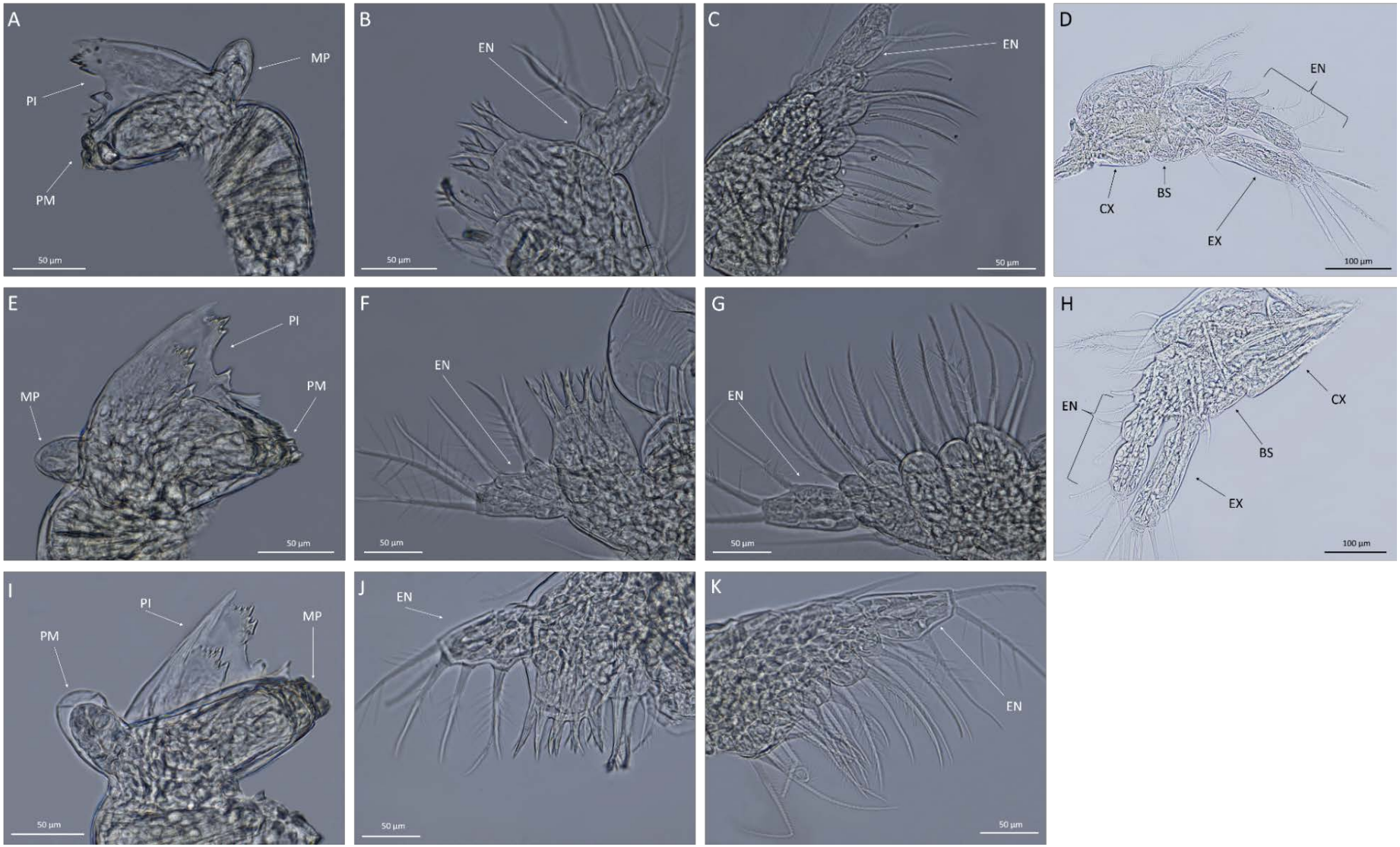

Figure B2. Feeding appendage morphology of *Thysanoessa macrura* early furcilia stages (F I – F III). **A**. F I mandible **B** F I maxillule **C**. F I maxilla **D** F I Thoracopod 2 **E**. F II mandible **F**. F II maxillule **G**. F II maxilla **H** F II thoracopod 2 **I**. F III mandible **J**. F III maxillule **K**. F III maxilla. Scale bar D and H = 100 µm, all other scale bars 50 µm. PI = pars incisiva, PM = pars molaris, MP = mandibular palp, EN = endopod, EX = exopod, CX = coxa, BS = basis.

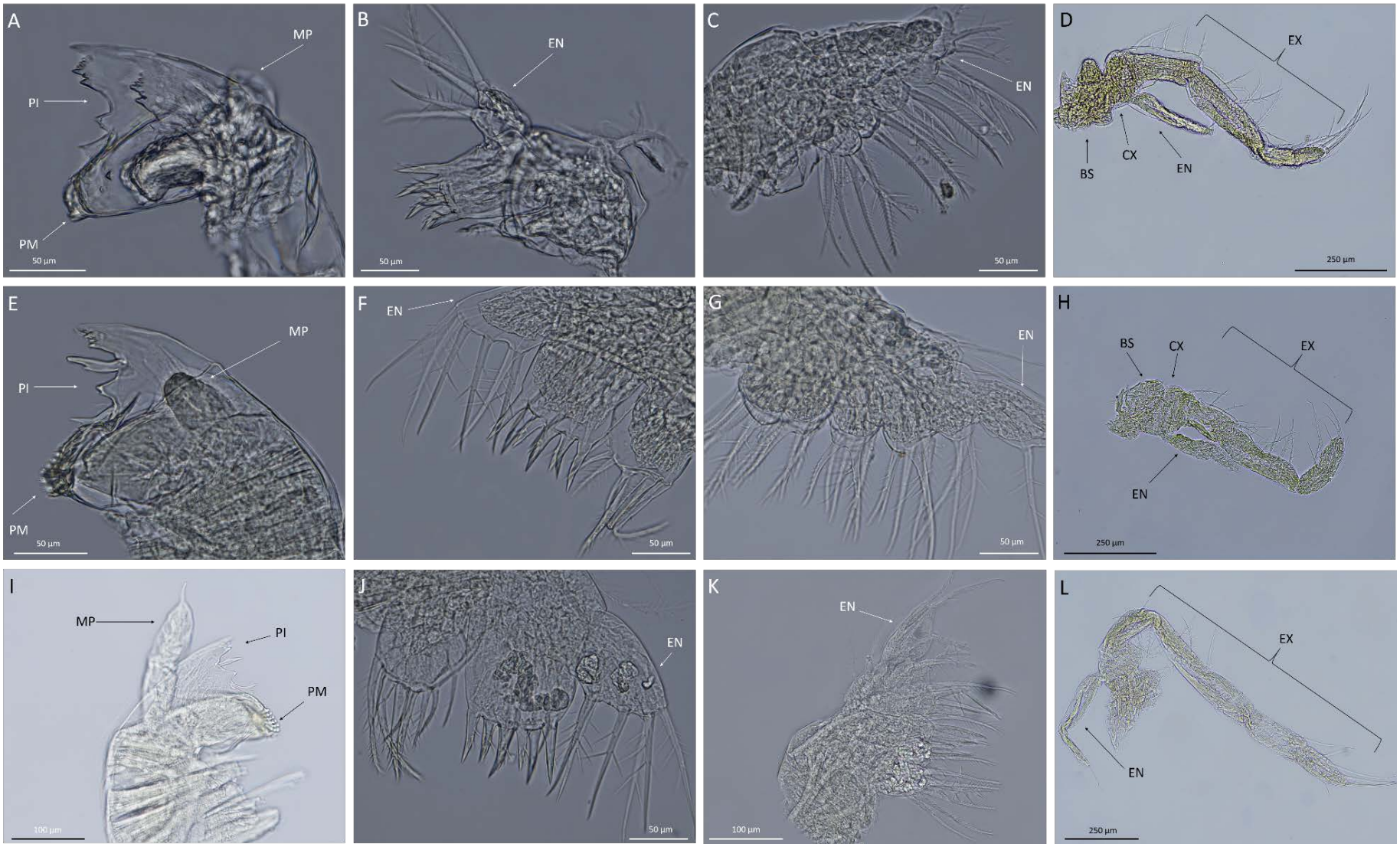

Figure B3. Feeding appendage morphology of *Thysanoessa macrura* late furcilia stages (F IV – F VI). **A**. F IV mandible **B** F IV maxillule **C**. F IV maxilla **D** F IV Thoracopod 2 **E**. F V mandible **F**. F V maxillule **G**. F V maxilla **H** F V thoracopod 2 **I**. F VI mandible **J**. F VI maxillule **K**. F VI maxilla. **L**. F VI Thoracopod 2. PI = pars incisiva, PM = pars molaris, MP = mandibular palp, EN = endopod, EX = exopod, CX = coxa, BS = basis.

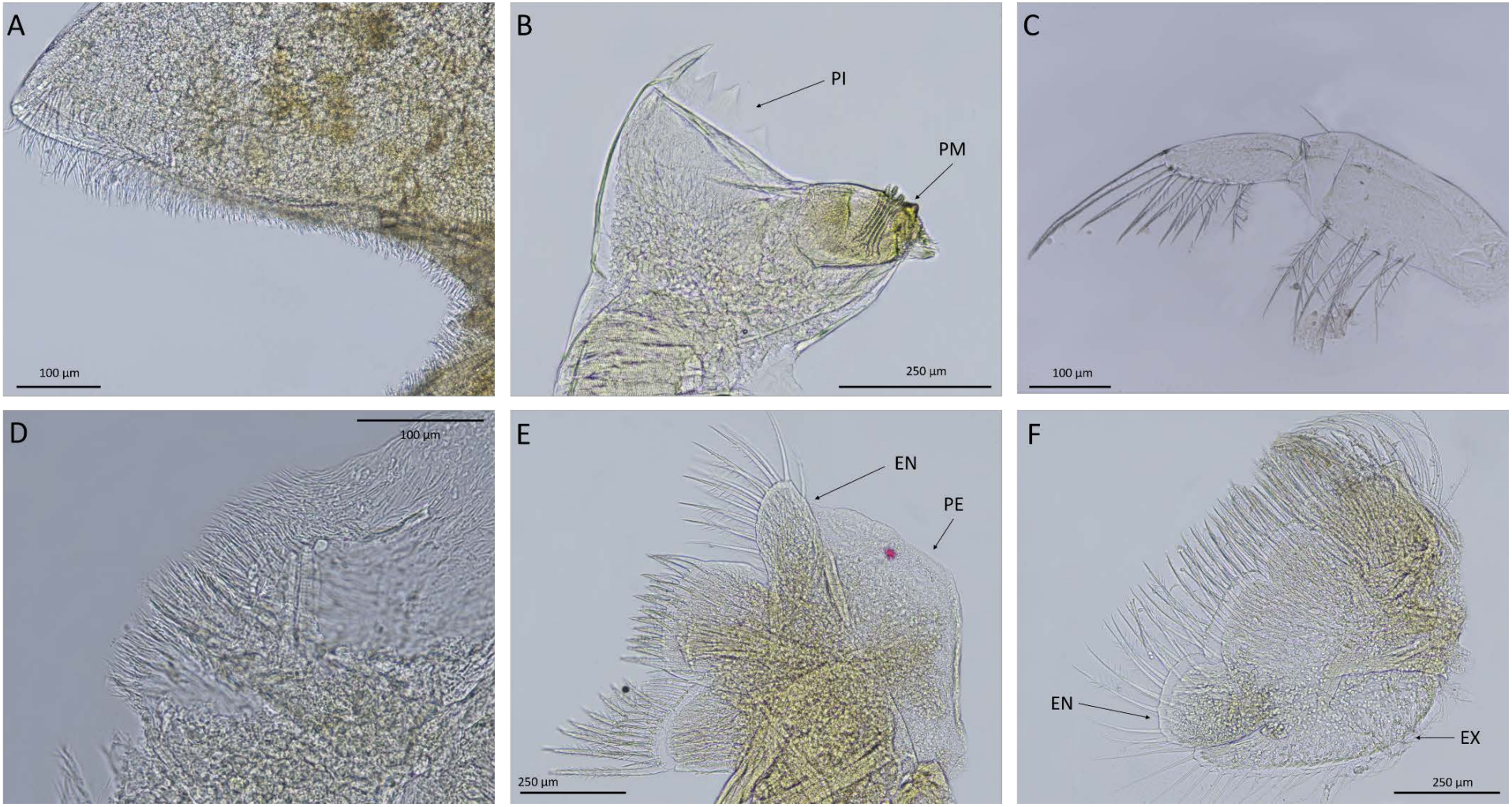

Figure B4. Feeding appendage morphology of adult *Thysanoessa macrura* **A**. Inner margins of the labium **B**. Mandible **C**. Mandibular palp **D**. Inner surface of the labrum **E**. Maxillule **F**. Maxilla. PI = pars incisiva, PM = pars molaris, EN = endopod, EX = exopod, PE = pseudo-exopod.

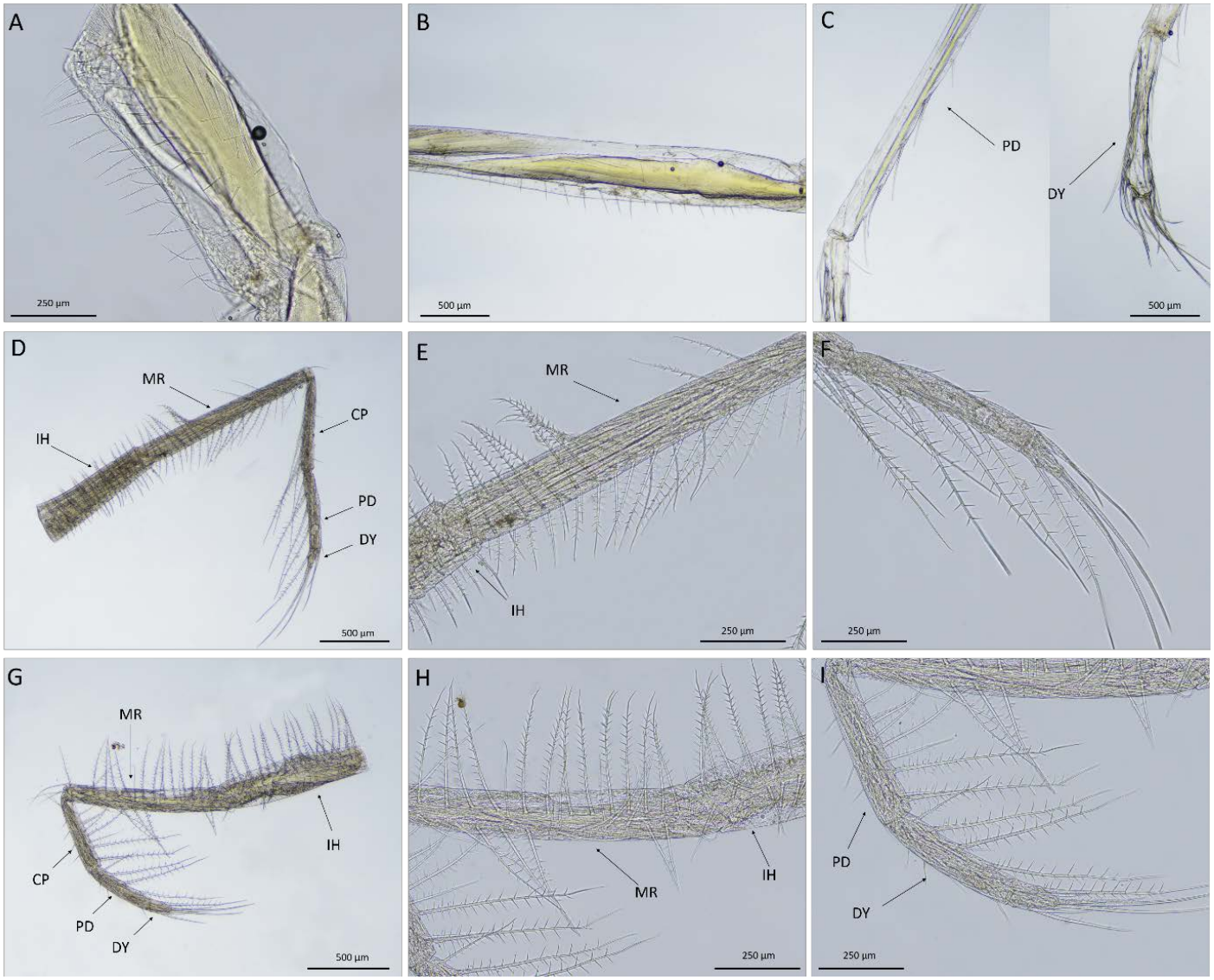

Figure B5. Thoracopod morphology of adult *Thysanoessa macrura*. The second thoracopod **A**. Ischium **B**. Merus and **C**. Dactylus and propodus joint. **D**. 3rd thoracopod **E**. Spine arrangement of the merus of the 3rd thoracopod **F**. 3rd thoracopod dactylus **G**. 4th thoracopod **H**. 4th thoracopod merus spine arrangement **I**. Dactylus of the 4th thoracopod.

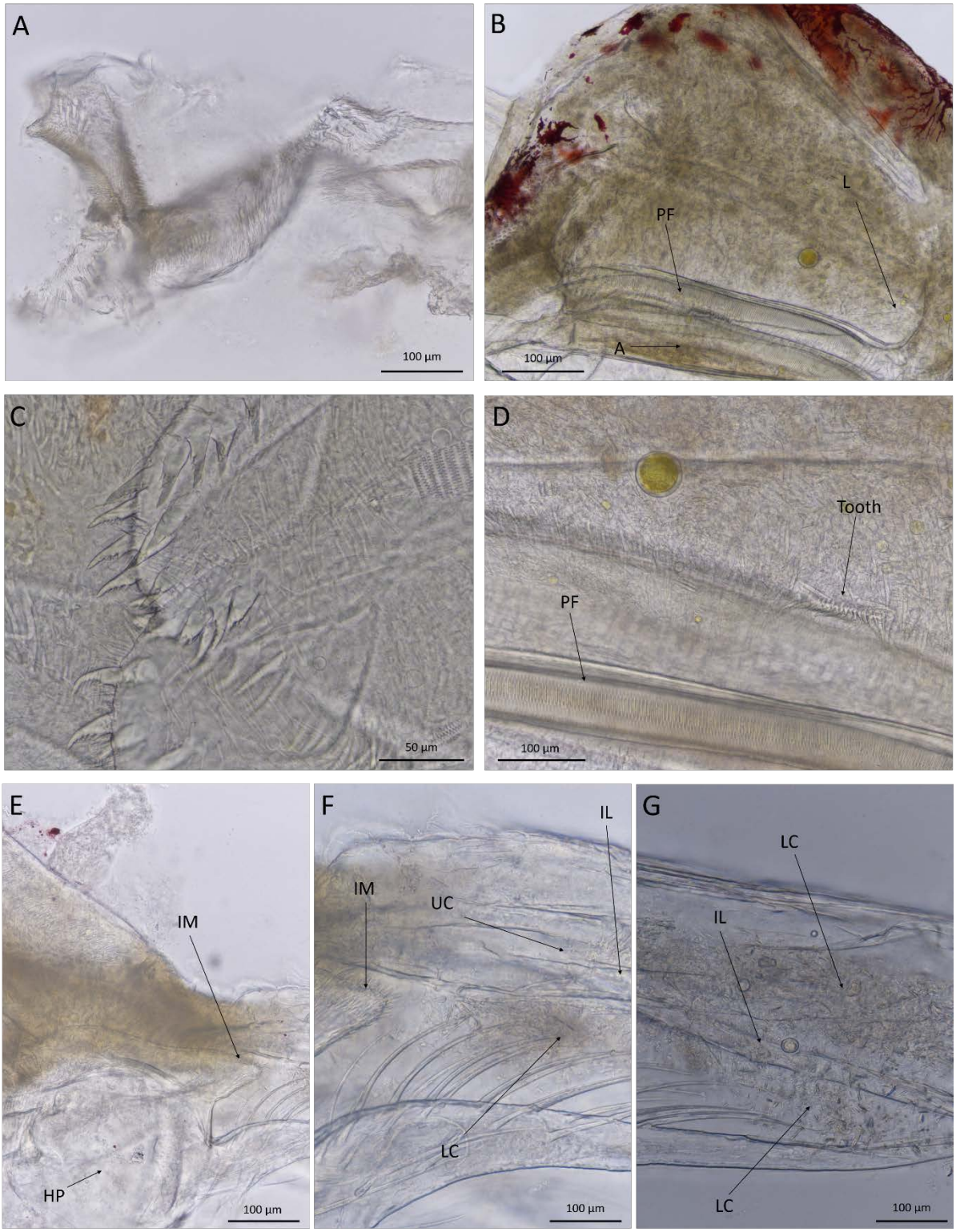

Figure B6. Fore and mid- gut structure of adult *Thysanoessa macrura*. **A**. Internal surface of the oesophagus **B**. The cardia chamber of the foregut **C**. Lateral teeth **D**. Primary filter and laterale **E**. Anterior region of the pylorus **F**. Mid pylorus region **G**. Posterior end of the pylorus. PF = Primary filter, L = lateralia, A = Anteromedianum, HP = hepatopancreaus, IM = inferomedianum, IL = Inferolateralia, UC = upper channel, LC = lower channel.

Appendix C

The following provides allometric relationships of *Thysanoessa macrura* established from individuals caught during the Kerguelen Axis voyage and accompanies the information provided in Chapter 5 "*Thysanoessa macrura* in the southern Kerguelen region: population structure and biomass"

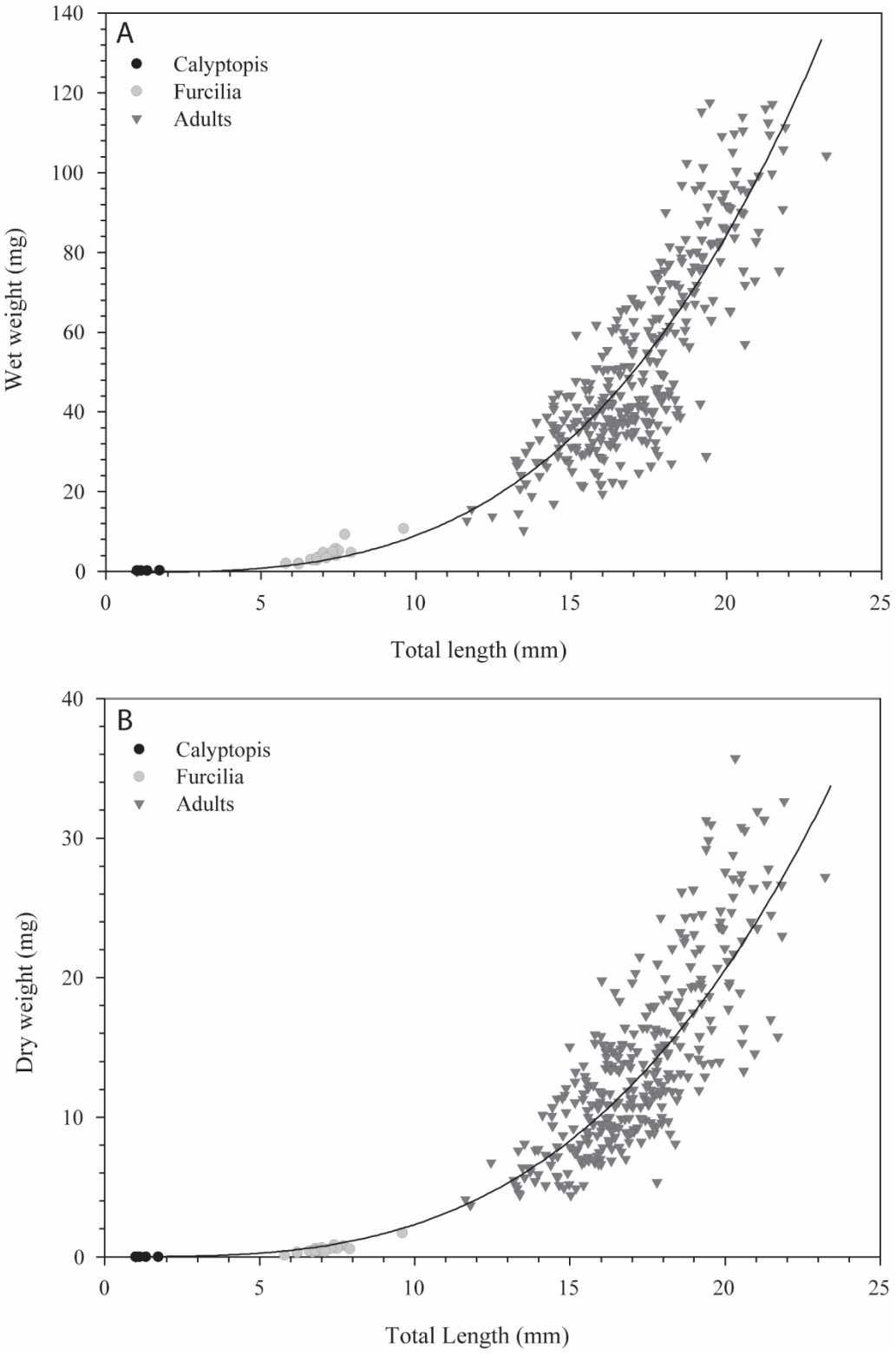

Figure C1. Allometric relationships of *Thysanoessa macrura* including calyptopis, furcilia and adult developmental stages. **A**. Total length – wet weight (wet weight = 0.0053 x total length$^{3.22}$) (R^2 = 0.769, *p* = <0.001). **B**. Total length – dry weight (dry weight = 0.0019 x total length $^{3.12}$) (R^2 = 0.769, *p* = <0.001).

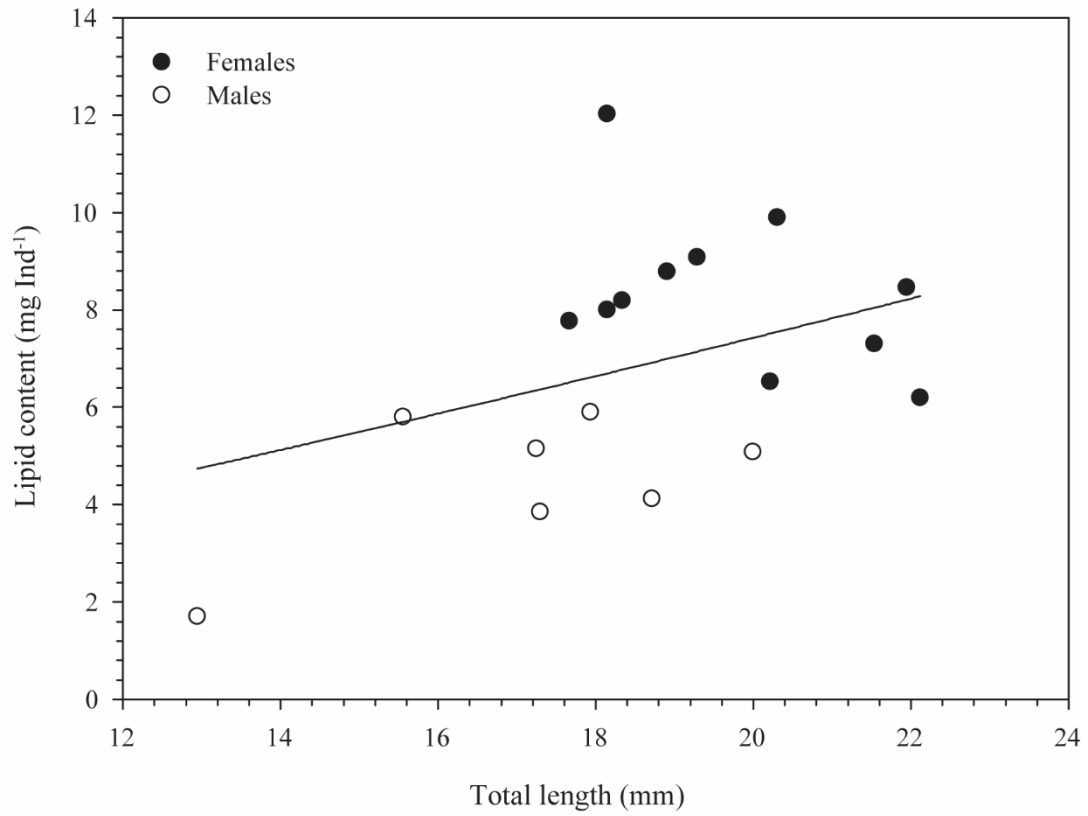

Figure C2. Relationship between adult *Thysanoessa macrura* total lipid content and total length (lipid content = 0.1956 x total length$^{1.22}$) (R^2 = 0.203, p = 0.061).

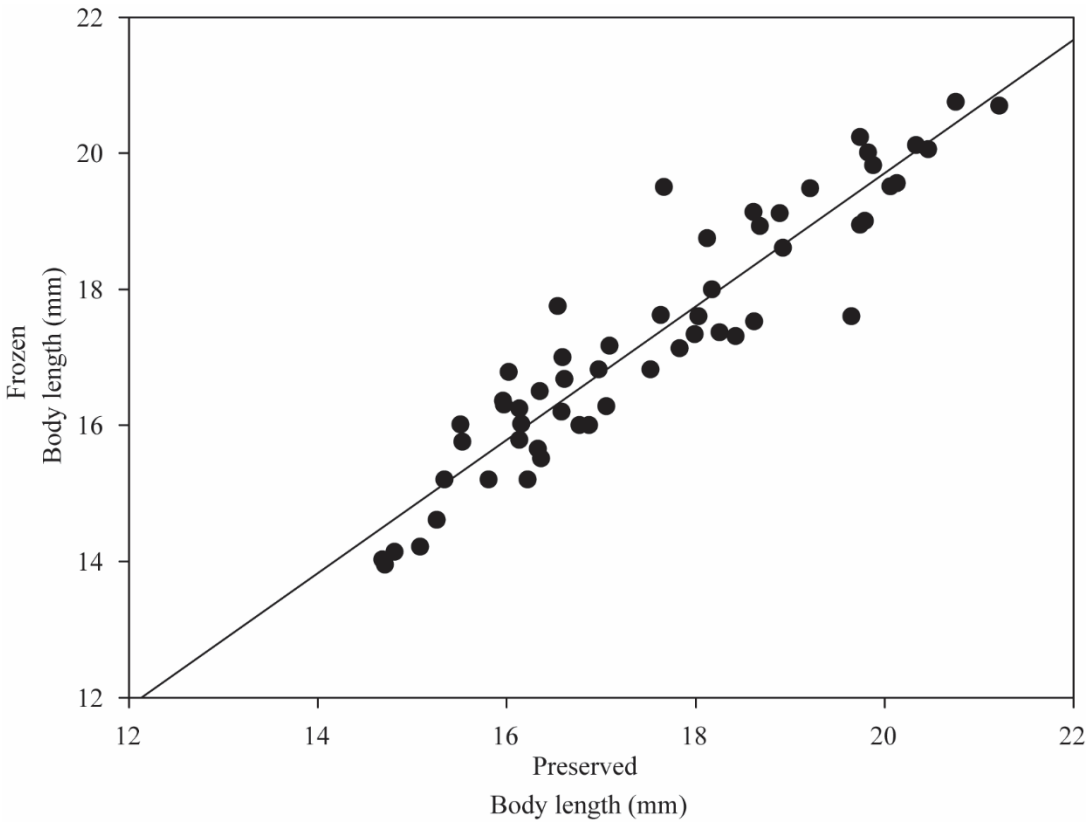

Figure C3. Relationship between frozen and preserved total length of *Thysanoessa macrura* (y = 0.896x + 2.04, R^2 = 0.88, *p* = <0.001).

Appendix D

The following provides detailed parametrisation and outputs from the General Additive Model (GAM) used to assess the abundance of *Thysanoessa macrura* across the southern Kerguelen Plateau and the biomass estimates produced at each site by statistical interpolations. This accompanies the information provided in Chapter 5 "*Thysanoessa macrura* in the southern Kerguelen region: population structure and biomass"

Table D1. Parameters and fit of the final general additive model (GAM) of adult *Thysanoessa macrura* abundance.

	df	Chi squared	*p*-value
Salinity	4	5.4	<0.001
Log_{10} (Abundance of *Calanoides acutus*)	2.7	3.6	0.018
Temperature at 200 m	1	1	0.371

Adjusted R^2	Deviance explained	n
0.126	56.70%	36

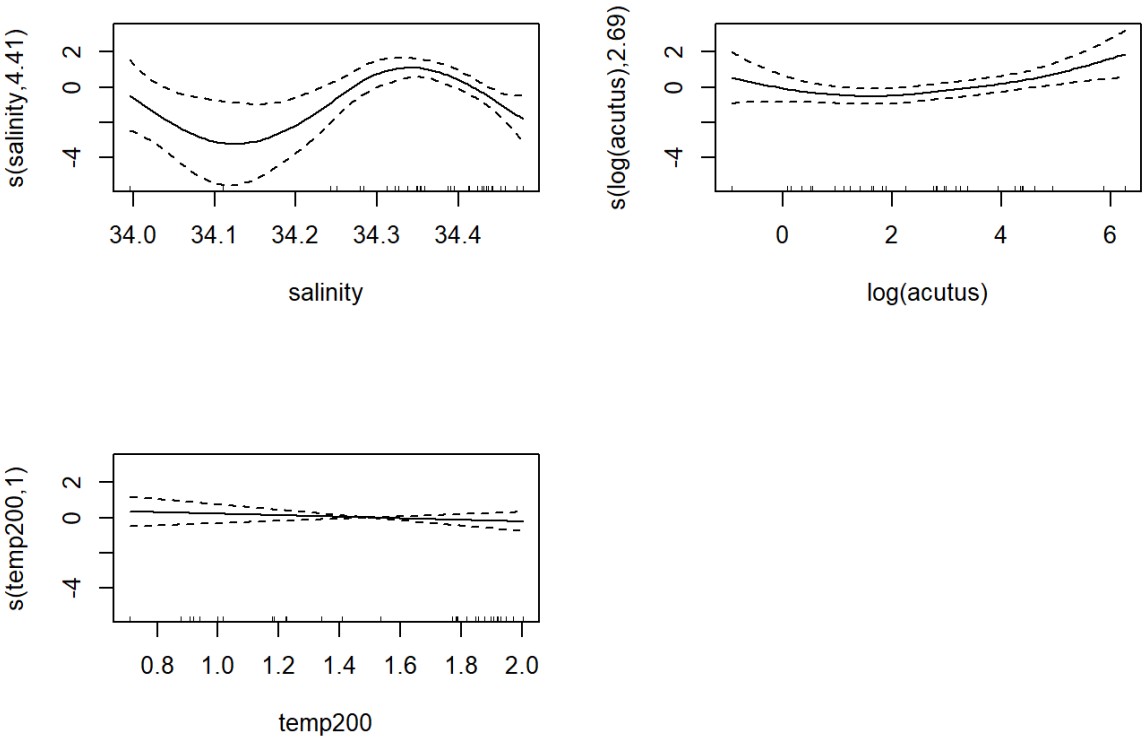

Figure D1. General additive model (GAM) smoothed for the abundance of adult *Thysanoessa macrura* over the southern Kerguelen Plateau including salinity, the abundance of the copepod *Calanoides acutus* (Log_{10}) and temperature at 200 m depth.

Table D2. Biomass estimates at the sites sampled for *Thysanoessa macrura* across the southern Kerguelen Plateau. The standard deviation and confidence intervals of biomass calculations are also provided.

Site	Biomass (mg m^{-3})	Standard deviation	Upper biomass estimate (mg m^{-3})	Lower biomass estimate (mg m^{-3})
1	3.43	0.09	3.60	3.26
2	4.25	0.19	4.64	3.87
3	1.71	0.04	1.79	1.64
4	6.64	0.21	7.05	6.23
5	3.43	0.11	3.66	3.21
8	9.53	0.41	10.36	8.70
9	2.04	0.15	2.35	1.74
10	0.93	0.07	1.07	0.79
11	8.81	0.40	9.60	8.01
12	1.90	0.10	2.11	1.69
13	6.04	0.56	7.16	4.92
14	2.14	0.09	2.31	1.96
15	4.62	0.42	5.46	3.79
16	0.59	0.04	0.67	0.52
17	0.83	0.05	0.94	0.73
18	0.86	0.03	0.92	0.80
19	4.75	0.22	5.19	4.31
20	3.62	0.12	3.87	3.37
21	3.07	0.09	3.26	2.89
22	0.95	0.03	1.00	0.90
23	0.85	0.04	0.93	0.78
24	1.45	0.11	1.67	1.22
25	2.37	0.09	2.54	2.19
26	0.38	0.02	0.42	0.33
27	0.20	0.01	0.22	0.17
28	0.92	0.05	1.03	0.82
29	0.04	0.00	0.05	0.04
30	0.76	0.05	0.85	0.67
32	0.15	0.02	0.18	0.12
33	0.05	0.00	0.06	0.04
38	0.11	0.01	0.13	0.08
39	0.20	0.01	0.22	0.18
40	1.20	0.08	1.35	1.05
41	4.02	0.14	4.29	3.75

Appendix E

Discovery of gregarine parasitism in some Southern Ocean krill (Euphausiacea) and the salp *Salpa thompsoni*

The following provides information on the discovery and description of gregarine parasites in the guts of *T. macrura* identified during gut contents analysis, with subsequent gregarines identified within the guts of several other species of krill and salp from the Southern Ocean. This publication provides additional information on the feeding ecology of *T. macrura* and contributes to the body of work provided by this thesis; however, it does not directly relate to the key aims of the research provided in the body of this thesis.

All the research presented in this appendix is currently published in Polar Biology

Wallis JR, Smith AJR, Kawaguchi S. (2017). Discovery of gregarine parasitism in some Southern Ocean krill (Euphausiacea) and the salp Salpa thompsoni*. Polar Biol 40:1913-1917*

Polar Biol
DOI 10.1007/s00300-017-2089-0

SHORT NOTE

Discovery of gregarine parasitism in some Southern Ocean krill (Euphausiacea) and the salp *Salpa thompsoni*

Jake R. Wallis[1,2] · **Abigail J. R. Smith**[1] · **So Kawaguchi**[2,3]

Received: 13 November 2016 / Revised: 10 January 2017 / Accepted: 23 January 2017

Abstract The presence and role of endoparasites in pelagic macrozooplankton within the Southern Ocean are poorly understood. Accounts of such parasites are generally restricted to the Antarctic krill species *Euphausia superba*, with little information on other possible host species. Endoparasitic gregarines were recorded for the first time in the euphausiids *Euphausia triacantha* and *Euphausia valentini* and the salp *Salpa thompsoni* during the Kerguelen Axis Antarctic research cruise (February–March 2016). Gregarines found in *E. triacantha* and *E. valentini* were morphologically similar to those previously identified in Antarctic krill, *E. superba*. Despite overlapping distributions, the smaller euphausiid *Thysanoessa macrura* possessed a different gregarine endoparasite, indicating parasite–host specificity in Southern Ocean euphausiids. Most notable was the discovery of large gregarines in the stomachs of aggregate individuals of *S. thompsoni*. The presence of gregarines in these dominant macrozooplankton indicates that endoparasitism within the Southern Ocean is more common than previously thought. Gregarines were observed in guts of krill and salps collected between 57.9 and 63.6°S. The continual presence of gregarines in the species examined indicates that these host-parasite interactions are not isolated events with differing life stages of gregarines within the same intestinal tract of some species indicating periodic infection. The impacts of gregarine parasitism on these newly identified hosts are unclear and require further investigation to understand the spatial and temporal patterns of gregarine-host interactions.

Keywords *Thysanoessa macrura* · *Euphausia triacantha* · *Euphausia valentini* · Indian Ocean

✉ Jake R. Wallis
jrwallis@utas.edu.au

[1] Institute for Marine and Antarctic Studies, University of Tasmania, Private Bag 129, Hobart, TAS 7001, Australia

[2] Antarctic Climate and Ecosystem Cooperative Research Centre, University of Tasmania, Private Bag 80, Hobart, TAS 7001, Australia

[3] Australian Antarctic Division, 203 Channel Highway, Kingston, TAS 7050, Australia

Introduction

Gregarines are a diverse group of endoparasites of the phylum Apicomplexa (Class Sporozoea, Order Eugregarinida). Parasitism by gregarines has been documented in both vertebrate and invertebrates in terrestrial and aquatic environments; however, the incidence and influence of these enodparasites on marine species are poorly understood (Gómez-Gutiérrez and Morales-Ávila 2016). Gregarines differ from other apicomplexans due to the lack of merogony (asexual reproduction by multiple fission), with the ingestion of oocysts from the environment responsible for infection (Takahashi et al. 2009). Continued presence and parasitism of the host, therefore, requires repeat ingestion of oocysts from the environment. There are very few reports of gregarine endoparasitism within Southern Ocean macrozooplankton, being confined to a few species of krill and amphipods. Avdeev (1985) first described the gregarine *Cephaloidophora pacifica* within the digestive tract and mid-gut gland (hepatopancreas) of the Antarctic krill *Euphausia superba*. Subsequent investigations have shown the high prevalence of this endoparasite in both larval and adult individuals of *E. superba* and a cosmopolitan distribution of *C. pacifica*, with the life-cycle of these gregarines conceptualised by Takahashi et al.

Published online: 10 February 2017

(2009). *Cephaloidophora thysanoessae* was later identified by Avdeev and Avdeeva (1989) in the krill *Thysanoessa macrura*, with the presence of gregarines in other Southern Ocean euphausiid species currently unknown. The influence of gregarines on marine hosts is poorly understood, with negative impacts ranging from sterility of adult females to blockages of the intestinal tract reducing nutrient absorption (Kulka and Corey 1984; Takahashi et al. 2011). In this study, we describe gregarines and their occurrence in the euphausiids *T. macrura, Euphausia triacantha*, and *Euphausia valentini* and the salp *Salpa thompsoni*.

Methods

Krill and salps were collected using a rectangular midwater trawl net (RMT) in the Indian sector of the Southern Ocean during the 2015/16 Australian marine science Kerguelen Axis voyage. Upon collection, individuals were frozen immediately at −80 °C for analysis of gut contents. Samples were collected along a latitudinal gradient encompassing several of the major oceanographic fronts in the region, with all three krill species collected at the northern extent of the study area (57.9°S, 83.4°E). *S. thompsoni* and *T. macrura* were both collected in the centre of the study area (61.9°S, 85.0°E), separated from the northern site by the Southern Antarctic Circumpolar Front. *T. macrura* was also collected from the southern extent of the voyage (63.6°S, 88.2°E) and was separated from the mid sampling site by the Southern-Boundary of the Antarctic Circumpolar Current. Each species of krill was dissected under stereomicroscope, removing both the entire length of the gut and the hepatopancreas. The foregut (including the stomach) and hind-gut were separated and examined separately. *S. thompsoni* guts were removed from the test and halved due to their large size. Compound microscopy was then used to examine the components of the guts (and hepatopancreas for krill). Twenty individual gregarine specimens were then measured from each host species to provide morphometric data for their identification.

Results and discussion

Gregarines were identified in all species examined with a minimum of 44% and maximum of 64% prevalence identified for *E. valentini* and *T. macrura*, respectively (Table 1). The size and shape of gregarines identified differed between *T. macrura* and *Euphausia* species, suggesting gregarine-host specificity (Table 2). Immature gamonts of *C. thysanoessae* were identified within the intestinal tract and hepatopancreas of *T. macrura* (Fig. 1a). Gamonts were elongated, with a clear septum separating the deutomerite and promerite, with a distinctive single nucleus within the deutomerite (Fig. 1b). Immature gamonts appeared translucent with disperse granules throughout the entire body. They had a mean total size (±SD) 47.6 ± 10.45 µm (Fig. 1b). Despite their smaller size due to being immature gamonts, morphometric characteristics are consistent with those provided by Avdeev and Avdeeva (1989) (Table 2).

The gregarines present within *E. triacantha* and *E. valentini* were larger than those found within *T. macrura*, with the morphological characteristics of the gamonts closely resembling *C. pacifica* commonly found in *E. superba*. Both immature and mature gamonts were identified in *E. triacantha* and *E. valentini*. Immature gamonts were small and oval in shape, with a mean size (±SD) 24.0 ± 4.1 µm for *E. triacantha* (Fig. 2a) and 22.4 ± 5.0 µm for *E. valentini* (Fig. 3a). In both host species, immature gamonts were translucent; however, both a clear nucleus within the deutomerite and a septum were visible. Mature gamonts from *E. triacantha* had a mean size of 41.8 ± 6.7 µm and *E. valentini* 46.92 ± 3.54 µm, and were 'pear-shaped', with dense granules and large vacuoles evident in both the deutormite and the promerite (Figs. 2b, 3b). Comparisons with morphometric data of *C. pacifica* identified in *E. superba* by Avdeev (1985) showed that they closely resembled that recorded for the gregarines identified in both *E. triacantha* and *E. valentini*, indicating that they were likely of the genus *Cephaloidophora* (Table 2). Variations in the total size and relative proportions of the promerite and deutomerite indicate the need for further investigation via molecular techniques to identify the gregarines and their relatedness to those described for *E. superba*. Gregarines were found in all individuals at each site in which they

Table 1 Number of each host macrozooplankton species examined for the presence of gregarines within their intestinal tract, their prevalence, and the presence of immature and mature gamonts in each host species

Host species	Number examined	Prevalence (%)	Immature gamont	Mature gamont
Thysanoessa macrura	45	64.4	✓	
Euphausia triacantha	25	68	✓	✓
Euphausia valentini	25	44	✓	✓
Salpa thompsoni	25	48		✓

Table 2 Comparison of gamont morphometric data from described gregarine species and their host species (indicated in bold) and those identified in this study

Gregarine species	Host species	TL (µm)	ProL (µm)	DeuL (µm)	ProL/TL	DeuL/TL	ProL/DeuL
Cephaloidophora thysanoessae[a]	*Thysanoessa macrura*	173	33	134	1:5.2	1:1.3	1:4
Cephaloidophora thysanoessae	*Thysanoessa macrura*	47.1 ± 10.45 (35–62)	8.6 ± 5.12 (3–16)	38.5 ± 5.35 (32–46)	1:5.5	1:1.2	1:4.5
Cephaloidophora pacifica[b]	*Euphausia superba*	96	17	68	1:5.6	1:1.4	1:5.6
Cephaloidophora-like specimens (Fig. 2)	*Euphausia tricantha*	41.8 ± 6.7 (32–49)	13 ± 3.5 (8–17)	28.8 ± 3.21 (24–32)	1:3.2	1:1.5	1:2.2
Cephaloidophora-like specimens (Fig. 3)	*Euphausia valaneitni*	46.92 ± 3.54 (42–50)	18.18 ± 1.65 (16–20)	28.8 ± 1.98 (26–31)	1:2.6	1:1.6	1:1.6
Thalicola flava[c]	*Pegea confoederata*	225	50	150	1:4.5	1:1.5	1:3
Thalicola- like specimens (Fig. 4)	*Salpa thompsoni*	144 ± 34.04 (116–200)	34.3 ± 9.75 (24–50)	109.8 ± 24.33 (91–152)	1:4.2	1:3.1	1:3.2

The mean ± standard deviation (and range) is provided for the total length (TL), promerite length (ProL), and deutomerite length (DeuL) based upon measurements of 20 individual gregarine specimens for each host species

[a]Avdeev and Avdeeva (1989)

[b]Avdeev (1985)

[c]Desportes and Schrével (2013)

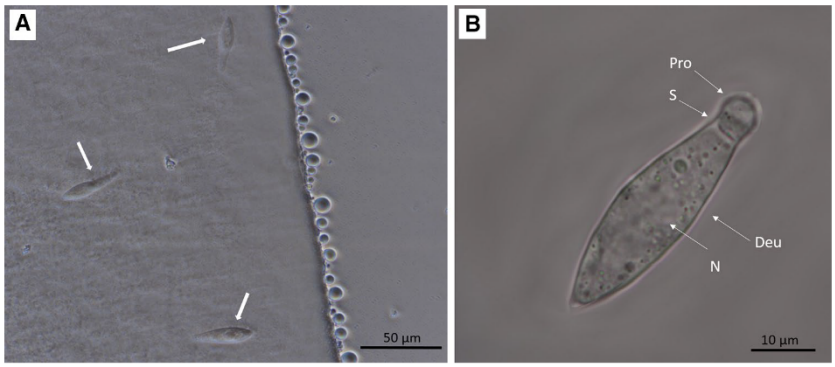

Fig. 1 Gregarine *Cephaloidophora thysanoessae* found within the hind-gut of *Thysanoessa macrura*. **a** Immature gamonts within the lumen of the hind-gut. Each *arrow* identifies an individual gamont. **b** Isolated immature gamont from the hind-gut indicating the major anatomical features. Septum (S), deutomerite (Deu), promerite (Pro), nucleus (N)

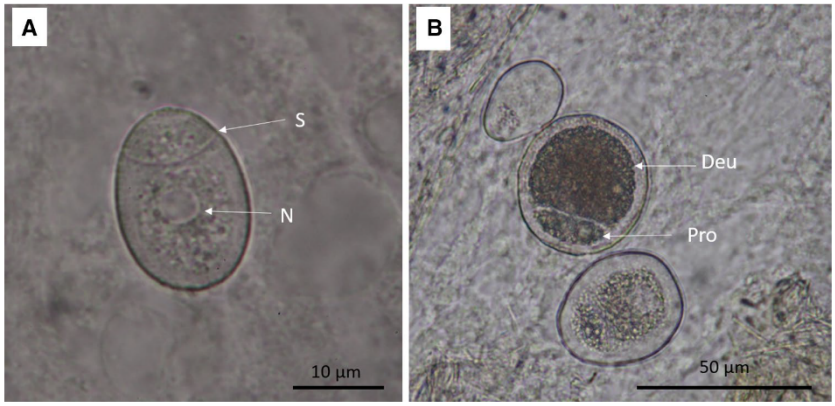

Fig. 2 Gregarine observed in *Euphausia triacantha*. **a** Immature gamont isolated from within the hind-gut. Septum (S), nucleus (N). **b** Mature gamonts found within the digested material of the hind-gut. Deutomerite (Deu), promerite (Pro)

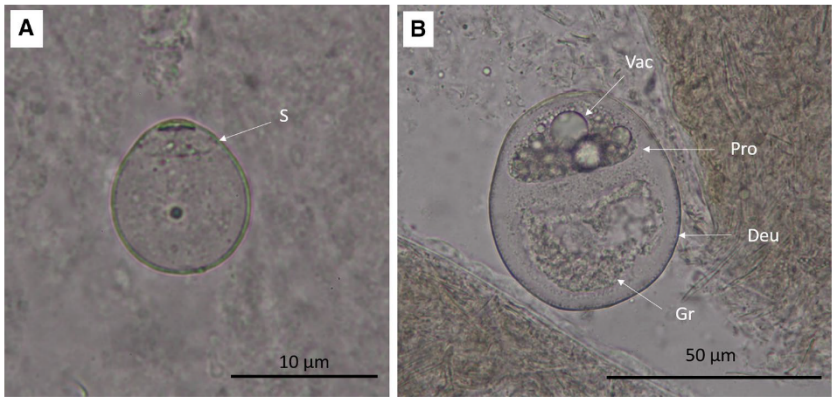

Fig. 3 Gregarine observed in *Euphausia valentini*. **a** Immature gamont found within the hind-gut lumen. Septum (S). **b** Mature gamont from within digested material of the hind-gut. Vacuole (Vac), dense granules (Gr), deutomerite (Deu), promerite (Pro)

were examined. *C. thysanoessae* was identified parasitising *T. macrura* over the entire region of the study. Furthermore, the presence of both mature and immature gamonts in the larger krill *E. tricantha* and *E. valentini* indicates that ingestion of oocysts from the environment is continual and may reflect their feeding behaviour. The distribution of gregarines within the digestive tract of each of the three euphausiids examined was not uniform, with gamonts only identified within the hind-gut and hepatopancreas. A similar pattern in gregarine distribution has been recorded for *E. superba*, with gregarines thought to both avoid the foregut due to the mechanical digestion of the gastric mill and their motility allowing them to migrate within the gut to avoid being shed with the cuticle of the stomach and hindgut during moulting (Takahashi et al. 2003). The lack of mature gamonts recorded within *T. macrura* may be due to larger, mature gamonts having been discharged during the previous moulting events. Further studies are required to determine if *C. thysanoessae* demonstrates a 'refuge seeking' behaviour that is described for gregarine parasitism of *E. superba* (Gómez-Gutiérrez and Morales-Ávila 2016).

Most notable was the identification of gregarines within aggregates of *S. thompsoni* (Fig. 4a). Gregarines have previously been identified in benthic tunicates; however, only two species of salps have been reported as hosts of these endoparasites (Clopton 2002). The gregarine genus

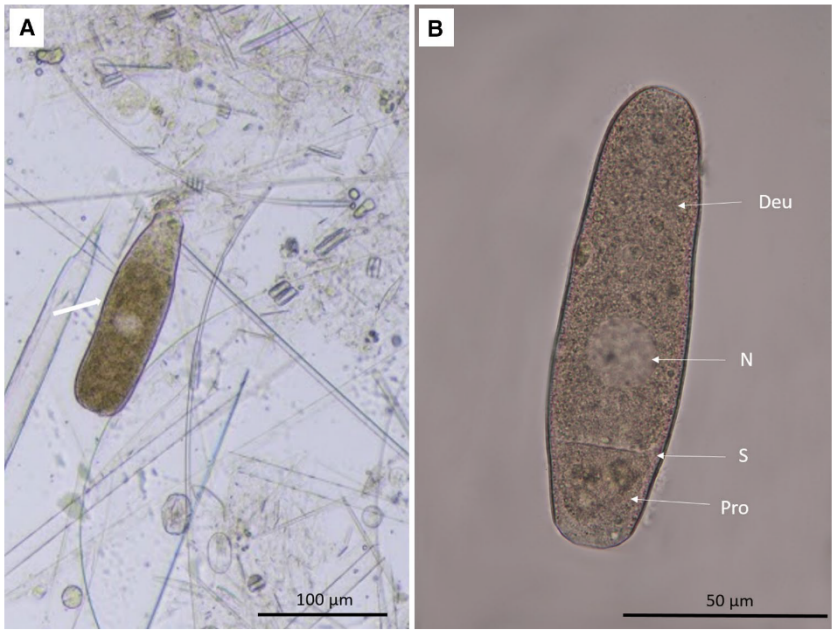

Fig. 4 Gregarine from the gut of an aggregate test of *Salpa thomponsi* **a** Gamont identified within material from the gut as indicated by the *white arrow*. **b** Isolated large gamont. Septum (S), deutomerite (Deu), promerite (Pro), nucleus (N)

Thalicola has been described for both *Salpa maxima* and *Salpa fusiformis* in the northern hemisphere; however, no such observation has been made for the dominant Southern Ocean species *S. thompsoni*. The gregarines observed in *S. thompsoni* were very large compared to those identified in the euphausiid species, with a mean size (±SD) of 144 ± 34.04 μm. Gamonts were distinctively 'bottle-shaped' and present throughout the entire length of the guts examined (Fig. 4a, b). Dense granules were present in both the deutomerite and the promerite, which were separated by a septum, and a spherical nucleus was clearly visible in the centre of the deutomerite (Fig. 4b). The morphology of gregarines identified in *S. thompsoni* is highly consistent with that of *Thalicola flava*, a species of gregarine that parasitise the salp species *Pegea confoederata* (Table 2) (Desportes and Schrével 2013). The established classification of gregarines that infect salps and the closeness in morphology to *T. flava* indicate that the gregarines identified within *S. thompsoni* are of the genus *Thalicola*, however, a detailed molecular study is required to determine if these gregarines belong to a currently described or new species. The impacts of gregarine parasitism on *S. thompsoni* are unclear. Reports of gregarines within other tunicates have been linked to disease, ultimately resulting in the death of the host (Mita et al. 2012). Whilst this remains to be seen in *S. thompsoni*, it is likely that parasitism at least impairs the ability to process ingested food and, therefore, assimilation of nutrients as witnessed for Antarctic krill (Takahashi et al. 2011). Given the potential importance of *S. tompsoni* in the Southern Ocean with respect to changing oceanic conditions associated with a warming climate and their relationship with *E. superba* (Atkinson et al. 2004), understanding the role that these endoparasites play in the reproductive efficiency of this gelatinous species is important.

The presence of gregarines in *E. triacantha, E. valentini*, and *S. thompsoni* indicates that parasitism of macrozooplankton within the Southern Ocean is more common than previously thought. The occurrence of gregarines over a large spatial distribution and the presence of both mature and immature gamonts within individuals suggest periodic infection. Detailed analysis of identified gregarines within *E. triacantha* and *E. valentini* is required to establish if they are the same species recorded for *E. superba* or a currently undescribed species. The identification of gregarines in these species raises important questions that need to be addressed: how does infection rate relate to feeding? What are the impacts of endoparasitism on *S. thompsoni* and are aggregates and solitary individuals impacted differently? Given the interest in the interaction of salps and krill in the Southern Ocean ecosystem, it is important that the impacts of these parasites on their hosts and their interactions over broad scales are better understood.

Acknowledgements We thank the captain and crew of the RV *Aurora Australis* and research expeditioners for their assistance during the voyage. We are especially thankful for the assistance and expertise provided by Paige Kelly. This project was supported by AAS Grants 4331, 4344, and 4037. This research was supported by the Antarctic Climate and Ecosystems Cooperative Research Centre (ACE CRC).

References

Atkinson A, Siegel V, Pakhomov E, Rothery P (2004) Long-term decline in krill stock and increase in salps within the Southern Ocean. Nature 432:100–103

Avdeev VV (1985) New species of gregarines of genus *Cephaloidophora* parasites of *Euphausia superba*. Parisitology 1:1–6

Avdeev VV, Avdeeva NV (1989) On gregarine fauna from planktonic crustaceans from Antarctica. In: Lebadev BI (ed) Parasites of animals and plants: collection papers. Far East Division of Russia Academy of Science, Vladivostok, pp 40–44

Clopton RE (2002) Phylum Apicoplexa Levine 1970: Order Eugregarinorida Léger, 1990. In: Lee JJ, Leedale G, Patterson D, Bradbury (eds) Illustrated guide to the protozoa, 2nd edn. Society of Protozoologists, Lawrence, pp 205–288

Desportes I, Schrével J (eds) (2013) Marine gregarines. In: Treatise on zoology—anatomy, taxonomy, biology. The gregarines, vol 1. Brill, Leiden, pp 197–375

Gómez-Gutiérrez J, Morales-Ávila JR (2016) Parasites and diseases. In: Siegel V (ed) Biology and ecology of Antarctic krill. Springer, Switzerland, pp 351–386

Kulka DW, Corey S (1984) Incidence of parasitism and irregular development of gonads in *Thysanoessa inermis* (Kroeyer) in the Bay of Fundy (Euphausiacea). Crustaceana 46:87–94

Mita K, Kawai N, Rueckert S, Sasakura Y (2012) Large-scale infection of the ascidian *Ciona intestinalis* by the gregarine *Lankesteria ascidiae* in an inland culture system. Dis Aquat Org 101:185–195

Takahashi KT, Kawaguchi S, Kobayashi M, Toda T (2003) Parasitic eugregarines change their spatial distribution within the host digestive tract of Antarctic krill, *Euphausia superba*. Polar Biol 26:468–473

Takahashi KT, Kawaguchi S, Toda T (2009) Observation by electron microscopy of a gregarine parasite of Antarctic krill: its histological aspects and ecological explanations. Polar Biol 32:637–644

Takahashi KT, Kawaguchi S, Kobayashi M, Toda T, Tanimura A, Fukuchi M, Odate T (2011) Eugregarine infection within the digestive tract of larval Antarctic krill, *Euphausia superba*. Polar Biol 34:1167–1174

Appendix F

In situ growth rate estimates of Southern Ocean krill, *Thysanoessa macrura*

The following provides the first estimates of *T. macrura* growth using the instantaneous growth rate method developed for live experiments with euphausiids. The results of this study do not directly answer the key aims of the research provided in the body of this thesis; however, provides supporting information for describing the population ecology of *T. macrura*.

All the research presented in this appendix is currently in press in Antarctic Science

Wallis JR, Melvin JE, King R, Kawaguchi S. (2019). In situ growth rate estimates of Southern Ocean krill, Thysanoessa macrura*. Antarct Sci DOI:10.1017/S0954102019000063*

Antarctic Science page 1 of 7 (*2019*) © Antarctic Science Ltd 2019 doi:10.1017/S0954102019000063

In situ growth rate estimates of Southern Ocean krill, *Thysanoessa macrura*

JAKE R. WALLIS[1,2], JESSICA E. MELVIN[1,2], ROBERT KING[3] and SO KAWAGUCHI[2,3]

[1]*Institute for Marine and Antarctic Studies, University of Tasmania, Private Bag 129, Hobart Tasmania 7001 Australia*
[2]*Antarctic Climate & Ecosystem Cooperative Research Centre, University of Tasmania, Private Bag 80, Hobart, Tasmania 7001, Australia*
[3]*Australian Antarctic Division, 203 Channel Highway, Kingston, Tasmania 7050, Australia*
jrwallis@utas.edu.au

Abstract: Growth, which is intrinsically linked to environmental conditions including temperature and food availability are highly variable both temporally and spatially. Estimates of growth rates of the Southern Ocean euphausiid *Thysanoessa macrura* are currently restricted to limited studies which rely upon repeated sampling and length-frequency analysis to quantify growth rates. The instantaneous growth method (IGR) was used to measure the growth rate of *T. macrura* successfully in the southern Kerulen Plateau region during summer, providing the first IGR parameters for the Southern Ocean euphausiid species. Results of the four-day IGR incubation indicate a period of low somatic growth for adult *T. macrura*. Males had a longer intermoult period (IMP) (62 days) than females (42 days), but the sexes exhibited similar daily growth rates of 0.011 mm day^{-1} and 0.012 mm day^{-1} respectively. Juveniles exhibited the fastest growth, with an IMP of 13 days and daily growth rate of 0.055 mm day^{-1} indicating a prolonged growth season, similar to the Antarctic krill *E. superba*. Consequently, we highlight the usability of the IGR method and strongly encourage its use in developing a comprehensive understanding of spatial and seasonal growth patterns of *T. macrura*.

Received 12 October 2018, accepted 27 January 2019

Key words: daily growth rate, instantaneous growth rate, intermoult period

Introduction

Quantifying growth and its seasonal patterns is integral to understanding the life history of euphausiids. Growth in krill, like other crustaceans, is not a continuous process but occurs periodically, punctuated by moulting of the exoskeleton. Growth is intrinsically tied to the environment, influenced by temperature and food availability in addition to the partitioning of energy between storage, reproduction and somatic growth (Kawaguchi *et al.* 2006, Tarling *et al.* 2006). Consequently, growth rates of krill are highly variable both spatially and temporally. Measuring the somatic growth of krill is often achieved by one of two methods: the analysis of length-frequency distributions of single populations or live experimentation (Nicol 2000).

Thysanoessa macrura G.O. Sars is a small, highly abundant species of krill in the Southern Ocean. Despite the recognition as the second most abundant krill species in this region and trends suggesting an increase in abundance in some areas including the Western Antarctic Peninsula, estimates of its growth are currently restricted to repeated sampling length-frequency analyses (Haraldsson & Siegel 2014, Steinberg *et al.* 2015). Due to the uncertainties and limitations associated with this method, including the assumption of the same population being repeatedly sampled with no immigration or emigration occurring, growth rates are reported as averages for periods that span 4–13 months, providing little information on seasonal cycles (Nordhausen 1992, Haraldsson & Siegel 2014). *Thysanoessa macrura* is thought to live for up to four years, growing to a maximum size of 35 mm and reaching sexual maturity at 13 mm in length (Haraldsson & Siegel 2014, Wallis *et al.* 2018). Recent investigations have provided valuable information on the winter reproductive cycle of *T. macrura* and the role of stored lipids in fuelling gonad maturation (Wallis *et al.* 2018). Understanding of seasonal growth patterns of *T. macrura* represents a remaining fundamental gap in knowledge of the life history of this species that is essential for quantifying the partitioning of energy between somatic growth, lipid storage and reproduction, and establishing conceptual models of population dynamics.

The instantaneous growth rate (IGR) method has proved to be a valuable means of quantifying growth at fine spatial and temporal scales (Nicol *et al.* 1992). Whilst this method requires the incubation of large numbers of krill (a minimum of 100 individuals) the information gained allows for a more accurate *in situ* determination of growth, accounting for environmental influences and mortality (Nicol 2000). Furthermore, the IGR method allows for the determination of the intermoult period (IMP) - the number of days between moulting events - which is influenced by temperature

and krill length, and daily growth rates (DGR) which incorporate both the IGR and IMP of the experiment (Tarling *et al.* 2006). Despite providing valuable, fine scale information, allowing for both regional and seasonal comparisons, this method is consistently only used for *Euphausia superba* in the Southern Ocean, with *T. macrura* often considered too fragile to use in live experiments (Haraldsson & Siegel 2014). The IGR method however, has been successfully applied to *Thysanoessa* species in the Northern Hemisphere (Pinchuk & Hopcroft 2007). Furthermore, Nicol (2000) indicates its effectiveness on other Southern Ocean euphausiids, including *T. macrura*, although quantitative data were not provided.

Advances in the methods and capabilities to provide fine scale estimates of growth and population structure are currently limited to *E. superba* in the Southern Ocean due to both their importance as a keystone species and the focus of large-scale fisheries (Melvin *et al.* in press). These techniques, especially the IGR method, are transferrable to other Southern Ocean euphausiid species, but have yet to be implemented to begin to fill major knowledge gaps in growth patterns, both spatially and seasonally. The present work demonstrates the successful application of the IGR method to *T. macrura* and provides the first *in situ* *T. macrura* growth parameters including IGR, IMP and DGR, information that is critical for future evaluations of the population dynamics of *T. macrura* and its role in the Southern Ocean ecosystem.

Methods

Sampling

Specimens of *T. macrura* were collected in the Kerguelen Plateau region of the Southern Ocean, as part of the Kerguelen Axis marine science voyage undertaken by the RV *Aurora Australis* during late January 2016. Live *T. macrura* were collected using a rectangular midwater trawl net (RMT 8) equipped with a flow meter (Baker *et al.* 1973). The ship-equipped scientific echo sounder was used to identify regions of potentially high *T. macrura* abundance, with aggregations of *T. macrura* appearing as dense 'patches' or 'mats' at the ocean surface (10–30 m depth), verified by routine trawls of the RMT. A dense mat of *T. macrura* was identified at 63.5°S, 93.6°E, located over the Princess Elizabeth Trough at a depth of 15 m. The RMT was subsequently deployed to this depth with a trawl time of seven minutes at a ship speed of < 2.0 knots to ensure minimal damage to individuals during trawling.

Upon collection, live *T. macrura* were immediately transferred into an on-board holding tank equipped with continuously flowing surface seawater. Two hundred and eighty-eight freely swimming individuals were then randomly selected and transferred into individual 250 ml jars equipped with small holes to allow water exchange and placed in a specially built flow-through system to maintain ambient ocean temperature for the duration of the experiment. For detailed technical information on the flow-through system see Kawaguchi *et al.* (2006). The experiment was conducted for a total of four days, with jars checked for moults every 24 hours. If an individual was found to have moulted, the animal and its moult were immediately frozen together and stored in liquid nitrogen for later measurement.

The remainder of the krill were then collected and a Motoda box plankton splitter (Motoda 1959) was used to fraction the sample, with a proportion immediately frozen at -80°C and the remainder stored in 10% buffered formalin. Preserved krill were counted, measured for their total length and sexed according to the descriptions provided by Wallis *et al.* (2018). Direct counts of *T. macrura* were also performed, accompanied by the flow meter reading to provide the abundance of the dense mat of *T. macrura* sampled.

Growth estimates

The relationship between uropod length and total body length was determined for *T. macrura*. A total of 50 frozen individuals caught during the sampling of live *T. macrura* were measured for their total body length, from the tip of the rostrum to the base of the uropod using digital callipers under a stereo microscope, and uropods were measured using a calibrated eyepiece micrometre (±0.01 mm). ANCOVA was used to evaluate the difference in this relationship between males and females.

Instantaneous growth rates were calculated using measurements of both the left and right uropod exopodites of both the moult and post-moult individual. Moulted individuals were sexed according to Wallis *et al.* (2018) and uropods analysed using a Leica MZ9.5 microscope equipped with a DFC380 digital colour camera. Moults and moulted individuals were placed ventral side down and the uropod arranged at an approximate 45° angle to the telson and photographed. The Leica Application Suite V2.4 image analysis software was then used to measure the length of the uropod. Damaged uropods were not measured, and an average of the length of left and right uropod was used for subsequent calculations if both were found to be intact and undamaged. The IGR of each individual was then calculated as the change in the length of the uropod from the moult (U_m) and the animal post-moult (U_a) by the following equation (Tarling *et al.* 2006):

$$IGR_{uro} = \left(\frac{U_a - U_m}{U_m}\right) \cdot 100. \quad (1)$$

To establish the changes in total body length (IGR_{TL}) based upon changes in uropod length, the following equation is used:

$$IGR_{TL} = \left(\frac{TL_a - TL_m}{TL_m}\right) \cdot 100, \quad (2)$$

where TL_a is the total length of the post-moult krill and TL_m is the total length of the moult. The total length of krill was first determined by applying the derived relationship between uropod length and total body length (Eq. 5). ANOVA was subsequently used to test for differences in estimates of IGR based upon the change in uropod length and total body length for males, females and juveniles.

Due to the surviving non-moulted krill not being sexed, the intermoult period (IMP) of *T. macrura* was calculated for the whole experiment. IMP was determined by the equation (Tarling *et al.* 2006):

$$IMP = \frac{(N + m) \cdot d}{m}, \quad (3)$$

where N is the number of surviving krill at the conclusion of the experiment, m is the number of krill that moulted, and d is the duration of the experiment (days).

IGR calculations provide growth information in terms of proportional change. The daily growth rate (DGR) of *T. macrura* was subsequently calculated by the follow equation (Tarling *et al.* 2006):

$$DGR = \left(\frac{TL_m \cdot IGR_{uro}}{IMP \cdot 100}\right). \quad (4)$$

Theoretical DGRs were also calculated for male, female and juvenile *T. macrura*. Despite not having quantitative information on the number of maturity stages of *T. macrura* within the IGR experiment (male, female and juvenile), the maturity stage ratio of the population obtained was used as a proxy for the ratio of males, females and juveniles used within the experiment. It is assumed that due to the random sampling of the 288 freshly caught individuals the IGR population was reflective of the ratio of maturity stage in the wild population, whilst also assuming that mortality within the experiment was constant across males, females and juveniles. Using this information, the IMPs for each sex and juveniles were calculated using Eq. 3 and a subsequent sex- and stage-specific DGRs determined (Eq.4).

Results

The aggregation of *T. macrura* had a density of 30 ind. m^{-3}. The ratio of maturity stages of *T. macrura* within this surface mat indicated a female dominant aggregation, with 67% female, 29% male and 4% juveniles identified. The length frequency of *T. macrura* indicated a relatively similar size distribution for both males and females, albeit with females at higher frequencies than males (Fig. 1).

Analysis of the relationship between total length and uropod length for males and females, shown in Fig. 2 indicated no significant difference based upon sex ($F = 0.23$, $P > 0.2$). Consequently, both males and females were combined to provide a single relationship to estimate total length based upon uropod length. This relationship was found to have a strong linear relationship ($R^2 = 0.93$, $P < 0.001$) and is described by:

$$Total\ length = 5.595 \cdot \text{Uropod length} + 1.804. \quad (5)$$

Instantaneous growth rates

Twenty-eight individuals had moulted by the end of the IGR experiment (Table I). The number of individuals that moulted per day was variable between days of incubation, with the most individuals moulting during the second and third days of incubation (Fig. 3). As shown in Fig. 4, the IGR calculated for each day of the incubation indicated a non-significant decrease of IGR over the duration of the experiment ($F = 1.52$, $P > 0.2$). Due to the limited number of juveniles and males that moulted over the course of the experiment, this relationship was assessed based upon cumulative IGR values for each day of the experiment rather than maturity stage trends. During the course of the experiment, 30 individuals died, accounting for 10.4% of the experimental *T. macrura* used.

IGR calculations based upon the change in uropod length and total length using the relationship derived from frozen individuals (Eq. 5) were both used to estimate the percentage growth of male, female and juvenile *T. macrura*. Based upon both methods for IGR calculation, juveniles were found to have the highest proportional growth of all three maturity stages (Table I). Juveniles had an average IGR_{uro} of 4.9% and IGR_{TL} of 4.3%, followed by males with an IGR_{uro} and IGR_{TL} of 4.3% and 3.8% respectively. Females had the lowest growth estimates at 3.1% (IGR_{uro}) and 2.8% (IGR_{TL}). Comparisons of IGR estimates based upon the change in length of uropods and total body length between moulting indicated that there was no significant difference in these estimates for males ($F = 0.28$, $p = 0.61$), females ($F = 0.66$, $p = 0.66$) or juveniles ($F = 0.12$, $p = 0.74$). Consequently, calculations of DGR for *T. macrura* were based upon IGR_{uro} to avoid increasing unnecessary errors associated with applying total length conversions.

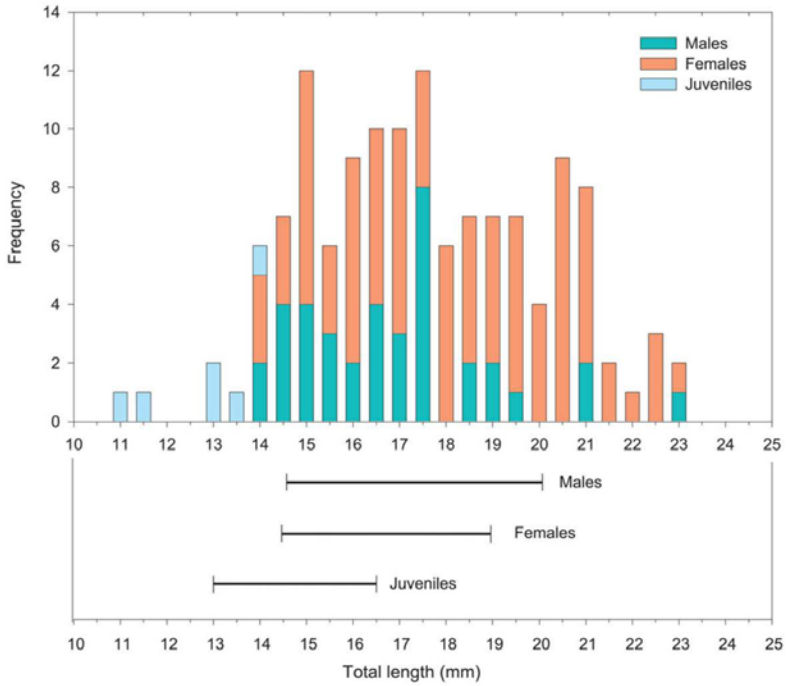

Fig. 1. Size-frequency distribution of *Thysanoessa macrura* for the maturity stages; male, female and juvenile from the aggregation sampled for the IGR experiment. The solid lines indicate the range in size of pre-moult individuals used in the IGR experiment.

Comparisons of the total lengths of males, females and juveniles used in the IGR experiment indicate that the spread in the size is relatively consistent with the size range of each maturity stage identified in the aggregation sampled, although males and females above 21 mm were not represented in the experiment (Fig. 1).

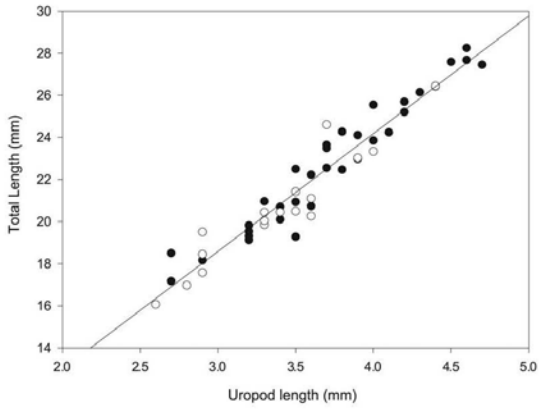

Fig. 2. Relationship between total body length and uropod length of adult *Thysanoessa macrura* males (empty circles) and females (filled circles). Total length = 5.595 × Uropod length + 1.804 ($R^2 = 0.93$, $p < 0.001$).

Intermoult period and daily growth rates

The IMP of *T. macrura* based upon cumulative information from the entire IGR experiment was found to be 41 days. The subsequent DGR of *T. macrura* irrespective of maturity stage ranged from 0.003–0.04 mm day^{-1} with a mean DGR of 0.009 mm day^{-1} (Table I). In order to provide quantitative growth rates for the different maturity stages present in the sample, the proportion of males, females and juveniles present in the *T. macrura* aggregation sampled was used to estimate the number of each present in the IGR experiment. The IMPs of all three maturity stages were then calculated assuming that mortality rates were consistent for males, females and juveniles within the experiment (Table I).

The theoretical IMPs were highly variable for the different maturity stages. Males had the largest IMP at 62, with a corresponding mean DGR of 0.011 mm day^{-1}. Females had a smaller IMP period than males, with an estimated IMP of 42 days, however DGR for females with a mean of 0.012 mm day^{-1} was not significantly different from the value for males ($F = 0.07$, $P = 0.77$). Juveniles had the lowest IMP of 14 days, with a corresponding mean DGR of 0.55 mm day^{-1}, significantly greater than both males and females ($F = 24.6$, $P < 0.001$).

Table I. Summary of the growth parameters for *Thysanoessa macrura* based upon the four-day experiment. Instantaneous growth rates (IGR) are provided based upon changes in uropod length (IGR_{uro}) and the total length of moulted *T. macrura* (IGR_{TL}). Subsequent intermoult period (IMP) and daily growth rate (DGR) are provided. Theoretical estimates of growth are based upon the ratio of developmental stages present within the aggregation of *Thysanoessa macrura* sampled. TL = total body length.

	Total in IGR experiment	Number of deaths	Number moulted	Pre-moult TL (mm)	Post-moult TL (mm)	IGR_{uro} (%)	IGR_{TL} (%)	IMP (days)	DGR (mm day^{-1})
Cumulative from experiment	288	30	28					41	0.009 ± 0.015
Males			5	16.7 ± 1.9	17.3 ± 1.9	4.3 ± 1.5	3.8 ± 1.3		
Females			18	17.6 ± 1.5	18.1 ± 1.4	3.1 ± 2.4	2.8 ± 2.1		
Juveniles			5	14.9 ± 1.4	15.6 ± 1.6	4.9 ± 2.7	4.3 ± 2.5		
Theoretical estimates*									
Males	81	8	5					62	0.011 ± 0.004
Females	193	20	18					42	0.012 ± 0.009
Juveniles	14	2	5					13	0.055 ± 0.034

Discussion

The results of this study demonstrate the practicability of applying the IGR method successfully to *T. macrura* in the field. The dense aggregation of *T. macrura*, appearing as a mat in surface waters demonstrated that this species can reach high densities in discrete regions, indicating behaviour not previously recorded for the species. *Thysanoessa macrura* is often thought of as a fragile species that does not survive net sampling (Haraldsson & Siegel 2014). Although *T. macrura* often do not survive the manual handling of long, standard trawls, often double oblique tows to 200 m, our observations demonstrate that *T. macrura* can survive short, targeted trawls, reducing the damage incurred during regular trawling by large nets. Furthermore, *T. macrura* were maintained alive in an on-board holding tank for one month (J. Wallis, personal observation). The structure of the *T. macrura* aggregation is consistent with other observations of *T. macrura* populations with a size range of 13–23 mm with a skewed sex ratio, dominated by females (Haraldsson & Siegel 2014).

The IGR method, established for the use of measuring *in situ* growth of *E. superba*, assumes that somatic growth is directly proportional to the change in uropod length between pre-moult (measured directly from the moult) and the moulted individual due to the linear relationship between uropod length and total length (Nicol 2000, Kawaguchi *et al.* 2006). The relationship between uropod and total length was also found to follow a linear relationship for *T. macrura*. No sexual differentiation was identified in this relationship, consistent with other somatic relationships for *T. macrura* (Fäber-Lorda 1990). Somatic relationships for *T. macrura* have been shown to display regional variability due to the influence of temperature and food availability and their influence on growth (Fäber-Lorda 1994). Accordingly, uropod-length relationships should

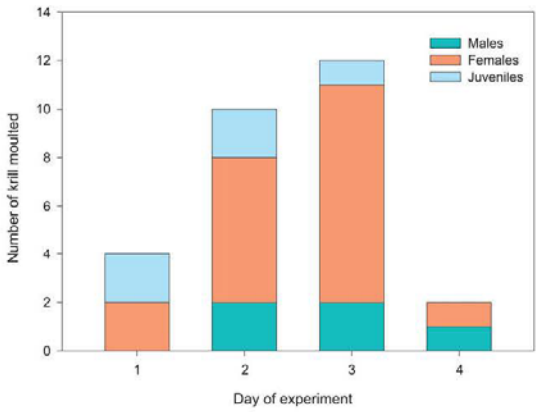

Fig. 3. Number of each *Thysanoessa macrura* maturity stage moulted for each day of the IGR experiment.

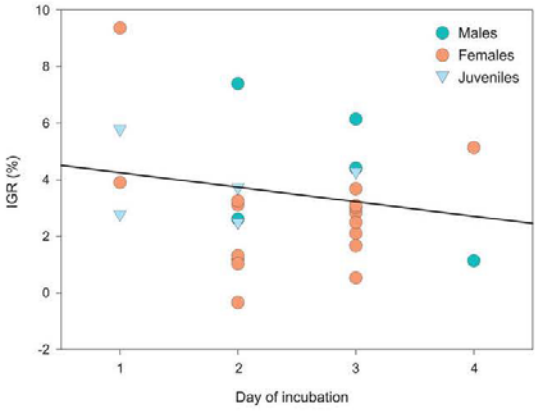

Fig. 4. IGR recorded for each day of the experiment for males, females and juveniles. The solid line indicates the linear regression relationship between cumulative IGR and day of incubation.

Table II. Estimates of *Thysanoessa macrura* growth rates based upon repeated measured length-frequency analysis.

Sex/stage	Method	Growth rate (mm d^{-1})	Time	Duration of experiment	Region
C II - F VI[1]	Length-frequency	0.073 0.05	December March	4 months	Gerlache Strait
C II - F VI[1]	Length-frequency	0.072 0.049	December March	4 months	Bransfield Strait
C II - F VI[1]	Length-frequency	0.057 0.042	December March	4 months	Drake Passage
Juveniles[2]	Length-frequency	0.017 0.023	Yearly average	12 months	Lazarev Sea
Adult Female[2]	Length-frequency	0.011	Yearly average	12 months	Lazarev Sea
Adult Male[2]	Length-frequency	0.015	Yearly average	12 months	Lazarev Sea
Adult[3]	Length-frequency	0.0383	January February average	9 years	Elephant Island - ACC waters
Adult[3]	Length-frequency	-0.0069	January February average	9 years	Bransfield Strait and Weddell Sea
Juveniles[4]	IGR	0.055	March	4 days	Princess Elizabeth Trough
Adult Males[4]	IGR	0.011	March	4 days	Princess Elizabeth Trough
Adult Females[4]	IGR	0.012	March	4 days	Princess Elizabeth Trough

[1]Nordhausen 1992.
[2]Haraldsson & Siegel 2014.
[3]Driscoll *et al.* 2015.
[4]This study.

be derived for each population of *T. macrura* sampled. A comparison of IGRs derived from uropod measurements and total body length, calculated from the relationship derived from the population sampled indicated no difference in IGR estimates and therefore indicates the feasibility of using uropods to estimate growth for *T. macrura* as per the established method for *E. superba* (Quetin & Ross 1991, Nicol *et al.* 1992)

Due to the lack of quantitative information regarding the ratio of maturity stages used in the experiment, only simple estimates of IMP and DGR of *T. macrura* (regardless of maturity stage) could be confidently calculated. The simple IMP for *T. macrura* of 41 days indicates a period of very little and slow somatic growth. Tarling *et al.* (2006) highlight the potential error associated with the calculation of IMP from a single IGR experiment if moult synchronicity is present. Due to the restrictions of only a single IGR experiment being performed, it was not possible to apply alternative methods of determining the IMP of *T. macrura*. Given that less than 10% of the incubated individuals moulted within the four-day experiment, it is likely that there was little moult synchronicity present and therefore the calculated IMP closely reflects the wild population. The large IMP is reflected by the low IGR values determined for *T. macrura* with females exhibiting the smallest growth increment (IGR_{uro}) at 3.1% followed by males at 4.3% and juveniles showing the highest growth at 4.9%. A growth rate of 0.009 mm day^{-1} is lower than yearly average growth rates previously reported for *T. macrura* (Haraldsson & Siegel 2014, Driscoll *et al.* 2015). Given that these previously reported growth estimates are yearly averages based upon repeated sampling length-frequency analysis, seasonal variation is not accounted for. Similar DGRs of northern hemisphere congener species, *T. inermis* and *T. spinifera* estimated using the IGR method have been determined during the onset of autumn, a period of low to negative growth for both species (Pinchuk & Hopcroft 2007). *Thysanoessa macrura* probably shows similar seasonal growth patterns, highlighting the need for the application of the IGR method during different times of the year in assessing these seasonal cycles.

The growth rate estimates of *T. macrura*, based upon cumulative information of the IGR experiment provide a broad overview of *T. macrura* growth and highlight the power of the IGR method. Despite the lack of quantitative information on the maturity stages present in the IGR experiment, using the assumptions of an equal maturity ratio to the wild population sampled allows for the first insights into the variation in growth for males, females and juveniles. The pattern in sex-specific IMPs observed by Tarling *et al.* (2006) for *E. superba*, with males possessing longer IMPs than females was reflected in the theoretical IMPs calculated for *T. macrura* in this study, with males having an IMP of 62 days and females 42 days. Juveniles had a much shorter IMP of only 13 days, indicating much higher growth than adult *T. macrura* and is reflective of the IGRs determined. Despite differences in the IMPs, males and females displayed highly similar DGRs. The DGRs determined for both males and females are very similar to previously reported growth estimates (Table II), however the DGR of juveniles, up to five times greater than adults, is substantially larger than current estimates for *T. macrura* (Haraldsson & Siegel 2014). These IMPs and DGRs of *T. macrura* are also consistent with the observed growth of *E. superba* during the same voyage (Melvin *et al.* in press). Whilst both patterns in IMP and growth rates are consistent with *E. superba* from the same time of year, the underlying mechanisms to explain these growth rates differ. During summer, *E. superba* is still actively reproducing, with energy used to fuel reproduction rather than somatic

growth, resulting in longer IMP and lower growth (IGR and DGR) (Tarling *et al.* 2006; Melvin *et al.* in press). *Thysanoessa macrura* however has finished its reproductive period by spring, accruing lipid reserves in the free space of the cavity during summer (Hagen & Kattner 1998, Wallis *et al.* 2018). The preferential partitioning of energy to lipid storage rather than somatic growth during late summer could help explain the growth identified for *T. macrura* and its similarity to that of *E. superba.* Furthermore, juveniles, with growth rates up to five times faster than adults, do not accumulate large lipid reserves until autumn, capitalizing on the high food availability in spring and summer for a sustained growth period, a similar trend as observed in *E. superba* (Hagen & Kattner 1998, Kawaguchi *et al.* 2006).

The results of the IGR experiment provided in this study demonstrates the success of the IGR method for *T. macrura*, providing the first IGR, quantitative IMP and DGR estimates for the species. Whilst the power of the IGR method is contingent upon multiple sampling locations to assess regional variations in growth and the ability to understand the influence of temperature and food availability on IMP and DGR, the limited sample size of our study currently precludes this ability. The theoretical growth parameters established for males, females and juveniles provide an interesting insight into variation between these maturity stages and prompt the need for further investigation. Answering the fundamental questions of the influence of sex and developmental stage, and environmental conditions on somatic growth rates is vital for producing a comprehensive understanding of the seasonal and regional patterns in *T. macrura* growth and should be the target of future investigations by employing the IGR method.

Acknowledgements

We would like to thank the captain and crew of the *Aurora Australis* and the members of the research expedition for their help and support during sample collection and the running of the experiment. We would also like to thank the reviewers for their help and expertise. This research was supported by the Antarctic Climate and Ecosystems Cooperative Research Centre (ACE CRC) and funded through the Australian Antarctic Science (AAS) grants 4331, 4344 and 4037.

Author contribution

J.R. Wallis performed the data analysis and was assisted by S. Kawaguchi with preparing the manuscript; R. King and J.E. Melvin performed the live experiment at sea.

References

Baker, A.C., Clarke, M.R. & Harris, M.J. 1973. The N.I.O. combination net (RMT 1+8) and further developments of rectangular midwater trawls. *Journal of the Marine Biological Association of the United Kingdom*, **53**, 176–184.

Driscoll, R., Reiss, C. & Hentschel, B. 2015. Temperature-dependant growth of *Thysanoessa macrura*: inter-annual and spatial variability around Elephant Island, Antarctica. *Marine Ecology Progress Series*, **529**, 10.3354/meps11291.

Fäber-Lorda, J. 1990. Somatic length relationships and ontogenetic morphometric differentiation of *Euphausia superba* and *Thysanoessa macrura* of the southwest Indian Ocean during summer (February 1981). *Deep-Sea Research A*, **37**, 1135–1143.

Fäber-Lorda, J. 1994. Length-weight relationships and coefficient of condition of *Euphausia superba* and *Thysanoessa macrura* (Crustacea: Euphausiacea) in southwest Indian Ocean during summer. *Marine Biology*, **118**, 645–650.

Hagen, W. & Kattner, G. 1998. Lipid metabolism of the Antarctic euphausiid *Thysanoessa macrura* and its ecological implications. *Limnology and Oceanography*, **43**, 1894–1901.

Haraldsson, M. & Siegel, V. 2014. Seasonal distribution and life history of *Thysanoessa macrura* (Euphausiacea, Crustacea) in high latitude waters of the Lazarev Sea, Antarctica. *Marine Ecology Progress Series*, **495**, 10.3354/meps10553.

Kawaguchi, S., Candy, S., King, R., Naganobu, M. & Nicol, S. 2006. Modelling growth of Antarctic krill. *I. Growth trends with sex, length, season, and region.* Marine Ecology Progress Series, **306**, 1–15.

Melvin, J., Kawaguchi, S., King, R. & Swadling, K. In press. The carapace matters: refinement of the instantaneous growth rate method for Antarctic krill *Euphausia superba* Dana, 1850 (Euphausiacea). *Journal of Crustacean Biology*, 10.1093/jcbiol/ruy069.

Motoda, S. 1959. Devices of simple plankton apparatus. *Memoirs of the Faculty of Fisheries, Hokkaido University*, **7**, 73–94.

Nicol, S. 2000. Understanding krill growth and aging: the contribution of experimental studies. *Canadian Journal of Fisheries and Aquatic Sciences*, **57**, 168–177.

Nicol, S., Stolp, M., Cochran, T., Geiisel, P. & Marshall, J. 1992. Growth and shrinkage of Antarctic krill *Euphausia superba* from the Indian Ocean sector of the Southern Ocean during summer. *Marine Ecology Progress Series*, **89**, 175–181.

Nordhausen, W. 1992. Distribution and growth of larval and adult *Thysanoessa macrura* (Euphausiacea) in the Bransfield Strait Region, Antarctica. *Marine Ecology Progress Series*, **83**, 185–196.

Pinchuk, A. & Hopcroft, R. 2007. Seasonal variations in the growth rates of euphausiids (*Thysanoessa inermis, T. spinifera,* and *Euphausia pacifica*) from the northern Gulf of Alaska. *Marine Biology*, **151**, 10.1007/s00227-006-0483-1.

Quetin, L. & Ross, R. 1991. Behavioural and physiological characteristics of the Antarctic krill, *Euphausia superba*. *American Zoologist*, **31**, 49–63.

Steinberg, D.K., Ruck, K.E., Gleiber, M.R., Garzio, L.M., Cope, J.S., Bernard, K.S., *et al.* 2015. Long-term (1993–2013) changes in microzooplankton off the Western Antarctic Peninsula. *Deep-Sea Research I*, **101**, 54–70.

Tarling, G., Shreeve, R., Hirst, G., Atkinson, A., Pond, D., Murphy, E. & Watkins, J. 2006. Natural growth rates in Antarctic krill (*Euphausia superba*): I. Improving methodology and predicting intermolt period. *Limnology and Oceanography*, **51**, 956–972.

Wallis, J., Kawaguchi, S. & Swadling, K. 2018. Sexual differentiation, gonad maturation, and reproduction of the Southern Ocean euphausiid *Thysanoessa macrura* (Sars, 1883) (Crustacea: Euphausiacea). *Journal of Crustacean Biology*, **38**, 10.1093/jcbiol/rux091.

Appendix G has been removed for copyright or proprietary reasons.

It has been published as: Wallis, J.R., Kawaguchi, S., Matsuno, K., Swadling, K. M., 2019. Big things come in small packages. Biomass contribution of the krill Thysanoessa macrura to the marine ecosystem in the Kerguelen Plateau region. In, Welsford, D., Dell, J., Duhamel, G. (Eds). The Kerguelen Plateau: marine ecosystem and fisheries. Proceedings of the Second Symposium. [PDF] Australian Antarctic Division, Kingston, Tasmania, Australia. ISBN: 978-1-876934-30-9.

Appendix G

Big things come in small packages. Biomass contribution of the krill *Thysanoessa macrura* to the marine ecosystem in the Kerguelen Plateau region.

The following eventuated from preliminary analysis to assess and estimate the biomass contribution of *T. macrura* to the Kerguelen Plateau region, explored in Chapter 5. The results of this study were presented at the 2nd International scientific symposium of the Kerguelen Plateau and drove the analysis approach of Chapter 5 of this thesis.

All the research presented in this appendix is currently in press in 2nd International scientific symposium on the Kerguelen Plateau

Wallis JR, Kawaguchi S, Matsuno K, Swadling KM (2019). Big things come in small packages. Biomass contribution of the krill Thysanoessa macrura *to the marine ecosystem in the Kerguelen Plateau region. Proceedings of the 2nd Kerguelen Plateau Marine Ecosystem and Fisheries Symposium. In press*